

# **Extracellular Granzyme B and Pathophysiological Implications**

by

Wendy Anne Boivin

B.Sc., Simon Fraser University, 2005

**A THESIS SUBMITTED IN PARTIAL FULFILLMENT OF  
THE REQUIREMENTS FOR THE DEGREE OF**

**DOCTOR OF PHILOSOPHY**

in

The Faculty of Graduate Studies

(Pathology and Laboratory Medicine)

**THE UNIVERSITY OF BRITISH COLUMBIA**  
(Vancouver)

July 2012

© Wendy Anne Boivin, 2012

## Abstract

Granzyme B (GzmB) is a serine protease that contributes to immune-mediated elimination of cells by initiating a tightly-regulated form of death known as apoptosis. However, during inflammation, GzmB leaks out and accumulates in the extracellular space, retains its activity, and proficiently cleaves extracellular matrix (ECM) proteins. I therefore hypothesized that extracellular GzmB is capable of cleaving novel ECM substrates, contributing to dysregulated ECM integrity and function in disease. In the present dissertation I identified eleven novel extracellular GzmB substrates. Further investigations revealed that GzmB-mediated proteoglycan cleavage was implicated in the dysregulation of active transforming growth factor-beta (TGF- $\beta$ ) sequestration and bioavailability. GzmB cleavage sites were identified in biglycan and betaglycan and active TGF- $\beta$  was shown to be released from decorin, biglycan and betaglycan. The pathophysiological role of my findings were further investigated and validated using animal models of disease in which inflammation and elevated GzmB are observed. Evidence of fibrillin-1 and decorin cleavage were observed in atherosclerosis, abdominal aortic aneurysm and in skin aging pathogenesis. I also assessed the activity of GzmB in advanced atherosclerosis using perforin/apolipoprotein E- double knockout (Perf/apoE-DKO) and granzyme B/apolipoprotein E-double knockout (GzmB/apoE-DKO) mice. Interestingly, unlike our aneurysm findings whereby only GzmB/apoE-DKO mice were protected, both Perf/apoE-DKO and GzmB/apoE-DKO mice were protected from atherosclerosis compared to apoE-KO controls, suggesting the intracellular Perf-dependent activities of granzymes are also important in the pathogenesis of atherosclerosis. In summary, GzmB is a protease that functions both intracellularly and extracellularly in disease. My findings suggest that the use of Perf knockout mice alone to study the role of GzmB in disease should be re-evaluated given the increasing

evidence in both animal models and in human disease showing elevated GzmB in bodily fluids is associated with inflammation and age.

## Preface

Figures and text from chapter 1 were published in the review manuscript “Intracellular versus Extracellular Granzyme B in Immunity and Disease: Challenging the Dogma.” Boivin WA, Cooper DM, Hiebert PR, Granville DJ *Lab Invest.* 2009 Nov;89(11):1195-220. Figures 1-3 and 5 were drawn by Paul Hiebert.

Chapter 5 contains content from the manuscript entitled, “Granzyme B Cleaves Decorin, Biglycan and Soluble Betaglycan, Releasing Active Transforming Growth Factor- $\beta$ 1”, by Boivin WA, Shackleford M, Vanden Hoek A, Zhao H, Hackett TL, Knight DA, and Granville DJ and is currently in press in *PLoS One*.

Chapter 6 contains a figure from “Granzyme B contributes to extracellular matrix remodeling and skin aging in apolipoprotein E knockout mice.” Hiebert PR, Boivin WA, Abraham T, Pazooki S, Zhao H, Granville DJ. (2011) *Exp Gerontol*,46(6):489-99 and a figure from “Perforin-independent extracellular granzyme B activity contributes to abdominal aortic aneurysm.” Chamberlain CM, Ang LS, Boivin WA, Cooper DM, Williams SJ, Zhao H., Folkesson M, Swedenborg J, Allard MF, McManus BM, and Granville DJ. (2010) *American Journal of Pathology*. 176(2):1038-49. The murine skin figure and animal work was performed by Paul Hiebert. For aneurysm experiments, animal work was carried out by Lisa Ang and Ciara Chamberlain.

In Chapter 7, hair cycle experiments contains animal work carried out by Dr. Kevin McElwee’s laboratory at the Skin Care Centre at the University of British Columbia. Electron Microscopy was carried out in collaboration with Dr. David Walker and Toluidine blue stain was done by Fanny Chu. A figure of a nerve from “Perforin-independent extracellular granzyme B activity contributes to abdominal aortic aneurysm.” Chamberlain CM, Ang LS, Boivin WA,

Cooper DM, Williams SJ, Zhao H., Folkesson M, Swedenborg J, Allard MF, McManus BM, and Granville DJ. (2010) *American Journal of Pathology*. 176(2):1038-49 was also included.

All animal procedures were performed in accordance with the guidelines for animal experimentation approved by the Animal Experimentation Committee of the University of British Columbia. All research studies were conducted with the approval of the University of British Columbia Animal Care Committee and research was carried out under the certificates A10-0119 and A06-0158.

# Table of Contents

<b>Abstract.....</b>	<b>ii</b>
<b>Preface .....</b>	<b>iv</b>
<b>Table of Contents.....</b>	<b>vi</b>
<b>List of Tables.....</b>	<b>ix</b>
<b>List of Figures .....</b>	<b>x</b>
<b>List of Acronyms and Abbreviations .....</b>	<b>xii</b>
<b>Acknowledgements .....</b>	<b>xiv</b>
<b>1. Introduction.....</b>	<b>1</b>
1.1 The Granzymes .....	1
1.2 Granzyme B .....	1
1.3 Perforin .....	2
1.4 GzmB in Apoptosis .....	3
1.5 GzmB Inhibition in vivo .....	6
1.6 Extracellular Matrix.....	6
1.6.1 Fibrillin-1 .....	7
1.6.2 Decorin .....	7
1.7 Extracellular GzmB Activity.....	8
1.8 Consequences of Extracellular Matrix Degradation by GzmB .....	16
1.9 Cytokine Activation and Release.....	19
1.10 Other Granzymes .....	19
1.10.1 Granzyme A and the Orphan Granzymes in Cell Death .....	20
1.10.2 Extracellular Activities of Granzymes A, H, K and M.....	21
1.10.3 Granzymes and Inflammation .....	22
1.11 GzmB in Disease .....	24
1.12 Cardiovascular Disease .....	31
1.12.1 Atherosclerosis .....	31
1.12.2 Abdominal Aortic Aneurysm.....	34
1.12.3 Cardiac Allograft Vasculopathy.....	37
1.13 Skin Disorders .....	37
1.14 Neurological Disorders .....	42
<b>2. Rationale, Hypothesis and Aims .....</b>	<b>45</b>

<b>Specific Aims .....</b>	<b>46</b>
<b>3. Methodology .....</b>	<b>48</b>
<b>3.1 In vitro Assays .....</b>	<b>48</b>
3.1.1 Elastin Binding Assay .....	48
3.1.2 Elastin Cleavage Assay .....	48
3.1.3 GzmB-ECM Cleavage Screening Assay .....	49
3.1.4 Smooth Muscle Cell-derived ECM Based Cleavage Assays .....	49
3.1.5 Recombinant Substrate Cleavage Assays .....	50
3.1.6 Proteoglycan Cleavage Assays .....	50
3.1.7 N-terminal Sequencing .....	51
3.1.8 Michaelis-Menten Kinetics .....	51
3.1.9 TGF- $\beta$ 1 Release Assays.....	52
3.1.10 TGF- $\beta$ 1 Bioavailability Assays.....	52
3.1.11 Statistics .....	53
<b>3.2 In vivo Assays.....</b>	<b>53</b>
3.2.1 Mice .....	53
3.2.2 Identifying a Decrease in Decorin in a Murine Model of AAA .....	53
3.2.3 Murine Atherosclerosis and Skin Pathologies Methodology.....	54
3.2.4 Depilation-induced Hair Follicle Cycling in Mice.....	54
3.2.5 Total Cholesterol and Triglyceride Quantification .....	55
3.2.6 En face Staining of Murine Aortas .....	55
3.2.7 Immunohistochemistry.....	56
3.2.8 Alcian Blue-safranin Staining of MCs, Counting and Data Analysis .....	56
3.2.9 Electron Microscopy of Skin Sections .....	57
3.2.10 GzmB Staining in Human AAA Vessels .....	57
3.2.11 Statistics.....	57
<b>4. Identification of Novel Extracellular Substrates .....</b>	<b>58</b>
<b>4.1 Introduction.....</b>	<b>58</b>
<b>4.2 Results.....</b>	<b>58</b>
4.2.1 GzmB has Affinity for Elastin and Displays Weak Elastolytic Activity .....	58
4.2.2 GzmB Cleaves Smooth Muscle Cell Extracellular Matrix .....	59
4.2.3 GzmB-mediated Cleavage of Microfibril Proteins .....	64
4.2.4 GzmB Cleaves Multiple Proteoglycan Substrates .....	64
4.2.5 GzmB Cleaves Fibromodulin, Thrombospondin-1 and Thrombospondin-2 .....	64
<b>4.3 Discussion .....</b>	<b>71</b>
<b>5. GzmB Cleaves Decorin, Biglycan and Soluble Betaglycan, Releasing Active Transforming Growth Factor-<math>\beta</math>1 .....</b>	<b>76</b>
<b>5.1 Introduction.....</b>	<b>76</b>
<b>5.2 Results.....</b>	<b>78</b>
5.2.1 GzmB Cleaves Decorin, Biglycan and Betaglycan .....	78
5.2.2 GzmB Cleavage Site Identification .....	80
5.2.3 Michaelis-Menten Kinetics .....	80

5.2.4 GzmB-dependent Cleavage of Biglycan, Decorin and Betaglycan Results in the Release of Active TGF- $\beta$ 1 .....	80
5.2.5 TGF- $\beta$ 1 Released by GzmB Remains Active and Induces SMAD Signalling in Smooth Muscle Cells .....	86
<b>5.3 Discussion .....</b>	<b>88</b>
<b>6. Investigating Perf-dependent and Perf-independent Roles for the Granzymes in Animal Models of Disease.....</b>	<b>94</b>
<b>6.1 Introduction.....</b>	<b>94</b>
<b>6.2 Results.....</b>	<b>95</b>
6.2.1 Evidence for GzmB-dependent Decreases in Fibrillin-1 and Decorin in Atherosclerosis, AAA and Skin Aging/xanthomatosis.....	95
6.2.1.1 GzmB-dependent Reduction in Fibrillin-1 in AAA and Atherosclerosis .....	95
6.2.1.2 GzmB-dependent Decrease in Adventitial Decorin in AAA.....	96
6.2.1.3 Reduction of Decorin in the Dermis of GzmB/apoE-DKO Mice .....	96
6.2.2 Characterization of GzmB/apoE-DKO and Perf/apoE-DKO Mice in Atherosclerosis .....	100
6.2.2.1 C57, ApoE-KO, GzmB/apoE-DKO and Perf/apoE-DKO Mice .....	100
6.2.2.3 Reduced Atherosclerosis in GzmB/apoE-DKO and Perf/apoE-DKO Mice .....	102
6.2.2.4 Cholesterol and Triglyceride Plasma Levels .....	102
6.2.2.5 GzmB Expression in ApoE-KO Plaques .....	102
<b>6.3 Discussion .....</b>	<b>106</b>
<b>7. Preliminary Studies in the Hair Follicle Cycle and in Ultrastructural Alterations of the Skin .....</b>	<b>110</b>
<b>7.1 Introduction.....</b>	<b>110</b>
7.1.1 Preliminary Study 1: GzmB in the Hair Follicle Cycle .....	110
7.1.2 Preliminary Study 2: Collagen and Nerve Abnormalities by Transmission Electron Microscopy .....	111
<b>7.2 Results.....</b>	<b>112</b>
7.2.1 Preliminary Study 1: GzmB in the Hair Follicle Cycle .....	112
7.2.1.1 GzmB Protein Expression in Hair Follicles Throughout the Hair Growth Cycle .....	112
7.2.1.2 Perf Expression Through the Hair Growth Cycle .....	116
7.2.1.3 GzmB Expression in Mast Cells Throughout the Hair Follicle Cycle .....	118
7.2.2 Future Direction 2: Collagen and Nerve Abnormalities by Transmission Electron Microscopy .....	121
7.2.2.1 GzmB Expression in Nerves .....	121
7.2.2.2 Collagen Abnormalities in ApoE-KO mice .....	125
<b>7.3 Discussion .....</b>	<b>129</b>
<b>8. Conclusion .....</b>	<b>133</b>
<b>Bibliography.....</b>	<b>137</b>



List of Tables

Table 1: Extracellular GzmB Substrates..... 11

Table 2: GzmB in Bodily Fluids..... 13

Table 3: GzmB in Disease ..... 25

Table 4: Summary of Identified ECM Substrates..... 75

Table 5: GzmB Localization Throughout the Hair Follicle Cycle ..... 116

## List of Figures

Figure 1. Classical GzmB/perf-mediated Apoptosis Pathway .....	5
Figure 2. Putative Extracellular (Perf-independent) Roles for GzmB in Age-related Chronic Inflammatory Disorders.....	18
Figure 3: The Role of GzmB in Atherosclerosis .....	33
Figure 4: GzmB in Abdominal Aortic Aneurysm .....	36
Figure 5: GzmB in Skin Pathologies .....	41
Figure 6: <i>In vitro</i> Elastin Binding Assay and Cleavage Assay.....	61
Figure 7: GzmB Cleaves Human Coronary Artery Smooth Muscle Cell Extracellular Matrix ..	62
Figure 8: GzmB-mediated Cleavage of Microfibrillar Proteins .....	63
Figure 9: Low Throughput Screen for Extracellular GzmB Substrates Using Recombinant Proteins .....	65
Figure 10: Cleavage of Fibromodulin by GzmB .....	66
Figure 11: GzmB-mediated Cleavage of Thrombospondin-1 and Thrombospondin-2.....	67
Figure 12: Inhibition of GzmB using a Specific Small Molecule Inhibitor (JT00025135 and JT00025102B) Prevents Decorin and Betaglycan Cleavage .....	69
Figure 13: Inhibition of GzmB using Small Molecule Inhibitors Prevents ECM Cleavage .....	70
Figure 14: GzmB-mediated Cleavage of Decorin, Biglycan and Betaglycan .....	79
Figure 15: GzmB-mediated PG Cleavage is Inhibited by DCI and Cleavage Site Identification	81
Figure 16: GzmB Cleaves Native Smooth Muscle Cell-derived Decorin and Biglycan.....	82
Figure 17: GzmB-mediated Cleavage of Decorin, Biglycan and Betaglycan Results in the Release of Active TGF- $\beta$ 1 .....	84
Figure 18: Inhibition of GzmB using a Specific Small Molecule Inhibitor (JT25102B) Prevents the Release of Proteoglycan-sequestered TGF- $\beta$ 1 .....	85
Figure 19: TGF- $\beta$ 1 Released by GzmB is Active and Induces SMAD-3 Activation in HCASMCs.....	87
Figure 20: Implications of Proteoglycan Cleavage in Wound Healing.....	93
Figure 21: Decreased Fibrillin-1 in ApoE-KO Aortas Compared to GzmB/ApoE-DKO Aortas in Models of Atherosclerosis and Aneurysm.....	97
Figure 22: GzmB –dependent Loss of Adventitial Decorin in Abdominal Aortic Aneurysm ....	98
Figure 23: Decorin in the Papillary Dermis of C57, ApoE-KO and GzmB/apoE-DKO Mice ...	99
Figure 24: Perf/apoE-DKO Mice and GzmB/apoE-DKO Weigh Significantly more than ApoE-KO Mice .....	101
Figure 25: En face Staining for Atherosclerotic Plaque .....	103
Figure 26: Cholesterol and Triglyceride Levels in Mouse Plasma.....	104
Figure 27: Reduced GzmB Staining in the Perf/apoE-DKO Mouse Aorta .....	105
Figure 28: GzmB Expression through the Hair Follicle Cycle.....	115
Figure 29: Perf Expression in the Hair Follicle Throughout the Hair Follicle Cycle.....	117
Figure 30: GzmB Expression in Mast Cells Throughout the Hair Follicle Cycle .....	121
Figure 31: GzmB Expression in the Nerven Ganglia of Aortic AAA Tissue .....	122
Figure 32: Dermal Nerves in ApoE-KO and C57 Mice .....	123

Figure 33: Transmission Electron Microscopy Images of Dermal Nerves in C57 and ApoE-KO Mice .....	125
Figure 34: ECM Morphology in ApoE-KO Mice .....	126
Figure 35: Collagen Fibrils Appear Smaller in the Xanthomas of ApoE-KO Mice Compared to C57 Controls.....	127
Figure 36: Collagen and ECM Abnormalities in the Skin of ApoE-KO Mice on a 30 Week High Fat Diet .....	128
Figure 37: Implications of Extracellular GzmB Activity .....	134

## List of Acronyms and Abbreviations

AAA: Abdominal aortic aneurysm

ANOVA: Analysis of variance

AMI: Acute myocardial infarction

ApoE-KO: Apolipoprotein E-knockout

AR: Aortic

BAL: Bronchoalveolar lavage

BSA: Bovine serum albumin

COPD: Chronic obstructive pulmonary disease

CS: Chondroitin sulphate

CSF: Cerebrospinal fluid

CTL: Cytotoxic lymphocyte

DCI: 3,4-Dichloroisocoumarin

DMSO: Dimethyl sulfoxide

DP: Dermal papilla

DS: Dermatan sulphate

ECM: Extracellular matrix

FBS: Fetal bovine serum

FHL: Familial hemophagocytic lymphohistocytosis

GAG: Glycosaminoglycan

HCASMC: Human coronary artery smooth muscle cells

HS: Hair shaft

Gzm: Granzyme

GzmB/apoE-DKO: Granzyme B/apolipoprotein E double knockout

IL: Interleukin

IRS: Inner root sheath

LDL: Low density lipoprotein

LDLr-KO: Low density lipoprotein receptor knockout

LPS: Lipopolysaccharide

LTBP: Latent transforming growth factor beta binding protein

MAPK: Mitogen activated protein kinase

MIF: Migration inhibitor factor

MMP: Matrix metalloproteinase

NK: Natural killer cells

ORS: Outer root sheath

Perf: Perforin

Perf/apoE-DKO: Perforin apolipoprotein E double knockout

PG: Proteoglycan

RA: Rheumatoid arthritis

ROS: Reactive oxygen species

SF: Synovial fluid

SK: Skin

SMC: Smooth muscle cell

SMGM: Smooth muscle cell growth medium

TGF- $\beta$ : Transforming growth factor-beta

TIMP: Tissue inhibitor of metalloproteinases

UV: Ultraviolet

VWF: Von willebrand factor

## Acknowledgements

I would like to thank my friends and family as without their support I would not be where I am today. My mom and my dad and sister Lisa have been amazing throughout the years. A special thanks to my fantastic friends and/or lab members Johanna Scheutz, Helen Burston, Virginia Le, Stephanie Warner, Hayley Hiebert, Paul Hiebert, Kristin Bowden, Ciara Chamberlain, Lisa Ang and Alon Hendel; you are all truly amazing people.

Thank you to my supervisor Dr. David Granville, whom has also been a great mentor, providing ongoing insightful feedback on my work. To my aunt Taryn Boivin, you have been an inspiration for me throughout my degree and to my amazing grandmother Eileen Boivin of whom I would love to have shared this with.

Thank you to our collaborator Dr Darryl Knight as well as Tillie Hackett for their technical expertise and insight into my TGF- $\beta$  work. Thank you to my committee members Dr. Bruce McManus, Dr. David Walker, Dr. David Hunt, Dr. Susan Porter and Dr Vincent Duronio for their guidance throughout my degree. An acknowledgement to David Hunt, my previous co-operative education supervisor, for his ongoing mentorship and guidance throughout my studies. Thank you to Dr. David Walker for his expertise and guidance in my transmission electron microscopy project. I would like to thank Amanda Vanden Hoek for her help with my enzyme kinetics studies. Special acknowledgement to the members of the Granville Laboratory for their insight into my projects and the friendly, supportive atmosphere we share in the laboratory. Thanks to the animal facility for their help with my animal models and in animal training.

# 1. Introduction

## 1.1 *The Granzymes*

The Granzymes (Gr) are a family of serine proteases that were originally predicted to function as intracellular and extracellular proteases [1]. There are 5 granzymes in humans (A, B, H, K and M) and 11 in mice (A, B, C, D, E, F, G, K, L, M and N) of which Granzyme A (GzmA) and Granzyme B (GzmB) are the most extensively studied. The other granzymes are often referred to as the orphan granzymes, as until recently, very little was known regarding their function. The granzymes are closely structurally related to chymotrypsin and all contain a conserved triad of residues in their active site (histidine, aspartic acid and serine), consensus sequences at their N-termini and conserved disulphide bridges [1, 2]. All granzyme transcripts are similarly organized and composed of 5 exons [1]. Both the human and mouse granzymes map to 3 corresponding loci: in humans the ‘tryptase’ locus is at 5q11-q12 for GzmA and GzmK, the ‘chymase’ locus is at 14q11-q12 for GzmB and GzmH and the ‘met-ase’ locus is at 19p13.3 for GzmM [2]. The tryptase subfamily has tryptase-like specificity, the chymase subfamily exhibits chymotrypsin-like specificity and the met-ase family has elastase-like specificity. Sequence homology across the subfamilies is about ~40%, homology within subfamilies is 55-70%, while human, rat and mouse GzmB are about 70% identical [1].

## 1.2 *Granzyme B*

GzmB, a 32 kDa aspartase, was discovered in the mid-1980’s and described as a protease in the cytotoxic granules of cytotoxic lymphocytes (CLs), namely cytotoxic T lymphocytes (CTLs) and natural killer (NK) cells [3-6]. GzmB can also be expressed in other immune cell types such as mast cells [7], macrophages [8], neutrophils [9], basophils [10], dendritic cells [11], CD4<sup>+</sup> T cells [12] and CD4<sup>+</sup>CD25<sup>+</sup> T-regulatory cells [13] and by non-immune cells including chondrocytes [14], keratinocytes [15], smooth muscle cells (SMC) [16],

type II pneumocytes [17], Sertoli cells [18], primary spermatocytes [18], granulose cells [19] and syncytial trophoblasts [18]. GzmB has a cleavage preference for P1 residues of aspartic acid in substrates, which interacts with an arginine residue on the side of the GzmB active site [20].

The GzmB gene is located on chromosome 14 and is ~3500 bp long [21]. The promoter region has binding sites for activating transcription factor/cyclic AMP-responsive element-binding protein-1, activator protein-1, ikaros and core-binding factor and mutations to any of the binding sites prevents GzmB expression [22-25]. Cytotoxic lymphocytes often express GzmB constitutively, but further transcription can be initiated upon cell activation [24, 26]. GzmB is tagged with mannose-6-phosphate for trafficking to granules through the mannose-6-phosphate receptor [27] and the inactive zymogen GzmB is activated en route or in cytotoxic granules by removal of the pro-peptide by cathepsin C [28, 29]. Within granules GzmB is stored on scaffolds of serglycin, a chondroitin sulphate proteoglycan and is rendered inactive due to the low pH of granules [30-33].

### *1.3 Perforin*

Perforin (Perf) is a 66 kDa cytolytic protein identified in the mid-1980s [34, 35]. It is a calcium-dependant protein that has homology to components of complement. Perf is localized on serglycin in the cytotoxic granules of cytotoxic lymphocytes where it is rendered inactive due to the low pH of granules. Perf expression is IL-2-dependent in CTLs and constitutive in NK cells [36]. It polymerizes to form pores in membranes to facilitate the transfer of GzmB into the cytosol of target cells for the induction of apoptosis (further discussed in the GzmB in apoptosis section). At concentrations below a target cell-dependent threshold (<62ng/ml for U937 cells), Perf won't deliver granzymes but at concentrations above threshold it can independently cause necrosis (500-1000ng/ml for U937 cells) [37]. In humans, nonsense or missense mutations in the Perf gene causes familial hemophagocytic lymphohistocytosis (FHL). FHL is characterized



by improper clearance of antigen-presenting cells by CTLs, resulting in uncontrolled expansion of T-cells and macrophages [38]. Perf is required for the internalization of granzymes into target cell cytosol but not necessary for extracellular granzyme activity. Thus intracellular granzyme activity is Perf-dependent but extracellular activity is Perf-independent.

#### *1.4 GzmB in Apoptosis*

Apoptosis or programmed cell death is a tightly-regulated means by which cell death is induced in the body to discretely remove unwanted cells, without provoking the pro-inflammatory response. There are 2 main cytotoxic pathways by which cytotoxic lymphocytes induce cell death, the receptor-mediated pathway involving TNF ligands (eg. FasL, TRAIL) and the granule-mediated pathway involving the granzymes. Upon target cell engagement, granule contents are released into the immunological synapse, the space between the cytotoxic cell and target cell. Granzymes then enter target cells in a Perf-dependent manner. The mechanism by which Perf mediates GzmB entry into target cells remains under debate. Early models suggested GzmB enters through pores created by Perf in the plasma membrane, although it became apparent GzmB could be endocytosed independent of Perf [39-42]. More recent models suggest the mannose-6-phosphate receptor is involved in the uptake of GzmB into endosomes where it enters target cell cytosol with the aid of Perf [43]. Another model suggests that GzmB-serglycin complexes can enter the cytosol through the cell surface receptor heparin sulphate, without the formation of Perf pores [31, 33, 43-45]. Finally other cell surface molecules such as heat shock protein-70 may also promote GzmB entry [46].

Once inside the target cell, GzmB can act on several cytosolic and nuclear substrates, ultimately inducing apoptosis (Figure 1) [47]. GzmB can cleave and subsequently activate several caspases such as caspase 3, 7 and 9 [48-50] leading to the processing of several other cellular substrates such as the sensor for DNA damage poly(ADP ribose) polymerase and

nuclear lamins, ultimately resulting in a loss of integrity of the nuclear membrane [51]. The BH3-only protein Bid is also a substrate for GzmB, whereby the truncated form gtBid translocates to the mitochondrial membrane and disrupts its integrity leading to the release of cytochrome C and other factors [52, 53]. Cytochrome C release results in the formation of the apoptosome composed of cytochrome C, dATP, apaf-1 and procaspase-9 which activates caspase 9, then subsequently caspases 3 and 7. In addition, GzmB can degrade other intracellular targets including  $\alpha$ -tubulin [54], HIP [55, 56] and Hop [57].

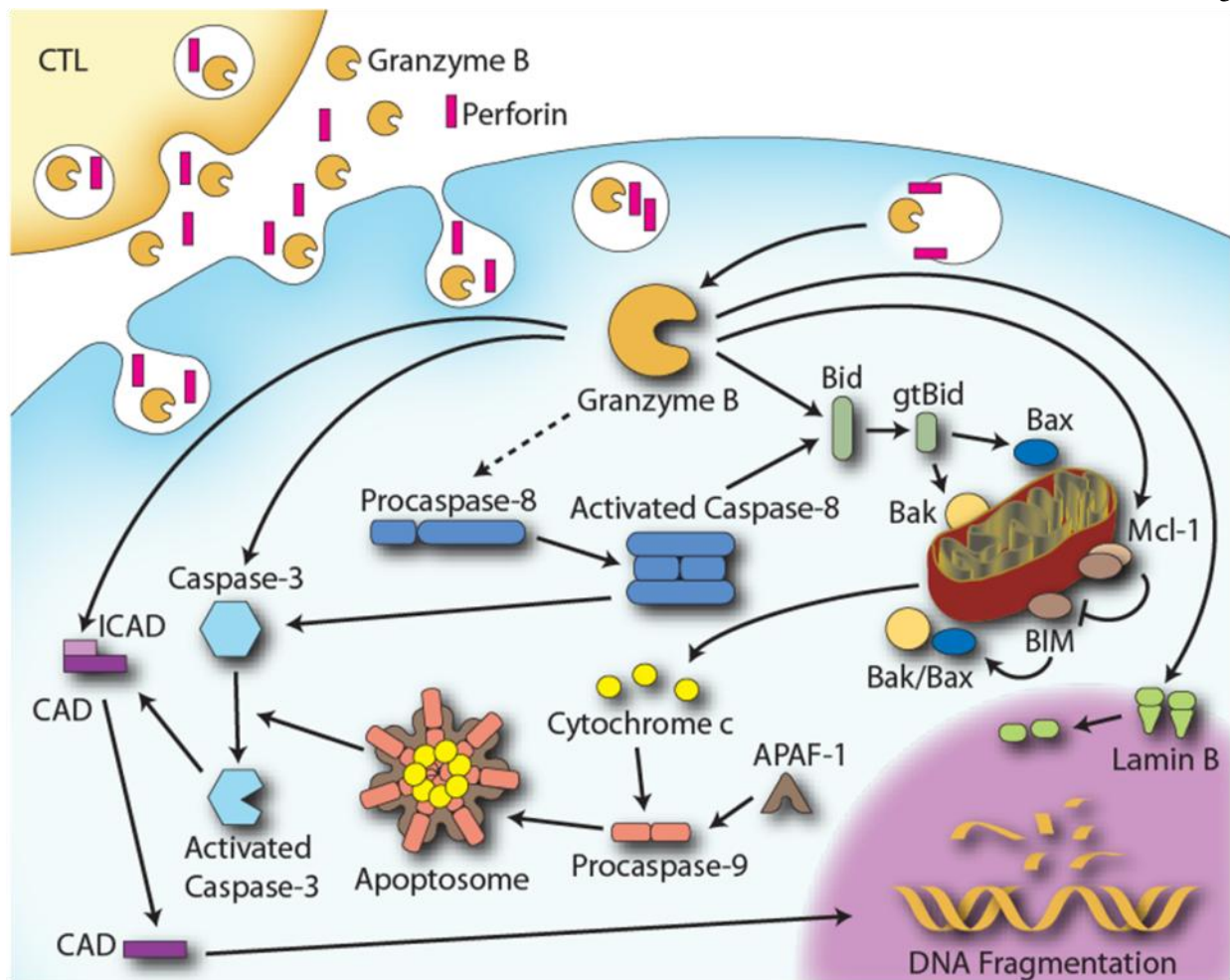


**Figure 1. Classical GzmB/perf-mediated Apoptosis Pathway**

GzmB internalization is facilitated by Perf. Upon internalization, GzmB initiates apoptosis primarily through the cleavage of Bid into a truncated form (gtBid) that triggers mitochondrial cytochrome c release and apoptosome formation leading to caspase activation and manifestation of the apoptosis phenotype. GzmB can also bypass the mitochondrial pathway and initiate caspase activation directly and/or cleave caspase substrates such as the inhibitor of caspase activated deoxyribonuclease (ICAD) thereby allowing CAD to translocate to the nucleus to fragment DNA. GzmB also cleaves the nuclear membrane protein lamin B, resulting in a loss of integrity of the nuclear membrane. Reproduced with permission from *Laboratory Investigation* [58]

### 1.5 *GzmB Inhibition in vivo*

The only known endogeneous inhibitor of GzmB *in vivo* is proteinase inhibitor-9 (PI-9), which is expressed by immune cells as protection against accidental GzmB leakage into the cytosol [59, 60]. Non-immune cells such as endothelial cells and vascular smooth muscle cells can also express the inhibitor to prevent targeted cytotoxicity [61, 62]. In mice, serine protease inhibitor-6 regulates GzmB activity similarly to PI-9 in humans. A second inhibitor, Serpina3n was also recently discovered in mouse Sertoli cells and is expressed in the brain, testis, lung, thymus and spleen [36, 63, 64].

### 1.6 *Extracellular Matrix*

The extracellular matrix (ECM) is a fundamental component of tissue, providing a structural framework for stability, organization and elasticity. It also provides an essential scaffold for cell survival, acts as a molecular filter, and influences cell signaling and phenotype. In particular relevance to this thesis, the ECM acts as a reservoir for growth factors and cytokines by influencing their storage, location, concentration, activation, synthesis and degradation [65]. Extracellular proteases such as the MMPs act in regulating growth factor bioavailability by cleaving ECM and releasing sequestered cytokines, as well as by activating latent growth factors [65, 66]. One such family of growth factors is TGF- $\beta$ , which is involved in numerous processes including differentiation, migration and ECM synthesis [67, 68]. TGF- $\beta$  is normally secreted as a latent protein but both the active and inactive forms of TGF- $\beta$  are bound and sequestered by ECM, albeit by different mechanisms. For example, fibrillin-1 sequesters inactive TGF- $\beta$  by interacting with the latent TGF- $\beta$  binding protein (LTBP) while active TGF- $\beta$  can bind directly to the ECM proteoglycans (PGs) decorin, biglycan and soluble betaglycan [65, 69-71].

### *1.6.1 Fibrillin-1*

Fibrillin-1 is synthesized as a dimer, linked with disulphide bonds. It is the major structural constituent of microfibrils, either elastin associated or non-elastin associated. Microfibrils act as a scaffolding to support elastin and is critical for tissue extensibility and elasticity. Fibrillin-1 binds to latent transforming growth factor- $\beta$ -binding proteins (LTBP) 1, 2, and 4 [72, 73], microfibril-associated glycoprotein 1 and 2 [74, 75], fibulins [76], bone morphogenetic protein 2, 4, 7, and 10 [77], and growth and differentiation factor 5 [77]. Microfibrils are involved in transforming growth factor- $\beta$  (TGF- $\beta$ ) bioavailability, sequestering the inactive growth factor through the LTBP proteins. Mutations in the fibrillin-1 gene causes Marfans Syndrome, a connective tissue disorder characterized by defects in the eyes, cardiovascular system (ascending aortic aneurysm, heart valve defects), nervous system, skin and skeleton .

### *1.6.2 Decorin*

Decorin is a 40 kDa small leucine rich proteoglycan, with one GAG chain composed of either chondroitin sulphate (CS) or dermatan sulphate (DS). The structure of decorin is horseshoe or arched in tertiary shape, which provides sites for interactions as a dimer or as a monomer complexed to other proteins. It is a small pericellular PG, similar in structure to biglycan and interacting with collagen [78], epidermal growth factor receptor [79], fibronectin [80, 81], thrombospondin [82] and tropoelastin [83]. Decorin also interacts with growth factors such as TGF- $\beta$  [84], fibroblast growth factor-2 [85], tumor necrosis factor- $\alpha$  [86], platelet derived growth factor [87], and insulin-like growth factor-1 [88]. It is involved in ECM assembly, composition and turnover and plays a role in collagen fibrillogenesis and spacing by binding to collagen type I [89]. Decorin allows the matrix to resist physical stress and regulates

intrafibrillar distances of collagen fibres. Decorin is cleaved by matrix metalloproteinases 2, 3 and 7. [66] and has been implicated in cellular processes such as cell adhesion [81], migration [90], proliferation [91, 92], cell survival and inhibition of apoptosis [93]. Disruption of the decorin gene in mice causes abnormal collagen fibril morphology and skin fragility [94] and decorin production and expression is altered during wound healing and scar formation [95, 96]. A catabolic fragment known as decorunt is found in the skin with increasing age, however the protease that cleaves the fragment remains to be identified [97].

### *1.7 Extracellular GzmB Activity*

Until recently, GzmB was largely studied intracellularly, specifically in the context of apoptosis. However, the granzymes were originally identified as both intracellular and extracellular proteases and over the past few years, increased research has focused on extracellular GzmB activity [98-102]. Several groups have reported that GzmB is present in the ECM of tissue and can be found extracellularly in bodily fluids (Table 2) [100, 103, 104]. Several novel extracellular substrates for GzmB have been identified. Potential implications of ECM cleavage have been described, and extracellular GzmB activity has been linked to arthritis, vascular pathologies, and other diseases. While cell types such as keratinocytes, chondrocytes and neutrophils are capable of expressing both GzmB and perforin simultaneously, other cell types such as mast cells and basophils express GzmB in the absence of Perforin and GzmA suggesting GzmB may act exclusively extracellularly in these cells [9, 10, 15, 105-107]. Differential expression of GzmB from Perforin and GzmA in mast cells and basophils is probably due to the GzmB gene localization to a cluster of genes along with mast cell proteases (separate from the Perforin and GzmA genes). As a result GzmB can be expressed by myeloid cells (dendritic cells, granulocytes) and others upon activation, independently of Perforin [10, 11, 108]. In addition, several of these cell types such as keratinocytes and chondrocytes are unable to form

immunological synapses, suggesting these cell types are incapable of inducing target cell-induced apoptosis.

GzmB is released from cytotoxic granules upon target cell recognition. Upon reaching the neutral pH of the extracellular environment, GzmB is instantly active and can readily cleave susceptible extracellular substrates at a P1 residue of aspartic acid or glutamic acid. Unlike its intracellular pathway which is Perf-dependent, GzmB does not require Perf to act extracellularly. The stimuli involved in GzmB release have not been fully elucidated; however several mechanisms have been described to date. GzmB may leak into the ECM from the immunological synapse during target cell engagement, it may be released non-specifically upon TCR signaling or after prolonged IL-2 stimulation and it is likely released after other currently unidentified stimuli [109, 110]. Recently, Prakash *et al* found that GzmB is constitutively released from CTLs and NK cells *in vivo* and that GzmB release can be independent of target cell engagement [111]. GzmB is released in both active and inactive forms, suggesting there may be an extracellular GzmB activator for the zymogen form of the enzyme [111]. The pro-form of GzmB may be regulated outside of cells in a process similar to the extracellular regulation of other ECM proteases, such as the pro-forms of matrix metalloproteases (MMP), although this has yet to be defined. Besides NK cells and CTLs, other immune and non-immune cell types also express and secrete GzmB, however the stimuli and signaling pathways regulating GzmB release is largely unknown in these cell types.

GzmB is present in the plasma of healthy individuals with median levels of approximately 20 to 40 pg/ml reported in the literature [100, 104]. Serum levels of GzmB are elevated in several diseases such as human immunodeficiency virus-1 infection, Epstein Barr virus infection, arthritis and others (Table 1) [100, 103, 104]. Apart from the potential blood clotting implications that will be described later, it is worth noting that although circulating

GzmB may be useful as a biomarker for several diseases, it may not have a large impact on disease progression and may be present in the serum due to leakage from tissues where it is more abundant. In diseased tissues, particularly in areas of inflammation, extracellular granzyme concentration would be expected to be much higher than that of the blood. In such focal areas, GzmB may exert its greatest impact due to the abundance of ECM substrates and the associated network of susceptible cells in tissue. In addition to plasma, GzmB is also present in the synovial fluid (SF) of rheumatoid arthritis patients [104], the cerebrospinal fluid (CSF) of multiple sclerosis [112] and Rasmussen encephalitis patients [113], as well as the bronchoalveolar lavage (BAL) in the inflamed lung [114] and atopic asthma [115] (Table 2) . Although the GzmB inhibitor PI-9 is present in normal human plasma, GzmB retains 70% of its activity in the plasma, suggesting PI-9 does not efficiently inhibit GzmB activity in the blood [116, 117]. There is a lack of evidence for an endogenous extracellular GzmB inhibitor that is physiologically effective, thus its extracellular activity may be largely unregulated in contrast to other ECM proteases such as MMPs, which are tightly regulated by the tissue inhibitors of metalloproteases (TIMPs). In support of this the major protease inhibitors in the bronchoalveolar lavage do not inhibit GzmB [114]. This lack of extracellular regulation of GzmB activity may have important implications with respect to a potential degradative role for GzmB in disease.



**Table 1: Extracellular GzmB Substrates**

*Substrates identified in my studies are italicized.*

<b>Protein</b>	<b>Implications</b>	<b>References</b>
<b>Proteoglycans</b>		
Aggrecan	Disruption of structural integrity in cartilage	[118]
Cartilage proteoglycans	Disruption of structural integrity in cartilage	[118]
<i>Decorin</i>	Release of active TGF- $\beta$ . Degradation results in a loss in collagen density, tight bundle formation and tensile strength.	
<i>Biglycan</i>	Release of active TGF- $\beta$	
<i>Betaglycan</i>	Release of active TGF- $\beta$	
<i>Fibromodulin</i>	Potential implications in collagen spacing and TGF- $\beta$ bioavailability	
<i>Brevican</i>	Potential role in neurite growth and synapse stabilization	
<i>Syndecan</i>	Potential role in wound healing	
<b>Blood proteins/clotting</b>		
Von Willebrand factor	GzmB cleavage site in domain of platelet interaction, prevention/delay of thrombosis	[119]
Plasminogen	Cleavage yields angiostatin which is anti-angiogenic. Implications in angiogenesis	[120]
Plasmin	As plasmin is pro-angiogenic, cleavage results in reduction of angiogenesis.	[120]
<b>Cell receptors</b>		
Neuronal glutamate receptor	GzmB cleaves the non-glycosylated form of the receptor into an autoantigenic fragment	[121]
Acetylcholine receptor	Cleavage results in a reduction of the receptor in neuromuscular junctions and yields an autoantigenic fragment	[122]
<b>Other ECM components</b>		
Vitronectin	GzmB cleavage site in integrin binding domain, implications in cell adhesion, migration and anoikis	[123]
Fibronectin	Cell adhesion, migration and anoikis	[123, 124]
Fibrinogen	Matrix form of fibrinogen is cleaved. The uncleaved protein responsible for platelet adhesion and thrombus growth. Cleavage results in anti-thrombosis implications	[119]
Laminin	Cell adhesion, anoikis	[123]
Smooth muscle cell matrix	Cell adhesion, anoikis	[124]
<i>Fibrillin-1</i>	May contribute to medial disruption in abdominal aortic aneurysm, disruption of microfibril component of elastin	

<b>Protein</b>	<b>Implications</b>	<b>References</b>
<i>Fibrillin-2</i>	Potential disruption of the microfibril component of elastin	
<i>Fibulin-2</i>	Potential disruption of the microfibril component of elastin	
<i>Thrombospondin-1</i>	Potential disruption of cell-matrix interactions	
<i>Thrombospondin-2</i>	Potential disruption of adhesion and migration	
<b>Cytokines</b>		
Interleukin 1 $\alpha$	GzmB processes full length IL-1 $\alpha$ into a fragment with enhanced biological activity.	[125]

**Table 2: GzmB in Bodily Fluids**

Disease	Bodily Fluid	GzmB levels*	Fold over control	Ref
<b>Infection</b>				
Melioidosis	Plasma	Bacteremic melioidosis: 27.3 pg/mL (55.0–571.3), Nonbacteremic melioidosis: 13.6 (5–628.9) pg/mL, Healthy controls: 19.3 (5.0–24.8) pg/mL	Bacteremic melioidosis 1.4x higher than healthy controls	[126]
<i>Neisseria meningitidis</i>	Plasma	Fulminant septicaemia: 247 (140–2280) pg/mL, Distinct meningitis and septic shock: 265 (90–341) pg/mL, distinct meningitis: 20 (9–36) pg/mL, controls: 18 (12–25)	Fulminant septicaemia 13.7x, Distinct meningitis and septic shock 14.7x higher than controls	[127]
<i>Plasmodium Falciparum</i> Malaria	Plasma	Uncomplicated Malaria: 42 (2–4132), Severe Malaria: 69 (2–1980), controls 9 (2–32)	Uncomplicated malaria 4.6x, severe malaria 7.6x higher than controls	[128]
CMV infection	Plasma	112 (38–363) pg/mL at peak, Control before rejection treatment: 30 (1 to 80) pg/mL	3.7x higher than controls	[129]
CMV infection	Serum	Subclinical rejection: 40 (2–4453) pg/mL, Acute rejection: 38 (3–1256) pg/mL, no rejection controls: 19 (range, 5–1244) pg/mL	Subclinical 2.1x and acute rejection 2x higher than controls	[117]
<b>Musculo-skeletal</b>				
Rheumatoid Arthritis (RA), Dengue fever, CMV infection	Plasma	No increase in GzmB in RA patients. CMV infection: ~50U/ml–5000U/ml. Dengue Fever: ~50U/ml–1000U/ml. 1u/ml ~ 1pg/ml	Control samples below detection limit	[130]
RA	Plasma/ synovial fluid (SF)	RA Plasma: 121 (7–6571) pg/mL, inflammatory osteoarthritis (OA) plasma: 8 (0–308), RA SF: 251 (33–44848) pg/mL, OA SF: 29 (0–120)	RA plasma 15.1x higher than OA plasma, RA SF 8.7x higher than OA SF	[103]
RA, EBV, HIV	Plasma/ SF	RA Plasma: 20 (1–1918) pg/mL, RA SF: 3183 (75–26538) pg/mL, EBV plasma: 60 (1–4000) pg/mL, HIV plasma: 20 (1–74) pg/mL healthy individuals plasma: 11.5 (1–130) pg/mL	RA plasma 1.7x, EBV plasma 5.2x and HIV plasma 1.7x higher than healthy individuals	[104]
<b>Pulmonary</b>				
Chronic allergic asthma	Bronchoalveolar lavage (BAL)	BAL: 1–348.1 pg/mL, control: 1.0–70.5 pg/mL	No medians reported	[115]
Hypersensitive pneumonitis	BAL/ serum	BAL: 10 pg/mL, control BAL: 0 pg/mL. No increase from controls in serum	Median control: 0 pg/mL	[114]

Disease	Bodily Fluid	GzmB levels*	Fold over control	Ref
Chronic obstructive pulmonary disease	BAL	Exact values not reported. Highest level approaching 2000 pg/mL in current smokers with COPD	Values not reported	[131]
<b>Cardiovascular</b>				
Acute Myocardial Infarction	Plasma	Day 1: 78±23, Day 7: 359±68, Day 14: 261±54pg/ml	4.6x higher on day 7 than day 1, 3.35x higher on day 14 than day 1	[132]
Carotid atherosclerosis	Plasma	Echolucent plaque (unstable): 492.0 (0.7–956.4), Echogenic/heterogenous plaque: 143.8 (0.7–981.1) pg/mL	No control value reported	[133]
<b>Neurological</b>				
Rasmussen's encephalitis	Cerebral Spinal Fluid (CSF)	CSF: 10.8 ± 15.5 pg/mL, controls: 1.2 ± 1.2 pg/ml	9x higher than controls	[113]
Relapsing Remitting Multiple Sclerosis	CSF/ plasma	CSF: ~3U/mL (1U/ml in controls). No increase in plasma	~3x higher than controls	[112]

In addition to ECM proteolysis, GzmB can act on extracellular substrates involved in the clotting cascade such as plasmin, plasminogen, von Willebrand Factor (VWF) and the matrix form of fibrinogen [119, 120]. GzmB cleaves VWF in domains that are necessary for platelet interaction and cleavage prevents platelet aggregation, spreading, tethering and adhesion to VWF multimer [119]. Since GzmB has a high affinity for ECM binding, Buzza *et al* suggest it would accumulate in areas of inflammation and prevent/delay thrombosis in these areas [119]. GzmB-dependent cleavage of plasmin and plasminogen has implications outside of clotting as degradation of these proteins may also inhibit angiogenesis: the growth of new blood vessels from pre-existing ones [120]. Plasmin is proangiogenic, releasing and activating growth factors and proteases [134] and the cleavage of plasminogen and plasmin yield angiostatin fragments, which are anti-angiogenic in nature [120].

GzmB is also capable of cleaving cartilage proteoglycans, and in particular, aggrecan. GzmB cleaves aggrecan at a faster rate than that of stromelysin-1 and has implications in cartilage degradation in and remodelling of interstitial ECM in rheumatoid arthritis (RA) [118]. A large number of synovial and tissue lymphocytes contain GzmB and GzmB is increased in the synovial fluid of RA patients [103, 135-138]. GzmB+ cells are present in the invasive front of the synovium suggesting GzmB may play a role in joint destruction in RA [137].

In terms of cleavage site identification, the site in vitronectin has been identified, along with fibrinogen, von Willebrand factor, neuronal glutamate receptor, acetylcholine receptor and IL-1 $\alpha$  [119, 121-123, 125]. The cleavage site is in the RGD domain of vitronectin, an integrin binding motif. GzmB-mediated cleavage of this domain disrupts cellular-vitronectin interactions and influences cell adhesion and migration properties [123]. Integrin-RGD binding is key in several extracellular processes such as cell migration, proliferation, differentiation and apoptosis and cleavage of ECM proteins at this domain may influence cell adhesion to matrix. Small

soluble RGD fragments can act as decoys and prevent cell adhesion. Apart from GzmB there is no extracellular protease shown to cleave at the RGD domain or at a P1 residue of aspartic acid, which yields potentially chemotactic fragments and may disrupt adhesion.

GzmB can cleave cell surface receptors such as the neuronal glutamate receptor, Notch1 and FGFR1 [121, 139]. The cleavage of these cell surface receptors may have implications in cell signaling affecting tumor survival as well as autoantigen generation. Cleavage fragments of receptors can also have physiological activities such as seen with the FGFR1 cleavage fragment, which can activate pro-cell death functions as well as inactivate pro-growth signals facilitated by FGFR1 in cancer [139].

### *1.8 Consequences of Extracellular Matrix Degradation by GzmB*

GzmB-mediated ECM cleavage may contribute to disease not only through mechanical damage, but also through other mechanisms (Figure 2). One consequence of ECM cleavage is anoikis; a form of cell death similar to apoptosis that is caused by a loss of cell/matrix interaction. Fibronectin, laminin and vitronectin are adhesive proteins that are involved in connecting cells to surrounding insoluble matrix. As all of these proteins are substrates for GzmB, GzmB-mediated cleavage may induce anoikis in various cell types. Choy *et al* described anoikis in cultured SMCs when treated with extracellular GzmB that cleaved fibronectin in the matrix [124]. Choy *et al* also showed that approximately 30% of smooth muscle cell death induced by cytotoxic lymphocytes was Perf-independent but GzmB-dependent, pointing towards anoikis as the mechanism of cell death [124]. Buzza *et al* further investigated this by seeding endothelial cells on pure fibronectin, laminin and vitronectin matrices and reported cell detachment and death by anoikis [123]. Cleavage of fibronectin was further confirmed by Hernandez-Pigeon *et al* (2007), who showed that keratinocytes can secrete GzmB that is capable of cleaving fibronectin.

GzmB-dependent cleavage of vitronectin and fibronectin can also inhibit cell motility and migration [123]. UVA light stimulates keratinocyte motility, however GzmB expression is induced by UV light and inhibits this process [140]. An area poorly understood is whether GzmB-generated ECM fragments can elicit chemotactic activities. GzmB ECM cleavage fragments could possess chemotactic properties, leading to the recruitment of immune cells and promotion of inflammation [141]. Indeed fibronectin fragments can attract both neutrophils and monocytes [141-144]. Fibronectin fragments also have other properties such as inducing MMP expression by chondrocytes [144]. ECM fragments may also act as signaling molecules in neighboring resident cells, as mentioned previously with the FGFR1 fragment [139]. As ECM has affinity for and serves as a reservoir for many growth factors and cytokines, the disruption of ECM by GzmB could also induce the release of these growth factors and influence surrounding cells in an indirect manner.

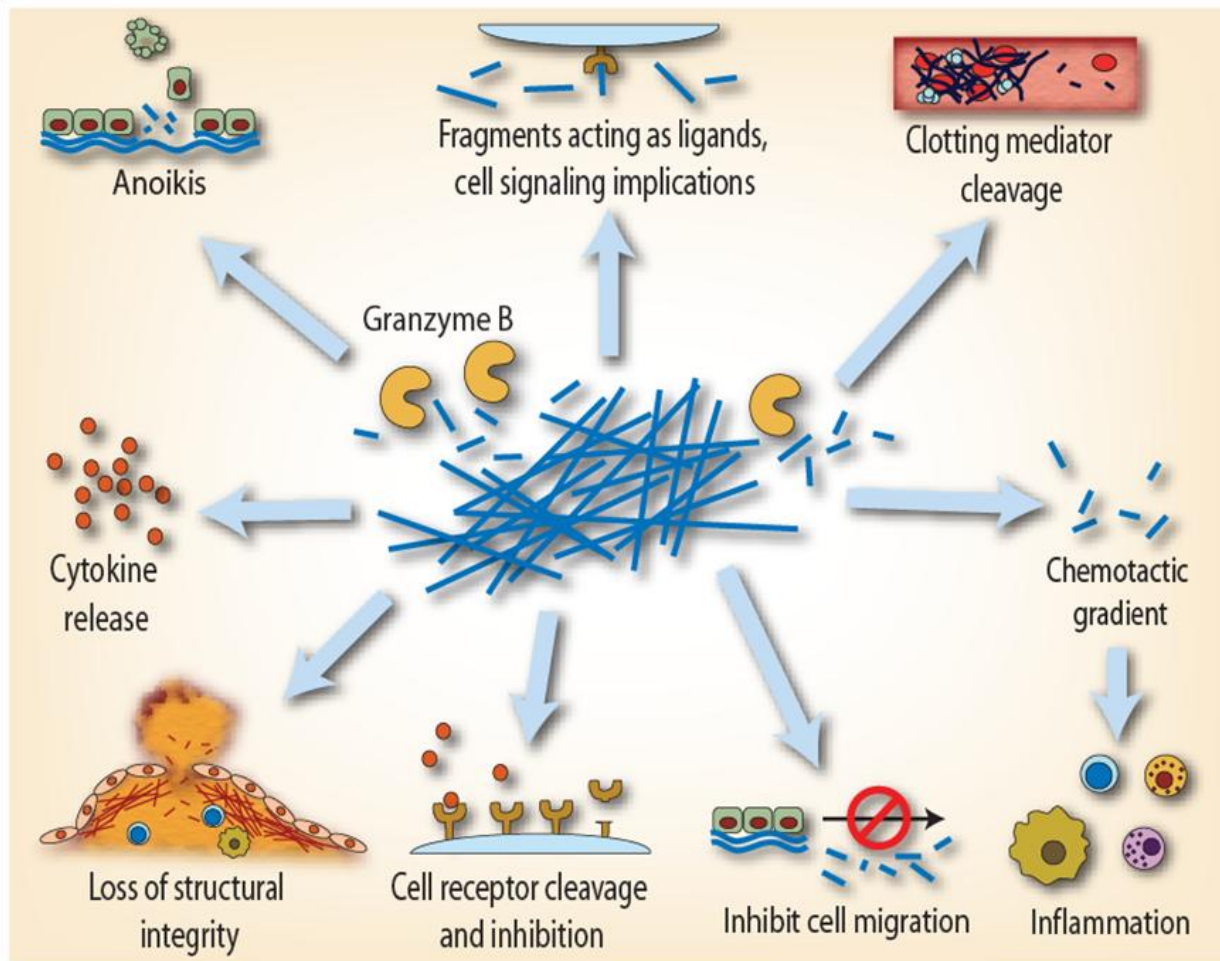


**Figure 2. Putative Extracellular (Perf-independent) Roles for GzmB in Age-related Chronic Inflammatory Disorders.**

Extracellular GzmB accumulation has been observed in a number of diseases associated with dysregulated inflammation and/or aging. GzmB has been shown to accumulate in the extracellular milieu of tissues, blood, and other bodily fluids. GzmB retains its activity in the blood suggesting that, unlike MMPs, cathepsins, and other extracellular proteases, extracellular mediators of GzmB activity may be limited. GzmB can cleave proteins involved in structural integrity and wound healing such as fibronectin. GzmB can also cleave proteins related to clotting (fibrinogen, vWf, plasminogen). GzmB can induce detachment-mediated cell death (anoikis) via the cleavage of ECM. Although not determined for granzymes, MMP-mediated fragments of fibronectin and elastin exhibit chemotactic properties and may promote inflammation. Fragments may also exhibit bioactive properties and augment the release of cytokines from the matrix. Granzymes may also play a role in the cleavage of cell surface receptors as seen with Notch1 and FGFR1. Reproduced with permission from *Laboratory Investigation* [58] .



### 1.9 Cytokine Activation and Release

GzmB has recently been shown to act as a molecular switch to potentiate the pro-inflammatory activity of IL-1 $\alpha$  [125]. Importantly, GzmB-mediated IL-1 $\alpha$  processing occurred both intracellularly and extracellularly and enhanced IL1 $\alpha$  activity both *in vitro* and *in vivo*. While absent in healthy patients, fragments with similar in size to GzmB-processed IL-1 $\alpha$  were found in bronchoalveolar lavage fluid (BAL) from patients with inflammatory lung conditions such as cystic fibrosis, chronic obstructive pulmonary disease and bronchiectasis. Additionally, when GzmB processed IL-1 $\alpha$  was added to an antigen-driven model using ovalbumin there was an increase in antibody responses and cytokine production, suggesting the processed IL-1 $\alpha$  was active *in vivo* [125].

GzmB can also activate proIL-18 into the same active fragment as converted by caspase-1, the well-described, endogeneous converting enzyme [145]. Supernatants of CD8<sup>+</sup> T cells (which were positive for GzmB and negative for caspase-1), activated proIL-18 in a process that was inhibited by the GzmB inhibitor Z-AAD-CMK, confirming the activation can occur extracellularly. GzmB-converted IL-18 is fully active and induces the same degree of IFN- $\gamma$  production by KG-1 cells as that produced by caspase-1.

Finally, as described in chapter 5 of this dissertation, GzmB can also release active TGF- $\beta$  from the sequestering extracellular proteoglycans decorin, biglycan and betaglycan. The released TGF- $\beta$  is fully active and capable of inducing p-SMAD-3 signaling by human coronary artery smooth muscle cells [146].

### 1.10 Other Granzymes

GzmA and the other granzymes are also expressed by immune cells and facilitate Perf-dependent cell death as well as Perf-independent extracellular activities. GzmA has been

extensively studied in the context of cell death, however, little is known regarding the pathways for apoptosis induction of the other granzymes. GzmA, GzmK and GzmM have been implicated in cytokine production and are present extracellularly in bodily fluids [103, 130, 147, 148]. GzmA also cleaves several receptors and extracellular matrix substrates. Our laboratory has also demonstrated an extracellular role for GzmK in inflammation through the cleavage and activation of protease-activated receptor-1 (PAR-1) [149]. An extracellular role for the other granzymes has yet to be established.

Although there are no intracellular GzmA inhibitors identified, there are several extracellular endogenous inhibitors of GzmA, namely  $\alpha$ -2 macroglobulin, antithrombin III and pancreatic secretory trypsin inhibitor (PSTI) [150-152]. When complexed to proteoglycans (PGs), GzmA is resistant to inhibition by macroglobulin and antithrombin III but not by PSTI [150-152]. SERPINB4 has been identified as an intracellular inhibitor of GzmM, and overexpression of the serpin inhibited NK-mediated cell death [153]. GzmM also cleaves PI-9, suggesting it is a regulator of GzmB inhibition [154]. Extracellular GzmK is inhibited by inter-alpha-trypsin inhibitor and free bikunin in the plasma [155]

#### *1.10.1 Granzyme A and the Orphan Granzymes in Cell Death*

Cell death induced by granzyme A is caspase-independent and characterized by single-strand DNA nicking rather than the double-strand nicks created by GzmB [156-158]. GzmA-mediated cleavage results in a loss in the inner membrane potential of the mitochondria as well as the release of reactive oxygen species (ROS) [158]. In contrast to GzmB, no pro-apoptotic mitochondrial proteins such as cytochrome C are released during cell death. GzmA mediates DNA damage through the SET complex, a complex containing the nucleosome assembly protein SET, the tumor suppressor pp32, the DNA bending protein HMG-2, the endonuclease Ape-1 and the DNase NM23-H1 [159]. The normal function of the SET complex remains to be

confirmed, although it is likely to be involved in processes such as regulating chromatin structure, integrity and gene expression [159]. In response to ROS, the SET complex located in the endoplasmic reticulum translocates to the nucleus where GzmA cleaves proteins involved in DNA repair; HMG-2, SET and Ape1 [160-162]. Cleavage of SET also releases the DNase NM23-H1 and allows it to nick DNA [160]. The endonuclease Trex-1 then extends the break [163]. GzmA also targets chromatin through the cleavage of histone H1 and targets the nuclear membrane through cleavage of lamins [164, 165].

Granzyme K induces caspase-independent apoptosis and induces ROS production, suggesting it may act similarly to GzmA [166, 167]. Indeed GzmK induces SET translocation to the nucleus and cleaves SET, Ape1 and HMGB2 [166]. Granzyme C cell death is caspase-independent, causing single-stranded DNA nicks and a loss of mitochondrial membrane potential [168]. Granzyme M induces cell death in a caspase and mitochondrial-independent mechanism involving rapid plasma membrane permeabilization, however a recent study has implicated it in caspase-dependent cell death [169-171]. Granzyme H may be involved in adenoviral defense and also induces caspase-independent cell death [172]. No cellular substrates involved in cell death have been identified for GzmC but substrates for GzmH includes Bid and for GzmM includes ICAD and PARP [173, 174].

#### *1.10.2 Extracellular Activities of Granzymes A, H, K and M*

Although functional extracellular roles for GzmH or GzmM have not been established, GzmA, GzmM and GzmK have been observed in the extracellular milieu. Low concentrations of GzmA and GzmK are found in the serum of healthy individuals. However, in acute inflammation and infection these granzymes are elevated in bodily fluids such as GzmA and GzmK in BAL fluid of the inflamed lung [114, 175], GzmK in the plasma of sepsis patients [147] and GzmA in the SF of RA patients [103]. In addition, GzmM has been found in the

plasma of patients with meningococcal sepsis [148]. As high concentrations of GzmA is required for apoptosis induction, it has been postulated that GzmA may act largely extracellularly. Indeed, GzmA cleaves fibronectin, pro-urokinase plasminogen activator, collagen IV, myelin basic protein and basement membrane proteoglycans. Cleavage of fibronectin has implications in anoikis as proteolysis induces cell detachment and reduces cell-basement membrane interactions [176, 177]. Cleavage of collagen IV also has implications in anoikis and migration as proteolysis results in the disruption of the basement membrane [176, 178]. Degradation of myelin may result in myelin destruction and pro-urokinase plasminogen activator results in alterations in plasmin generation and immune cell migration in clots [179, 180]. GzmA also cleaves receptors including proteinase-activated receptor-2, which may lead to inflammation and infectious colitis [181]. GzmA-mediated cleavage of the thrombin receptor in neuronal cells results in neurite retraction and in platelets GzmA binding of the receptor prevents platelet aggregation [182-184]. GzmM has been implicated in extracellular activity as it has been shown to cleave VWF. Cleavage of VWF did not affect platelet aggregation but did result in an abrogation of factor VIII binding and potentially controlling blood coagulation [148].

### *1.10.3 Granzymes and Inflammation*

Recently a role for GzmA in inflammasome-mediated cytokine activation has been proposed that challenges long-held notions that GzmA is a pro-apoptotic protease [35]. In the latter study, GzmA was shown to activate IL-1 $\beta$  by cleavage of its propeptide, into the active 17 kDa form [185]. Furthermore, in this study it was suggested that previous work showing GzmA involvement in the induction of cell death is not physiologically relevant as it only occurs when cells are exposed to high levels of Perf that are not found *in vivo*. As such, although still under debate, it is now widely viewed that the primary role for GzmA is actually in the promotion of inflammation and plays a minimal role in cell death [106]. GzmA also activates monocytes,

fibroblasts and epithelial cells to secrete the cytokines IL-1 $\beta$ , IL-6, IL-8 and TNF- $\alpha$  [186-188]. Further studies are required to determine the mechanism of cytokine production, but cleavage of a cell surface receptor may facilitate the process [189]. However, the process does not occur through cleavage of the thrombin receptor, as is the case with thrombin [187, 189]. Additionally, intracellular mechanisms have also been proposed as cytokine production is elevated after internal delivery of GzmA [188]. Production of IL-1 $\beta$ , TNF- $\alpha$  and IL-6 by a monocyte cell line was almost completely abolished with a pan-caspase inhibitor, and production of these cytokines was determined to be in part caspase-1-dependent [188].

Cooper *et al* (2011) showed that GzmK activates the protease activated receptor-1 (PAR-1) on fibroblasts through an extracellular, Perf-independent mechanism, inducing the secretion of IL-6, IL-8 and MCP-1, which may promote inflammation [149]. GzmK also induces fibroblast proliferation through the activation of Erk-1/2 and p38 MAPK [149]. Alternatively, Joeckel *et al* [190] have also shown that GzmK induces IL-1 $\beta$  production from macrophages, at low concentrations with the Perf analog streptolysin O and at high concentrations (600nM-1000nM) without the lytic component .

In addition, a proinflammatory role for GzmM in Toll-like receptor-4/ lipopolysaccharide (LPS) signalling has been forwarded [191]. GzmM-deficiency results in reduced IL-1 $\alpha$ , IL-1 $\beta$ , TNF- $\alpha$  and IFN $\gamma$  levels in the serum of knockout mice post LPS injection. GzmM produced by NK cells is responsible for augmenting the inflammatory cascade induced by TLR4 signaling, resulting in lethal endotoxemia. However, GzmM was not responsible for directly processing the cytokines such as carried out by caspase-1 and was determined to be downstream temporally of caspase-1. These reductions in cytokines also occurred in GrA-deficient mice, but not GzmB knockout mice and mice deficient in GzmM and GzmA were more resistant to LPS than mice lacking just one of the proteases.

In summary, while the past two and a half decades have focused almost exclusively on attempting to delineate the pro-apoptotic roles of granzymes A, H, K and M, it is becoming clear that these proteases may not be involved in cell death under physiological conditions and that roles in inflammation may be their primary function. However, further research is still required to confirm this new paradigm.

### *1.11 GzmB in Disease*

GzmB can cleave both intracellular and extracellular substrates. Recently, with the discovery of new immune cell and non-immune cell sources of the protease, its importance in normal bodily processes, infection and cancer is evolving and its contribution to other chronic diseases is emerging. The extracellular role of GzmB is further supported by the fact that immune cells such as mast cells and basophils express GzmB but do not express Perforin which is necessary for internalization [10, 107]. Infiltrating immune cells during chronic inflammation results in elevated levels of GzmB to diseased tissue and induces apoptosis in damaged and inflamed areas. Extracellular concentrations of GzmB in bodily fluids are elevated in various diseases and the extracellular activity of this protease in chronic inflammation is an emerging area of research. Extracellular levels of GzmB are elevated in the bodily fluids in chronic inflammatory diseases such as atherosclerosis [133], chronic obstructive pulmonary disease (COPD) [131] and rheumatoid arthritis (RA) [192]. As further direct support for an extracellular role for GzmB in disease, GzmB contributes to murine abdominal aortic aneurysm (AAA) pathogenesis through the cleavage of ECM proteins [193, 194]. In the skin of aging mice, GzmB deficiency attenuated collagen disorganization, reduction of thick collagen bundles and skin thinning by preventing decorin cleavage [195]. An overview of the activity of GzmB in disease is provided in Table 3. The remainder of this chapter will focus on the role of GzmB in cardiovascular, skin and neurological diseases.

**Table 3: GzmB in Disease**

Condition	Intracellular vs. Extracellular	Description	References
<b>Lung Diseases</b>			
Chronic Obstructive Pulmonary Disease (COPD)	Intracellular/ extracellular	Increased CTL's and NK cells expressing GzmB in the blood and BAL of patients with COPD. Type II pneumocytes and alveolar macrophages in the lung express GzmB. Increased Perf expression by CD8+ cells in the lung of smoking subjects with COPD. CD8/CD28(null) cells are increased in COPD and express GzmB upon stimulation.	[17, 131, 196, 197]
Asthma	Intracellular/ extracellular	Increase in lymphocytes expressing GzmB in the BAL fluid of patients suffering from allergic asthma following allergen challenge. Induction of GzmB expression by basophils upon stimulation with IL-3 released by mast cells. Of note, mast cells and basophils only express GzmB and do not express Perf. This would support an extracellular role for GzmB.	[10, 115]
Acute Respiratory Distress Syndrome (ARDS)	Intracellular/ extracellular	GzmB and Perf mRNA is up regulated in the BAL of patients in the acute phase of ARDS.	[198]
Pulmonary Sarcoidosis	Intracellular/ extracellular	GzmB and Perf is expressed by CD8+ and some CD4+ T cells in the BAL fluid. Serum levels of GzmB are decreased in patients with sarcoidosis.	[199, 200]
Hypersensitivity Pneumonitis	Extracellular	GzmB is increased in the BAL fluid of patients with hypersensitivity pneumonitis	[114]
<b>Oral</b>			
Chronic Obstructive Sialadenitis / Sialolithiasis	Intracellular(?)	GzmB is expressed by periductal and periacinar lymphocytes in patients with chronic sialadenitis.	[201]
Papillon-Lefèvre Syndrome (PLS)		NK cells in patients with PLS fail to induce the caspase cascade in target cells due to an inactive form of GzmB as a result of a mutation in cathepsin C.  Reduced active GzmB in cytotoxic cells in patients with PLS compared to controls.	[202, 203]
Oral lichen planus		GzmB expression is higher in oral lesions than in cutaneous lichen planus. Apoptotic keratinocytes are also evident.	[204]
<b>Blood Disorders</b>			
Aplastic Anemia	Intracellular/ extracellular	No difference in GzmB expressing cytotoxic effector cells in disease patients compared to controls.  Increase in Perf but no increase in GzmB in bone marrow clot sections of disease patients compared to controls.	[205, 206]
Idiopathic Neutropenia		No difference in GzmB expressing CD16+ cells in the blood between patients with chronic idiopathic neutropenia.	[207]

Condition	Intracellular vs. Extracellular	Description	References
Chronic Idiopathic Thrombocytopenic Purpura (ITP)	Intracellular(?)	Increased GzmB expressing T cells in the blood of patients with ITP compared to controls.  Increased GzmB mRNA levels in CD8+ cells in patients with ITP compared to controls.	[208-210]
<b>Skin Diseases</b>			
Alopecia	Intracellular	GzmB expressing CTLs are closely associated with hair follicles and may damage follicles. Substance P increases CD8+ T cells expressing GzmB which may cause hair follicle regression	[211-213]
UV Light Photoaging	Intracellular/ Extracellular	GzmB is expressed by keratinocytes in response to confluency, UVA light and UVB light. UVB light-treated keratinocytes have cytotoxic potential against co-cultured cells and GzmB from UVA light-treated keratinocytes can cleave fibronectin.	[15, 140, 214]
Acne		GzmB is up regulated in acne lesions	[215]
Atopic Dermatitis/ Allergic Contact Dermatitis	Intracellular	GzmB expressing CD4+ and CD8+ T cells are observed in the perivascular infiltrate and focally at spongiosis sites. In contact dermatitis keratinocytes neighboring GzmB expressing cells are damaged	[216-219]
Vitiligo	Intracellular	GzmB expressing CTLs cluster around disappearing melanocytes and may induce apoptosis in these cells	[220, 221]
Lichen Planus	Intracellular	GzmB expressing cells are found in close proximity to apoptotic keratinocytes. DCs expressing GzmB are found in lesions	[217, 222-226]
Lichen Sclerosus		GzmB is expressed in dermal infiltrate close to keratinocytes. Vasculitis associated with the disease contains GzmB-positive cells in the perivascular infiltrate	[227-229]
Stevens-Johnson Syndrome/Toxic Epidermal Necrolysis	Intracellular/ Extracellular	CTLs expressing GzmB may induce apoptosis in keratinocytes. GzmB-positive lymphocytes in blister fluid. GzmB upregulation correlated to disease severity. GzmB expression around microvessels. High GzmB corresponds to a high co-efficient of disease .	[230-235]
Pityriasis Rosea		GzmB is expressed by immune cells in pityriasis rosea lesions	[216]
Psoriasis		GzmB is expressed by some lymphocytes in psoriasis lesions	[218, 219]
Bullous Blistering Skin Lesions		GzmB is expressed in bullous lesions by T cells	[236]
Discoid Lupus Erythematosus		GzmB is expressed on lesional lymphocytes expressing the skin homing proteins CLA and MxA. GzmB-positive cells are perivascular and located in the dermal-epidermal junction	[217, 237]
Pemphigus Vulgaris (PV)		Decreased ex vivo expression of GzmB by circulating NK cells in patients with PV compared to controls.	[238]
Skin Aging and Xanthomatosis	Extracellular	GzmB/apoE-DKO mice are protected from skin thinning, xanthomatosis, decorin degradation, and a decrease in collagen density	[195]



Condition	Intracellular vs. Extracellular	Description	References
<b>Bones and Joints</b>			
Rheumatoid Arthritis (RA)	Extracellular/ Intracellular	GzmB cleaves aggrecan and other cartilage components. Levels of GzmB are markedly elevated in the synovial fluid and plasma of patients. All GzmB-expressing cell types may also contribute to RA through GzmB-mediated apoptosis, including chondrocytes which display the surface antigens of NK cells. NK-22 cells express GzmB and Perforin in the synovial fluid	[8, 12, 14, 103-105, 118, 135-138, 192, 239-241]
Juvenile Idiopathic Arthritis		Increase in GzmB in duodenal and ileal mucosal cytotoxic lymphocytes	[242]
Osteoarthritis		mRNA and protein expression of GzmB in the synovium of joints	[136]
Reactive Arthritis	Extracellular	GzmB expressed in the synovial tissue	[243]
<b>Neurological Disorders</b>			
Rasmussen's Encephalitis (RE)	Intracellular/ Extracellular/ Autoimmunity	GzmB-expressing CTLs described in RE brains. GzmB from CTLs is polarized towards neurons and astrocytes that express MHC I. Extracellular GzmB levels in cerebrospinal fluid (CSF) are elevated. GzmB cleaves the GLUR-3 receptor yielding an autoantigenic fragment.	[113, 121, 244-247]
Multiple Sclerosis (MS)	Intracellular/ Extracellular	CTLs are involved in neuronal toxicity and T <sub>H</sub> 17 cells, which cross the blood brain barrier, express GzmB and can kill neurons <i>in vitro</i> . Increase in extracellular GzmB levels in the CSF in relapsing remitting MS. Purified GzmB induces neuron cell death, potentially Perforin-independently. GzmB cleaves transaldolase causing a loss of enzymatic activity but retention of antigenicity	[112, 248-252]
Amyotrophic Lateral Sclerosis (ALS)		GzmB is present in the serum of patients and corresponds to disease severity	[253]
Guillain Barre Syndrome	Intracellular	GzmB-expressing CTLs are increased and MHC I expressing Schwann cells may be GzmB targets. Implications in myelin sheath damage	[254]
Vasculitic Neuropathy		GzmB is expressed in the peri-vascular infiltrate.	[255]
Sensory Perineuritis	Intracellular	GzmB-expressing CTLs contribute to perineurial cell apoptosis	[256]
Ischemic Stroke	Intracellular	GzmB from CTLs and NK cells induce apoptosis of brain cells	[257]
Spinal Cord Injury	Intracellular	GzmB levels elevated and CTLs in close proximity to neurons in regions of damage	[258]
Myasthenia Gravis	Extracellular/ Autoantigen	GzmB cleaves the autoantigen AChR. GzmB is present in Myasthenia Gravis thymus glands but absent in controls	[122]
Autoimmune Encephalomyelitis		Activated interferon-producing killer DCs express GzmB	[259]
Stroke	Intracellular	Human stroke tissues contained higher levels of GzmB. GzmB co-localized to TUNEL in degenerating neurons. GzmB inhibition prevented neurotoxicity <i>in vitro</i>	[260]

Condition	Intracellular vs. Extracellular	Description	References
<b>Autoimmune Disease</b>			
Systemic Lupus Erythematosus (SLE)	Intracellular/ Extracellular/ Autoimmunity	Frequency of GzmB expressing CTLs coincides with disease progression. GzmB is involved in autoantigen processing of XRCC4 and other potential SLE autoantigens. CD4+GzmB+ cells correspond to disease activity. Increased soluble GzmB was found in the serum of SLE patients.	[261-267]
Neonatal Lupus Erythematosus		GzmB expression in the left ventricle of hearts from fetuses/infants with complete atioventricular block	[268]
Scleroderma (SSc)	Autoimmunity/ Extracellular	GzmB cleaves the autoantigens topoisomerase I, NOR-90, fibrillarin, B23 and others. SSc patients with ischemic digital loss have autoantibodies for CENP-C, which may be useful as biomarkers for IDL. The GzmB cleavage product angiostatin inhibits angiogenesis and may be responsible for the poor circulation in SSc	[120, 261, 269, 270]
Sjögren Syndrome (SS)	Intracellular/ Autoimmunity	GzmB cleaves the autoantigens SS-B (La) autoantigen, $\alpha$ -fodrin, $\beta$ -fodrin, type 3 muscarinic acetylcholine receptor and others. CD4+ and CD8+ T cells induce apoptosis of epithelial cells through the granule pathway and these cells are only present in SS glands.	[261, 271-278]
Myositis	Intracellular/ Autoimmunity	GzmB cleaves autoantigens such as PMS-1 and HisRS. GzmB expressing cells are found in the endomysial sites of polymyositis and are proposed to cause muscle cell damage.	[261, 279-282]
Type 1 Diabetes	Intracellular	Human and mouse $\beta$ cells undergo apoptosis in the presence of GzmB, which correlates with a loss in islet insulin secretion capacity. Bid deficient islets are protected from GzmB-mediated killing. Autoreactive CTLs in islets of NOD mice expressed higher levels of GzmB and Perf than those from the pancreatic lymph node.	[283-285]
Wiskott-Aldrich Syndrome	Intracellular	WAS-KO T-regulatory cells do not suppress B cell proliferation, have reduced capacity to kill B cells and have reduced degranulation of GzmB	[286]
<b>Bile/Liver/Intestinal Diseases</b>			
Lymphocytic Gastritis (LG)	Intracellular(?)	Intraepithelial CD8+ cells from LG children with celiac disease lack GzmB.  Increase in GzmB expressing intraepithelial lymphocytes in patients with acute gastric mucosal lesions compared to controls.  Increased GzmB expressing intraepithelial lymphocytes in patients with non-celiac disease associated LG compared to patients with celiac disease associated LG.	[287-289]
Autoimmune Cholangitis (AC) and Primary Biliary Cirrhosis (PBC)		GzmB expressing T cells found in the bile duct epithelium. No difference in the number of GzmB expressing lymphocytes between patients with AC versus PBC. Effector memory T cells express more GzmB than other CD8+(high) cells	[290, 291]

Condition	Intracellular vs. Extracellular	Description	References
Nodular Regenerative Hyperplasia (NRH)		Increased CD8+ lymphocytes expressing GzmB in liver biopsy samples from patients with NRH compared to controls.	[292]
Inflammatory Bowel Disease		Increased GzmB expressing intraepithelial lymphocytes in patients with Crohn's disease and ulcerative colitis.	[293]
<b>Vascular Diseases</b>			
Atherosclerosis	Extracellular/ Intracellular	<p>GzmB levels increase with increased disease severity. Present in high levels in advanced atherosclerotic and TVD plaques. Elevated in lipid-rich regions. Activated caspase 3 in SMC corresponded to decreased PI-9 expression and the presence of GzmB suggesting SMC are susceptible to GzmB-mediated apoptosis in atherosclerosis</p> <p>Gzm in the blood is significantly higher in patients with unstable atherosclerotic plaques. The study also demonstrated that raised plasma levels of Gzm in unstable carotid plaques were associated with an increased frequency of cerebrovascular events (ie. Strokes) suggesting that GzmB may be a marker of plaque instability.</p> <p>GzmB expressed in macrophages in atherosclerotic plaques</p> <p>Perf deficiency in LDLR-KO mice does not affect atherosclerosis. Supports role for extracellular GzmB or its role in late-stage/advanced atherosclerosis</p> <p>GzmB in absence of Perf can induce smooth muscle cell apoptosis via the cleavage of extracellular matrix proteins. Fibronectin identified as a substrate.</p> <p>GzmB production from PBMCs of unstable angina pectoris (UAP) patients was significantly higher than patients with stable angina (SAP). GzmB production from PBMCs increased with the increasing TIMI risk score in UAP patients. The percentage of GzmB-positive lymphocytes to CD3-positive lymphocytes in UAP patients was significantly higher than in SAP</p>	[8, 16, 124, 132, 133, 294-297]
Acute transplant rejection	Intracellular	GzmB-mediated apoptosis that occurs during the recruitment of inflammatory cells following the non-specific injury to graft vessels. GzmB can contribute to lesion formation through processes that include GzmB-mediated apoptosis, and the promotion of EC activation and SMC migration.	[298-306]
Allograft Vasculopathy	Intracellular	GzmB/perf pathway involved in allograft vasculopathy-a form of accelerated arteriosclerosis associated with transplanted organs and leading cause of organ failure. Increased GzmB associated with increased disease severity	[16, 307, 308]
Kawasaki disease	Extracellular	Children with Kawasaki's exhibit elevated vascular inflammation and often die from fatal aortic dissections or aneurysms. Elevated levels of GzmB observed in lesions, aneurysms and plasma of Kawasaki's patients, however its involvement of GzmB disease pathogenesis requires further elucidation.	[309-311]

Condition	Intracellular vs. Extracellular	Description	References
Abdominal Aortic Aneurysm	Extracellular	GzmB is expressed in human and mouse aneurysm tissue. GzmB/apoE-DKO mice are protected from AAA incidence and rupture whereas Perf/apoE-DKO develop AAA and have a similar rate of rupture as apoE-KO mice. A GzmB-dependent reduction in medial fibrillin-1 levels is evident in AAA tissues and corresponds to medial elastic lamella breakage. Infusion with the extracellular GzmB inhibitor Serpina3n protects against AAA rupture. Serpina3n mice had more adventitial decorin and higher collagen density than apoE-KO controls	[193, 194]
<b>Kidney diseases</b>			
Crescentic Glomerulonephritis (CG)	Intracellular	Perf neutralizing antibody protects against the progression of CG in rats.	[312]
Goodpasture's Disease (GD)		Glomerular GzmB expression and GD pathogenesis is reduced upon administration of anti-CD8+ antibody.	[313]
Chronic Kidney Disease		Plasma GzmB levels are higher in patients with coronary artery disease and may be a risk factor	[314]
<b>Esophagus</b>			
Achalasia		The inflammatory infiltrate found in the myenteric plexus contains cytotoxic T cells, some of which express GzmB.	[315]
Esophagitis		Significant increase in GzmB expressing intraepithelial lymphocytes in biopsy specimens from patients with esophagitis compared to controls.	[316]
Crohn's Disease		Increase in GzmB expressing cells in esophagus biopsy specimens taken from patients with CD compared to controls.	[317]
<b>Other</b>			
Eosinophilic Fasciitis		The inflammatory infiltrate in eosinophilic fasciitis contains some CD8+ cells expressing GzmB suggesting a cytotoxic immune response.	[318]
Cryptorchidism		Lymphocytes expressing GzmB are decreased in the testis of patients with cryptorchidism.	[319]
Histiocytic Necrotizing Lymphadenitis (HNL) / Kikuchi Disease	Intracellular/ apoptotic necrosis	GzmB expressing cells found in necrotizing lesions of patients with Kikuchi disease.  The majority of lymphocytes found in the necrotic foci in HNL are GzmB expressing CD8+ cells.	[320, 321]
Chediak-Higashi Syndrome		CTL granules are unable to release their contents upon recognition of a T cell receptor, express normal levels of GzmB.	[322]
Duchenne Muscular Dystrophy (DMD)/ Facioscapulo-humeral Dystrophy (FSHD)	Intracellular	GzmB expression detected in muscle biopsy specimens from patients with DMD and FSHD but absent in control samples.	[323]
Atypical Allergic Rhinitis	Intracellular	Granzyme release from CTLs upon antigen exposure	[324]

Condition	Intracellular vs. Extracellular	Description	References
Histiocytic Necrotizing Lymphadenitis		GzmB expression in lymphocytes in apoptotic areas and in histiocytes	[325]

## 1.12 Cardiovascular Disease

### 1.12.1 Atherosclerosis

Atherosclerosis is an inflammatory disease characterized by lipid accumulation, cell migration, proliferation and apoptosis as well as ECM accumulation and degradation [326, 327]. Atherosclerosis is a major predecessor to myocardial infarction, stroke and lower limb loss [328]. This pathologic condition is characterized by the accumulation of macrophage and SMC derived foam cells, which accumulate in the neo-intimal layer of the vessel. CTLs, macrophages, NK cells, mast cells, dendritic cells and neutrophils are present in plaques [329-333] and CTL's, NK cells, macrophages and SMCs have been shown to express GzmB in lesions [8, 16].

The role of GzmB in atherosclerosis progression is proposed in figure 3. In human atherosclerotic tissues, GzmB expression is associated with increased disease severity and cell death. GzmB was not present in vessels with mild atherosclerosis but was in abundance in the intima and adventitia of vessels with advanced disease [16]. GzmB also localized to TUNEL positive cells, suggesting it was responsible for inducing target cell death in atherosclerosis [16]. The endogenous inhibitor PI-9 is decreased in smooth muscle cells in unstable plaques compared to stable plaques, suggesting SMC may be more susceptible to apoptosis in unstable plaques [61]. In the SMC of advanced plaques, there was increased activated caspase-3 in areas of reduced PI-9 expression [297]. GzmB also colocalized to these areas suggesting SMC are susceptible to GzmB-mediated cell death in advanced atherosclerosis [297]. However, compared to low density lipoprotein (LDL) receptor knockout mice (LDLr-KO), Perf/LDLr double

knockout mice were not protected from atherosclerosis, suggesting that removal of the intracellular pro-apoptotic GzmB pathway does not affect atherosclerosis in this model [294].

Extracellular GzmB activity may also play a role in atherosclerosis. GzmB was found in the shoulder regions of atherosclerotic plaques and has been linked to plaque instability [16]. High plasma GzmB levels were linked to unstable versus stable carotid lesions and an increased incidence of cerebrovascular events. As such, plasma GzmB was suggested to be a potential plasma marker for plaque instability. Plasma levels of GzmB are elevated in patients with carotid atherosclerosis compared to healthy controls. Levels were highest in patients with echolucent plaque (plaques with a thin rupture-prone fibrous cap, Table 2) [133]. GzmB levels in plasma are also increased after acute myocardial infarction (AMI), peaking at 7 days post infarct suggesting GzmB may play a role in left ventricle remodelling after AMI [132].

Choy *et al* showed that GzmB could induce SMC apoptosis in the absence of Perf through the loss of cell matrix contact, a process known as anoikis [124]. Along these lines, GzmB may contribute to plaque instability through degradation of ECM in the cap region, induction of apoptosis in the fibrous cap and/or release or activation of cytokines. Through these extracellular activities combined with immune-mediated apoptosis, GzmB may contribute to the formation of a necrotic core, thinning of the fibrous cap and ultimately plaque rupture.

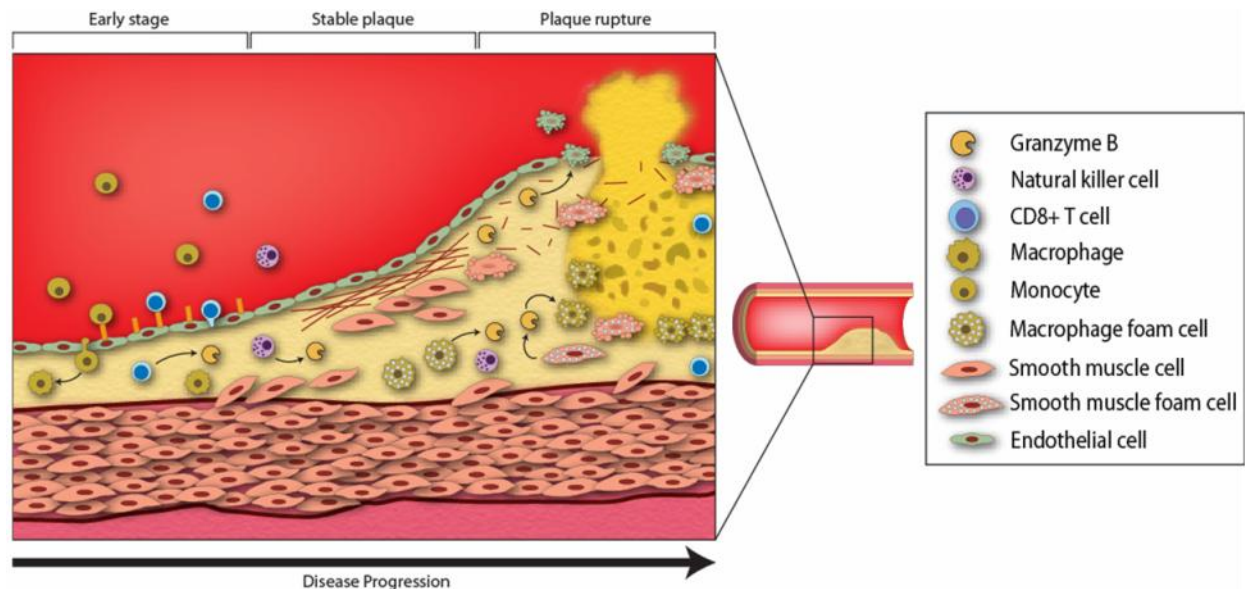


**Figure 3: The Role of GzmB in Atherosclerosis**

At the early stages of atherosclerosis, following endothelial dysfunction and intimal lipid retention, CTLs and monocytes infiltrate the vessel wall and migrate into the intima. SMC and macrophages engulf oxidized lipoproteins and become lipid-laden foam cells, leading to GzmB expression in these cells. The latter may promote foam cell apoptosis in developing plaques. GzmB can also cleave various extracellular matrix proteins that maintain fibrotic cap stability. In addition to a loss in matrix integrity, ECM cleavage will also result in a loss of SMC-ECM interactions which may promote apoptosis. SMC expression of PI-9 is decreased in unstable plaques, rendering SMCs susceptible to GzmB-dependent apoptosis and further promoting plaque instability and rupture. Reproduced with permission from *Laboratory Investigation* [58].

### *1.12.2 Abdominal Aortic Aneurysm*

An aneurysm is a permanent focal dilation of an artery that results in weakening of the artery wall and vessel dilation, which can ultimately lead to medial rupture of the vessel (Figure 4). Elastin and collagen degradation along with flow changes lead to a progressive weakening of the wall. There is extensive remodelling in the luminal expansion phase and the appearance of the thrombus which subsequently progresses into fibrotic tissue. A general loss of ECM, neovascularization and protease accumulation, growth factors and immune cells such as macrophages and mast cells are hallmarks of aneurysm pathogenesis (reviewed in [334]). GzmB is present in murine and human AAA particularly in mast cells and macrophages in the media and adventitia of aneurysms as well as lymphocytes in the thrombus [193]. In the mouse model of AAA, angiotensin II infusion is used to induce aneurysm formation in apolipoprotein E mice. GzmB/apoE-DKO mice were examined. The rate of rupture of GzmB/apoE-DKO mice was only 7.1% compared to 46.7% for apoE-KO mice [193]. Perf deficiency had no protective effect on rupture, suggesting the mechanism behind GzmB pathogenesis is peforin-independent and extracellular. When mice were infused with serpin3n, an extracellular GzmB inhibitor, there was a reduction in rupture and death, implicating extracellular GzmB activity in AAA progression [194]. Medial fibrillin-1 levels were reduced in apoE-KO mice compared to controls, and GzmB/apoE-DKO mice were protected from the loss in fibrillin-1 [193]. Fibrillin-1 fragments were also found in the serum of apoE-KO mice but not GzmB/apoE-DKO mice. Medial disruption was evident in apoE-KO mice and prevented in GzmB/apoE-DKO mice suggesting cleavage of fibrillin-1 may play a role in vessel stability as further described in subsequent chapters. A loss in adventitial decorin was apparent in apoE-KO mice but not in GzmB/apoE-DKO mice or mice infused with the extracellular GzmB inhibitor, serpin3n [194]. Collagen density was increased in mice receiving the inhibitor compared to apoE-KO without



serpina3n infusion, suggesting GzmB cleavage of decorin may play a role in collagen density and spacing.

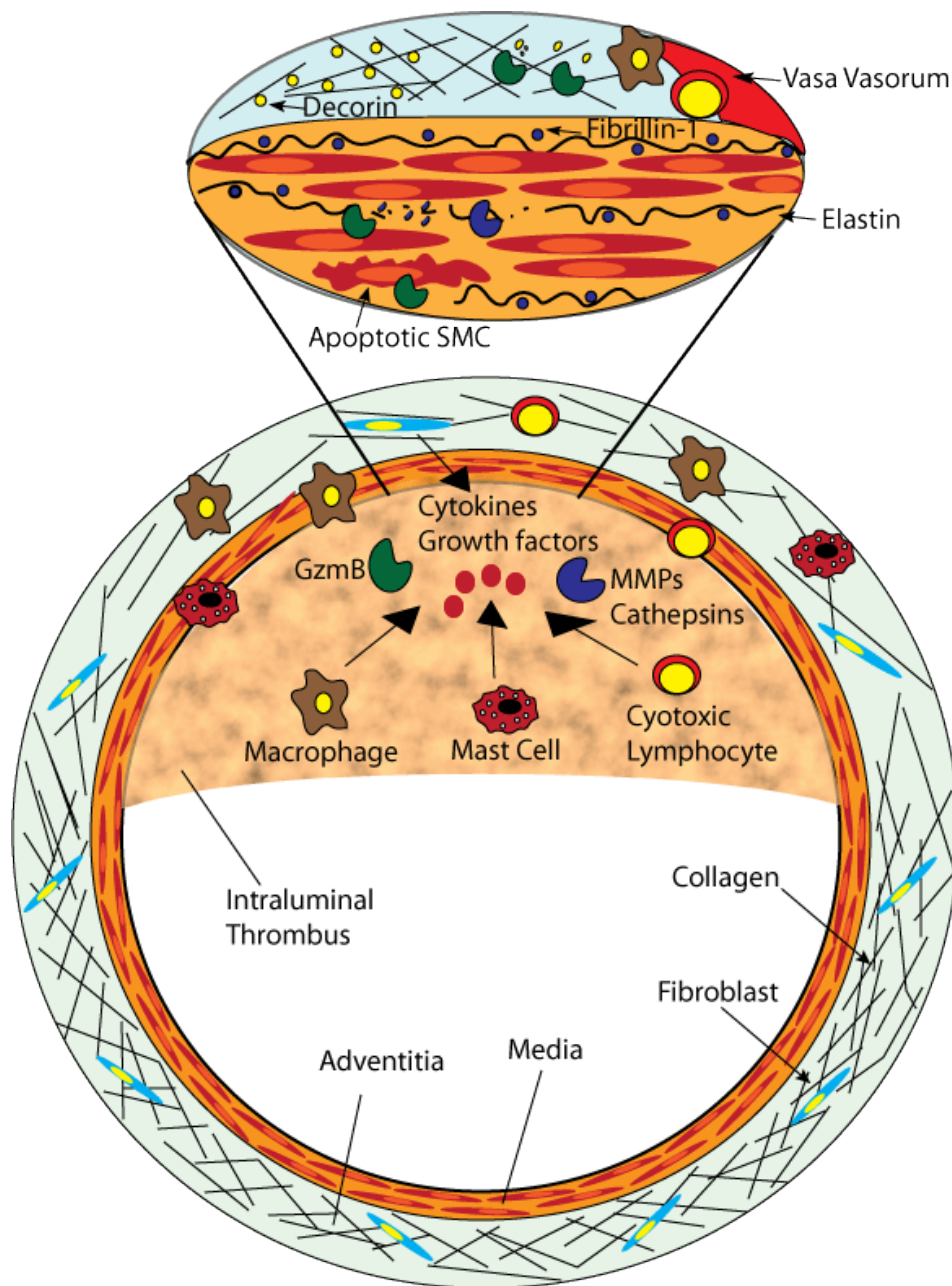


**Figure 4: GzmB in Abdominal Aortic Aneurysm**

Macrophages, mast cells and cytotoxic lymphocytes enter the adventitia through the vasa vasorum and also accumulate in the intraluminal thrombus and media. They secrete cytokines, growth factors and proteases such as GzmB, MMPs and cathepsins. Fibroblasts also secrete cytokines such as VEGF and MCP-1. GzmB cleaves fibrillin-1, a scaffolding protein key in elastin fibre integrity and cleavage is linked to medial instability. GzmB also cleaves decorin, a protein involved in collagen fibrillogenesis and spacing, resulting in decreased collagen density and tensile strength thereby rendering the vessel prone to dilatation and possibly rupture. GzmB can also induce SMC apoptosis either intracellularly or extracellularly by anoikis through the cleavage of ECM.

### 1.12.3 Cardiac Allograft Vasculopathy

GzmB has been implicated in cardiac allograft vasculopathy (CAV), an accelerated immune-mediated arteriosclerotic disease, resulting in the occlusion of the vasculature of transplanted cardiac allografts. Elevated GzmB is linked to increased CAV disease severity and GzmB has been localized to macrophage and SMC foam cells in the neo-intima as well as CTLs and extracellularly in the media and adventitia of allograft lesions [16]. GzmB localization corresponds to TUNEL positive cells in the intima, suggesting it plays a role in apoptosis [16]. GzmB mRNA was apparent in infiltrating leukocytes but not in foam cells. The role of GzmB and Perf in CAV has been further characterized in a mouse heterotopic heart transplant model where hearts transplanted into GzmB-KO [307] or Perf-KO [308] mice displayed a reduction in luminal narrowing and endothelial cell apoptosis compared to wildtype hearts. There was a similar amount of immune cell infiltration and vasculitis in hearts transplanted into GzmB-KO and Perf-KO mice compared to wildtype hearts suggesting differences in luminal narrowing was not due to inflammatory infiltrate. There was strong Perf expression in the vasculature and myocardium of transplanted hearts. Perf-KO mice were protected from endothelial disruption and cell death as indicated by TUNEL positivity compared to wildtype hearts, suggesting that GzmB-mediated endothelial cell apoptosis is key in CAV.

## 1.13 Skin Disorders

### 1.13.1 GzmB Expression in the Skin

The role of GzmB in dermatological conditions is emerging and the contribution of GzmB to skin aging, alopecia and other dermatological diseases is illustrated in Figure 5. There are several potential sources of GzmB in the skin, namely CLs, DCs, macrophages, mast cells, and keratinocytes [107, 214]. Keratinocytes expressed GzmB *in vitro* after treatment with UVA light, UVB light and at high cell density [15, 140, 214]. Interestingly, UVB light and cell

confluency induce both GzmB and Perf expression, where as GzmB is expressed without Perf in response to UVA light. UVA light also induces GzmB expression in human skin *in vivo* [140]. In the latter study, UVA light treatment of cultured keratinocytes caused a ROS-dependent release of macrophage migration inhibitor factor (MIF) and MIF induced GzmB expression by keratinocytes. GzmB expression was p38 mitogen activated protein kinase (MAPK)-dependent and resulted in the phosphorylation of its subsequent substrate MAPKAPK2. During UVB light treatment, ROS production results in signaling through EGFR, MAPK activation and subsequent MAPKAPK-2 phosphorylation [15]. It should be noted that it is unclear as to whether these pathways are involved in the induction of GzmB expression in other cell types.

As keratinocytes cannot form an immunological synapse with target cells, it is likely that GzmB expression in this cell type mediates its effects extracellularly. Indeed, GzmB from UVA light-irradiated keratinocytes degraded fibronectin *in vitro* and keratinocyte-derived GzmB may play a role in degrading ECM in photoaging. UVA light induces keratinocyte cell detachment and cell death and treatment with an antisense oligonucleotide against GzmB prevents these processes. The antisense also induced migration through fibronectin and vitronectin matrices, and GzmB induced factors inhibitory in migration [140].

GzmB is also expressed by mast cells in mouse skin *in vivo*, as well as in cultured skin mast cells after IgE treatment [7, 107]. Mast cells do not express Perf and GzmB that is released extracellularly from these cells induces fibroblast anoikis suggesting that it plays a role in ECM degradation in the skin. No follow up studies have been published describing GzmB from mast cells or keratinocytes contributing to skin diseases *in vivo* and the majority of dermatological studies to date exclusively examine CTLs as the lone source of GzmB in the skin. As mast cells do not express Perf and keratinocytes express GzmB (but not Perf) in response to stimuli such as UVA light, there is clearly a potential extracellular, Perf-independent capacity for GzmB in the

skin. As the skin contains a high proportion of ECM such as collagen, elastin and ground substance, future studies will be useful in further examining the extracellular activity of GzmB and its role in disease.

Our laboratory has shown using the apoE accelerated aging model that GzmB/apoE-DKO mice are protected against the xanthomatosis, skin thinning, loss of dermal collagen density and ECM degradation characteristic of apoE-KO mice [195]. The protection is through an extracellular means, through the inhibition of cleavage of extracellular matrix, decorin in particular. The skin is an ideal organ to study the process of aging due to its abundance of extracellular matrix and ease in accessibility and is ideal for studying fraility in the elderly who are more prone to skin tearing and skin ulcers.

#### *1.13.2 Other Skin Disorders*

GzmB has been linked to other skin conditions such as acne [215], vitiligo [221], atopic dermatitis [216], allergic contact dermatitis [216, 218], pityriasis rosea [216], lichen planus [224], lichen sclerosis [227], Stevens-Johnson syndrome (SJS) [230] and toxic epidermal necrolysis (TEN) [230, 231]. GzmB expression in most of these diseases was found to be localized to CTLs and GzmB-specific disease implications were almost exclusively thought to be through intracellular CTL-mediated apoptosis of keratinocytes and other resident cell types. As more cellular sources of GzmB have been identified as of late and the emerging role of extracellular activity gains traction, determining other GzmB sources and examining the importance of extracellular GzmB activity will be a necessity in dermatological research involving GzmB.

SJS and TEN are rare and potentially life threatening diseases involving keratinocyte apoptosis and epidermal necrosis, which are largely thought to be drug induced [231]. GzmB-positive peripheral blood mononuclear cells are found in blister fluid and GzmB upregulation

correlates to increased disease severity [233]. T cells in lesions express Perf and GzmB and it has been suggested that T cells may trigger keratinocyte cell death in these skin conditions [230-234]. In addition, GzmB positive cells were shown surrounding the superficial dermal vessels in SJS/TEN as an indicator of disease [335].

### *1.13.3 Hair Loss - Alopecia Areata*

Hair loss or alopecia occurs when follicles remain in the resting telogen phase longer than normal. Alopecia areata (AA) is an inflammatory condition that results in non-scarring patchy hair loss. Perifollicular and intrafollicular CTLs have been implicated in AA suggesting there is an immune cell attack on the normally immune privileged hair follicle during the growth phase (anagen) of the hair cycle [336, 337]. GzmB-expressing cytotoxic cells were found closely associated with human hair follicles in chronic AA patients, suggesting GzmB may contribute to CTL-mediated follicular damage [211]. However, in a contradictory study, Sato-Kawamura *et al* did not detect GzmB-positive cells around follicles in lesions of AA [213]. In a C3H/HeJ mouse model of AA, GzmB expression was described in immune cells in the intrafollicular dermis, although few of these cells expressed CD8 [212]. Interestingly, supplying the neuropeptide substance P to the skin of AA-affected mice led to an increase in CD8<sup>+</sup> cells expressing GzmB, possibly leading to an increase in cytotoxicity in the skin. Substance P also resulted in regression of hair follicles out of the growth phase into catagen suggesting this could be related to a substance P-dependent increase in CD8<sup>+</sup> GzmB expressing cells [212]. Although more studies are required to define the mechanism by which GzmB contributes to AA, there is indeed an association between the disease and GzmB expression.

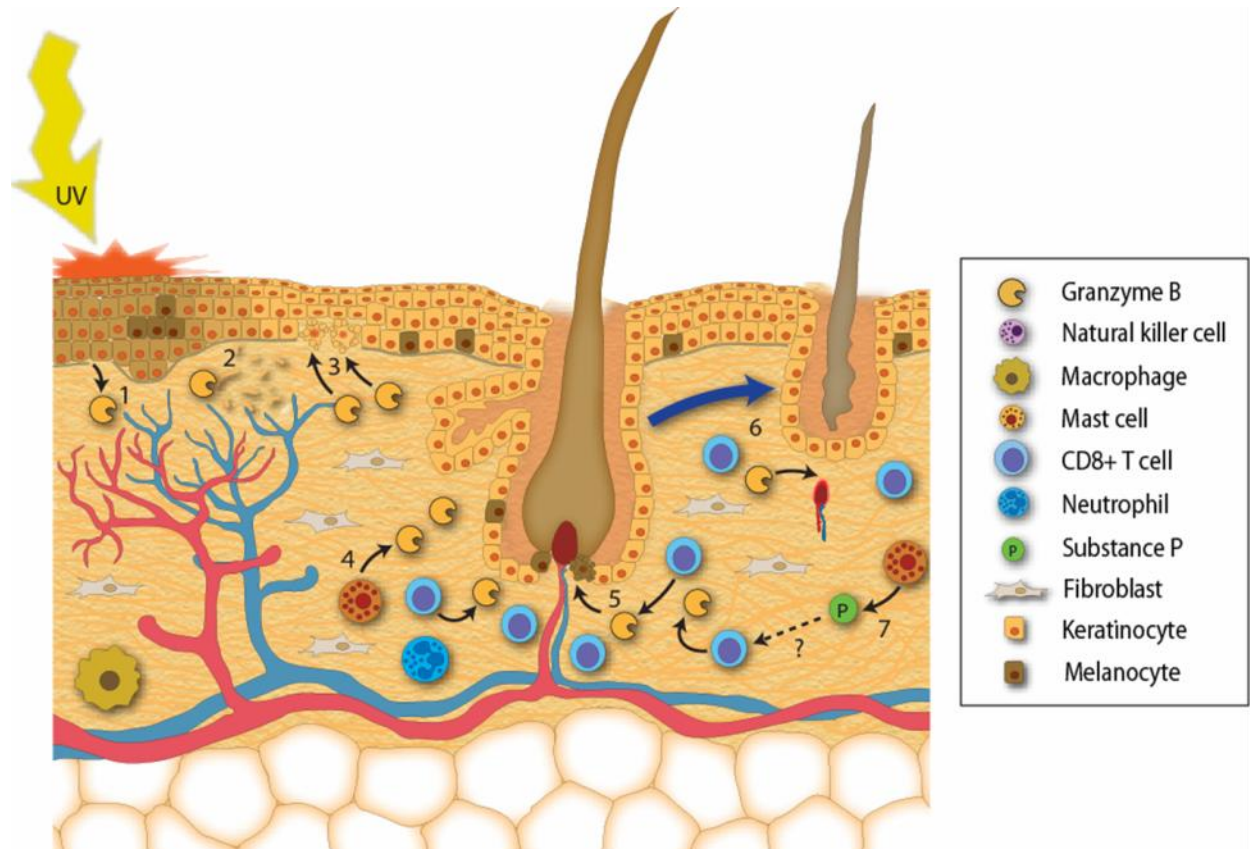


**Figure 5: GzmB in Skin Pathologies**

GzmB may contribute to skin disease through various intracellular and extracellular pathways. UVA light, which is believed to be responsible for most of the visible aging that occurs in the skin, induces reactive oxygen species production which leads to GzmB expression in keratinocytes (1). GzmB from keratinocytes is capable of cleaving the ECM protein fibronectin (2), can inhibit cell migration and can also induce apoptosis in neighboring cells (3). Mast cells from the skin are another cell type that express GzmB (4). GzmB from CTLs has been proposed to induce melanocyte apoptosis in Vitiligo (5). Invading CTLs express GzmB in alopecia areata and influence hair follicle regression (6). Substance P secreted by skin mast cells increases GzmB+ CTLs in the skin, further promoting AA (7). Whether substance P induces mast cell degranulation leading to the release of GzmB is unknown. Reproduced with permission from *Laboratory Investigation* [58].

### 1.14 Neurological Disorders

The central nervous system is regarded as an immune privileged site due to the blood brain barrier and an immunosuppressive environment. However, in many neurological conditions there is a loss of immune privilege and, as a result, GzmB has been implicated in the pathogenesis of a number of neurological disorders through mechanisms of immune cell-mediated apoptosis, receptor cleavage, autoantigen synthesis and potential extracellular activities, as described below.

There are several neurological diseases where the role of GzmB is just emerging, largely in an immune cell-mediated, pro-apoptotic role. In vasculitic neuropathy, the characteristic perivascular infiltrate expresses GzmB and GzmB positive cells are significantly up regulated [255]. In sensory perineuritis, GzmB expressing infiltrates were detected and T cells are believed to contribute to perineural cell apoptosis [256]. During cerebral ischemia, in a rat model of ischemic stroke, GzmB secreted from CTLs and NK cells results in the breakdown of Hsp-70 and AIF translocation from mitochondria to the nucleus, ultimately resulting in apoptosis of brain cells [257]. Finally, in a rat model of spinal cord injury, GzmB levels were elevated and CTLs were found in close proximity to neurons in damaged regions of the spinal cord. Many of the neurons undergoing death were positive for GzmB suggesting that GzmB is responsible for neuron cell death in spinal cord injury [258].

In addition to inducing apoptosis intracellularly, GzmB may contribute to neurological disease through other extracellular mechanisms, such as through receptor signaling or through direct cleavage of receptors. In Myasthenia Gravis (MG) a decrease in acetylcholine receptors (AChR) at neuromuscular junctions is observed as a result of autoimmune attack. Furthermore, GzmB and the autoantigen fragments of AChR are observed in the thymus of MG patients but are not present in healthy controls. Casciola-Rosen *et al* showed that GzmB cleaves AChR



suggesting GzmB-mediated cleavage of this protein exposes cryptic antigens that facilitate an autoimmune response in the disease and results in a loss of functional AChR [122].

Rasmussen's encephalitis (RE) is an autoimmune chronic inflammatory disease occurring mainly in childhood, characterized by seizures and a loss of motor skills and speech. Immune infiltrates consisting mainly of GzmB-positive CTLs are found in the brains of these patients. Using confocal microscopy, Bien *et al* found that GzmB was polarized towards neurons, some of which expressed MHC-I [246]. In similar studies, Bauer *et al* described GzmB-positive lymphocytes in close proximity to astrocytes on the border of astrocyte-deficient lesions. Extracellular GzmB activity has also been linked to RE as extracellular GzmB levels in CSF are elevated in patients with RE, with the original cellular source thought to be CTLs [113]. It is possible that an elevation in extracellular GzmB could be used as a biomarker for RE as it is present at earlier stages of the disease and remains slightly elevated as the disease progresses.

Multiple sclerosis (MS) is a complex autoimmune disease of the central nervous system resulting in demyelination of nerves and GzmB has been implicated in MS pathogenesis. In patients with relapsing remitting MS, GzmB levels in peripheral T-cells decrease while plasma GzmB levels do not change. However, there is an increase in extracellular GzmB in CSF as quantified by ELISA, suggesting extracellular granzyme may contribute to the disease. Although it has yet to be shown, the extracellular localization of GzmB in CSF implies that the enzyme has access to extracellular matrix in the spinal cord and brain, suggesting it may be actively cleaving this matrix, perhaps similar to what has been described in arthritis [137]. There have been several studies reporting an intracellular pro-apoptotic role for GzmB in MS. Since oligodendrocytes and neurons express MHC-I, GzmB-expressing CTLs may be responsible for the induction of cytotoxicity resulting in axonal damage and demyelination [249]. In addition,

neurons expressing MHC-1 resist Fas-mediated killing but are susceptible to granule-mediated apoptosis [250].

## 2. Rationale, Hypothesis and Aims

The pathologic role of GzmB in disease is an emerging area quickly gaining momentum (reviewed in [58]). Our laboratory has examined GzmB in allograft vasculopathy, atherosclerosis, aneurysm, xanthomatosis and skin aging while other groups have characterized GzmB in diseases such as cancer, infectious disease, rheumatoid arthritis, autoimmune diseases, diabetes, lung disease and neurological disorders. However, our knowledge of the relative impact of intracellular versus extracellular GzmB in disease remains elusive as many studies are qualitative, using histology to examine GzmB expression in disease tissues and implicating them in cell-mediated cytotoxicity. As discussed, other studies have identified elevated GzmB levels in bodily fluids of a variety of diseases linking extracellular GzmB to disease. Despite this preliminary evidence, there is limited mechanistic work published on the extracellular activity of GzmB in disease. Our laboratory has published findings from murine models of transplant vascular disease, skin aging and AAA but the use of animal models for mechanistic and proof of concept studies is sparse outside of those used to study infectious disease and/or cancer pathogenesis.

For the last few decades, the bulk of granzyme studies focused on an intracellular pro-apoptotic role for granzymes, which has been critical in our understanding of immune-mediated cytotoxicity. An example of the importance of this pathway is evident in the case of familial hemophagocytic lymphohistiocytosis, where patients are severely immunocompromised and a loss-of-function results in an overactivation of cytotoxic cells. However, the granzymes were originally identified as intracellular and extracellular proteases and recent work has identified an extracellular role for GzmB as it is present extracellularly, retains its activity in the extracellular milieu and appears to be unregulated by inhibitors extracellularly. In addition, non-immune cells express GzmB. These cells are not considered cytotoxic in nature and are

incapable of forming an immunological synapse, suggesting the role of GzmB in these cells is outside the scope of apoptosis. Even immune cells such as basophils and mast cells do not express Perf in conjunction with GzmB, suggesting they are unable to deliver GzmB intracellularly and must be secreting this protease into the extracellular space. In the past, Perf-KO mice were utilized to rule out a role for the granzymes in disease. If there was no difference in phenotype, it was assumed that the granzymes were not a driving force in the process or disease in question. The critical issue with this conclusion is that Perf-independent roles of the granzymes were often overlooked as Perf is required for granzyme internalization into target cells but not for extracellular granzyme activity such as receptor cleavage, growth factor bioavailability and extracellular matrix cleavage. Despite the clinical evidence supporting an extracellular role for GzmB in disease, little work has been carried out to examine the extracellular mechanisms of GzmB in disease. Even less is known regarding extracellular GzmB substrates as only a handful have been identified to date and limited physiological implications have been documented.

*I hypothesize that extracellular GzmB plays an important role in pathogenesis through the cleavage of ECM.* Through the use of *in vitro* and *in vivo* assays differentiating the extracellular and intracellular activities of Granzyme B, we characterize its role in disease.

### *Specific Aims*

1. *To identify novel extracellular matrix substrates with a focus on extracellular proteoglycans.* Prior to my studies, there were a limited number of extracellular matrix substrates identified and no systematic approach for extracellular substrate characterization. We focussed on proteoglycan substrates as the cationic sites of GzmB may draw it to PG substrates as GzmB is stored on serglycin in cytotoxic granules and GzmB exhibits affinity for cell surface PGs.

2. *To examine GzmB-mediated ECM cleavage on the bioavailability of transforming growth factor- $\beta$ .* Extracellular proteases such as the MMPs can release TGF- $\beta$  from decorin, influencing bioavailability. The role of GzmB in cytokine bioavailability was unknown and TGF- $\beta$  is a critical cytokine in wound healing and chronic diseases, such as AAA. As such, GzmB could disrupt the tightly regulated ECM/MMP-mediated TGF- $\beta$  sequestration and release, respectively.
3. *To examine GzmB activity in atherosclerosis, aneurysm, skin aging and other chronic inflammatory diseases.* We have shown that GzmB localization in atherosclerotic plaques increases with increasing disease severity. However, little was known regarding the intracellular (Perf-dependent) versus extracellular mechanisms by which GzmB contributes to atherosclerosis pathogenesis. In addition, the cleavage of extracellular matrix proteins by GzmB in atherosclerosis, AAA or skin pathologies/aging had not been investigated.

### 3. Methodology

#### 3.1 *In vitro* Assays

##### 3.1.1 *Elastin Binding Assay*

Purified human GzmB (Axxora, San Diego, CA) at 50, 100, and 300 ng was incubated with 15 µg human insoluble skin (Sk) and aortic (Ar) elastin (Elastin Products Company, Owensville, MO) in PBS for 3 hours at room temperature. The samples were centrifuged at 1000 x g at room temperature for 3 minutes and the insoluble elastin collected in the pellet. The supernatants, which contained unbound GzmB, were denatured with SDS loading buffer and run on a 10% SDS-PAGE gel. GzmB was detected by Western blot.

##### 3.1.2 *Elastin Cleavage Assay*

Tritiated elastin was prepared as previously described, with the following modifications [338, 339]. Briefly, 1 mg of skin or aortic elastin was diluted in 1 ml dH<sub>2</sub>O and pHed to 9.2. 1 mCi NaB<sub>3</sub>H<sub>4</sub> (PerkinElmer, Waltham MA) and 2 mg of non-radioactive NaB<sub>3</sub>H<sub>4</sub> (Sigma, St. Louis, MO) was added. After a 2 hour incubation, the pH was adjusted to 3.0 and the elastin was incubated for an additional 30 minutes. The elastin was centrifuged for 3 minutes at 5000 x g and the pellet was repeatedly washed to remove excess NaB<sub>3</sub>H<sub>4</sub>. For the cleavage assays, 0.15 mg 3H-elastin was incubated with GzmB (0.75 µg was added a total of 5 times) at room temperature for 7 days. At day 7 of incubation, 25 µg of elastase (Elastin Products Company, Owensville, MO) was incubated with elastin for 2 hours, as a positive control. After incubations, reactions were centrifuged at 5000 x g for 3 minutes. The radioactivity of the soluble, cleaved elastin fragments in the supernatant was counted in Ready Safe Scintillation Fluid (Beckman-Coulter, Fullerton, CA).

### 3.1.3 *GzmB-ECM Cleavage Screening Assay*

Potential GzmB substrates were identified by the presence of aspartic acid residues and pre-screened using GraBCas software [340]. If full length recombinant or purified substrates were available, cleavage assays were run in test tube based assays. If full length substrates were not available, cleavage assays were run on smooth muscle cell-derived extracellular matrix.

### 3.1.4 *Smooth Muscle Cell-derived ECM Based Cleavage Assays*

Human coronary artery smooth muscle cells (HCASMC, Clonetics) were grown to 80% confluency in 6 well plates, then serum starved in smooth muscle cell growth medium (SmGM, Clonetics/Lonza, Watersville, MD) + 0.2% fetal bovine serum (FBS) for 2-7 days, to allow for adequate extracellular matrix synthesis. After serum starvation, cells were washed with phosphate buffered saline (PBS, pH 7.4, Invitrogen, Burlington, ON, Canada) and lysed with 0.25mM ammonium hydroxide (Sigma-Aldrich, St. Louis, MO) for 10min, leaving the surrounding ECM intact. Cell debris was removed with distilled water and after a final wash with PBS, 80-100nM GzmB (Axxora) and 345nM trypsin (Sigma-Aldrich) was incubated on SMC ECM for 24h at room temperature. Following incubation, supernatants (containing cleavage fragments) were removed from the plates, run on an SDS-PAGE gel and transferred to a nitrocellulose membrane (BIO-RAD). To observe general ECM cleavage, ECM was biotinylated with EZ-link-Sulfo-NHS-LC-Biotin (Thermo Scientific/Pierce, Rockford, IL) and run on an SDS-PAGE gel and transferred to a nitrocellulose membranes. Biotin labelled ECM was detected using horseradish peroxidase labelled rabbit-anti-biotin antibody (Cell Signalling Technologies, Boston, MA), the ECL plus detection system (GE Healthcare, Buckinghamshire, UK) and developed on the ChemiGenius imaging system (Syngene, Frederick MD). Substrates were identified using rabbit-anti-fibronectin (Abcam, Cambridge, MA), mouse-anti-fibrillin-1 (Thermo Scientific), rabbit-anti-fibrillin-2 (Elastin Products Company, Owensville, MO ) anti-

fibulin-2 (Santa Cruz Biotechnology, Santa Cruz, CA), decorin (R&D Systems, Minneapolis, MN) and biglycan (R&D Systems) antibodies and IRDye® 800 conjugated secondary antibodies (Rockland Inc, Gilbertsville, PA). Bands were imaged using the Odyssey Infrared Imaging System (LI-COR Biotechnology, Lincoln, NE).

### *3.1.5 Recombinant Substrate Cleavage Assays*

To determine whether GzmB cleaved substrates that were commercially available, simple test tube based cleavage assays were carried out with purified substrates. Recombinant decorin, syndecan-1 and fibromodulin were ordered from Abnova. biglycan, betaglycan, brevican, thrombospondin-1 and thrombospondin-2 were obtained through R&D Systems. Decorin and syndecan (in 50mM Tris buffer, pH 8), as well as biglycan, and brevican (in PBS, pH 7.4) were run in test tube based cleavage assays at room temperature for 24h, stopped with SDS-PAGE loading buffer (50 mM Tris, 2%SDS, 6% Glycerol and 100 mM DTT) run on an SDS-PAGE gel, transferred to a nitrocellulose membrane and imaged using Ponceau stain (Fisher Scientific, Waltham, MA). Membranes were scanned using the LI-COR imaging system (LI-COR Biotechnology, Lincoln, NE). Fibromodulin was run in 50mM Tris pH 8.0 buffer for 24h at room temperature, stopped with SDS-PAGE loading buffer, run on a SDS-PAGE gel and imaged using Ponceau stain. Thrombospondin-1 and thrombospondin-2 were run in PBS, pH 7.4 for 2h at 37C, stopped with SDS-PAGE loading buffer, run on an SDS-PAGE gel and imaged through a Biosafe G-250 Coomassie stain (Bio-rad) of the gel using the LICOR imaging system.

### *3.1.6 Proteoglycan Cleavage Assays*

The recombinant human PGs, decorin (full length and glycosylated; 1-360 a.a., 0.5 ug, Abnova, Walnut, CA), biglycan (partial protein and glycosylated; 38-368 a.a., 1.5-5 µg, R&D Systems) and betaglycan (partial protein and glycosylated; 21-781 a.a., 2.5-5 µg, R&D Systems)



were incubated at room temperature for 24 h with 25-500 nM purified human GzmB (Axxora, San Diego, CA). Reactions were carried out in 50 mM Tris buffer, pH 7.4. For inhibitor studies, GzmB was incubated in the presence or absence of 200  $\mu$ M of the serine protease inhibitor 3,4-dichloroisocoumarin (DCI; Santa Cruz Biotechnology Inc, Santa Cruz, CA) or inhibitor solvent control, dimethyl sulfoxide (DMSO; Sigma-Aldrich, St Louis, MO) for 4h or 24h. After incubation, proteins were denatured, separated on a 10% SDS-polyacrylamide gel and transferred to a nitrocellulose membrane. Ponceau stain (Fisher Scientific, Waltham, MA) was used to detect cleavage fragments.

### *3.1.7 N-terminal Sequencing*

For Edman degradation, 2-5  $\mu$ g/lane of biglycan and betaglycan were incubated with 100-500 nM GzmB for 24h. Once run on a gel and transferred to a PVDF membrane, cleavage fragments were identified by Ponceau staining. The stain was removed by washes with distilled water and the membrane was dried and analyzed at the Advanced Protein Technology Center at the Hospital for Sick Kids (Toronto, ON).

### *3.1.8 Michaelis-Menten Kinetics*

For Michaelis-Menten kinetics, 0.05-4 $\mu$ M of decorin (in 50mM Tris, pH 7.4), biglycan or betaglycan (in PBS, pH 7.4) was incubated with 100nM GzmB for 2.5h at 37C. Reactions were stopped with SDS-PAGE loading buffer, run on an 8% gel and detected with G-250 Biosafe Coomassie Stain (Bio-Rad, Hercules CA). Proteoglycan cleavage was quantified by appearance of product for decorin and betaglycan and loss of substrate for biglycan. Enzyme kinetics calculations were carried out with GraphPad Prism software using linear regression curves for kinetics analysis.

### 3.1.9 TGF- $\beta$ 1 Release Assays

TGF- $\beta$ 1 release assays were carried out using a method similar to that previously described for the assessment of MMP-induced TGF- $\beta$ 1 release from ECM [66]. Briefly, decorin, biglycan and betaglycan (15  $\mu$ g/mL) were coated onto 48 well tissue culture plastic plates and allowed to incubate overnight at 4°C in PBS, pH 7.4. After blocking with 1% bovine serum albumin, 20 ng of active TGF- $\beta$ 1/well (Peprotech Inc, Rocky Hill, NJ) was added in dPBS containing calcium and magnesium (Invitrogen, Carlsbad, CA) for 5 h at RT. GzmB, with or without DCI, was incubated on the wells and after 24 h, supernatants were removed, denatured, and run on a 15% SDS-PAGE gel. Nitrocellulose membranes were probed using a rat anti-human TGF- $\beta$ 1 antibody (BD Biosciences, Franklin Lakes, NJ) and IRDye® 800 conjugated affinity purified anti-rat IgG (Rockland Inc, Gilbertsville, PA). Bands were imaged using the Odyssey Infrared Imaging System (LI-COR Biotechnology, Lincoln, NE).

For TGF- $\beta$ 1 release from endogenous ECM, SMC-derived ECM was isolated as described above for the SMC-derived ECM cleavage assays. ECM was blocked with 1% BSA and incubated with 0.6ng/ $\mu$ l TGF- $\beta$ 1 for 3h at RT. Unbound TGF- $\beta$ 1 was washed away with PBS and GzmB groups were incubated on the wells for 24h. Supernatants, containing released TGF- $\beta$ 1, were run on a SDS-PAGE gel as described above.

### 3.1.10 TGF- $\beta$ 1 Bioavailability Assays

For bioavailability assays, HCASMCs were seeded in 6 well plates in smooth muscle cell growth media (SmGM, Clonetics) +5% fetal bovine serum (FBS, Invitrogen) and grown to confluence. At this time, cells were quiesced by serum removal for 24 h, after which 150  $\mu$ l of release assay supernatants (as described above) and 5ng/ml TGF- $\beta$ 1 positive control were added to the cells for 20 min. Cell lysates were assessed by SDS-PAGE/Western blotting for phosphorylated-SMAD-3 (p-SMAD3; Epitomics, Burlingame, CA) total SMAD-2/3 (t-SMAD-

2/3; BD Biosciences) and the loading controls  $\beta$ -actin (Sigma-Aldrich) or  $\beta$ -tubulin (Millipore, Billerica, MA). Secondary IRDye® 800 conjugated antibodies (Rockland Inc) were utilized and imaged with the Odyssey Infrared Imaging System (LI-COR Biotechnology, Lincoln, Nebraska). Densitometric analysis was conducted on the Odyssey Infrared Imaging System and displayed graphically by p-SMAD-3/total-SMAD-3.

### *3.1.11 Statistics*

For densitometric analysis on pSMAD-3 activity assays, a one way analysis of variance (ANOVA) with a Dunnett's post test was carried out and significance was determined at  $P < 0.05$ .

## *3.2 In vivo Assays*

### *3.2.1 Mice*

All research studies were conducted with the approval of the University of British Columbia Animal Care Committee. For AAA, atherosclerosis and skin pathology experiments GzmB-KO, apoE-KO and Perf-KO mice were purchased through The Jackson Laboratory (Bar Harbor, ME) and GzmB/apoE-DKO and Perf/apoE-DKO mice were bred in house in the Genetic Engineered Models (GEM) facility at the James Hogg Research Centre. For hair plucking experiments, subjects were all female C3H/HeJ mice supplied from colonies at The Jackson Laboratory specific pathogen-free production facility. Mice had access to food and water *ad libitum*, and were housed in community cages in 12 h light/dark cycles. Mice were monitored daily post-procedure and provided with sufficient environmental enrichment.

### *3.2.2 Identifying a Decrease in Decorin in a Murine Model of AAA*

The AngII model was carried out as previously described by our laboratory [193] and all animal procedures were performed in accordance with the guidelines for animal experimentation approved by the Animal Care Committee of the University of British Columbia.

Briefly, apoE-KO and GDKO mice, aged 3 months, received AngII (Sigma Aldrich, St Louis MO) or a saline vehicle control at an infusion rate of 1000 ng/min/kg from a subcutaneous ALZET® mini osmotic pump (DURECT Corporation, Cupertino, CA). After 28 days, mice were euthanized by CO<sub>2</sub> inhalation, vessels were perfused at a flow rate of 100 mm Hg and aortas were embedded in paraffin and sectioned into 5 µm sections. Sections were immunohistologically stained for decorin (apoE-KO, n=4; GDKO, n=7) using a mouse anti-decorin primary antibody (R&D Systems), biotinylated rabbit anti-goat secondary, ABC reagent and NovaRED substrate (Vector laboratories, Burlingame, CA).

### *3.2.3 Murine Atherosclerosis and Skin Pathologies Methodology*

At 6-8 weeks of age c57, apoE-KO, GzmB-KO GzmB/apoE-DKO, Perf-KO and Perf/apoE-DKO mice were fed a high fat diet (21.2% fat, Harlan Teklad, Madison WI) for 30 weeks. At harvest mice were weighed, euthanized by CO<sub>2</sub> inhalation, photographed and blood was collected by cardiac puncture. Vessels were perfused at a constant pressure of 100mm hg with saline using a pressurized tubing system for 5min or until no blood was observed at the incision in the right atria. Organs were collected and fixed in 10% formalin and stored in 70% ethanol. Tissue sections were embedded in paraffin and sectioned into 5 µm sections.

### *3.2.4 Depilation-induced Hair Follicle Cycling in Mice*

Mice were anesthetized at 65 days old when the dorsal skin is uniformly in a telogen resting state [341, 342]. Hair fiber was plucked using a wax-rosin gum mixture from an area of the dorsal skin approximately 2cm x 5cm [343]. Plucking hair fibers from telogen stage follicles is a known method of inducing synchronised anagen growth in a uniform manner [341, 344]. At each time point; 0 (1 hour after hair plucking), 4, 8, 12, 16, and 20 days post hair removal, 3 mice were euthanized and their skin collected per time point. Skin samples from each mouse were subdivided and were fixed in Tellyesniczky / Fekete (Telly's) fixative for routine histology

and immunohistology. Tissue sections were embedded in paraffin and sectioned into 5  $\mu\text{m}$  sections.

### *3.2.5 Total Cholesterol and Triglyceride Quantification*

To determine total cholesterol levels in mouse plasma for the atherosclerosis project, the Cholesterol E enzymatic colorimetric assay (Wako, Richmond VA) was utilized. In brief, a 1:100 dilution of mouse serum and appropriate cholesterol standards were added to a colour reagent containing cholesterol ester hydrolase, cholesterol oxidase, peroxidase, 4-aminoantipyrine 3,5-Dimethoxy-N-ethyl-N-(2-hydroxy-3-sulfopropyl)-aniline sodium salt and ascorbate oxidase. Cholesterol esters were converted to free cholesterol and fatty acids and cholesterol was oxidized to generate hydrogen peroxide which then reacts to form a blue pigment. After 5min incubation at 37°C, the blue pigment was measured at an absorbance of 600nm.

To determine total triglycerides in mouse plasma the Triglyceride Colorimetric Assay Kit was utilized (Cayman Chemical Company, Ann Arbor MI). A triglyceride enzyme mixture in was added to a sodium phosphate assay buffer and then reacts to form a purple pigment to be read at 540nm. Plasma was added to the plate at a 1:16 ratio.

### *3.2.6 En face Staining of Murine Aortas*

Aortas were trimmed for removal of excess fat and tissue surrounding the aorta. Vessels were then pinned to a paraffin tray and tissue was covered in staining solution (0.5% sudan IV (Fisher Scientific), 35% ethanol and 50% acetone) for 15min. Solution was removed and replaced with 80% EtOH for decolourization for 5min. Aortas were washed in dH<sub>2</sub>O for 1h, photographed and plaque area was then traced using ImageProPlus software.

### 3.2.7 Immunohistochemistry

Paraffin sections were treated with xylene and rehydrated with ethanol and PBS. The tissues were treated in boiling citrate buffer and endogenous peroxidase was quenched in 3% H<sub>2</sub>O<sub>2</sub>. 10% rabbit serum or 10% goat serum was used for blocking after which goat anti-GzmB (Abcam or Santa Cruz Biotech, Santa Cruz, CA), rabbit anti-Perf (Santa Cruz Biotech), rabbit anti-fibrillin-1 (Abcam), rabbit anti-fibronectin (Abcam) or goat anti-decorin (R&D Systems) in 10% serum was incubated overnight at 4°C. The secondary antibody biotinylated rabbit anti-goat or goat anti-rabbit (Vector Laboratories, Burlingame, CA) was incubated at room temperature for 30 minutes. ABC reagent was used as directed (Vectastain Elite ABC kit, PK-6100, Vector Laboratories) and was visualized with Nova-RED reagent (Vector Laboratories) or DAB (Vector Laboratories). Tissue was counterstained with hematoxylin. A negative control lacking primary antibody was used to confirm there was no nonspecific staining and Perf-KO mouse skin (mouse acquired from Jackson Laboratories, Bar Harbor, ME, stock# 002407) was also used as a negative control for the Perf antibody.

### 3.2.8 Alcian Blue-safranin Staining of MCs, Counting and Data Analysis

Combined immunohistological and histological staining was achieved by first completing immunohistochemistry for GzmB and then incubating skin sections with alcian blue. For the alcian blue stain, paraffin embedded sections were stained with 1g 8GX alcian blue in 100 ml of 0.7 N HCl (Sigma-Aldrich, Oakville, Canada) pH 0.2 followed by washing in 0.7 N HCl. MCs and GzmB<sup>+</sup> cells were counted in at least 3 visual fields per specimen and the average quantifications were carried out using ImageProPlus<sup>TM</sup> Software (MediaCybernetics, Silver Spring, MD) per mm<sup>2</sup> of skin. The total number of MCs, GzmB<sup>+</sup> cells, and GzmB<sup>+</sup> MCs, were counted. These values were then used to calculate the percentage of MCs that expressed GzmB and the percentage of GzmB<sup>+</sup> cells that were MCs.

### *3.2.9 Electron Microscopy of Skin Sections*

Skin in the upper back of C57 and apoE-KO mice, was removed from mice and cut into 2mm pieces. Tissues were fixed in 2.5% glutaraldehyde and washed. They were then post fixed in 1% osmium, dehydrated, and embedded in Epon 812. Blocks were sectioned at 5µm, perpendicular to the plane of the skin and stained with toluidine blue (TBO) to examine the full section by light microscopy. For transmission electron microscopy (TEM), thin sections at 70nm were cut from the same blocks. Thin sections were viewed on the FEI Tecnai 12 TEM in the iCAPTURE Centre. All EM work was completed in collaboration with Dr. David Walker, in our iCAPTURE imaging facility.

### *3.2.10 GzmB Staining in Human AAA Vessels*

Human AAA samples were obtained according to ethical protocols at the Karolinska Institute (Sweden). GzmB staining on AAA nerve ganglia was carried out as described in method 3.2.9 with a mouse anti-GzmB (gift from Dr. Joseph Trapani, Melbourne Australia).

### *3.2.11 Statistics*

For en face staining and mouse weights a one way ANOVA with Bonferronis post test was utilized.

## 4. Identification of Novel Extracellular Substrates

### 4.1 Introduction

Although the granzymes were initially characterized as intracellular and extracellular proteases, over the past 30 years the focus has been almost exclusively on intracellular GzmB activity. Intracellular GzmB substrates have been well characterized and the implications of their cleavage have been well documented. However, increasing evidence towards an extracellular activity for GzmB is emerging. GzmB is constitutively released from cytotoxic lymphocytes, retains its activity extracellularly and is elevated in chronic disease in bodily fluids (reviewed in [58]). In addition, there is no known extracellular GzmB inhibitor, suggesting it may be essentially unrestrained in the extracellular milieu. Cleavage of several ECM proteins such as fibronectin, vitronectin, and laminin have been established and implicated in processes such as anoikis [123, 124]. Although the granzyme field has shifted focus to extracellular GzmB activity, this area remains in its infancy.

A limited number of extracellular GzmB substrates have been identified and even fewer have been implicated in disease (Table 1). There has not been a targeted screen for extracellular substrates described in the literature. Potential extracellular substrates key in wound healing, atherosclerosis and aneurysm are also not well known. We therefore set forth to identify extracellular GzmB substrates and characterize these substrates using a low throughput extracellular substrate screen.

### 4.2 Results

#### 4.2.1 GzmB has Affinity for Elastin and Displays Weak Elastolytic Activity

As previous work carried out by our laboratory suggested that GzmB localized to the elastic lamellae of the mouse aorta, we examined whether GzmB had affinity for elastin and if it

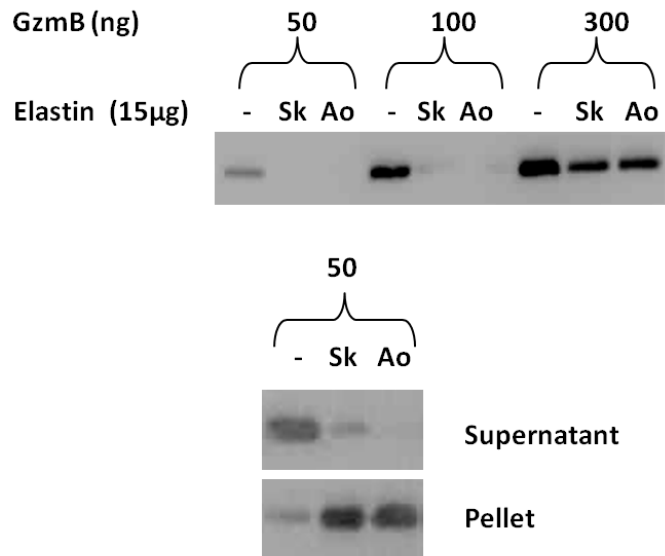
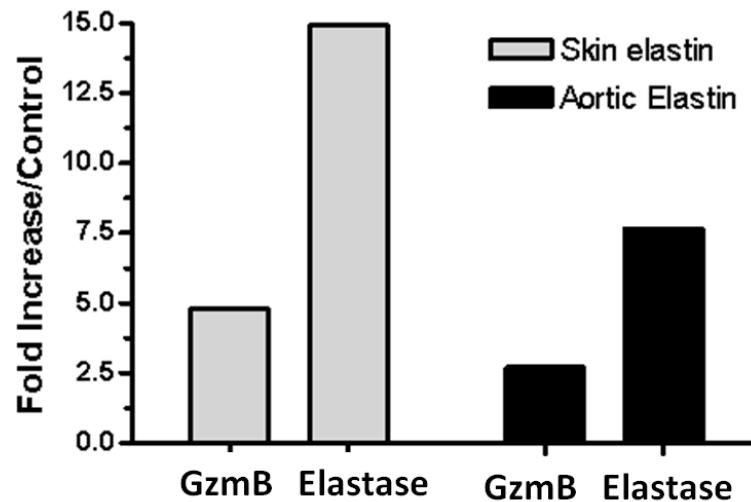


displayed elastolytic activity. To confirm the interaction of GzmB with elastin, we incubated GzmB with insoluble skin and aortic elastin. Upon incubation with elastin and a low speed centrifugation step, there was less GzmB present in the supernatant and instead GzmB associated with the elastin in the pellet (Figure 6). This was dose-dependent and was not restricted to the type of elastin used (i.e. skin elastin or aortic elastin). In a separate experiment designed to detect elastin degradation, after a 7 day incubation of GzmB with elastin, the radioactivity of the cleaved, soluble elastin fragments was 4.8 times and 2.7 times higher than background for skin and aortic elastin, respectively (Figure 6). Proteolysis of elastin by elastase yielded a radioactivity increase over background of 14.9 fold for skin elastin and 7.7 fold for aortic elastin. These data suggest that GzmB has affinity to elastin and when incubated for prolonged periods, may have elastolytic activity.

#### *4.2.2 GzmB Cleaves Smooth Muscle Cell Extracellular Matrix*

To develop a straightforward system to screen extracellular matrix substrates, we modified an extracellular matrix cleavage assay previously developed in our laboratory by Dr. Jonathan Choy [124]. We allowed HCASMC's to secrete ECM for up to 7 days, then removed cells from the plate using ammonium hydroxide. The remaining ECM was digested with GzmB and cleavage fragments (which detach from the plate and localize in the supernatant) were removed. As the ECM contains a minimal amount of protein compared to cell lysates, protein is not detectable by conventional coomassie or ponceau stains, therefore we biotinylated the ECM to be visualized by western blotting with an anti-biotin antibody. As shown in Figure 7, 80nM GzmB digested HCASMC ECM to a similar degree as 345nM trypsin over a 24h period, as shown by the biotinylated fragments in plate supernatants. To validate the assay and test for the detection of a known ECM substrate, we probed the supernatants with an anti-fibronectin

antibody and found that GzmB-mediated cleavage of fibronectin was detectable in HCASMC ECM.

**A****B**

**Figure 6: *In vitro* Elastin Binding Assay and Cleavage Assay**

To determine whether GzmB had affinity for and cleavage activity against elastin, binding and cleavage assays were carried out. (a) GzmB was incubated with 15μg human insoluble skin and aortic elastin for 3h at room temperature. The samples were centrifuged and the insoluble elastin collected in the pellet. The supernatants, which did not contain insoluble elastin and the pellets which contained insoluble elastin, were denatured and subjected to SDS-PAGE and GzmB was detected by Western blotting. (b) GzmB was incubated with  $^3\text{H}$ -elastin for 7d at RT, with fresh enzyme added 5 times throughout the experiment. Elastase was incubated with  $^3\text{H}$ -elastin for 2h. Samples were centrifuged for 3m at 5000g and supernatants containing the soluble cleavage fragments were collected and counted. Data is represented as fold increase in radioactivity over the control (elastin only), with n=2.

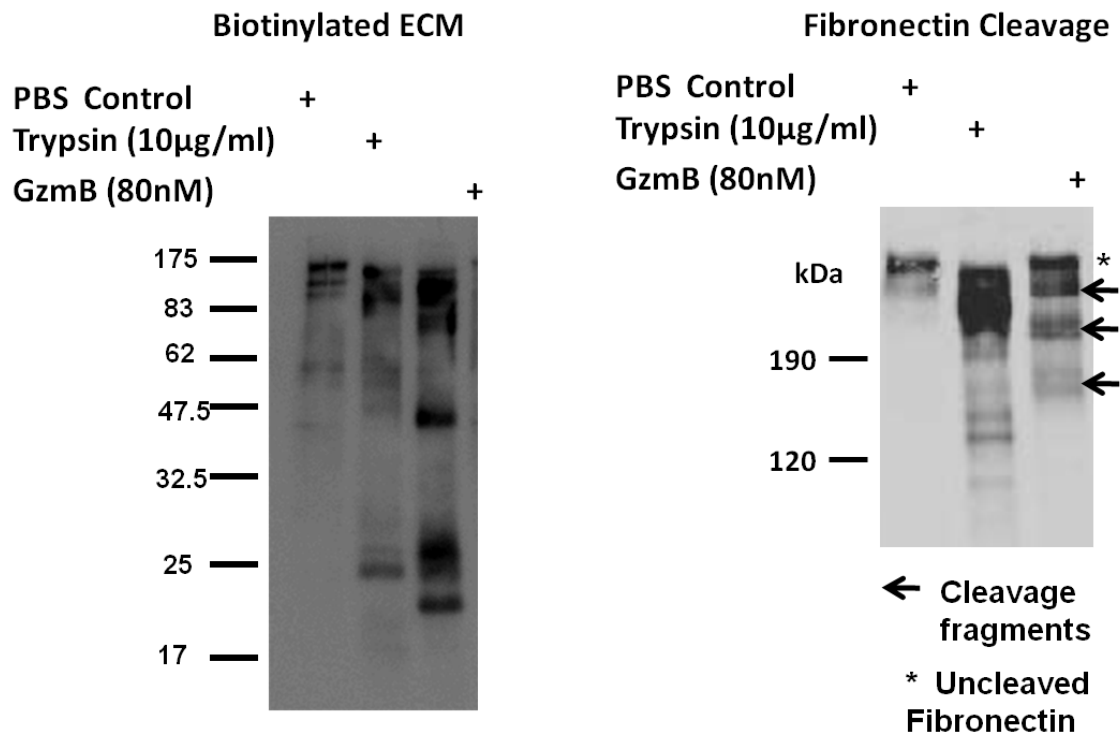


**Figure 7: GzmB Cleaves Human Coronary Artery Smooth Muscle Cell Extracellular Matrix**

To examine whether GzmB cleaves SMC-derived ECM, cleavage assays were utilized and confirmed with fibronectin cleavage. Smooth muscle cells were serum starved for 48h, the cells were removed with ammonium hydroxide and the remaining ECM was incubated with PBS, 345nM trypsin, and 80nM GzmB for 24h at room temperature. Supernatants (containing cleaved ECM) were collected, biotinylated, run on a 6% SDS-PAGE gel and resolved via Western blotting.

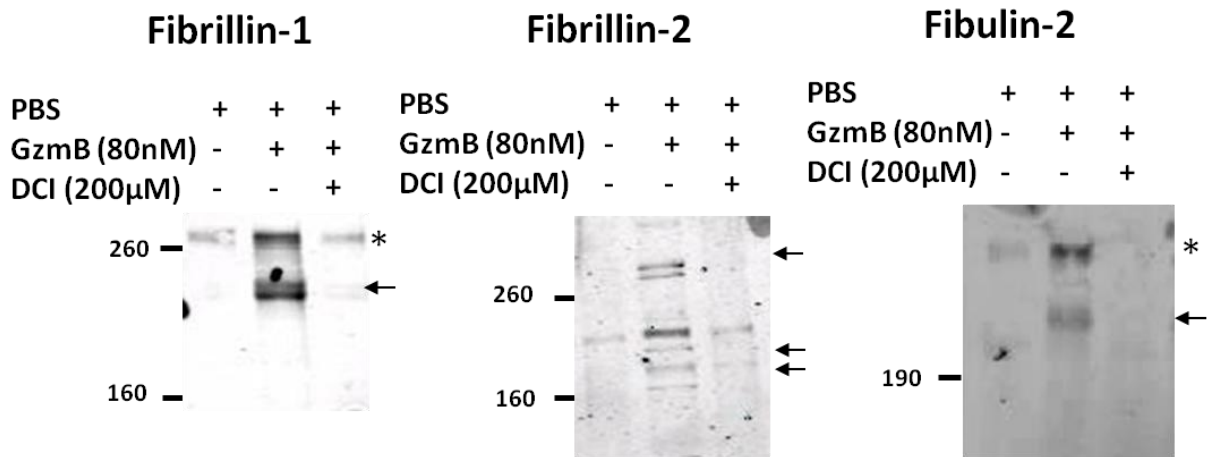


**Figure 8: GzmB-mediated Cleavage of Microfibrillar Proteins**

To determine whether microfibril components of elastin were substrates for GzmB, SMC ECM cleavage assays were conducted. For cleavage from SMC-derived ECM, following 5-7 days serum starvation for ECM synthesis, human coronary artery smooth muscle cells were removed from 6 well plates using ammonium hydroxide. GzmB was incubated on ECM for 24h and supernatants were western blotted for fibrillin-1, fibrillin-2 or fibulin-2. Star denotes full length and arrows indicate cleavage fragments

#### 4.2.3 *GzmB-mediated Cleavage of Microfibril Proteins*

HCASMC-derived ECM was used to detect the cleavage of elastin microfibril components and fibrillin-1, fibrillin-2 and fibulin-2 were determined to be GzmB substrates (Figure 8). Likely due to limitations in fragment detection by the antibodies, only 1 fragment was detected for fibrillin-1 and fibulin-2. However, five cleavage fragments were detected for fibrillin-2. To determine cleavage was mediated by GzmB, the GzmB inhibitor DCI was also used, preventing the cleavage of each substrate.

#### 4.2.4 *GzmB Cleaves Multiple Proteoglycan Substrates*

To examine various PG substrates, commercially available recombinant substrates were utilized. Decorin, biglycan, betaglycan, syndecan and brevican were all cleaved by the protease into several fragments (Figure 9). As ponceau stain was used to detect these fragments and not western blot, all stable cleavage fragments should be detectable using this methodology, unless they are too small to run through the SDS-PAGE gels. Cleavage was prevented with the inhibitor DCI, suggesting fragmentation was GzmB-dependent. For syndecan, Granzyme A and Granzyme K were also shown to cleave the substrate into distinct cleavage fragment patterns.

#### 4.2.5 *GzmB Cleaves Fibromodulin, Thrombospondin-1 and Thrombospondin-2*

Fibromodulin was also determined to be a substrate for GzmB, and the GzmB inhibitor V2248 (also known as compound 20), prevented fibromodulin cleavage after 2h incubation at 37°C (Figure 10). In addition, thrombospondin-1 and thrombospondin-2 were both cleaved by GzmB after a 2h incubation at 37°C (Figure 11). Cleavage fragments sizes were similar for both proteins, suggesting GzmB may degrade both substrates at the same or similar cleavage sites.

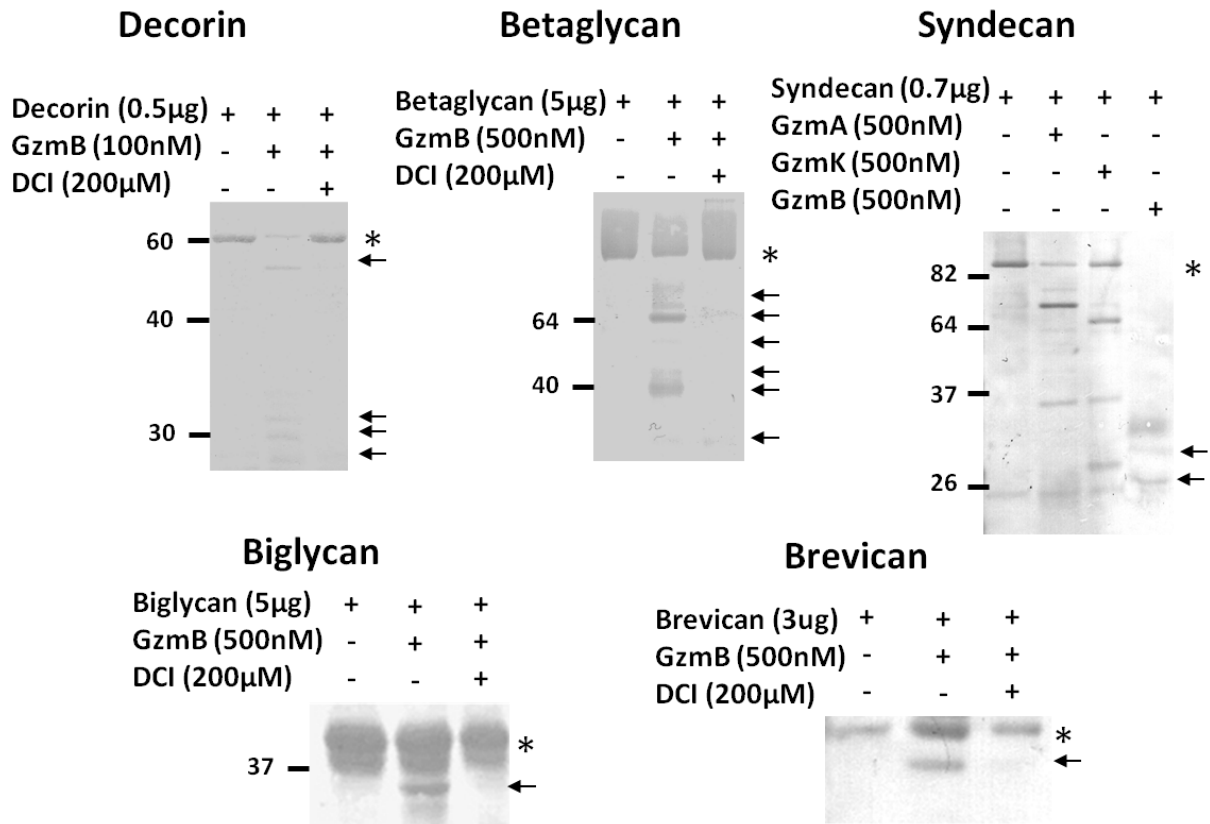


**Figure 9: Low Throughput Screen for Extracellular GzmB Substrates Using Recombinant Proteins**

Recombinant PG cleavage assays were conducted to identify novel GzmB substrates. Recombinant decorin, biglycan, betaglycan, syndecan, or brevican was incubated with purified GzmB for 24h at room temperature. Reactions were stopped with SDS-PAGE loading buffer, run on an SDS-PAGE gel and imaged by ponceau staining of a nitrocellulose membrane. \* denotes full length protein and arrows indicate cleavage fragments.

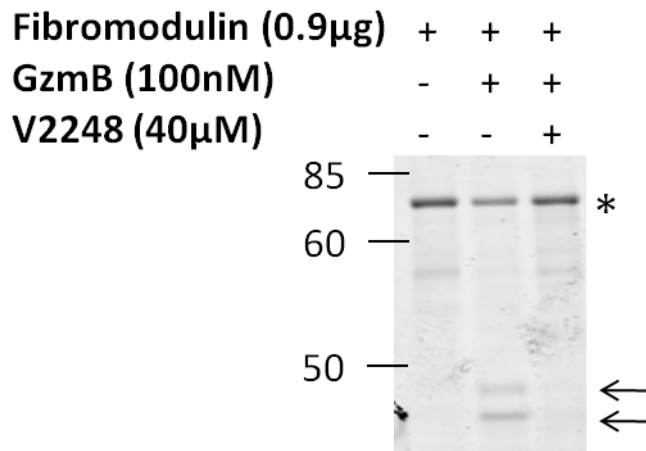


**Figure 10: Cleavage of Fibromodulin by GzmB**

A fibromodulin cleavage assay was conducted to characterize its cleavage by GzmB. Recombinant human fibromodulin was incubated with GzmB for 2h at 37C. Reactions were stopped with SDS-PAGE loading buffer, run on an SDS-PAGE gel, Coomassie stained and imaged on the licor imaging system. \* denotes full length protein and arrows indicate cleavage fragments.



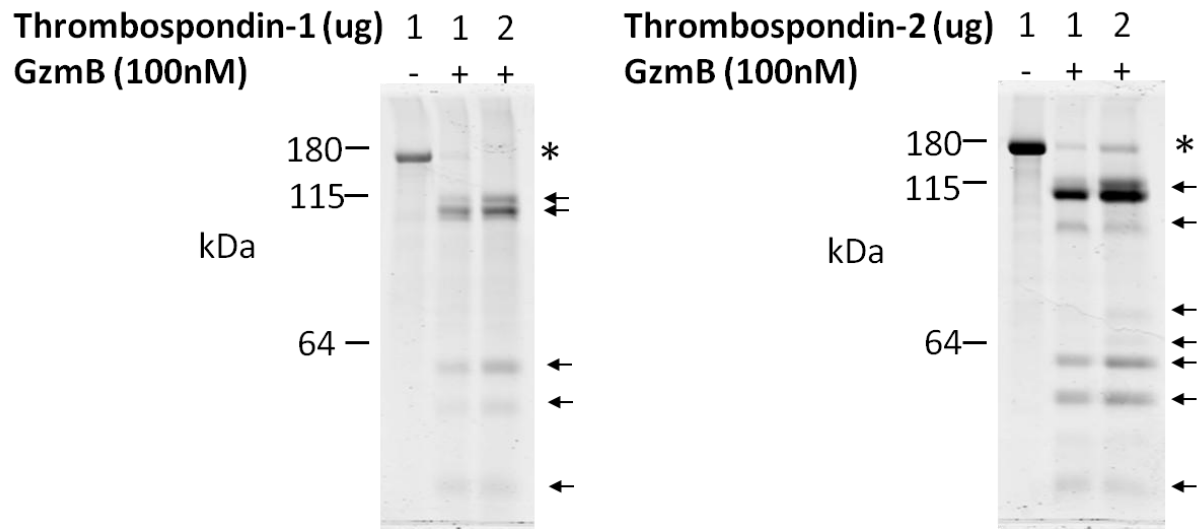


**Figure 11: GzmB-mediated Cleavage of Thrombospondin-1 and Thrombospondin-2**

To examine whether thrombospondin 1 and 2 were substrates for GzmB, recombinant protein tube based assays were utilized. Recombinant human thrombospondin-1 and thrombospondin-2 were incubated with GzmB for 2h at 37°C. Reactions were stopped with SDS-PAGE loading buffer, run on an SDS-PAGE gel, Coomassie stained and imaged on the Licor imaging system. \* denotes full length protein and arrows indicate cleavage fragments.

#### 4.3.5 Characterization of Extracellular Matrix Cleavage Inhibitors

To characterize compound 20 [345] as an ECM cleavage inhibitor, we ran two different lots of the inhibitor, JT00025135 and JT00025102B (Generated by UBC CDRD) on decorin and betaglycan cleavage respectively (Figure 12). For decorin, 20 $\mu$ M of JT00025135 was sufficient for complete inhibition. For betaglycan 5 $\mu$ M of JT00025102B prevented cleavage. The inhibitor was also tested on HCASMC ECM and we found that 50  $\mu$ M fully inhibited fibronectin and decorin cleavage (Figure 13). We also tested NCI compounds NCI644752 and NCI644777 on decorin cleavage and 150 $\mu$ M of NCI644752 partially inhibited decorin cleavage whereas 150 $\mu$ M of NCI644777 fully inhibited cleavage. We thus determined that these inhibitors could prevent GzmB-mediated ECM cleavage.

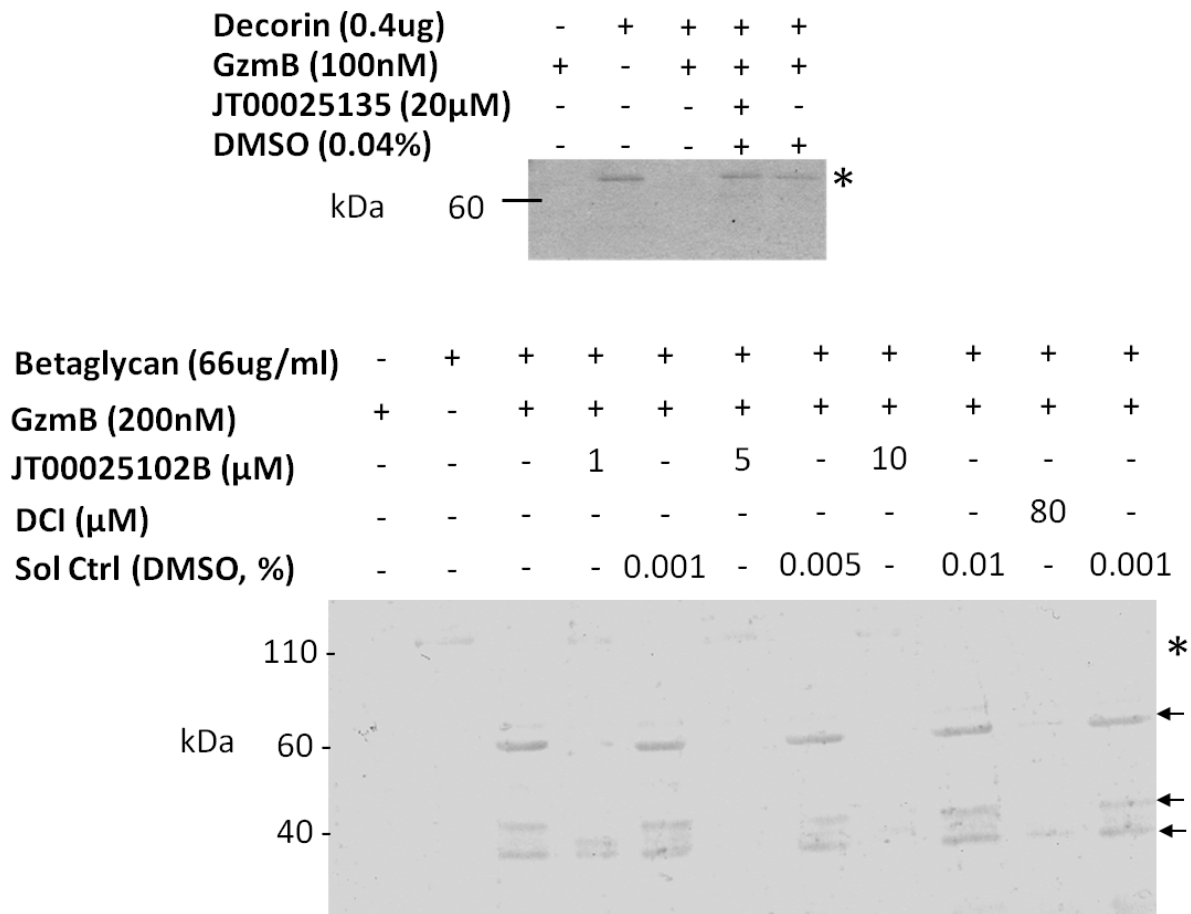


**Figure 12: Inhibition of GzmB using a Specific Small Molecule Inhibitor (JT00025135 and JT00025102B) Prevents Decorin and Betaglycan Cleavage**

To examine GzmB inhibition by the small molecule inhibitor compound 20, cleavage assays on recombinant decorin and betaglycan were conducted. Incubations were performed at RT for 24h in a total reaction volume of 30ul. Samples were run on a 10% gel and imaged by Coomassie Blue stain. Asterisk = full length protein, arrows indicate cleavage fragments.

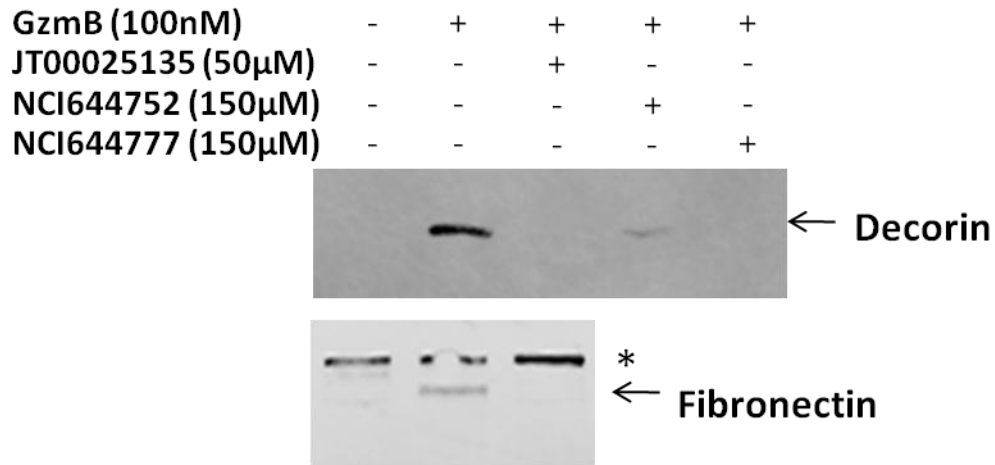


**Figure 13: Inhibition of GzmB using Small Molecule Inhibitors Prevents ECM Cleavage**

Compound 20-mediated GzmB cleavage inhibition was further characterized in decorin and fibronectin cleavage assays. To synthesize endogenous ECM, human coronary artery smooth muscle cells were seeded in 6 well plates and incubated at confluency for 7 days in serum starvation media (SMGM + 0.2% FBS). Cells were removed from the plates by incubation with 0.25M ammonium hydroxide for 20min. This treatment removes cells while leaving the surrounding extracellular matrix intact. Subsequently, 100nM GzmB and the inhibitor of interest was incubated on the endogenous ECM for 24h. Supernatants from the plates (containing cleavage fragments) were run on an SDS-PAGE gel and Western blotted for fibronectin or decorin. DMSO solvent control was not included due to redundancy. Asterisk = full length protein; Arrow = cleavage fragments, star denotes full length.

### 4.3 Discussion

GzmB is a pro-apoptotic serine protease initially characterized in the granules of CTLs and NK cells. GzmB is released towards target cells along with the pore-forming protein, Perf, resulting in its Perf-dependent internalization into the cytoplasm and subsequent induction of apoptosis [58, 346]. However, while once thought to be primarily involved in CTL/NK cell-mediated apoptosis, it is now recognized that GzmB can be expressed by other inflammatory cells (eg. macrophages, mast cells, dendritic cells, basophils) as well as non-immune cells (eg. chondrocytes, smooth muscle cells, keratinocytes, reviewed in [347]). As non-immune cells do not possess cytotoxic granules, rarely express Perf and do not readily form immunological synapses with target cells, GzmB is secreted from these cells into the extracellular milieu. Indeed mounting evidence suggests that GzmB exhibits non-apoptotic, Perf-independent roles involving matrix degradation in the pathogenesis of chronic inflammatory diseases (Summarized in [58, 347]).

In this chapter, 11 novel extracellular GzmB substrates were identified. Substrates were initially screened for probable cleavage sites using GraBCas before testing for cleavage. Not all potential substrates were cleaved as several ECM proteins that made it through the initial screen were determined not to be GzmB substrates such as collagen III, collagen IV and tenascin C. A summary of functions for each substrate is shown in Table 4 and nearly all are either elastin microfibril proteins or proteoglycans.

We also characterized 3 specific extracellular GzmB inhibitors; compound 20, NCI644752 and NCI644777. Compound 20 was quite efficient at preventing GzmB-mediated cleavage as 5 $\mu$ M sufficiently inhibited 200nM GzmB. Compound 20 has previously been characterized as a GzmB inhibitor and has a K<sub>i</sub> of 7nM and blocks CTL mediated killing with an IC<sub>50</sub> of 3 $\mu$ M [345]. NCI 644752 and NCI644777, which were not previously characterized as

GzmB inhibitors, inhibited decorin cleavage of SMC ECM. These candidate inhibitors were identified using a virtual screen of compounds using the crystal structure of GzmB from a virtual library from the United States National Cancer Institute. NCI644752 partially inhibited cleavage at 150 $\mu$ M and NCI644777 fully inhibited at 150 $\mu$ M.

We found that GzmB had affinity for elastin through the elastin binding assay and we have previously shown that GzmB localizes to elastic lamellae *in vivo* (unpublished results), suggesting the protease is likely in close vicinity to elastin and elastin microfibrils. This is the first report of weak elastolytic activity by GzmB over a prolonged time period. However, as cleavage of elastin itself was minimal, we examined microfibrillar components of elastin and found fibrillin-1, fibrillin-2 and fibulin-2 were substrates for GzmB, suggesting GzmB may play a role in elastin and microfibrillar stability *in vivo*. This could have implications in blood vessels where fibrillin-1 is important for vessel stability and associates with elastin in the elastic lamellae of the aorta. Indeed, a GzmB-dependent reduction in fibrillin-1 was apparent in apoE-KO mice infused with angiotensin II for aneurysm formation, as described in chapter 6 [193]. This was paralleled with elastic lamellae disruption and breakage. As elastin microfibrils are key in load bearing support in vessels, cleavage of fibrillin-1 by GzmB may weaken the vessel wall and increase susceptibility to aneurysm rupture.

Previously, GzmB-mediated cleavage of another extracellular PG, aggrecan, was described [118] and other unidentified cartilage PGs, were shown to be cleaved in rheumatoid arthritis [137]. Whether or not the PG we have identified were among the PGs cleaved in this study is not known but in our experience, it does appear that GzmB has a preference for extracellular PG substrates.

In this chapter, we found several proteoglycan substrates for GzmB. GzmB may also have affinity for ECM upon release, particularly in PG-rich ECM as GzmB has been previously

described to bind sulfated glycosaminoglycans. During the storage and release of GzmB from cytotoxic granules, GzmB binds to the heparan sulfate GAG chains of the PG serglycin [348]. Additionally, cells with reduced membrane GAG chain content displayed a decrease in GzmB-mediated cell death, likely due to reduced electrostatic GzmB transfer from serglycin to membrane associated GAG chains, such as chondroitin sulfate or heparan sulfate [43-45]. GzmB affinity for these GAG chains has been proposed to be due to GzmB cationic sites that bind electrostatically to anionic GAGs [45]. As decorin, biglycan and brevican contain chondroitin sulfate GAG chains, betaglycan and syndecan contains both chondroitin sulfate and heparin sulfate chains and fibromodulin contain keratan sulphate chains it is probable that GzmB may also have affinity for these ECM PGs, potentially accumulating in PG-rich ECM.

Decorin and biglycan are members of the small leucine rich PG family and are involved in the sequestration of active TGF- $\beta$  and in collagen fibre spacing [71, 349, 350]. A reduction in decorin levels has been found in wound healing models such as keloids, a variant of Ehlers-Danlos syndrome chronic skin ulcer and in the skin upon ultraviolet light exposure [351-354]. Of particular interest, 32kDa and 45kDa decorin fragments were identified in human keloid tissue of similar size to GzmB-derived fragments [352, 353] suggesting cleavage fragments of similar size to those seen by GzmB-mediated decorin cleavage are present *in vivo*. The protease that synthesized these fragments has yet to be reported and it is interesting to speculate future identification of GzmB-synthesized ECM fragments in bodily fluids.

Decorin and biglycan bind to collagen fibres and regulate spacing and structure [89, 94, 355]. Decorin-knockout mice have fragile skin with reduced tensile strength [94]. Ultrastructural analysis of collagen yielded uncontrolled lateral fusion of fibrils and courser irregular fibril outlines [94]. Biglycan-KO mice have thinning of the dermis but no skin fragility, however collagen fibril morphology was similar to decorin-KO mice [355]. Therefore, GzmB-

mediated cleavage of decorin and biglycan could result in an alteration in collagen fibril structure. Our laboratory examined collagen density in GzmB-deficient mice in a model of skin aging and found a GzmB-dependent reduction in collagen fibre density by second harmonic generation, suggesting GzmB-mediated cleavage of these proteins may be altering collagen fibre structure or special arrangement *in vivo* [195]. In AAA, a reduction in collagen fibre density is also apparent in the adventitia of aneurysm tissue [194]. This collagen structural alteration is prevented upon infusion with an extracellular GzmB inhibitor.

Thrombospondin-1 is involved in tissue repair, wound healing and fibrosis (reviewed in [356]). It stimulates cell adhesion, cell migration, resistance to anoikis, expression of collagen and deposition of matrix. Thrombospondin-1 also binds and activates latent TGF- $\beta$  by binding to the latency associated peptide and disrupting its interaction with the mature domain of TGF- $\beta$  [357]. Cleavage of thrombospondin-1 by GzmB may inhibit these processes, playing a role in wound healing. The proteases cathepsin G and ADAMTS-1 cleave thrombospondin-1 into soluble fragments, suggesting GzmB may also cleave it into a soluble form, however further studies are required to characterize the implications of GzmB-mediated cleavage of thrombospondin [358, 359].



**Table 4: Summary of Identified ECM Substrates**

<b>Substrate</b>	<b>Size* and Cleavage Fragments</b>	<b>Functions*</b>
<b>Fibrillin-1</b>	Full length 312kDa 1 fragment detected at ~200kDa	Major structural component of elastin microfibrils and involved in elastin fibre assembly. Sequestration of latent TGF- $\beta$ [72, 360]
<b>Fibrillin-2</b>	Full length 315kDa 4 fragments detected at ~260kDa and 160-200kDa	Elastic fibre assembly, microfibrillar component [360]
<b>Fibulin-2</b>	Full length 127kDa 1 fragment detected at ~200kDa	Organ development: differentiation of the heart, skeletal and neuronal structures. Microfibrillar component. [361, 362]
<b>Decorin</b>	With glycosylation runs at 60kDa. 1 fragment at 50kDa and 3 fragments at 30kDa	Binds type 1 collagen, involved in collagen fibre assembly. Binds active TGF- $\beta$ , Inhibits apoptosis and promotes cell survival, responsible for tight bundle formation and tensile strength of collagen [71, 78, 84, 91, 93, 349]
<b>Biglycan</b>	With glycosylation runs at 40kDa. 2 Fragments at 30kDa and 20kDa	Binds type 1 collagen, involved in collagen fibre assembly. Binds active TGF- $\beta$ [71, 350]
<b>Betaglycan</b>	With glycosylation runs at 100kDa. Multiple fragments at 60kDa and 40kDa	Undergoes ectodomain shedding and involved in TGF- $\beta$ bioavailability when present in the ECM [70]
<b>Syndecan-1</b>	With glycosylation runs at 90kDa. 2 fragments at 20-30kDa	Undergoes ectodomain shedding. Elevated in dermal wound fluid and the ectodomain inhibits wound repair. Binds proteases and limits their activities. [363, 364]
<b>Brevican</b>	With glycosylation full length runs at 140kDa. 1 cleavage fragment detected at ~100kDa	Expressed in the brain. Stabilizes synapses and neurite outgrowth [365-367]
<b>Fibromodulin</b>	With glycosylations runs at 70kDa. 2 cleavage fragments at 40-50 kDa	Binds type 1 collagen, inhibits fibrillogenesis <i>in vitro</i> . Role in TGF- $\beta$ bioavailability. [71, 368]
<b>Thrombospondin-1</b>	Runs at 165 kDa. Fragments at 115kDa, 60kDa, 50kDa and 30kDa	Cell-cell and cell-matrix interactions. Platelet aggregation, angiogenesis and wound healing. [369-371]
<b>Thrombospondin-2</b>	Runs at 170 kDa. Fragments at 115kDa, 110kDa, 60kDa, 50kDa and 30kDa	Cell adhesion and migration. Tumor growth, angiogenesis and wound healing. [372-374]

\*Information from Genecards.org

## **5. GzmB Cleaves Decorin, Biglycan and Soluble Betaglycan, Releasing Active Transforming Growth Factor- $\beta$ 1**

### *5.1 Introduction*

The extracellular matrix provides as scaffolding for cells to spread and attach and filters nutrients and other factors to surrounding cells. The pericellular matrix contains ECM proteins that are in close vicinity to cells and can thus bind growth factors in close quarters to cells. In this way ECM acts as a repository for growth factors and regulates their synthesis, activation and degradation. Growth factor binding to the ECM can alter their local concentrations, affect soluble levels and limit their mobility and uptake by neighboring cells. Extracellular proteases act in concert with ECM in the process of growth factor bioavailability, cleaving the ECM, activating latent growth factors and releasing these sequestered molecules so that they are accessible to nearby cells. The matrix metalloproteases (MMPs) have been established in these processes in the context of both normal physiological remodeling and in pathological ECM degradation [375, 376]. They have also been implicated in cytokine bioavailability as MMP-2, MMP-3 and MMP-7 release TGF- $\beta$  from decorin matrices [66]. Several known extracellular GzmB substrates are involved in cytokine banking, namely fibronectin which sequesters transforming growth factor-beta (TGF- $\beta$ ), vascular endothelial growth factor (VEGF), platelet-derived growth factor (PDGF), and tumor necrosis factor (TNF- $\alpha$ ), vitronectin which binds TGF- $\beta$  and PDGF and fibrillin-1 which sequesters TGF- $\beta$  [65, 73]. However, whether GzmB-mediated cleavage of these substrates results in the release of sequestered cytokines has not been elucidated. Decorin, biglycan and soluble betaglycan all bind active TGF- $\beta$ , sequestering it away from cells. [65].

TGF- $\beta$  regulates development, cell proliferation and ECM deposition and is involved in the pathogenesis of cancer, cardiovascular disease, diabetes, marfans syndrome among others. Inactive TGF- $\beta$  is associated with a non-covalently bond propeptide called a latency-associated peptide (LAP), in a complex known as the small latent TGF- $\beta$  complex (SLC) [377]. The SLC associates with the latent TGF- $\beta$  binding protein (LTBP) to form the large latent TGF- $\beta$  complex (LLC). The extracellular storage of TGF- $\beta$  is critical in regulating its bioavailability and both the active and inactive forms of TGF- $\beta$  are sequestered in extracellular matrix. Fibrillin-1 sequesters the LLC by associating with the LTBP and active TGF- $\beta$  can be bound to the ECM proteoglycans decorin, biglycan and soluble betaglycan [65, 70, 71, 378].

Decorin and biglycan are members of the small leucine rich proteoglycan family. They are involved in collagen density and spacing, active TGF- $\beta$  sequestration, cell division and proliferation, and migration. Betaglycan, also known as TGF- $\beta$  receptor III, is a PG receptor involved in TGF- $\beta$  signaling. Its extracellular domain acts as a soluble receptor following cleavage by membrane type-matrix metalloproteinase (MT-MMP1), in a process known as ectodomain shedding [379, 380]. This soluble betaglycan resides in the ECM and functions in TGF- $\beta$  sequestration [70, 378].

TGF- $\beta$  signaling occurs when active TGF- $\beta$  binds to TGF-receptor II (TGFR-II), a process that is promoted by membrane-associated betaglycan [67, 70]. TGFR-II then phosphorylates TGF receptor I, activating its kinase domain, which then phosphorylates downstream effectors such as SMAD-2 and SMAD-3 [68]. TGF- $\beta$  can also signal independently of the SMADs through proteins such as Erk and RhoA [381].

In the present chapter, we demonstrate that GzmB cleaves decorin, biglycan and betaglycan and identify sites of proteolysis. We show that the released TGF- $\beta$ 1 is active and induces the phosphorylation of SMAD-3 in HCASMCs.

## 5.2 Results

### 5.2.1 GzmB Cleaves Decorin, Biglycan and Betaglycan

Incubation of decorin, biglycan and betaglycan with GzmB resulted in the concentration-dependent generation of multiple cleavage fragments (Figure 14a-c). Full length decorin (~65 kDa) and 4 decorin cleavage fragments at ~50 kDa and ~30 kDa, were evident following GzmB incubation. Biglycan was identified at ~40 kDa, with cleavage fragments evident at ~30 kDa and 20 kDa, while incubation of recombinant soluble betaglycan (~100 kDa) with GzmB resulted in multiple cleavage fragments at ~60 kDa and 40 kDa. As all of these substrates are PGs and contain glycosaminoglycan (GAG) chains, the apparent molecular weight of the full length proteins and fragments may not be accurate, as glycosylation can alter movement through the gel. As such, several of the proteins and protein fragments are observed as a smear as opposed to a condensed band.

To confirm that decorin, biglycan and betaglycan proteolysis was mediated by GzmB, DCI was included in reactions for 4 h or 24 h (Figure 15 a-c). Higher concentrations of PG substrates and GzmB were utilized in this assay for favorable detection of cleavage fragments. DCI effectively inhibited decorin, biglycan and betaglycan cleavage at both time points while the vehicle control (DMSO) had no effect (Figure 15a-c).

To verify these PGs are indeed GzmB substrates in endogenous ECM, we repeated the cleavage assay with smooth muscle cell-derived ECM. As shown in Figure 16, decorin and biglycan were indeed cleaved by GzmB when associated with an endogenous ECM. Cleavage fragments for

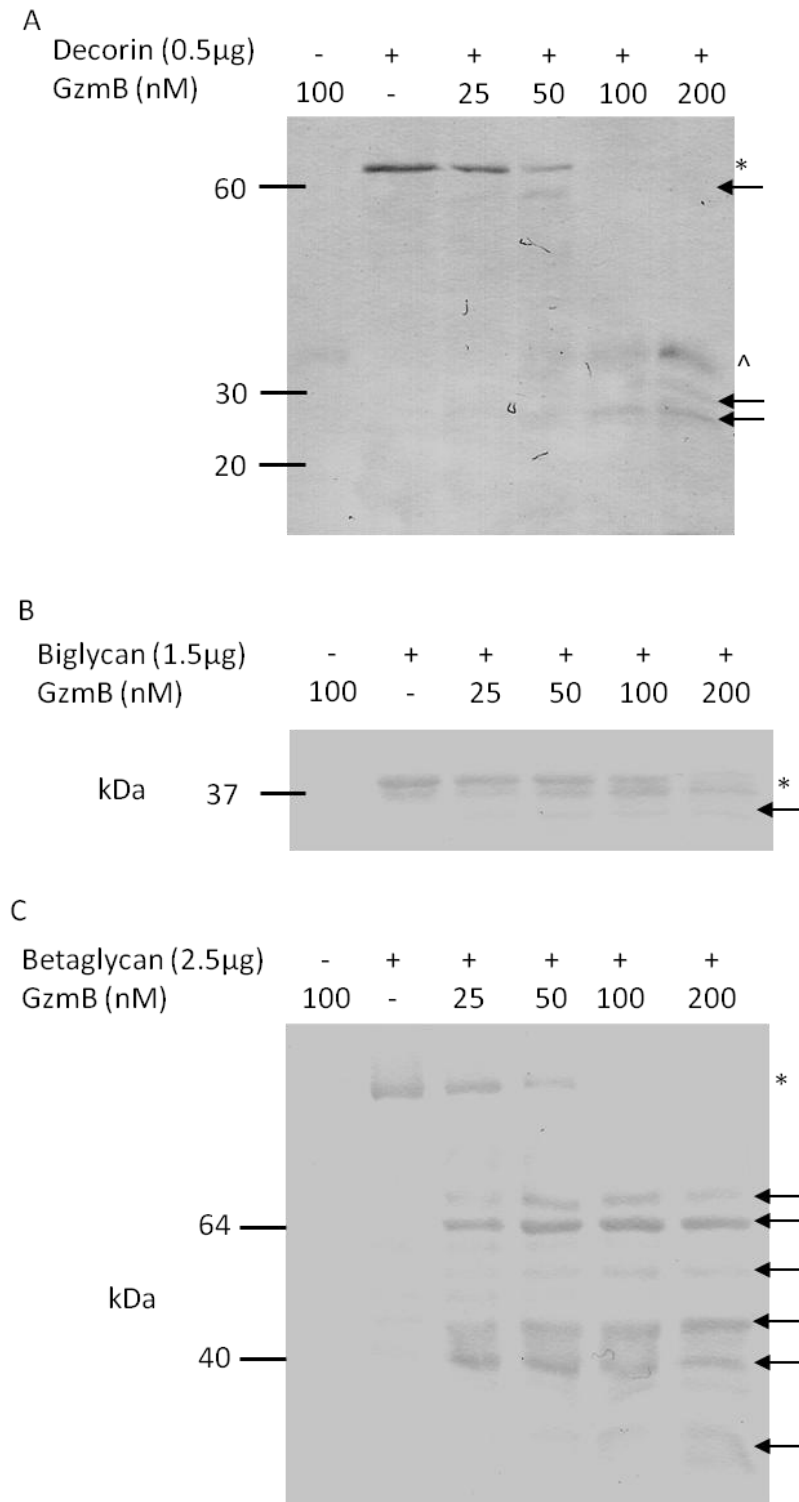


**Figure 14: GzmB-mediated Cleavage of Decorin, Biglycan and Betaglycan**

To determine if decorin, biglycan and betaglycan are substrates for GzmB, recombinant cleavage assays were conducted. Increasing concentrations of GzmB (25, 50, 100 and 200nM) were incubated with decorin (a), biglycan (b), and betaglycan (c) for 24h at RT. \* denotes full length protein, arrows indicate cleavage fragments and ^ indicates GzmB. Permission to reproduce facilitated by an open access Creative Commons License for *PLoS ONE*.

both proteins were apparent in the supernatant at around ~32kDa, the same cleavage fragment sizes seen in recombinant protein assays.

### 5.2.2 *GzmB Cleavage Site Identification*

GzmB cleavage sites were characterized in biglycan and betaglycan by Edman degradation (Figure 15 b-c). N-terminal sequence results for decorin were unable to be obtained due to low fragment yields, despite multiple trials. In biglycan, the cleavage site was identified at Ile-Ser-Pro-Asp<sup>91</sup>Thr-Thr-Leu-Leu-Asp, with a P1 residue of Asp (Figure 15 b). Interestingly, despite sequencing 6 unique bands for betaglycan, only one unique cleavage site was characterized, Asp-Glu-Gly-Asp<sup>558</sup>Ala-Ser-Leu-Phe-Thr, near the c-terminus of the protein (Figure 15c). The n-terminal sequence results of betaglycan fragments labeled by '1' corresponded to the n-terminus of the protein and the n-terminal sequence of fragments labeled with '2' corresponded to the cleavage site (Figure 15 c).

### 5.2.3 *Michaelis-Menten Kinetics*

To determine if the cleavage of decorin, biglycan and betaglycan occurs at physiologically relevant rates, Michaelis-Menten kinetics was carried out on Coomassie stained gels after 2h incubation at 37C. Kcat/Km ratios for biglycan:  $1.7 \times 10^3 \text{ M}^{-1}\text{s}^{-1}$ , betaglycan:  $5.89 \times 10^3 \text{ M}^{-1}\text{s}^{-1}$  and decorin:  $1.0 \times 10^3 \text{ M}^{-1}\text{s}^{-1}$ .

### 5.2.4 *GzmB-dependent Cleavage of Biglycan, Decorin and Betaglycan Results in the Release of Active TGF- $\beta$ 1*

As decorin, biglycan and betaglycan sequester active TGF- $\beta$ 1 [70, 71], TGF- $\beta$ 1 release assays were performed to determine if GzmB-mediated cleavage of these proteins resulted in active TGF- $\beta$ 1 release (Fig 17 a). Following 24h of incubation, negligible TGF- $\beta$ 1 had dissociated from the plate in the absence of GzmB, suggesting that the PG/TGF- $\beta$ 1 complexes were stable throughout the incubation time. After 24 h of GzmB treatment, TGF- $\beta$ 1 was

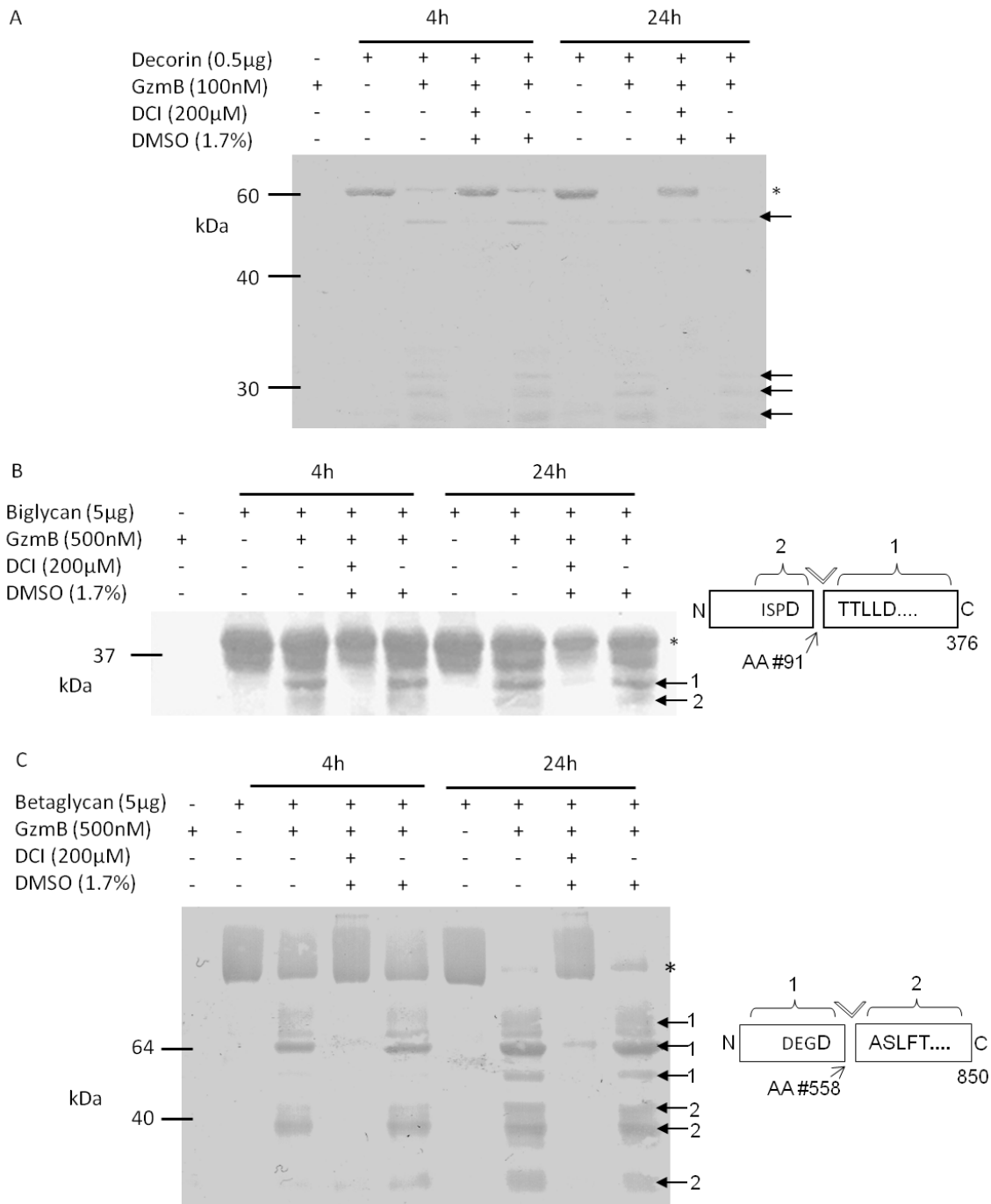


**Figure 15: GzmB-mediated PG Cleavage is Inhibited by DCI and Cleavage Site Identification**

To confirm GzmB cleavage was specific, cleavage assays were run using the inhibitor DCI and cleavage sites in biglycan and betaglycan were characterized. GzmB was incubated with decorin (a), biglycan (b) and betaglycan (c), +/- DCI and the solvent control DMSO, for 4h and 24h. Cleavage sites in biglycan and betaglycan were identified by N-terminal Edman degradation. \* denotes full length protein, arrows indicate cleavage fragments, and cleavage sites are displayed on the right. Permission to reproduce facilitated by an open access Creative Commons License for *PLoS ONE*.

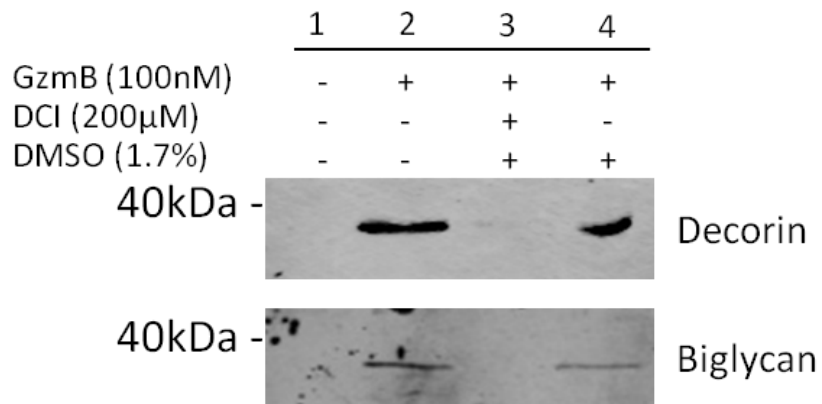


**Figure 16: GzmB Cleaves Native Smooth Muscle Cell-derived Decorin and Biglycan**

To determine that decorin and biglycan were cleaved in a physiological system, SMC ECM cleavage assays were conducted. HCASMCs were incubated at confluency for adequate ECM synthesis. Cells were removed, GzmB was incubated with the ECM and decorin and biglycan cleavage fragments were detected by western immunoblotting. Permission to reproduce facilitated by an open access Creative Commons License for *PLoS ONE*.



released into the supernatants, from all three PGs. This release was inhibited by DCI, suggesting the process was dependent on active GzmB. TGF- $\beta$ 1 release was observed at GzmB levels as low as 25 nM (Unpublished observations). In addition, TGF- $\beta$  release from betaglycan was also inhibited by 10 $\mu$ M compound 20, lot JT00025102B, a more specific GzmB inhibitor (Figure 18).

To confirm GzmB can also release TGF- $\beta$  from a heterogenous, endogenous ECM, SMC-derived ECM was utilized. However, in this closed *in vitro* setting TGF- $\beta$  is present only as a latent complex, most likely due to a lack of extracellular activators in the culture system (Figure 17 b). As decorin, biglycan and betaglycan bind and sequester active TGF- $\beta$  only, recombinant active TGF- $\beta$ 1 was supplemented on isolated ECM prior to GzmB incubation. Upon GzmB treatment, TGF- $\beta$ 1 was released from the ECM, while DCI prevented release (Figure 17 c). This suggests that GzmB can release recombinant TGF- $\beta$ 1 from a native, heterogeneous ECM, in addition to recombinant PG matrices.

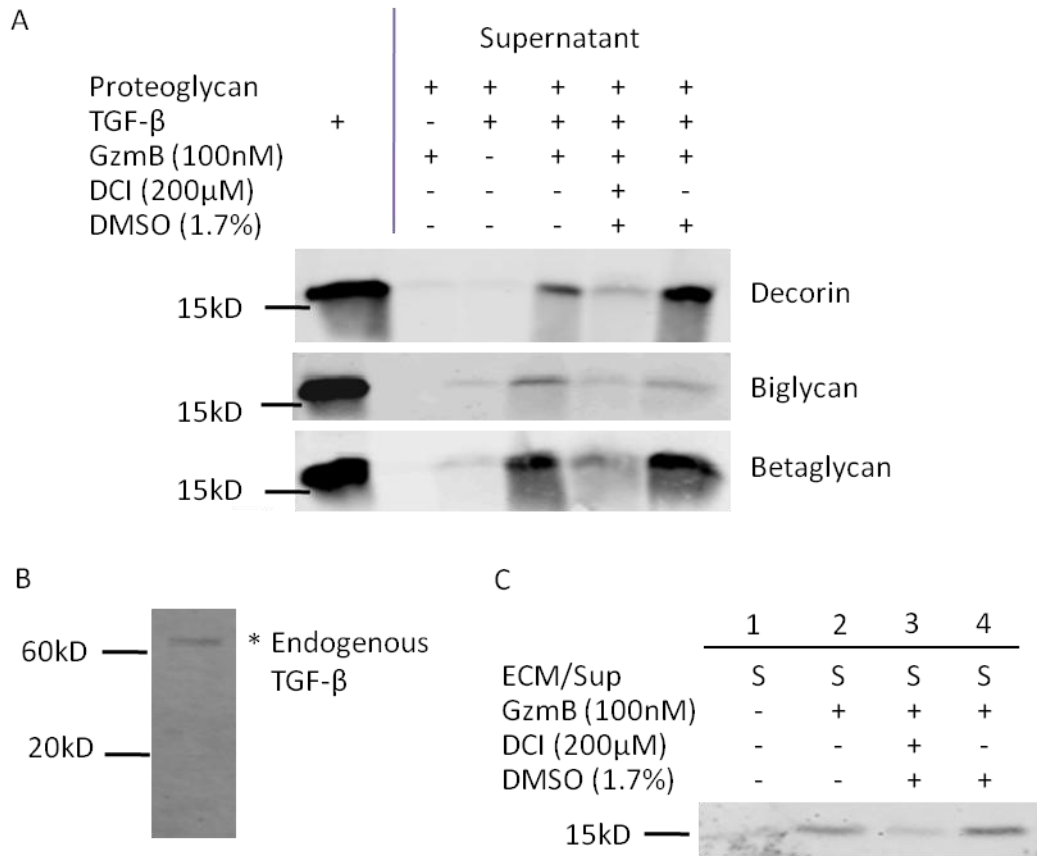


**Figure 17: GzmB-mediated Cleavage of Decorin, Biglycan and Betaglycan Results in the Release of Active TGF- $\beta$ 1**

To examine whether PG cleavage resulted in the release of active TGF- $\beta$ 1, release assays were conducted. Decorin, biglycan and betaglycan complexed with TGF- $\beta$ 1 were treated with GzmB. Supernatants (containing released TGF- $\beta$ 1), were collected and released TGF- $\beta$ 1 was detected by Western blotting. Results shown are representative western blots from at least 3 separate experiments for each PG (a). As endogenous SMC-derived ECM only contains latent TGF- $\beta$  (as shown in (b)), GzmB-mediated release from active TGF- $\beta$ 1 supplemented ECM was also examined (c). Permission to reproduce facilitated by an open access Creative Commons License for *PLoS ONE*.

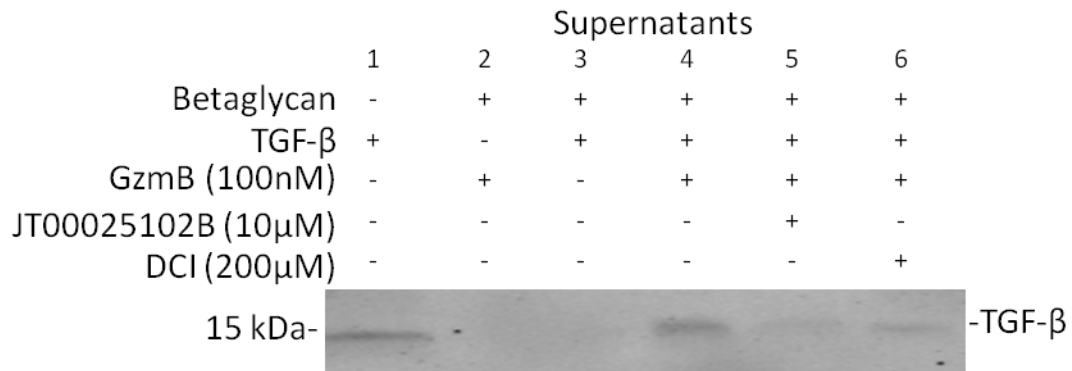


**Figure 18: Inhibition of GzmB using a Specific Small Molecule Inhibitor (JT25102B) Prevents the Release of Proteoglycan-sequestered TGF-  $\beta$ 1**

The small molecule inhibitor, compound 20, was utilized to confirm TGF-  $\beta$ 1 release by GzmB. 20  $\mu$ g/ml betaglycan was coated onto 48 well plates and incubated with 10ng of TGF- $\beta$ . Excess TGF- $\beta$  was washed off the plate and betaglycan/TGF- $\beta$  complexes were incubated with GzmB +/- inhibitors for 24h at RT. Supernatants (containing released TGF- $\beta$ ) were collected and Western blotted for TGF- $\beta$ . There is little non-specific dissociation of TGF- $\beta$  into supernatants in the absence of GzmB (2). TGF- $\beta$  is released by GzmB after 24h of incubation (4). Release is inhibited by JT00025102B (5) and partially inhibited by DCI (6).

#### *5.2.5 TGF- $\beta$ 1 Released by GzmB Remains Active and Induces SMAD Signalling in Smooth Muscle Cells*

To determine that the TGF- $\beta$ 1 released by GzmB remained active and was not bound to an inhibitory fragment, supernatants from the betaglycan release assay were incubated on HCASMC for 20 min (Fig 19). TGF- $\beta$  signaling was examined through the phosphorylation and activation of SMAD-3. HCASMC responded well to 5 ng/ml TGF- $\beta$ 1, with SMAD-3 phosphorylation observed at 20 min ( $P < 0.05$ ). The TGF- $\beta$ 1 released from betaglycan by GzmB induced SMAD-3 signaling, confirming that it remained active ( $p < 0.05$ ). Total SMAD-3 levels also did not change.

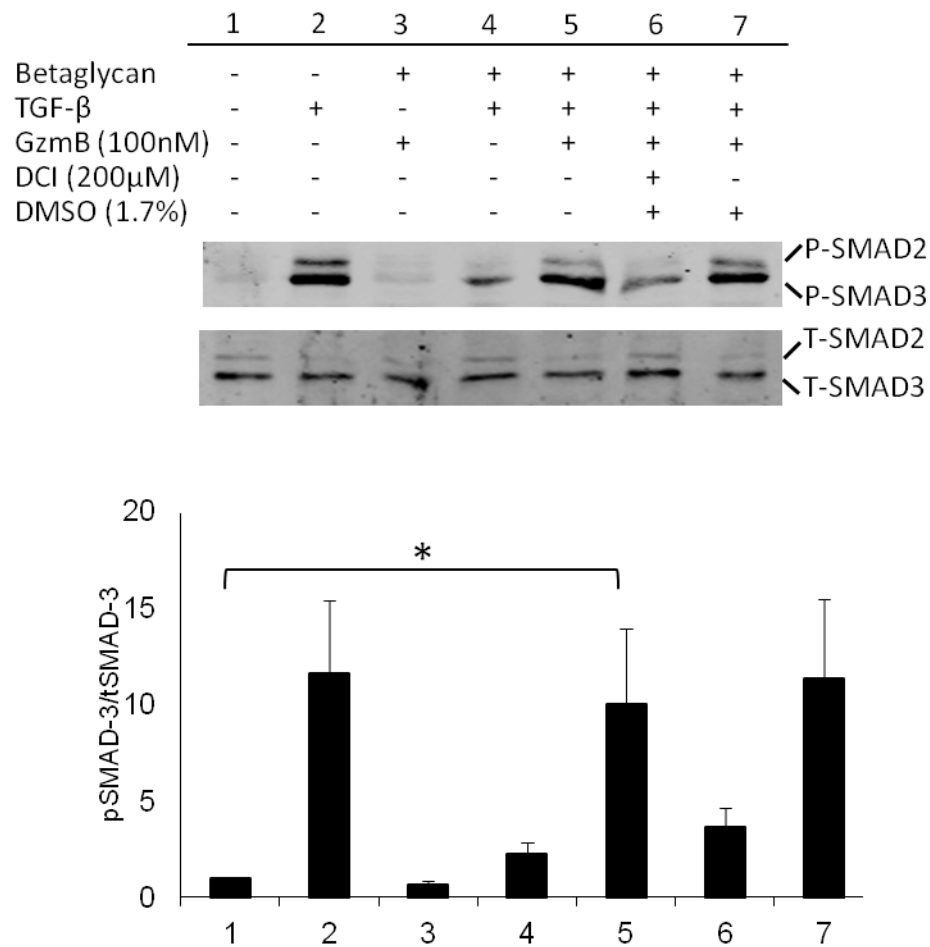


**Figure 19: TGF- $\beta$ 1 Released by GzmB is Active and Induces SMAD-3 Activation in HCASMCs**

TGF-  $\beta$ 1 bioavailability assays were carried out to verify that the GzmB released growth factor was active. GzmB +/- DCI was incubated on betaglycan/TGF- $\beta$ 1 complexes for 24h. Supernatants (containing released TGF- $\beta$ 1) were added to HCASMC for 20 m and phosphorylated SMAD-2 and SMAD-3 levels were examined. TGF- $\beta$ 1 released by GzmB is active and induces SMAD-3 signalling in HCASMCs ( $P < 0.05$ ). The result shown is representative of 5 experiments. Permission to reproduce facilitated by an open access Creative Commons License for *PLoS ONE*.

### 5.3 Discussion

In this study, we identify three novel extracellular substrates of GzmB; decorin, biglycan and betaglycan. Furthermore we demonstrate that upon cleavage of these PGs by GzmB, active TGF- $\beta$ 1 is released.

Approximately one third of GzmB is released non-specifically into the extracellular milieu during immune cell engagement/degranulation and cytotoxic lymphocytes constitutively release GzmB in the absence of target cell engagement [109, 111]. In further support of the biological relevance of non-specific release, the GzmB released into the extracellular milieu during NK killing assays is sufficient to process IL-1 $\alpha$  into a fragment with increased pro-inflammatory potential [125]. As such, even in cell culture studies there is sufficient leakage of GzmB outside of cells to promote a biological response. Additionally, under certain conditions, other non-inflammatory cell types can express and secrete GzmB (reviewed in [347]). As many of these cell types do not express Perf or form immunological synapses, an extracellular role for GzmB in pathogenesis is plausible. Indeed, in multiple chronic inflammatory conditions, GzmB accumulates in extracellular fluids including plasma, cerebral spinal fluid, synovial fluid and bronchoalveolar lavage fluid (BAL, Reviewed in [58]). In addition, IL-1 $\alpha$  fragments of similar size to GzmB processed fragments were detected in BAL from patients with cystic fibrosis, chronic obstructive pulmonary disease and bronchiectasis [125]. Given that GzmB is often detectable at levels 10 to 100-fold higher than normal in such fluids and retains its activity, it is highly probable that this protease could elicit a biological effect in the source tissues where its concentration would be expected to be significantly higher. In direct support of this, we have shown using both GzmB and Perf knockout mice that GzmB contributes to abdominal aortic aneurysm and skin aging through a Perf-independent mechanism involving ECM cleavage [193, 195].

Although the concentration range of GzmB in inflamed tissues is presently unknown, the concentrations of GzmB used in this study (25 and 50nM) are likely to be physiologically relevant in chronic inflammatory disease. Mean levels of GzmB in the plasma and synovial fluid of rheumatoid arthritis patients have been reported to be as high as 1 ng/ml and 3ng/ml respectively (compared to <40pg/ml in healthy patients), and similar increases of GzmB in bodily fluids have been reported in other inflammatory diseases [103, 104]. Levels of circulating GzmB would be expected to be several magnitudes lower than in source tissues, where GzmB is being produced and released and where ECM cleavage is observed [58].

In this study, PG cleavage was detected at GzmB concentrations as low as 25 nM, however, as the sensitivity of ponceau staining is relatively low, cleavage of these proteins may also occur at lower GzmB concentrations. In addition to recombinant protein cleavage assays, we examined biglycan and decorin cleavage from a heterogeneous matrix synthesized by smooth muscle cells (SMCs). A ~32 kDa cleavage fragment for both decorin and biglycan was detected in this assay, which were similar in size to the fragments derived from the recombinant substrate. As fragments were detected using monoclonal antibodies that recognize only one epitope of the proteins, other cleavage fragments were not detected. Soluble betaglycan was not detectable in ECM in this *in vitro* setting, suggesting it is either weakly expressed by SMCs or rarely shed by these cells *in vitro*.

In the present study, Michaelis-Menten kinetic analyses were carried out to examine if GzmB-mediated cleavage of these substrates was physiologically relevant in a biochemical context. In this environment, rates were lower than that for GzmB-mediated cleavage of aggrecan, suggesting GzmB may have a greater affinity for aggrecan than other proteoglycans [118]. It was also considerably lower than that determined for decorin cleavage by MMP 2, 3 and 7 [66]. However, biochemical assessment of *in vivo* relevance in an artificial test tube

environment obviously has its limitations with respect to recapitulating other factors and what is actually occurring the extracellular milieu that is found *in vivo*. In the context of chronic diseases such as aneurysms and skin aging, this rate is likely significant as GzmB has a high affinity for PGs leading to its increased accumulation and cleavage would occur over a prolonged period of time in areas of extracellular GzmB accumulation, as suggested in previous publications [194, 195]. In addition, several other proteases have been characterized to cleave substrates at similar rates, and have been determined to be catalytically efficient [382-386]. Nonetheless, future studies are necessary to examine GzmB-mediated proteoglycan cleavage *in vivo* and to identify GzmB-derived cleavage fragments in chronic human disease.

Despite the fact that several extracellular GzmB substrates have been identified, very few of the cleavage sites have been determined. In this study we define the GzmB cleavage sites for biglycan and betaglycan. GzmB residue preferences have been previously described, and GzmB cleavage sites have generally been characterized with a P1 residue of aspartic acid [387, 388]. Less frequently however, cleavage at non-Asp P1 residues have been reported. The most commonly characterized alternate P1 residue is Glu acid but P1 residues of Ser, Asn and Met have also been shown but are suspected to occur at lower kinetics and may be nonspecific [389, 390]. In addition to its P1 specificity, GzmB also has a preference for P3 residues that are negatively charged and P4 residues that are hydrophobic [389, 390]. P3, P2 and P1' tended to be smaller residues, most likely due to the size restrictions of the peptide binding pocket [390]. In this study, we show that GzmB cleaved these PG substrates at a P1 residue of Asp (biglycan: D<sup>91</sup>, betaglycan: D<sup>558</sup>), consistent with the literature described above. Biglycan contains a hydrophobic residue at P4 (Ile), betaglycan has a negative charge at P3 (Glu) and both contained relatively small residues in the P3, P2, P1' area, reflecting the cleavage site trends described previously [390].



Interestingly, GzmB is the only known extracellular protease capable of cleaving extracellular substrates at a P1 residue of aspartic acid. This unique specificity could potentially be used as a tool to initially screen for potential GzmB-derived fragments in bodily fluids, of these substrates and others. In addition, the acidic side chain of aspartic acid is key for ionic interactions and molecular recognition by receptors. This is of particular interest for fragments containing RGD sequences, which have various biological activities in cell signaling and disease.

Decorin, biglycan and betaglycan are known to sequester active TGF- $\beta$  [70, 71]. Therefore, we asked whether cleavage of these PGs by GzmB could release the growth factor. Matrix metalloproteases (MMP) are well characterized in their role in ECM degradation [375, 376] and cytokine/growth factor bioavailability as MMP-2, -3 and -7 have all been shown to release TGF- $\beta$ 1 from decorin [66]. To examine if GzmB may have a similar effect we utilized a similar TGF- $\beta$ 1 release assay in our studies [66]. TGF- $\beta$ 1 was released from all three substrates. In addition, the TGF- $\beta$ 1 released by GzmB induced SMAD-3 phosphorylation, confirming that GzmB releases active TGF- $\beta$ 1 and does not alter TGF- $\beta$ 1 activity. As GzmB liberates active TGF- $\beta$ 1 from the three most well described active TGF- $\beta$  reservoirs, it may be a potent factor in influencing TGF- $\beta$  bioavailability. To this end, we are not aware of another protease that has been described to release TGF- $\beta$  from all three of these extracellular proteins. In addition, there are no confirmed extracellular inhibitors of GzmB, as opposed to the MMPs, which are tightly-regulated extracellular proteases. One could speculate that GzmB may not have an extracellular means of inhibition, as it appears to accumulate specifically during sustained inflammation. As such, increased extracellular GzmB could lead to dysregulated TGF- $\beta$  release and contribute to a multitude of deleterious effects at the site of injury. However, more work is necessary to confirm this hypothesis.

TGF- $\beta$  down-regulates GzmB and Perf expression in cytotoxic T cells [391]. However, the effect of TGF- $\beta$  on GzmB expression by other cell types is currently unknown. There is potential for TGF- $\beta$  to act in a negative feedback loop in human tissue, whereby an increase in extracellular GzmB levels would lead to an increase in TGF- $\beta$  bioavailability. This could influence subsequent GzmB expression, perhaps as a safety mechanism in disease. The effect GzmB-mediated release of TGF- $\beta$  on subsequent GzmB expression warrants further investigation.

The implications of biglycan, decorin and betaglycan cleavage are illustrated in Figure 20. Proteolysis of these three proteins result in active TGF- $\beta$  release, increasing the bioavailability of the cytokine and subsequent signalling. TGF- $\beta$  signalling induces collagen synthesis, cleavage of decorin and biglycan cause an alteration in collagen structure and tensile strength and cleavage of decorin results in an increase in collagen production, all leading to fibrosis, as we see in our disease models of aneurysm and skin aging. A GzmB-dependent alteration in collagen fibre density is apparent in the adventitia of AAA vessels and in the skin of aging mice. This also corresponded with a decrease in decorin levels, suggesting these structural collagen changes were decorin-dependent.

In conclusion, the present knowledge of extracellular GzmB activity in health and disease is in its infancy [392]. In addition to identifying three novel substrates for GzmB, the present study provides further insight as to how an accumulation of GzmB in the extracellular milieu could negatively impact and/or alter growth factor sequestration by the ECM.

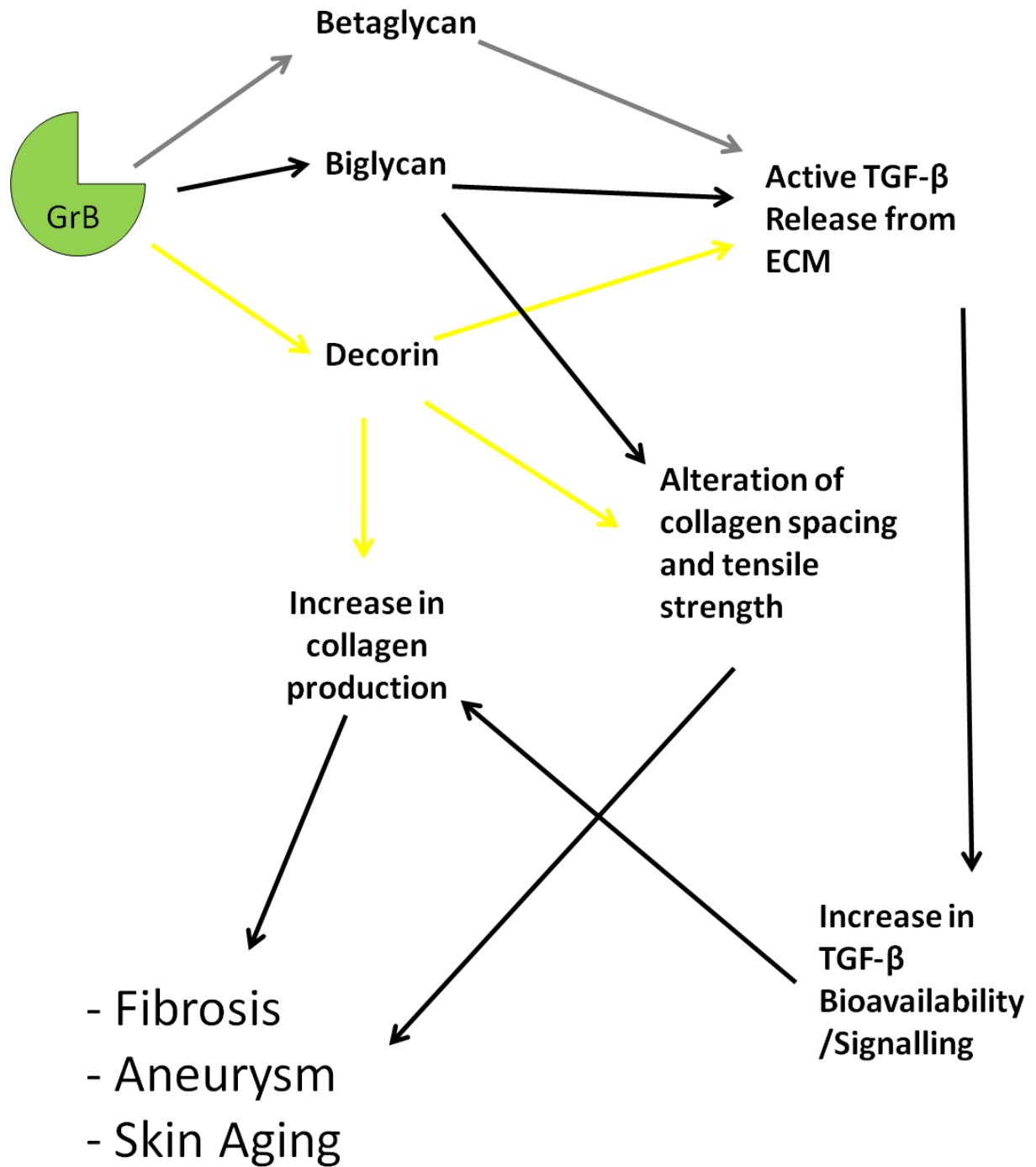


**Figure 20: Implications of Proteoglycan Cleavage in Wound Healing**

## **6. Investigating Perf-dependent and Perf-independent Roles for the Granzymes in Animal Models of Disease**

### *6.1 Introduction*

Apolipoprotein E is a mediator of the transport and clearance of circulating cholesterol. ApoE-knockout mice are hyperlipidemic and develop atherosclerosis which can be accelerated by a high fat diet. These mice tend to age faster than wild type c57 and develop hair loss and graying as well as cutaneous xanthomatosis as they age. When infused with angiotensin II, apoE-KO mice can be utilized as a model of AAA.

Perf-KO mice were used to indirectly determine whether the granzymes play a role in disease as granzymes require Perf for trafficking into target cells. However, often overlooked in this process was the Perf-independent extracellular activity of GzmB. Perf/apoE-DKO mice do not exhibit a functional intracellular GzmB activity as the protease requires Perf to enter the cytosol of target cells. However, as GzmB is released into the extracellular space in an active form and as Perf is not required for extracellular GzmB activity, these mice have fully functional extracellular GzmB activity. Thus, Perf/apoE-DKO mice can be utilized to study the extracellular activity of GzmB in isolation of its intracellular activities. As such, if Perf/apoE-DKO mice are protected against disease, the absence of the intracellular pathway of GzmB and potentially other granzymes, is likely aiding in the decrease in pathogenesis and if there is no change, intracellular GzmB activity has no effect. In the case of AAA, Perf/apoE-DKO mice had similar aneurysm incidence and rupture compared to apoE-KO controls, whereas GzmB/apoE-DKO mice were protected. This suggests the intracellular apoptosis-inducing capacity of GzmB does not play a role in aneurysm pathogenesis and that the extracellular activity of GzmB was more critical [193]. Further examination of extracellular matrix degradation through multiphoton microscopy, histology/immunohistochemistry for ECM

substrates and infusion of an extracellular GzmB inhibitor, Serpina3n, confirmed this was the case [193, 194].

Although extracellular substrates have been characterized for GzmB, the implications of their cleavage in disease was not known. Outside of infectious disease and cancer, the examination of the mechanism of GzmB activity in disease is limited in animal models. In this chapter, we examine the extracellular activity of GzmB in the apoE-KO models of skin aging, xanthomatosis, atherosclerosis and aneurysm. We also use Perf/apoE-DKO mice to examine the extracellular activity of GzmB in atherosclerosis.

We have previously shown that GzmB/apoE-DKO mice are protected from skin aging, xanthomatosis and AAA, with a reduction in incidence and severity of these phenotypes in GzmB/apoE-DKO mice compared to apoE-KO mice. We have also demonstrated that GzmB/apoE-DKO mice are protected from the collagen disorganization and structural abnormalities found in skin aging and AAA, suggesting GzmB is contributing to these diseases extracellularly. In this chapter we examine the cleavage of extracellular matrix substrates such as fibrillin-1 and decorin in atherosclerosis, skin aging and aneurysm. We also examine atherosclerosis in Perf/apoE-DKO mice.

## 6.2 Results

### 6.2.1 Evidence for GzmB-dependent Decreases in Fibrillin-1 and Decorin in Atherosclerosis, AAA and Skin Aging/xanthomatosis

#### 6.2.1.1 GzmB-dependent Reduction in Fibrillin-1 in AAA and Atherosclerosis

Fibrillin-1 levels were examined in the aortas of mice with atherosclerosis and AAA (Figure 21). After 28 days of Angiotensin II infusion for AAA and 30 weeks on a high fat diet for atherosclerosis, aortas were removed, fixed in formalin and stained by immunohistochemistry. There was reduced levels of fibrillin-1 in the media of apoE-KO mice in

both the AAA and atherosclerosis models. Interestingly, GzmB/apoE-DKO mice were protected against the loss in fibrillin-1 positivity, suggesting the loss in fibrillin-1 was GzmB-dependent.

#### 6.2.1.2 *GzmB-dependent Decrease in Adventitial Decorin in AAA*

To examine whether GzmB is capable of cleaving decorin *in vivo*, mouse AAA vessels from apoE-KO and GzmB/apoE-DKO mice were examined for decorin staining and localization. ApoE-KO mice receiving AngII-infusion exhibited a thin adventitia with diminished levels of decorin (Figure 22 a-c). The injured side of the vessels and regions adjacent to the thrombus exhibited minimal decorin positivity compared to the less damaged side of the vessel. In contrast, the majority of GzmB/apoE-DKO mice did not develop advanced AAA or experience rupture, as observed previously in Chamberlain *et al* [193] (Figure 22 d-e). With respect to the one GzmB/apoE-DKO mouse that did exhibit aneurysm in this study, decorin staining remained strong in the adventitia, suggesting there is reduced decorin degradation in GzmB-deficient mice (Figure 21 F-H)).

#### 6.2.1.3 *Reduction of Decorin in the Dermis of GzmB/apoE-DKO Mice*

To determine whether decorin levels were decreased in apoE-KO mouse skin, c57, apoE-KO and GzmB/apoE-DKO mice were grown to 30 weeks of age, euthanized and skin was stained with an anti-decorin antibody (Figure 23). In non-xanthoma skin in apoE-KO mice, decorin staining was strong in the dermis. However, in GzmB/apoE-DKO mice, decorin staining was stronger, particularly in the dermal-epidermal junction, an area critical in skin wrinkling. In xanthoma tissue, weak decorin staining was observed in lesions, whereas GzmB/apoE-DKO mice displayed stronger decorin staining in these lesions. This suggests that GzmB-deficiency is protective against decorin loss in the skin of apoE-KO mice.

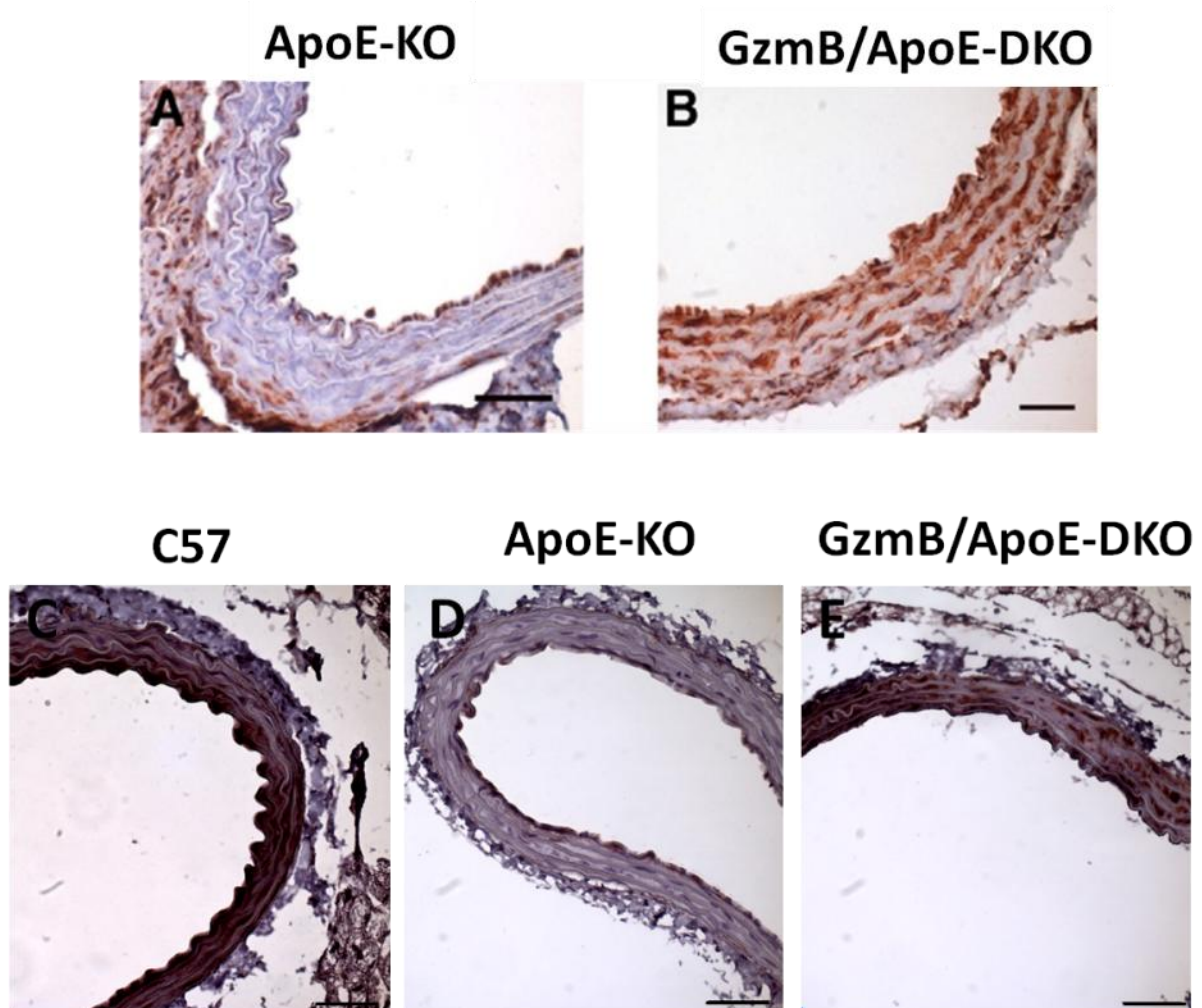
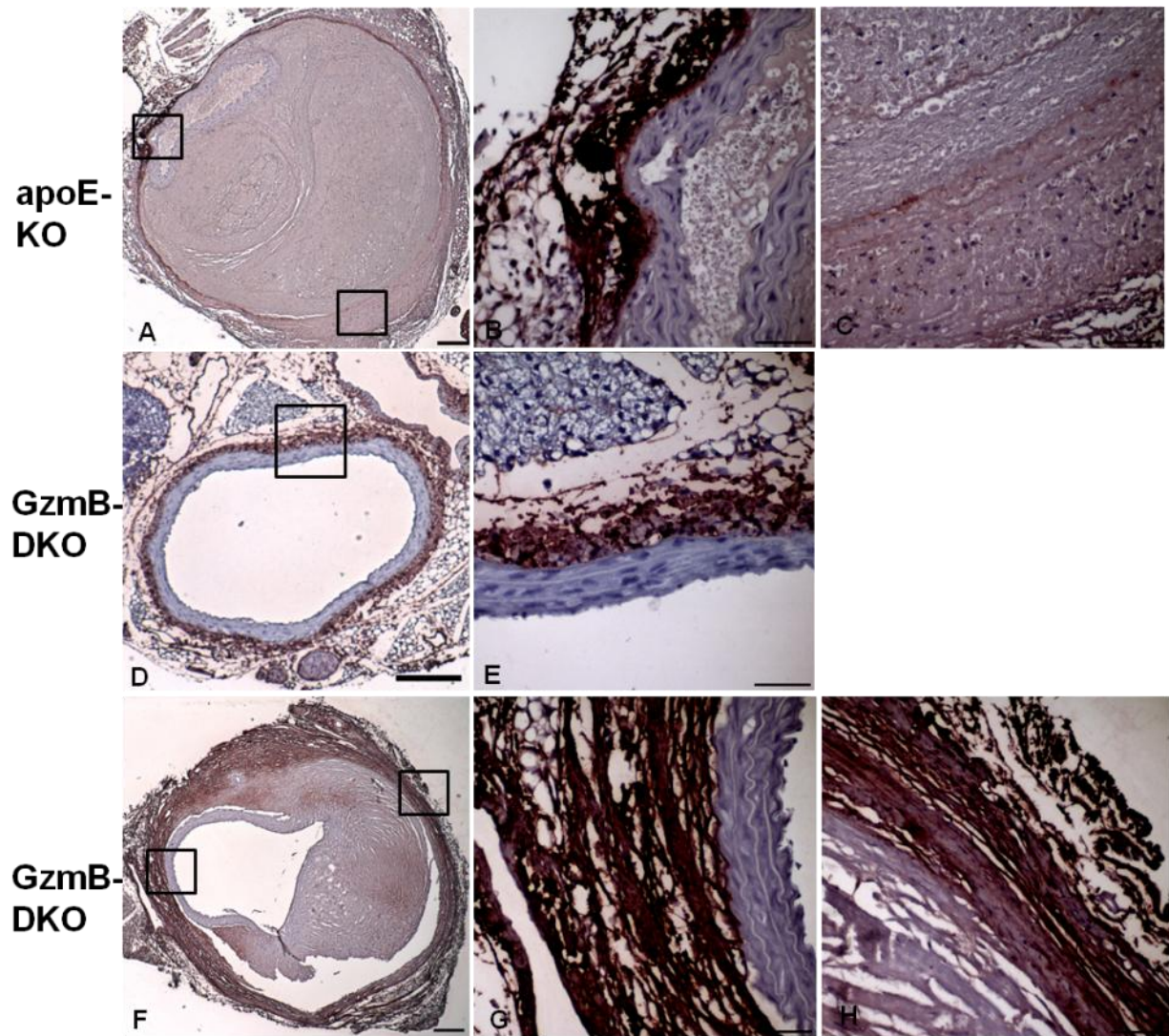


Figure modified with permission from [193]

**Figure 21: Decreased Fibrillin-1 in ApoE-KO Aortas Compared to GzmB/ApoE-DKO Aortas in Models of Atherosclerosis and Aneurysm**

Immunohistochemistry for fibrillin-1 was performed to examine the protein in atherosclerosis and AAA. For AAA, mice at 3 months of age were infused with angiotensin II for 28 days. Mice were euthanized by CO<sub>2</sub> inhalation, vessels perfused and aortic sections were fixed, embedded, sectioned and stained for fibrillin-1. Decreased fibrillin-1 staining, as indicated by red, was observed in Ang II-infusion ApoE-KO (a) mice versus Ang II-infusion GzmB/apoE-DKO mice (b). For atherosclerosis, after 30 weeks on a high fat diet, c57, apoE-KO and GzmB/apoE-DKO mice were euthanized, vessels perfused and aortas were also stained for fibrillin-1. C57 (c) and GzmB/apoE-DKO (e) mouse aortas contained strong fibrillin-1 staining compared to the aortas of apoE-KO mice (d) (Scale bars = 50  $\mu$ m). Permission to republish granted through the Copyright Clearance Center for *The American Journal of Pathology*.





**Figure 22: GzmB –dependent Loss of Adventitial Decorin in Abdominal Aortic Aneurysm**

To examine adventitial decorin levels in AAA vessels immunohistochemistry for decorin was conducted. Three month old apoE-KO and GzmB/apoE-KO mice were implanted with mini-osmotic pumps containing angiotension II, to induce aneurysm formation. After 28 days of infusion, mice were euthanized, perfused with saline and 10% formalin and aortas were fixed and embedded. In apoE-KO mice (a-c) (which are prone to AAA and aortic rupture) there is minimal decorin localization in the adventitia (b), with virtually no localization on the side of the rupture (c). However, in GzmB/apoE-DKO mice (which were less prone to AAA development and rupture), there is strong adventitial decorin staining (d-h). a, d, e scale bars 200 $\mu$ M, b, c, e, g, h scale bars 50 $\mu$ M.



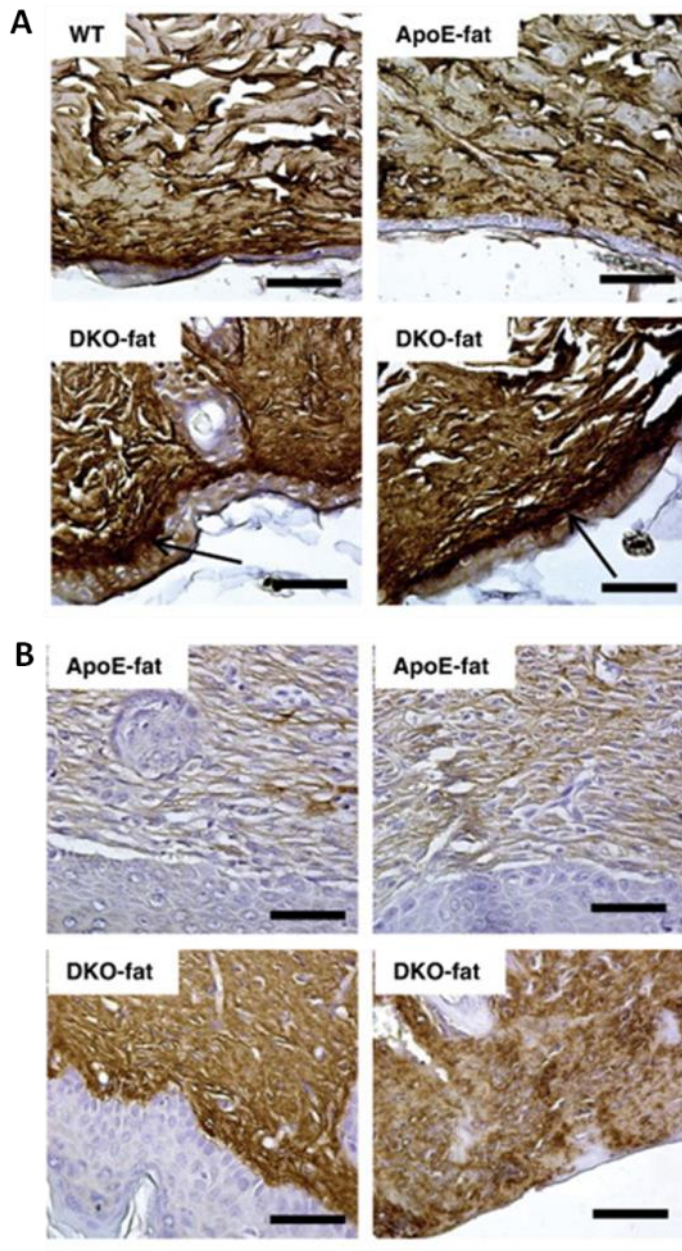


Figure modified with permission from [195]

### Figure 23: Decorin in the Papillary Dermis of C57, ApoE-KO and GzmB/apoE-DKO Mice

To examine decorin levels in the skin of apoE-KO mice, immunohistochemistry for decorin was conducted. At 30 weeks of age c57, apoE-KO and GzmB/apoE-DKO were euthanized and skin was fixed in 10% formalin. Normal skin (a) and xanthoma skin (b) were stained for decorin (brown). C57 and GzmB/apoE-DKO mice displayed strong immunostaining for decorin at the dermal-epidermal junction of the skin whereas apoE-KO skin had weak staining at the junction. In xanthoma skin, GzmB/apoE-DKO skin contained strong decorin staining throughout the dermis compared to apoE-KO skin which contained only weak patchy diffuse staining. Scale

bars= 25 Permission to republish granted through the Copyright Clearance Center for the journal of *Experimental Gerontology*.

## 6.2.2 Characterization of *GzmB/apoE-DKO* and *Perf/apoE-DKO* Mice in Atherosclerosis

### 6.2.2.1 *C57, ApoE-KO, GzmB/apoE-DKO and Perf/apoE-DKO Mice*

For atherosclerosis studies C57 (n=25), apoE-KO (n=26), Perf/apoE-DKO (n=26) and *GzmB/apoE-DKO* (n=19) mice were fed a high fat diet for 30 weeks. Prior to euthanasia at 36 to 38 weeks of age, mice were weighed (Figure 24). C57 mice had a large amount of adipose tissue due to the high fat diet and averaged  $48\text{g} \pm 1.3$ . ApoE-KO mice were significantly lighter with much less adipose than c57 mice and averaged  $30\text{g} \pm 0.9$ . Interestingly, Perf/apoE-DKO and *GzmB/apoE-DKO* mice were significantly heavier than apoE-KO mice and significantly lighter than C57 mice at  $42\text{g} \pm 1.5$  for Perf/apoE-DKO and  $41.7 \pm 1.8$  for *GzmB/apoE-DKO* mice.

Upon euthanasia, apoE-KO *GzmB/apoE-DKO* and Perf/apoE-DKO mice had enlarged spleens compared to c57 controls. There was less visceral fat surrounding the aortas of apoE-KO and Perf/apoE-DKO mice compared to that of c57 mice. Several Perf/apoE-DKO mice had visible tumours on their livers. No tumours were observed in *GzmB/apoE-DKO*, apoE-KO or c57 mice. Two Perf/apoE-DKO mice died suddenly but upon dissection, the cause of death was unknown.

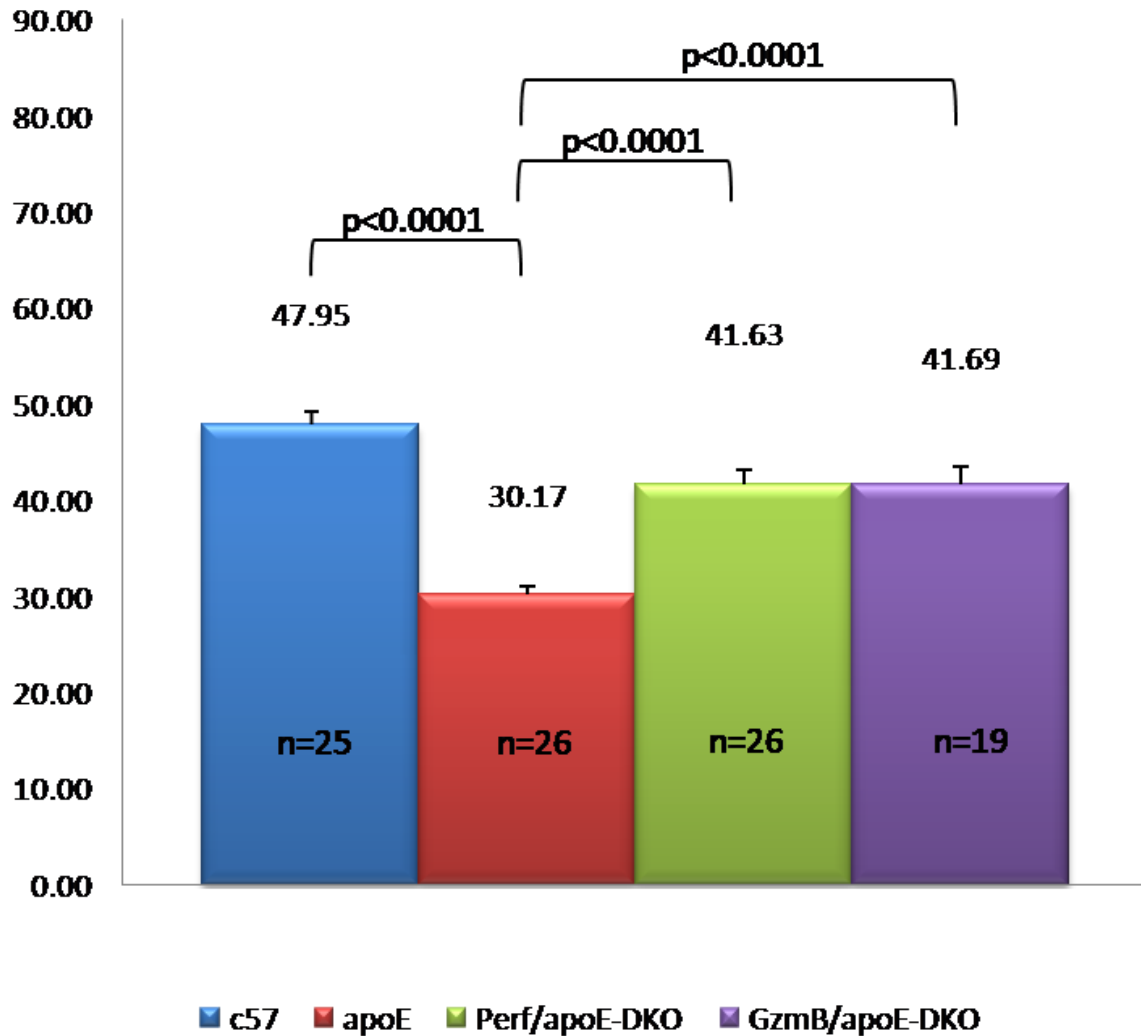


**Figure 24: Perf/apoE-DKO Mice and GzmB/apoE-DKO Weigh Significantly more than ApoE-KO Mice**

Weights across C57, apoE-KO, Perf/apoE-DKO and GzmB/apoE-DKO mice are graphed. Mice were fed a high fat diet for 30 weeks and at 36-38 weeks of age final weights were taken. ApoE-KO mice were significantly lighter than C57 controls. GzmB/apoE-DKO and Perf/apoE-DKO mice were significantly lighter than C57 and significantly heavier than apoE-KO mice.

#### *6.2.2.3 Reduced Atherosclerosis in GzmB/apoE-DKO and Perf/apoE-DKO Mice*

At 30 weeks on the high fat diet, aortas were removed, opened and en face stained with Sudan IV (Figure 25). No plaque was detected in C57 controls. Both Perf/apoE-DKO and GzmB/apoE-DKO mice had reduced atherosclerotic plaque area compared to apoE-KO mice by en face staining. Percent plaque area was  $38.32\% \pm 2.45$  for ApoE-KO mice versus  $29.11\% \pm 2.81$  for GzmB/apoE-DKO mice and  $18.56\% \pm 2.53$  for Perf/apoE-DKO mice. There was no apparent difference in the distribution of plaque throughout the aorta between the different genotypes.

#### *6.2.2.4 Cholesterol and Triglyceride Plasma Levels*

To determine whether the decrease in aortic plaque was due to changes in plasma lipid levels, total cholesterol and triglycerides were quantified (Figure 26). There was no decrease in plasma lipid levels in Perf/apoE-DKO mice or GzmB/apoE-DKO mice, suggesting the protection against atherosclerosis was not lipid-dependent.

#### *6.2.2.5 GzmB Expression in ApoE-KO Plaques*

To examine GzmB in atherosclerotic plaques, GzmB immunohistochemistry was carried out (Figure 27). GzmB/apoE-DKO mice displayed no staining as expected, confirming the antibody was specific. ApoE-KO mice displayed high levels of extracellular GzmB throughout the plaques. Perf/apoE-DKO mice showed much less staining, suggesting that the absence of Perf reduced GzmB expression in atherosclerosis.

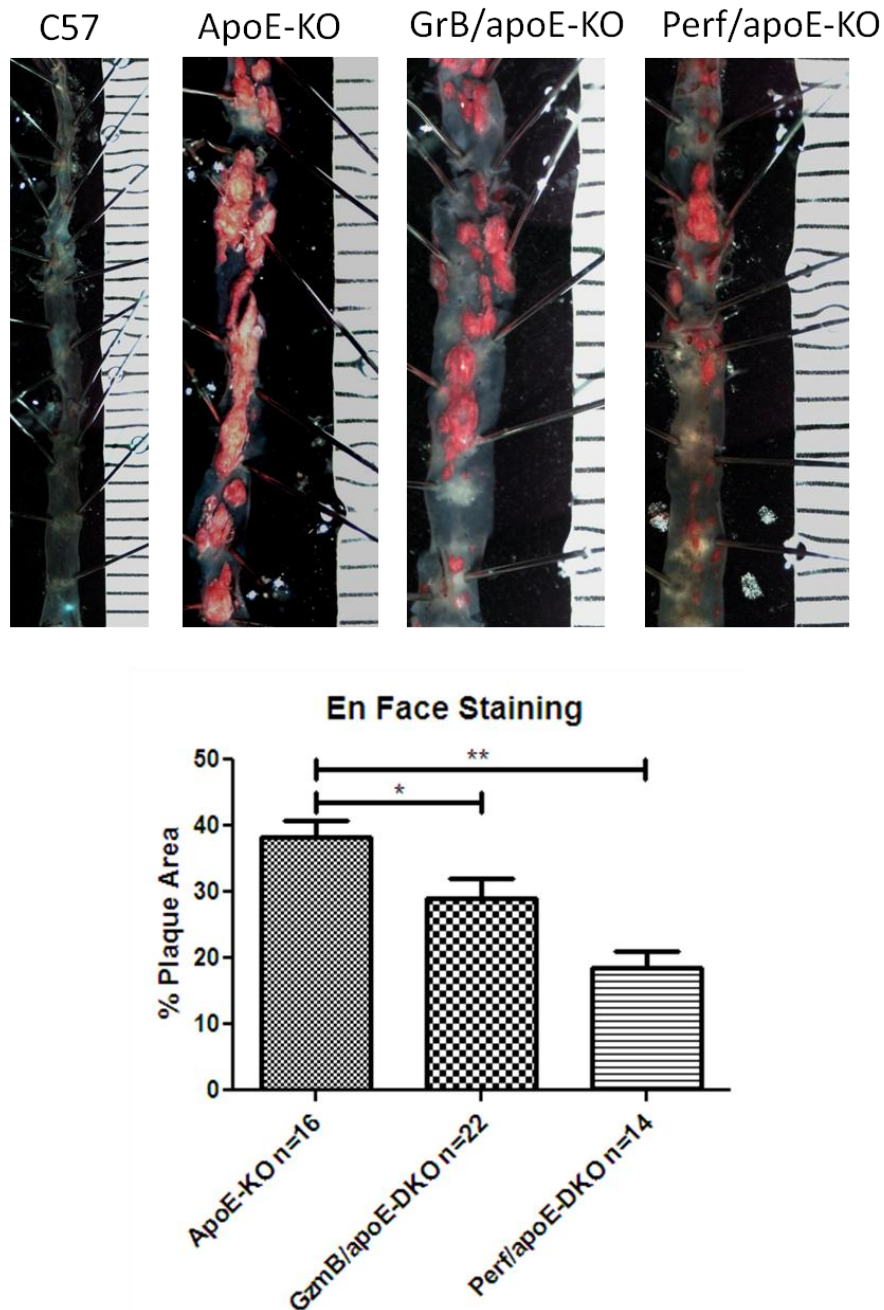


**Figure 25: En face Staining for Atherosclerotic Plaque**

En face staining of mouse aortas were performed to examine aortic plaque areas across the different genotypes. C57 controls, ApoE-KO, GzmB/apoE-DKO and Perf/apoE-DKO mice were euthanized at 30 weeks on a high fat diet. Aortas were opened and stained en face. GzmB/apoE-DKO and Perf/apoE-DKO mice had significantly less plaque than apoE-KO mice (apoE-KO: 38.32%, GzmB/apoE-DKO: 29.11%, Perf/apoE-DKO: 18.56%). A one way ANOVA with a Bonferroni's post test was utilized with Prism Graphpad software. \* p < 0.05, \*\* p < 0.0001

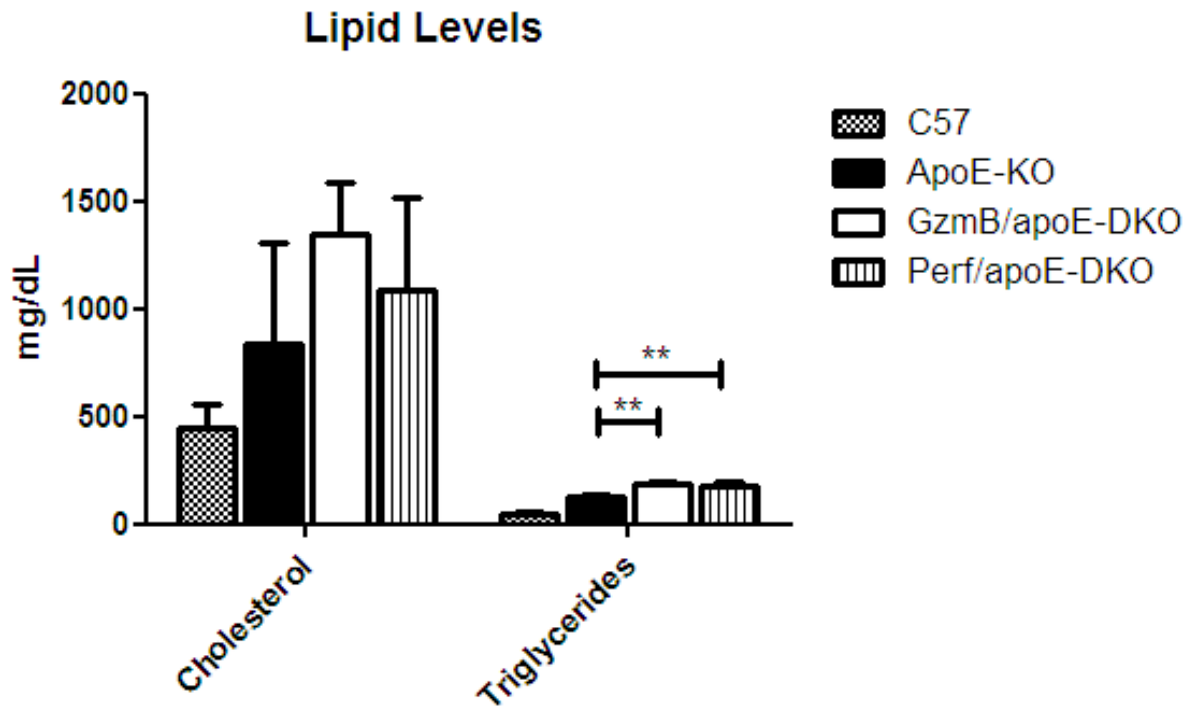


**Figure 26: Cholesterol and Triglyceride Levels in Mouse Plasma**

The decrease in aortic plaque in Perf/apoE-DKO mice is not due to a decrease in lipid levels. Cholesterol was detected at a 1:100 dilution of plasma and triglycerides was detected at a 1:16 dilution. A one way ANOVA with a Bonferroni's post test was utilized with Prism Graphpad software. \*\* p<0.0001

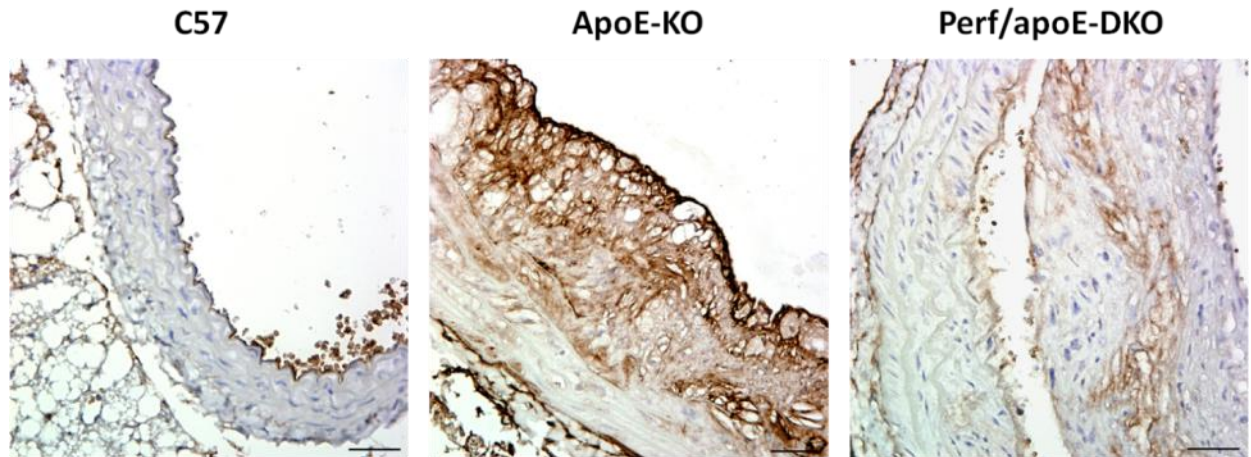


**Figure 27: Reduced GzmB Staining in the Perf/apoE-DKO Mouse Aorta**

C57, ApoE-KO and Perf/apoE-DKO mice were immunohistologically stained for GzmB. Strong extracellular GzmB staining was apparent in the plaques of ApoE-KO mice, however GzmB levels were vastly decreased in Perf/apoE-DKO mice. Scale bars = 50 $\mu$ m.



### 6.3 Discussion

In this chapter we describe a reduction in fibrillin-1 levels in apoE-KO mice compared to GzmB/apoE-DKO mice in AAA and in atherosclerosis, suggesting that GzmB is cleaving fibrillin-1 *in vivo*. In AAA, this loss in fibrillin-1 occurs in the media of vessels where there is elastin breakage and medial disruption in apoE-KO mice [193]. Fibrillin-1 fragments were also found in the serum of apoE-KO mice in AAA [193]. The medial disruption is inhibited in GzmB/apoE-DKO mice, suggesting that cleavage of fibrillin-1 in the microfibrils of elastin may be disrupting elastin structure and stability. Fibrillin-1 is the major scaffolding component of microfibrils and is important in vessel stability. It is associated with elastin in the elastic lamellae in the tunica media of the vessel wall. Fibrillin-1 also connects elastic lamellae to each other, SMC and endothelial cell basement membranes providing structural support to the vessel [393, 394]. Fibrillin-1-knockout mice die due to aneurysm rupture and have abnormal elastic lamellae [395, 396], thus degradation of fibrillin-1 by GzmB could lead to medial disruption and aneurysm rupture.

In the present chapter we demonstrate that adventitial decorin is reduced in apoE-KO aneurysms at sites adjacent to thrombi and in areas of injury. GzmB-deficiency prevented this reduction in decorin leading to a thickened, potentially healed, adventitia. It is interesting to note that decorin levels remained elevated in the adventitia in the only aneurysm observed in the GzmB/apoE-DKO group. Although it is unclear as to why medial disruption occurred in this vessel, it does illustrate a marked difference in adventitial thickness and decorin staining compared to that of the AngII-treated apoE-KO group. Whether reduced decorin degradation leads to increased circumferential strength requires further elucidation, however, in previous work we did observe a reduced incidence of rupture in GzmB/apoE-DKO mice compared to apoE-KO mice [193]. In a subsequent study, we demonstrate that adventitial decorin is reduced



in apoE-KO aneurysms at sites adjacent to thrombi and in areas of injury [194]. GzmB-deficiency and/or inhibition prevented this reduction in decorin leading to a thickened, healed, adventitia. Of further interest, elevated GzmB [193] and reduced decorin [397, 398] are observed in human aneurysm specimens. Adventitial collagen is critical for vessel strength/stability and collagen homeostasis/spacing is regulated by decorin, suggesting that decorin degradation would exert a negative impact on aortic wall strength and increased susceptibility to rupture [94].

Decorin levels are also decreased in normal and xanthoma skin in apoE-KO mice compared to GzmB/apoE-DKO mice. We have recently shown that GzmB/apoE-DKO mice are protected from the skin aging and frailty characteristic of aged apoE-KO mice and that GzmB localization corresponds to areas of decorin degradation in apoE-KO mice [195]. The collagen fiber density loss evident in apoE-KO mice was not evident in GzmB/apoE-DKO mice, suggesting GzmB-mediated degradation of decorin may result in collagen remodeling in aging skin. Importantly with respect to the present work, these studies support the premise that GzmB-mediated decorin cleavage occurs *in vivo*.

Our laboratory has previously shown that GzmB is present in human atherosclerotic lesions and that increased expression corresponds to increased disease severity [16]. However, no work on murine knockout models had been previously described. In this study we found high GzmB levels in atherosclerotic plaques from apoE-KO mice and vastly decreased levels in Perf/apoE-DKO mice. In addition, GzmB/apoE-DKO mice and Perf/apoE-DKO have reduced aortic plaque area compared to apoE-KO mice by en face staining. Interestingly, GzmB/apoE-DKO mouse plaque content was higher than that of Perf/apoE-DKO mice, which suggests that the Perf-dependent roles of GzmB may contribute to atherosclerosis. However, as Perf/apoE-DKO mice are less atherosclerotic than GzmB/apoE-DKO mice, this also suggests the other

granzymes may be important in atherosclerosis progression. The Perf-dependent roles of the other granzymes are less established than that of GzmB and will be the topic of future investigation. GzmA and GzmK have been shown to induce caspase-independent apoptosis through cleavage of the SET complex, but the concentrations of GzmA required for apoptosis induction are in the millimolar range [106, 399]. Other Perf-dependent roles for GzmA has been established in the inflammasome and cytokine production, suggesting Perf may be important for granzyme -induced inflammation [106]. It is also possible Perf may be facilitating atherosclerosis progression independent of the granzymes, however such a role for the pore forming protein has yet to be established. Either way, future studies are required to determine the functional roles of the other granzymes and Perf. We attempted to examine the other granzymes in our sections through immunohistochemistry but unfortunately the antibodies that we received from a non-commercial source were non-specific and unusable.

A previous study using the LDLr-KO model showed that Perf/LDLr-KO mice were not protected against atherosclerosis pathogenesis compared to LDLr-KO controls [294]. This is contradictory to our study but discrepancies may be indicative of the different models or perhaps the variation in time points (our studies were carried out at 30 weeks on high fat diet compared to the LDLr-KO study of 16 weeks). This was the case with previous work carried out in our laboratory which found no difference in atherosclerosis between apoE-KO and GzmB/apoE-DKO mice at 3 months on a high fat diet (data not shown). This suggests GzmB may play a more critical role in advanced atherosclerosis compared to the early stages of the disease. Unfortunately there are no good models of plaque rupture in mice to assess this hypothesis. However, our studies in angiotensin II treated mice and aneurysm rupture may support such a phenomenon.

In summary there is a GzmB-dependent decrease in fibrillin-1 levels in mouse models of atherosclerosis and AAA and a decrease in decorin in mouse models of skin aging and AAA, suggesting GzmB is acting extracellularly on these substrates *in vivo*. Perf/apoE-DKO mice had a decreased incidence in atherosclerotic plaque and a smaller plaque cross-sectional area compared to ApoE-KO and GzmB/apoE-DKO mice, suggesting that the Perf-dependent activities of the granzymes are critical in atherosclerosis.

## **7. Preliminary Studies in the Hair Follicle Cycle and in Ultrastructural Alterations of the Skin**

### *7.1 Introduction*

#### *7.1.1 Preliminary Study 1: GzmB in the Hair Follicle Cycle*

The skin is the largest organ of the body and the largest component of the skin is extracellular matrix. The skin consists of an outermost layer called the epidermis which is largely composed of keratinocytes and the dermis which consists of extracellular matrix, hair follicles, blood vessels, lymphatic vessels, nerves and glands. GzmB is expressed in the skin and sources of GzmB in the skin include immune cells such as mast cells, basophils and CTLs and non-immune cells such as keratinocytes [7, 10, 15, 107, 140, 214].

GzmB is present in alopecia areata but in order to examine the pathogenesis of hair loss, an understanding of normal hair follicle cycling is necessary. The hair follicle consists of the hair shaft (HS), the dermal papilla which regulates hair cycling, the inner root sheath (IRS) which helps mold the hair, the outer root sheath (ORS) which is an extension of the epidermis, the hair bulge which contains dermal stem cells, the pili muscle which can elevate the hair shaft and the sebaceous gland. Mammalian hair follicles undergo a growth cycle which involves transitions through a rapid growth phase (anagen), an apoptotic regression phase (catagen) and a quiescent resting phase (telogen) [400, 401]. During the telogen to early anagen transition, the DP transiently proliferates and down grows into the dermis followed by proliferating epithelial cells derived from the hair bulge stem cell region. Epithelial cells in the hair bulb undergo rapid proliferation during later anagen stages to form the HS and the inner root sheath (IRS) that surrounds the shaft also grows and differentiates. During the anagen to catagen transition, cell proliferation halts and cells in the bulb begin to undergo apoptosis as the hair follicle structure involutes. In catagen, extensive apoptosis promotes regression into the telogen resting phase in

which no proliferation, differentiation or apoptosis occurs and follicles rest before entering a new anagen phase. Potential mediators of hair follicle cycling have been characterized such as the growth factors TGF- $\beta$  and EGF but the detailed mechanisms of anagen to catagen transition are not well understood [402, 403]. The length of the hair shaft is dependent on the length of anagen and alterations in hair follicle cycling and hair fiber shedding may lead to hair loss [404].

The role of GzmB in hair follicle cycling has not been described but in order to understand how it may play a role in alopecia, it is first necessary to examine its role in normal cycling. In this chapter, we characterize Perf and GzmB expression throughout the hair follicle cycle using a depilation model of hair follicle cycling in C3H HeJ mice.

#### *7.1.2 Preliminary Study 2: Collagen and Nerve Abnormalities by Transmission Electron Microscopy*

Apolipoprotein E-knockout mice are an established model of aging as mice develop cardiovascular and neurological aging as well as skin/hair thinning [405]. ApoE-KO mouse skin displays altered collagen spacing and structure [195] and as described in chapter 6, display less decorin in the skin compared to C57 controls. On a high fat diet, these mice display hair loss and greying [195, 405]. ApoE-KO mice also have neurological defects as the blood barrier permeability increase with age is even higher for apoE-KO mice [406]. When fed a high fat diet, loss of cochlear ganglion cells was evident in apoE-KO mice [407]. However, nothing is known regarding the nerves in the skin of aging apoE-KO mice.

Transmission electron microscopy is an excellent methodology for examining structural changes in the extracellular matrix and nerves in the skin. By first examining structural changes in apoE-KO mouse skin, we can examine the potential protection from such changes in GzmB/apoE-DKO mice. In this chapter we examine structural changes in the extracellular matrix and in skin nerves of ApoE-KO mice using toluidine blue histology and transmission electron microscopy.

## 7.2 Results

### 7.2.1 Preliminary Study 1: GzmB in the Hair Follicle Cycle

#### 7.2.1.1 GzmB Protein Expression in Hair Follicles Throughout the Hair Growth Cycle

GzmB expression was evident in various phases of the follicle cycle in various cell types of the hair follicle and skin, and its expression changed distinctively throughout the hair cycle (Table 5, Figure 28a). Positive labeling was not apparent in control sections lacking secondary antibody and positive labeling localization changed with the stages of the follicle cycle, indicating the antibody was specific.

On day zero, one hour after hair plucking, GzmB was present in follicles. In particular, the arrector pili muscle was positive for the protein, most strongly at the point of insertion with the hair follicle bulge (Fig 28a). The epithelial bulge was also positive at this stage.

At 4 and 8 days post-depilation (early anagen I-III and early anagen III-V), the lower portion of the pili muscle and epithelial bulge were again positive. At day 8, in contrast to previous stages, the matrix was slightly positive for GzmB. GzmB immunopositivity was also evident in the DP cells as well as in the differentiating inner root sheath. GzmB expression by these cells has not been previously documented.

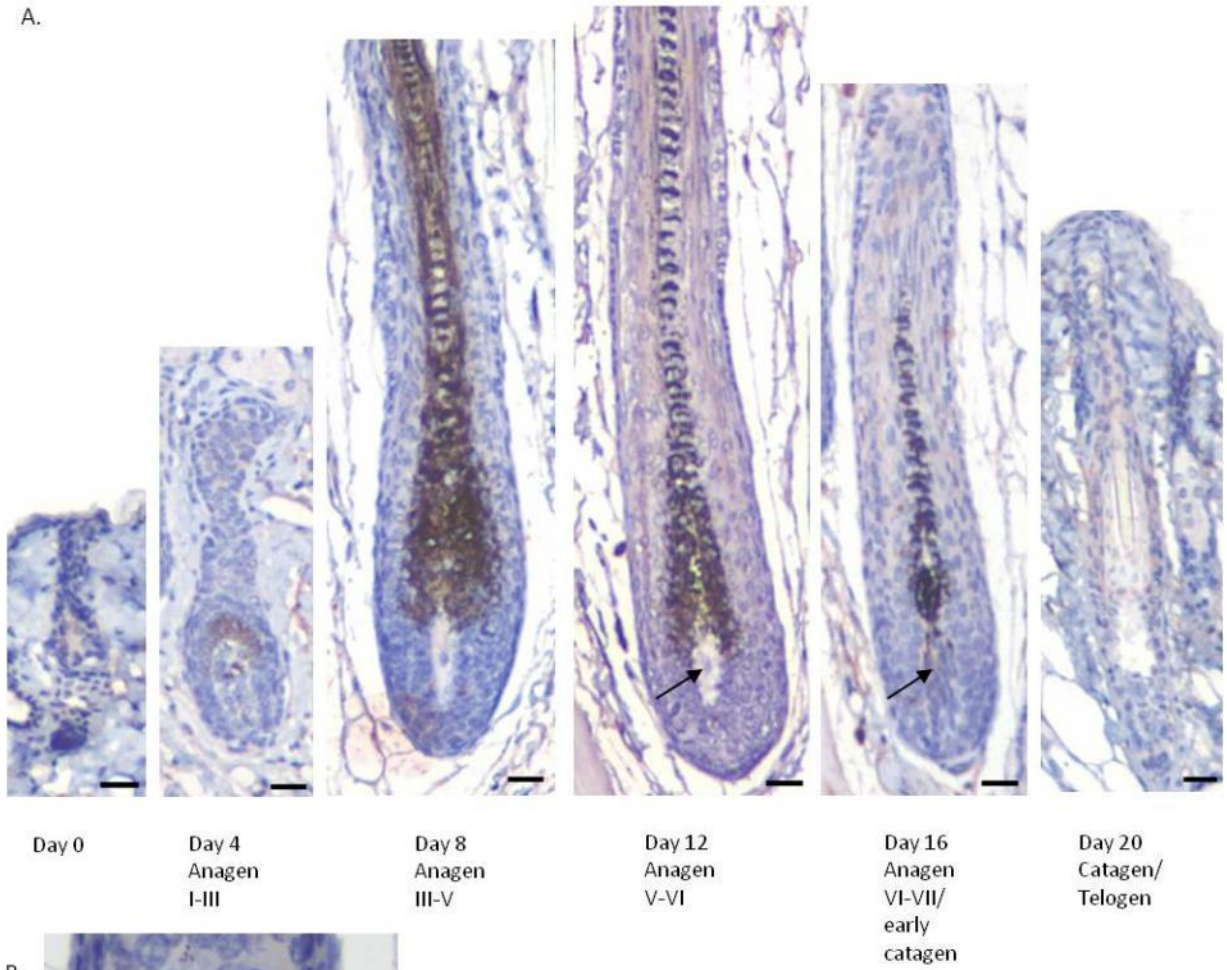
At day 12 (anagen V-VI) no difference in GzmB expression was apparent in the arrector pili muscle or the epithelial bulge. In contrast to early anagen, there was no GzmB expression in the matrix. However the apex of some DP and inner root sheath remained positive during this stage (Figure 28a, b).

At late anagen VI-VII-early catagen (day 16 post depilation), there was no GzmB in the pili muscle, however the epithelial bulge exhibited stronger positivity. Similarly to anagen V-VI, the apexes of select DP were positive and the inner root sheath displayed slight positivity. The GzmB labeling in DP was distinct from the dark black melanin pigment present in the

melanocytes, hair shaft matrix, and hair shaft. The matrix did not contain GzmB. At day 20 (late catagen, telogen) some follicles exhibited GzmB expression in the arrector pili muscle and the epithelial bulge was positive. The DP did not express GzmB and matrix remnants were negative.

The inner root sheath, whenever present, was consistently positive for GzmB, indicating these cells actively expressed the protein. The apex of the DP was positive for GzmB in late anagen and early catagen, during hair follicle regression (a stage of active apoptosis), as shown in Figure 28b, where positive GzmB expression is better illustrated in a section lacking the natural hair shaft melanin pigment. The non-follicular epithelium did not exhibit GzmB expression at any point of the cycle.

A.



B.

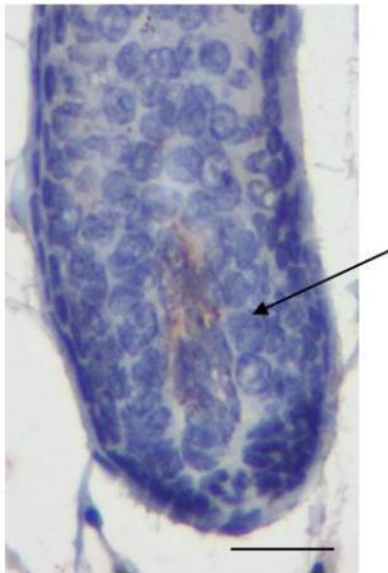




**Figure 28: GzmB Expression throughout the Hair Follicle Cycle**

GzmB was expressed in the inner root sheath and the apex of the DP from day 8-16 (anagen III-early catagen, denoted by arrows) (a) This light brown GzmB-labeling should not be confused with the dark black melanin pigment present in melanocytes and the hair shaft. A high magnification image (60x) of a representative DP from day 16, clearly displaying GzmB<sup>+</sup> positivity, in a section lacking melanin pigment (b). The negative control displayed no labeling throughout the follicle cycle. Scale bars = 20μm.

**Table 5: GzmB Localization Throughout the Hair Follicle Cycle**

	Pili Muscle	bulge	Dermal papillae	Inner root sheath	Matrix	Mast cells
0	+	+	+/-	-	-	++
Anagen I- (day 4)	+	+	-	-	-	++
Anagen -V (day 8)	+	+	+	+	+	++
Anagen V-VI (day 12)	+	+	+	+	-	++
Anagen VI-/ early catagen (day 16)	-	++	+	+	-	++
Catagen/ Telogen (day 20)	+/-	++	-	-	-	++

### 7.2.1.2 *Perf Expression Through the Hair Growth Cycle*

Perf expression, as determined by immunohistochemistry, was minimal throughout the follicle cycle (Figure 29). Apart from positivity in immune cells throughout the dermis and weak positivity in the inner root sheath, there was little expression in the skin. The hair follicle was largely negative for Perf, however weak expression was apparent in the stalk region of the DP from anagen V to catagen (day 12-20), a point of active apoptosis in the hair follicle cycle (Figure 29).

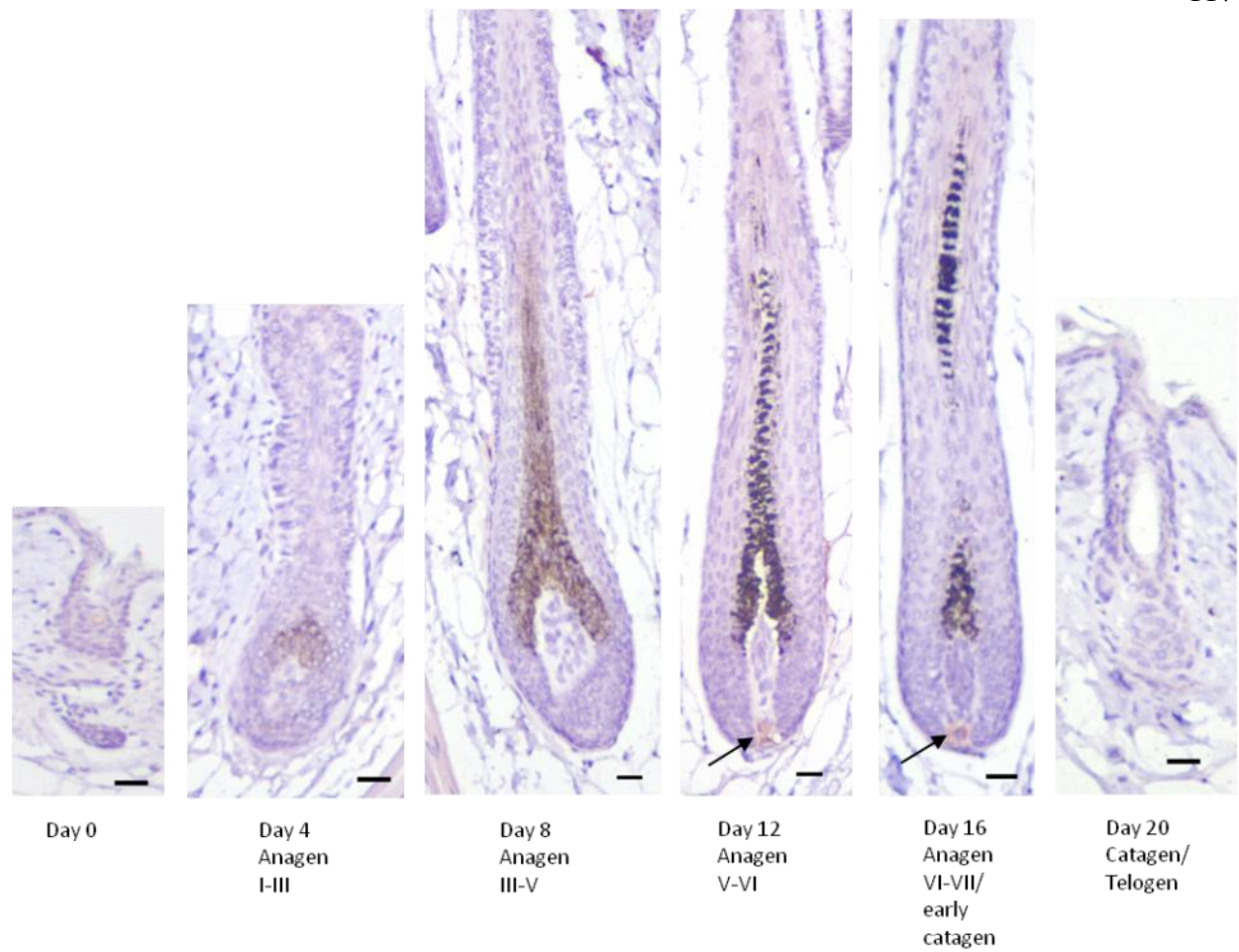


**Figure 29: Perf Expression in the Hair Follicle Throughout the Hair Follicle Cycle**

Perf was expressed in the follicle cycle in the stalk region of the DP from day 8-16 (anagen III-early catagen, denoted by arrows). The negative control displayed no positivity throughout the follicle cycle. Scale bars = 20 $\mu$ m

### 7.2.1.3 *GzmB* Expression in Mast Cells Throughout the Hair Follicle Cycle

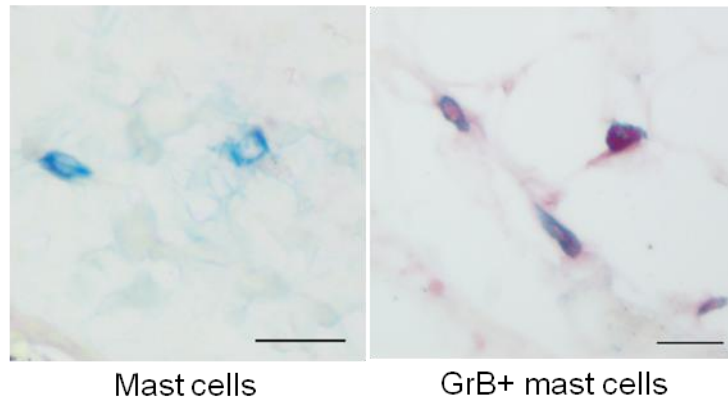
The majority of strongly *GzmB*<sup>+</sup> cells identified in the dermis around hair follicles were morphologically consistent with MCs; large cells with round to oval nuclei. To further characterize and identify MCs, skin sections from all phases of the cycle were incubated with alcian blue; a phthalocyanine dye that stains the acid mucopolysaccharide content of MCs' granules, and then assessed for *GzmB* co-localization (Figure 30 a). MCs were mostly located in the superficial papillary dermis and at the junction of the dermis and subcutaneous tissue. At the dermal/subcutaneous junction MCs were most commonly localized in proximity to hair follicles or nearby blood vessels.

The number of *GzmB* expressing cells, MCs and *GzmB*-expressing MCs, per mm<sup>2</sup> of skin, was quantified throughout the follicle cycle and counts displayed similar patterns throughout the cycle (Figure 30b). Numbers of cells for all 3 groups were high at anagen I-III (*GzmB*<sup>+</sup>: 68±17/mm<sup>2</sup>, MCs: 79±25/mm<sup>2</sup>, *GzmB*<sup>+</sup> MCs: 53±19/mm<sup>2</sup>) but not significantly different than at day 20, the resting, telogen stage. However, there was a significant decrease in cell density through the remainder of anagen and in catagen for all 3 counts (Day 12: *GzmB*<sup>+</sup>: 36±10/mm<sup>2</sup>, MCs: 32±6/mm<sup>2</sup>, *GzmB*<sup>+</sup> MCs: 23±6/mm<sup>2</sup>, P<0.05), before the marked increase at telogen. The only difference in MC density across *GzmB*<sup>+</sup> cells, MCs and *GzmB*<sup>+</sup> MCs was that *GzmB*<sup>+</sup> cell density was highest at day 0 (P<0.05) [124]. Although the number of MCs and *GzmB* expressing cells decrease in the mid-anagen to telogen stages, the number of *GzmB*<sup>+</sup> MCs decrease in a similar fashion, suggesting there is no cycle-dependent difference in *GzmB* expression in MCs.

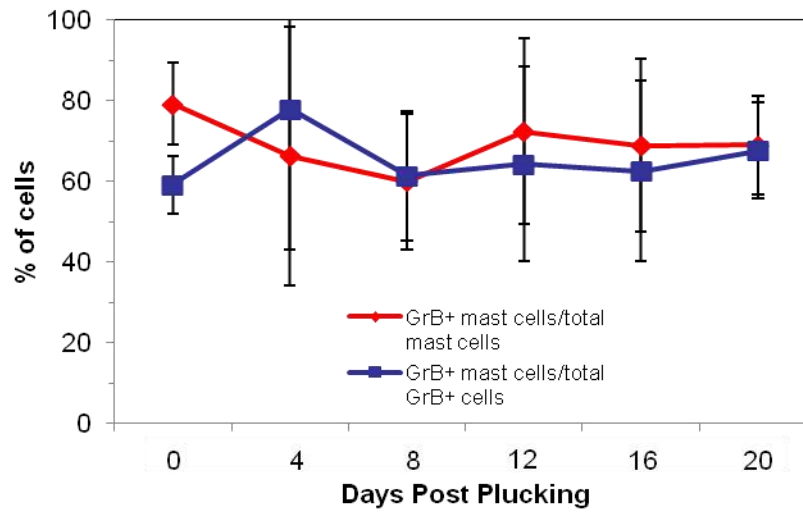
Approximately 70% of MCs were found to express *GzmB*, and this proportion did not change though the cycle (Fig 30 c). The proportion of non-follicular *GzmB* expressing cells that were MCs was 65% and also did not change throughout the cycle, suggesting that MCs may be

the main immune cell source of GzmB in the skin. Interestingly, through mid-anagen to catagen, papillary dermal MCs were largely negative for GzmB, however the lower dermal/subcutaneous MCs were nearly 100% positive, suggesting that GzmB expression may be dependent on localization.

A.



B.



C.

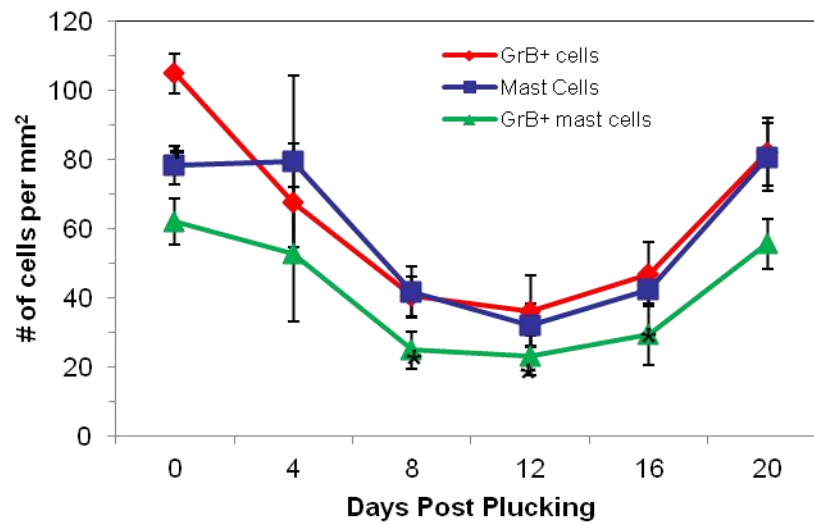


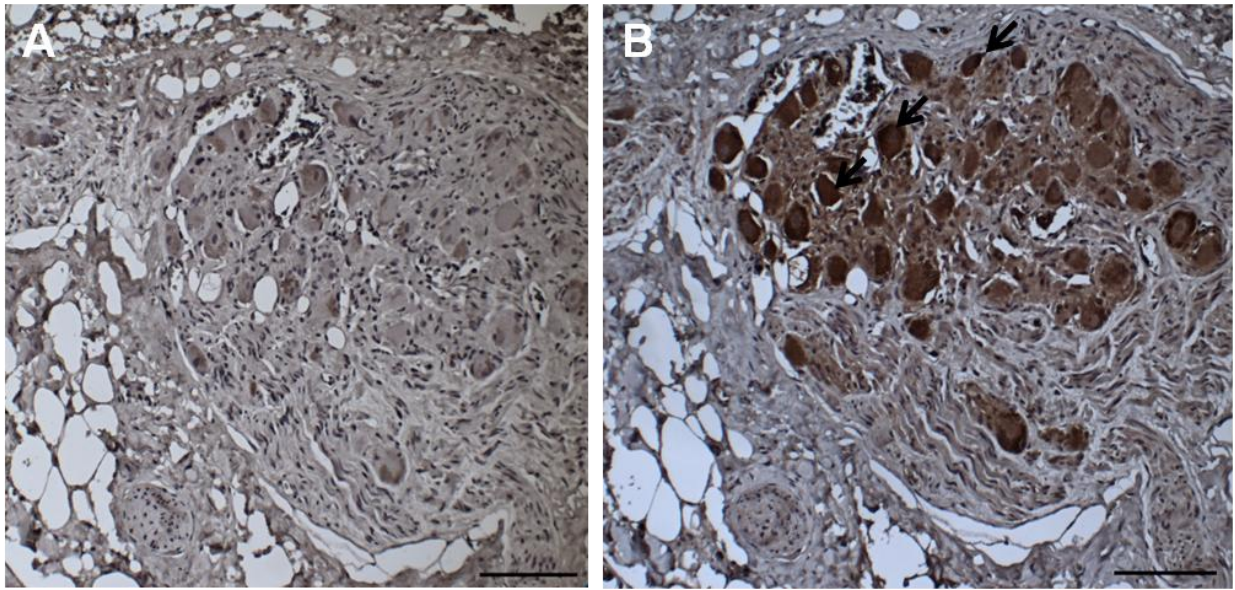
### **Figure 30: GzmB Expression in Mast Cells Throughout the Hair Follicle Cycle**

To examine GzmB expression by mast cells through the hair cycle an alcian blue/mast cell stain was conducted. Representative alcian blue stained mast cells (left) and GzmB<sup>+</sup>/alcian blue mast cells (right) in the dermis of C3H HeJ mouse skin (a). A graphical representation of GzmB<sup>+</sup> cells (red diamond), mast cells (blue square) and GzmB<sup>+</sup> mast cells (green triangle) throughout the follicle cycle is shown in (b). Approximately 70% of mast cells expressed GzmB (red diamond), 65% of GzmB expressing cells were mast cells (blue square) and these proportions did not significantly change throughout the follicle cycle (b). Asterisk indicates  $p < 0.05$  for all 3 groups (GzmB<sup>+</sup>, mast cells, and GzmB<sup>+</sup> mast cells) compared to telogen counts. + indicates  $p < 0.05$  for the GzmB<sup>+</sup> group only, compared to telogen counts. Scale bar = 20  $\mu$ m

#### *7.2.2 Future Direction 2: Collagen and Nerve Abnormalities by Transmission Electron Microscopy*

##### *7.2.2.1 GzmB Expression in Nerves*

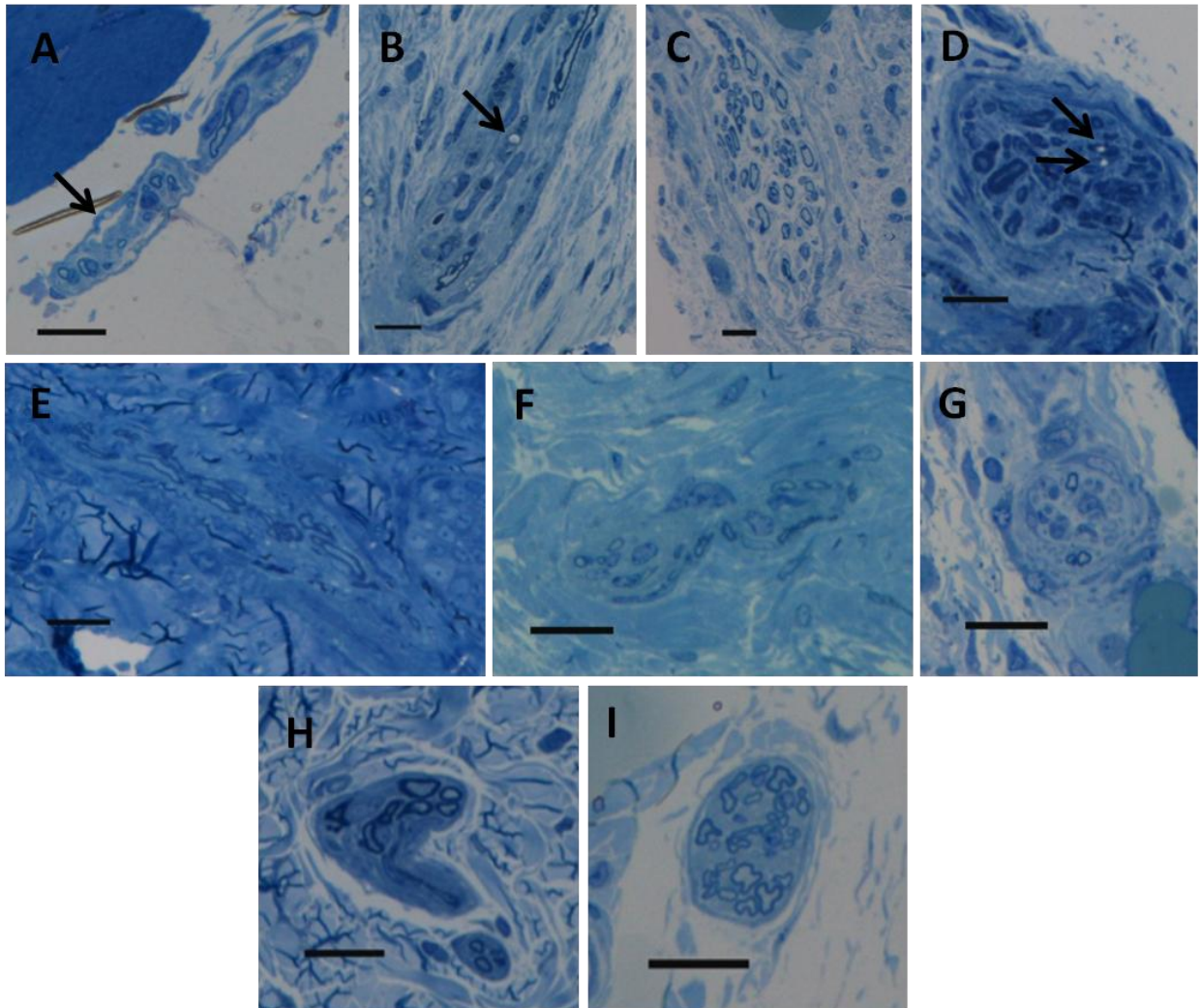
When staining for GzmB expression in human abdominal aortic aneurysm, we discovered strong GzmB expression in the nerve cell bodies of nerve ganglia of human vessels as shown by the brown stain in Figure 31. To examine the peripheral nerves in apoE-KO (Figure 32 a-g) and c57 (Figure 32 h, i) mice, skin was stained with toluidine blue, which stains myelin sheaths dark blue for visualization of myelinated nerves. Normal c57 nerves had a well defined epineurium and dark myelin sheaths. Lipid accumulation within apoE-KO nerves was observed (Figure 32, a, b, d, denoted with arrow) which was absent in c57 controls. In addition, the epineurium was not well defined in many apoE-KO nerves (Figure 32, e, f, g) and the endoneurium in some cases was poorly defined (Figure 32 c, e). In the nerves of c57 mice there were well defined and compact myelin sheaths by TEM (Figure 33). ApoE-KO mice skin displayed lipid accumulation and cholesterol clefts within nerves (Figure 33 j, k. Cholesterol arrows, lipid asterisk). The myelin sheath in myelinated axons was often disorganized, expanded, loose and uneven in apoE-KO mice compared to C57 controls, suggesting apoE-KO mice have abnormalities in myelin (Figure 33 g, h, i, l, j).



**Figure 31: GzmB Expression in the Nerve Ganglia of Aortic AAA Tissue**

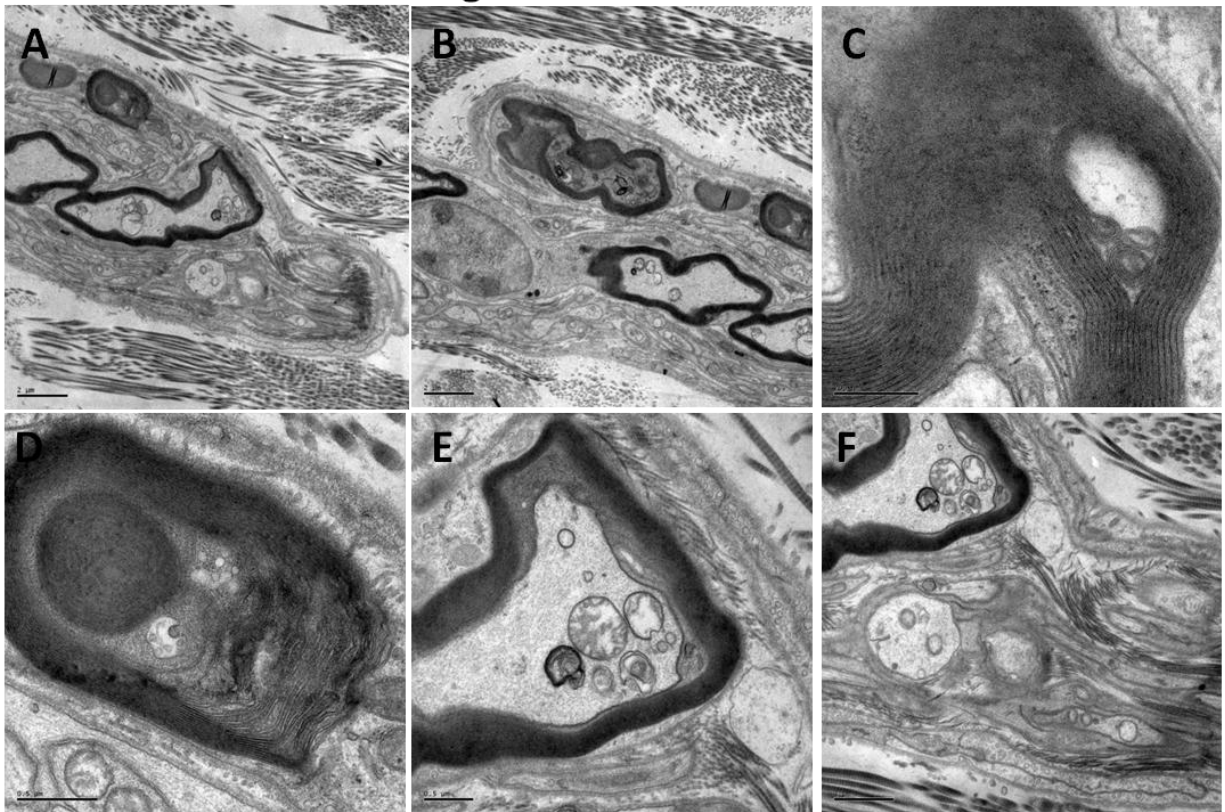
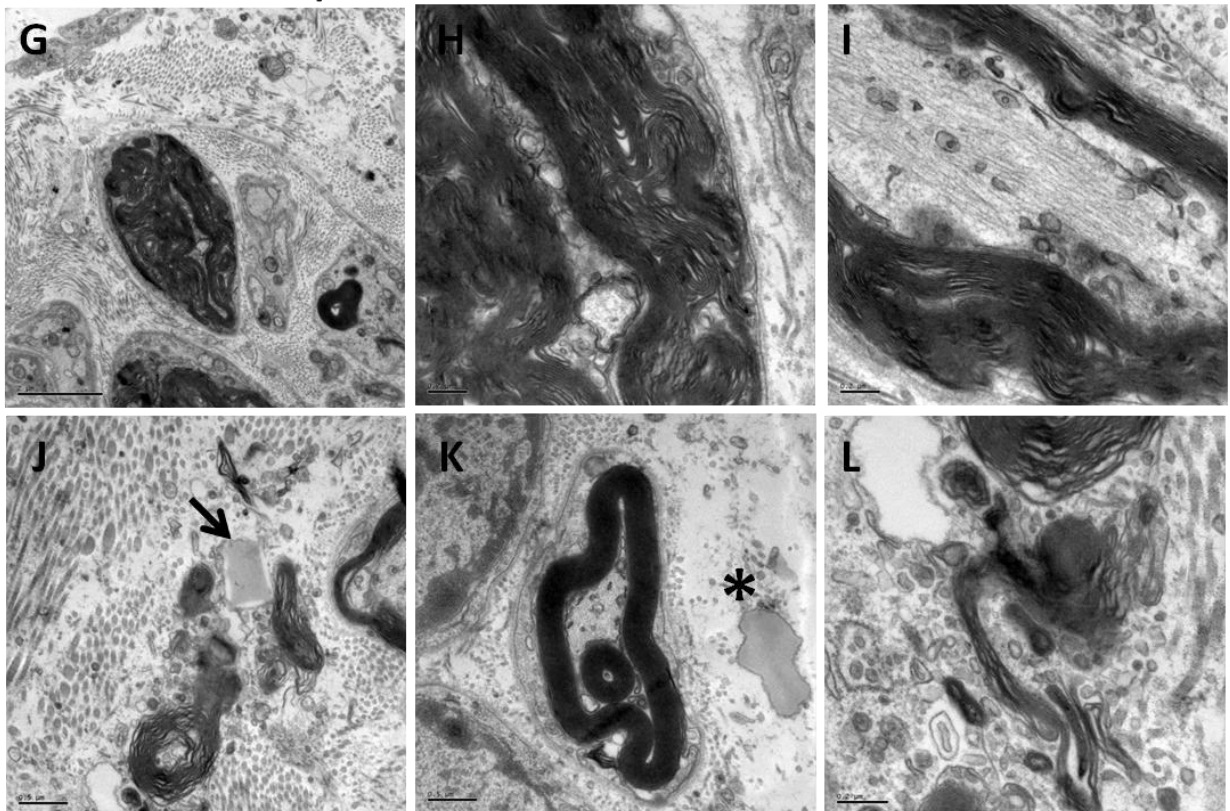
GzmB is expressed in the nerves of aortic AAA tissue. (a) Negative control, (b) GzmB immunohistochemistry. Arrows indicate nerve cell bodies positive for GzmB staining. Scale bar = 100  $\mu\text{m}$ . Permission to republish granted through the Copyright Clearance Center for *The American Journal of Pathology*.





**Figure 32: Dermal Nerves in ApoE-KO and C57 Mice**

To visualize dermal nerves in apoE-KO mice, toluidine blue stained tissues were examined for abnormal morphology. Peripheral nerves in apoE-KO mice (a-g) compared to the normal nerves of c57 mice (h-i). Toluidine blue stained sections of dermal nerves reveal lipid accumulation (denoted by arrows), myelin loss and general degeneration of nerves in apoE-KO mice. Scale bars = 50μm

**C57 reg diet – normal nerves****ApoE-KO xanthoma abnormal nerves**

### **Figure 33: Transmission Electron Microscopy Images of Dermal Nerves in C57 and ApoE-KO Mice**

Transmission electron microscopy was performed to examine the ultrastructural alterations in dermal nerves of apoE-KO mice compared to c57 controls. Myelin disorganization and expansion, lipid accumulation and cholesterol cleft localization in apoE-KO mice, that are absent in C57 dermal nerves. Arrow denotes cholesterol clefts and asterisk indicates lipid droplets. Scale bars: a, b, g = 2 $\mu$ m, c, h, i, l = 0.2 $\mu$ m, d, e, j, k = 0.5 $\mu$ m, f = 1 $\mu$ m

#### *7.2.2.2 Collagen Abnormalities in ApoE-KO mice*

The dermis of C57 mouse skin contained normal, organized collagen fibres with very little immune cell infiltration (Figure 34 a). In apoE-KO mouse skin, these collagen fibres were dispersed and replaced by numerous immune cells, foam cells and fragmented ECM (Figure 34 b, c). Figure 34 d displays a lipid-laden foam cell with a cholesterol cleft on the top left of the cell. The ECM surrounding the cell contains only a few collagen fibrils and elastic fibres. In c57 mice, normal collagen fibres were found in the dermis as displayed in Figure 35 and Figure 36, longitudinally and cross-sectionally by TEM. In apoE-KO mice, collagen fibres were smaller in diameter (Figure 35) and the absence of normal collagen fibres was apparent in many sections (Figure 36). In Figure 36, abnormal ECM is displayed, including collagen fibrils irregularly spaced and of varying size crosssectionally.



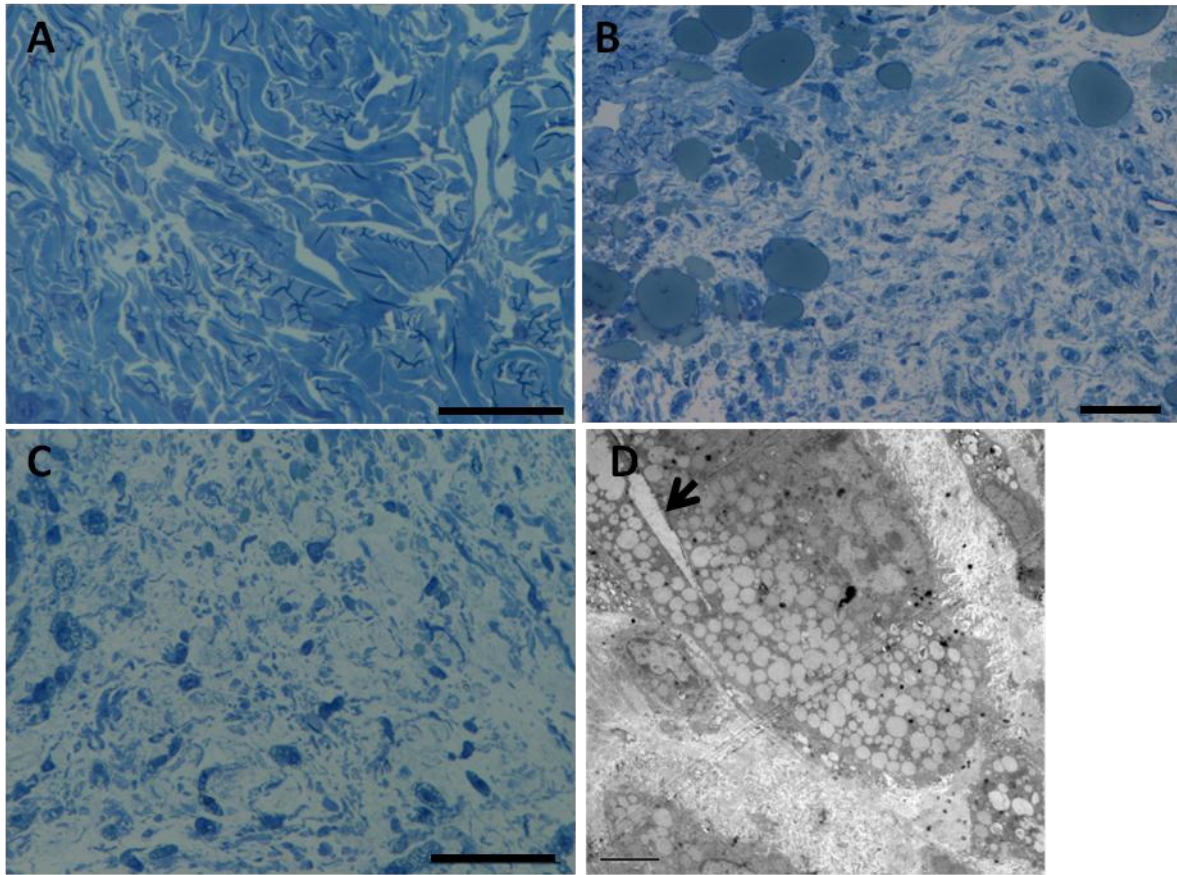


**Figure 34: ECM Morphology in ApoE-KO Mice**

TBO staining was conducted to examine extracellular matrix changes in the dermis of apoE-KO mice. (a) Toluidine Blue staining of normal dermal connective tissue from an apoE-KO mouse. (b) Abnormal connective tissue in the area within/surrounding a xanthoma, note the loss of collagen fibres. (c) More absence of collagen in the highly immune cell infiltrated xanthoma. (d) Abnormal ECM morphology surrounding a foam cell. Scale bars a-c = 50μm and d = 5μm

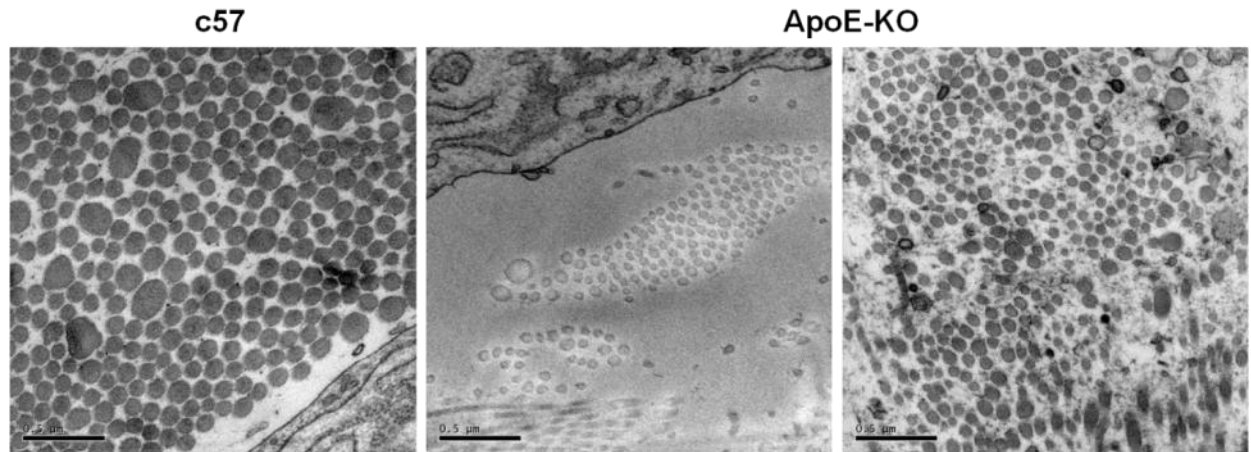


**Figure 35: Collagen Fibrils Appear Smaller in the Xanthomas of ApoE-KO Mice Compared to C57 Controls**

To observe cross-sectional collagen fibre size, TEM sections of the dermis of c57 and apoE-KO mice were examined. Skin from 37 week old C57 and apoE-KO mice on a high fat diet was collected, fixed and prepared for imaging by TEM. Collagen fibres in apoE-KO xanthoma skin are generally smaller than fibres in normal C57 skin. Scale bars = 0.5 $\mu$ m

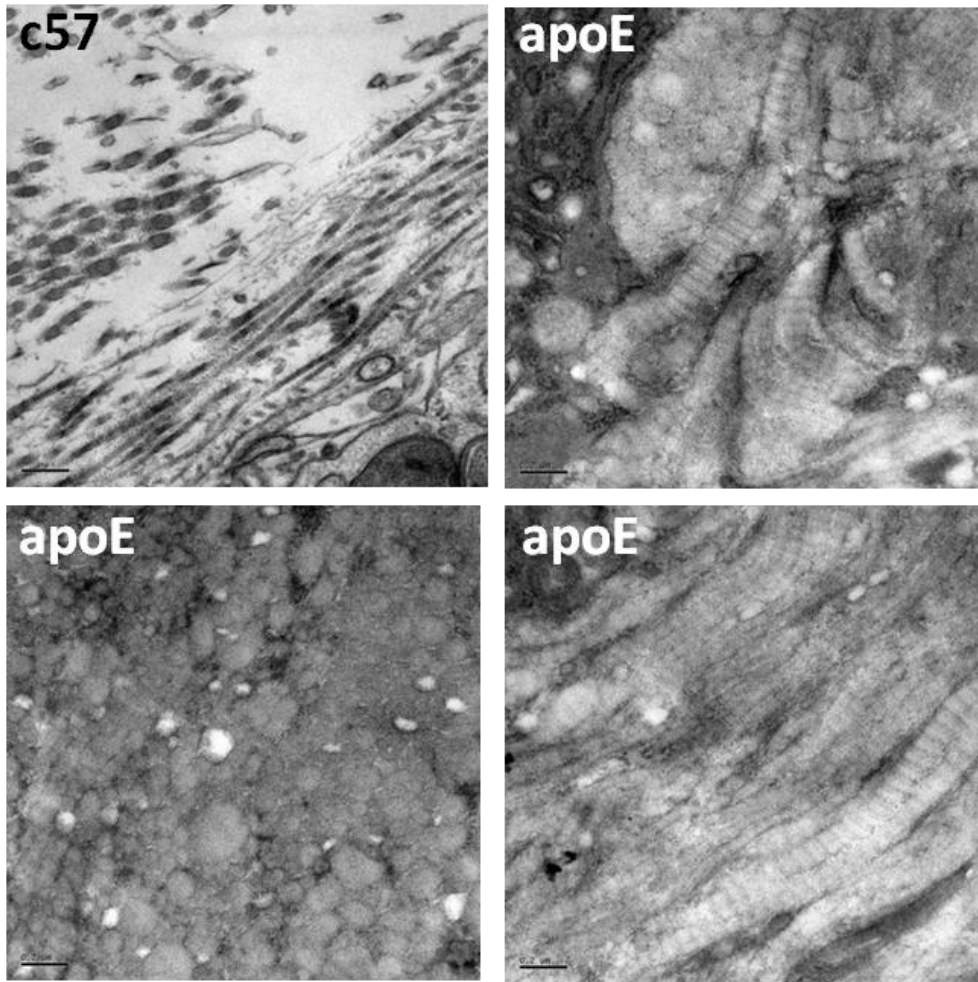


**Figure 36: Collagen and ECM Abnormalities in the Skin of ApoE-KO Mice on a 30 Week High Fat Diet**

To examine collagen fibre spacing, dermal sections of c57 and apoE-KO mice were photographed using TEM. C57 or apoE-KO mouse skin was fixed in glutaraldehyde, stained with osmium and imaged using transmission electron microscopy. apoE-KO mice skin contain areas of altered collagen structure and spacing compared to the normal collagen in c57 mice. Scale bars = 1  $\mu\text{m}$  top left image, all others 0.2  $\mu\text{m}$ .

### 7.3 Discussion

This chapter demonstrates that GzmB is differentially expressed by various skin and follicular cell types throughout the hair cycle and that GzmB and Perf are expressed by the DP at the anagen to catagen transition, a time of active apoptosis. MCs expressed GzmB throughout the cycle and may be involved in this transition. Although GzmB has been implicated in physiological processes such as immune-mediated apoptosis of damaged or virally infected cells, little is known regarding its patho-physiological role outside of T cell-mediated surveillance and the immune system. However, GzmB is differentially expressed and secreted from non-lymphoid cells under certain conditions and retains its activity upon its release into the extracellular space [58]. The present study indicates that GzmB is expressed by cells of the arrector pili muscle, epithelial bulge, DP and inner root sheath of the hair follicle and that its expression pattern changes distinctively throughout the hair cycle, suggesting that GzmB may influence hair follicle growth and regression.

The DP is composed of specialized, fibroblast-like cells whose activity can regulate the growth of the follicle through growth factor signaling. Both GzmB and Perf are expressed by the DP during the anagen to catagen transition. However, Perf expression in the DP was limited to the stem region of the papillae, whereas GzmB expression was specific to the DP apex. GzmB-mediated apoptosis is generally accepted as a Perf-dependent process. As Perf is required for GzmB entry into the cytosol of target cells [38, 408], the lack of substantial co-localization suggests GzmB is likely not inducing cell death in a Perf-dependent manner. However, GzmB can also induce cell death in a Perf-independent manner through cleavage of extracellular matrix, which results in a loss of cell-matrix contacts, and ultimately, a form of cell death known as anoikis [123, 124]. Perf can induce cell death in target cells in a GzmB-independent manner, through facilitating cytosolic entry of other granzymes and granule proteins. Thus, although

GzmB and Perf are not consistently co-localized in the DP, this does not rule out the possibility that they may be promoting apoptosis independently of each other in this region. Also, the extracellular function of GzmB is Perf-independent. As such, GzmB may also contribute to tissue remodeling during the hair follicle cycle.

In addition to CTLs and NK cells, the present study provides further evidence of MCs expressing GzmB. GzmB, but not Perf, is expressed in MC granules and secreted by MCs. MC-derived GzmB induces Perf-independent cell death through anoikis [7, 107]. MCs are specifically located in close proximity to hair follicles and skin regions with limited numbers of MCs typically corresponding to areas devoid of follicles [409, 410]. In this depilation-induced model of hair cycling, 70% of MCs express GzmB and 65% of GzmB<sup>+</sup> cells are MCs, suggesting that the majority of MCs in the skin express GzmB and that the majority of dermal GzmB expressing cells are MCs. GzmB-expressing MCs were localized to the deep dermis, near hair follicle bulbs, ideal positioning to potentially act on the bulb and contribute to apoptosis and regression of the follicle.

The density of MCs, GzmB-expressing MCs and GzmB-expressing cells in the dermis decrease in mid to late anagen and catagen, but increase to levels similar to early anagen during telogen. A similar decrease in MC density in anagen is consistent with previous literature, where it has been suggested that the reduction in MCs may be due to degranulation in early anagen and a lower histological detection as a result [411-414]. Inhibitors of MC degranulation prevent anagen development and an increase in MC degranulation has been implicated in the anagen-catagen transition [411] suggesting MCs may promote the onset of anagen as well as the anagen-catagen transition.

MCs are implicated in hair growth diseases and are increased in androgenetic alopecia [415]. In a mouse model of alopecia areata, the neuropeptide substance P increased MC



degranulation and promoted CD8<sup>+</sup>/GzmB<sup>+</sup> T cell migration to hair follicles [212]. Substance P induces GzmB expression and release *in vitro* and has been reported to potentially promote catagen [7, 212, 416]. These findings suggest that MCs are important for hair follicle cycling and may be linked to the development of some follicular diseases. As GzmB is strongly expressed by MCs throughout the cycle (70% of MCs) and is released upon degranulation, it could be capable of influencing the follicle cycle. Further studies are required to assess the link between substance P-induced MC release of GzmB and its specific contribution to early onset catagen hair loss in the context of alopecia.

The expression of GzmB in the panniculus carnosus and arrector pili muscle is consistent with our previous work demonstrating that smooth muscle cells may express GzmB [124] and suggests that GzmB may be commonly expressed by both smooth and striated muscle cells under certain, as yet undefined, conditions. The expression level and pattern of GzmB in the panniculus carnosus varied throughout the follicle cycle. GzmB localized in a granular-like punctuate stain in late anagen, catagen and telogen, which was not apparent in the earlier cycle stages. The protein was also more commonly polarized to the dermal membranes of the muscle cells. It is possible that even subcutaneous muscle may be influenced by factors involved in hair follicle cycling and that they may even be a dermal source of GzmB during the anagen-catagen transition. However, it is not known if GzmB can be secreted from muscle cells or if it is localized in granules, thus the functional role of GzmB in these cells requires further elucidation.

This chapter also demonstrates nerve abnormalities in the skin of apoE-KO mice, including myelin disorganization by TEM. It describes collagen abnormalities and smaller collagen fibrils in the skin and xanthomas of apoE-KO mice. Previously our laboratory has shown a loss of collagen organization/density in the skin of apoE-KO mice by multi-photon microscopy [195]. Collagen density was restored in GzmB/apoE-DKO mice yielding an even

stronger signal than C57 controls. Whether or not nerve and collagen pathologies are absent in GzmB/apoE-DKO mice remains to be established. However, this work does illustrate collagen and nerve abnormalities in apoE-KO mouse skin.

## 8. Conclusion

The granzymes were initially discovered as both intracellular and extracellular proteases, however until recently the field has focused on their intracellular apoptosis-inducing capacity. It has long been known that upon Perf-mediated delivery, the granule secretory pathway is essential for the elimination of tumor and virally-infected cells. Perf-KO mice were traditionally utilized to examine the role of the granzymes in disease and if there was no change in the disease phenotype it was assumed that the granzymes did not play a role in pathogenesis. However, often overlooked was the Perf-independent extracellular activities of the granzymes. GzmA, GzmB and GzmK are detected extracellularly in bodily fluids such as plasma, cerebral spinal fluid, bronchoalveolar lavage and synovial fluid [58, 100, 147, 175]. GzmB can be released from cells in the absence of target cell engagement and is immediately active in the extracellular space [111]. Moreover, cells such as basophils and mast cells express GzmB in the absence of Perf, and as Perf is required for internalization of the granzymes for apoptosis induction, these cells do not have the capacity to induce apoptosis [7, 10, 107]. Furthermore, non-immune cells such as chondrocytes also express GzmB [14]. As these cells do not have the capacity to form immunological synapses for granzyme delivery to target cells, they are unlikely cytotoxic in nature. Finally, GzmB retains 70% of its activity in plasma [116] and no extracellular GzmB inhibitor has been described, suggesting it is largely uninhibited in the extracellular milieu, in contrast to other extracellular proteases such as the MMPs.

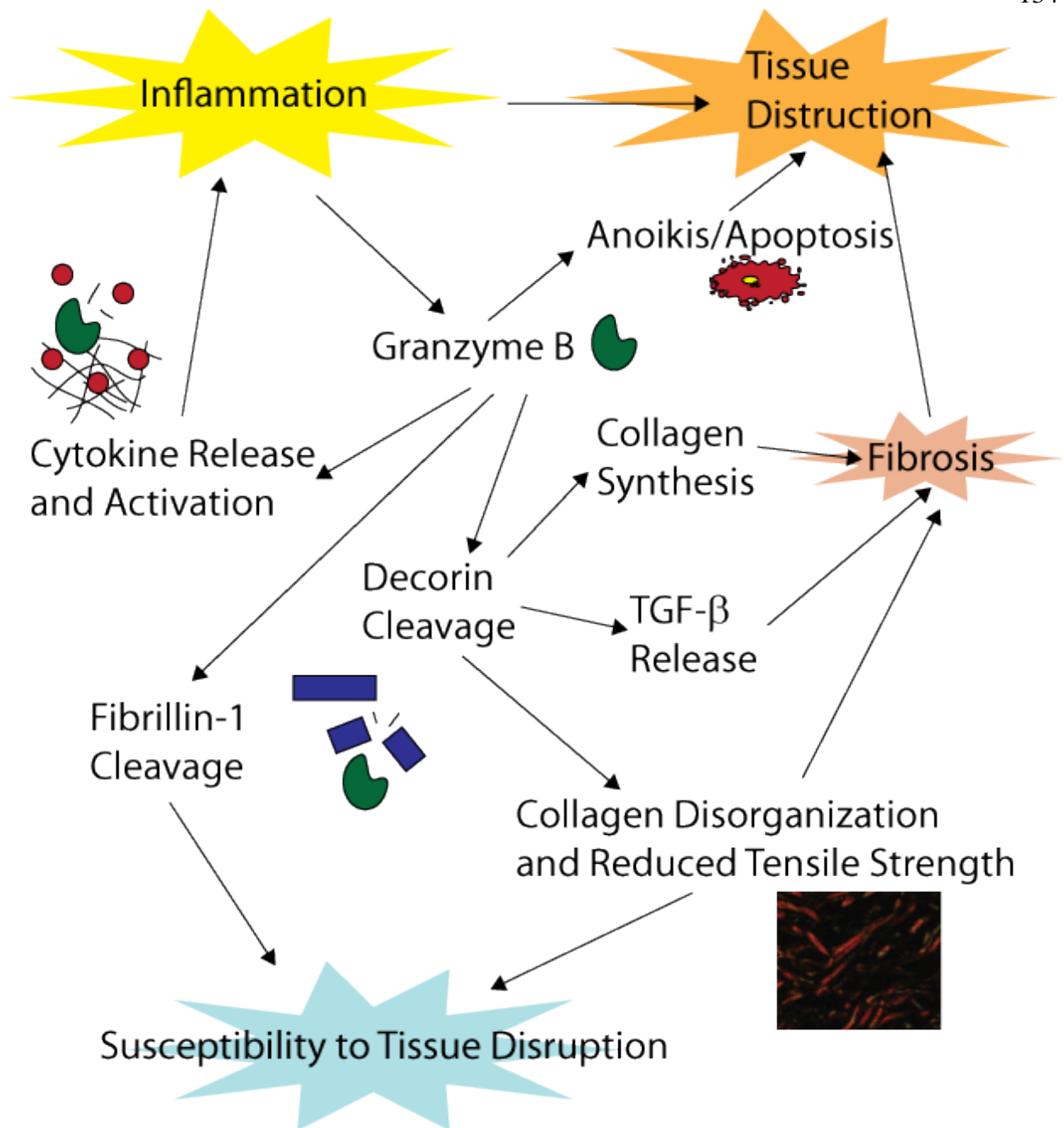


**Figure 37: Implications of Extracellular GzmB Activity**

GzmB cleavage of ECM can induce the release of cytokines such as TGF- $\beta$ . GzmB can also cleave and activate IL-18 and IL-1 $\alpha$ . This can lead to inflammation and subsequently tissue destruction. GzmB cleavage of decorin and fibrillin-1 leads to elastic tissue breakdown and collagen disorganization/reduction in tensile strength. Decorin cleavage results in TGF- $\beta$  release and collagen synthesis, all leading to fibrosis and further tissue destruction. Cleavage of ECM can also induce anoikis, cell death due to a detachment from surrounding matrix.

The degree to which the other granzymes are involved in the induction of apoptosis remains unclear as high concentrations of GzmA (micromolar range) and Perf have been utilized in the past to initiate cell death and more recent studies suggest that GzmA is not cytotoxic under physiological conditions [106, 188, 399]. Despite the fact that the granzymes were identified several decades ago, a clear role for GzmH, K and M in cell death has not been established, suggesting these proteases may be more involved in inflammation and cytokine production. Indeed, recent evidence points toward a non-cytotoxic capacity for granzymes such as the processing of proinflammatory cytokines, cleavage of extracellular matrix proteins and proteolysis of cell receptors (reviewed in [106, 347]). Extracellular matrix cleavage by GzmB can also cause anoikis, cell death induced by a loss of cell attachment [123, 124].

In this dissertation I identified 11 novel extracellular substrates and characterized the cleavage sites of 3 of these substrates. The majority of substrates characterized were proteoglycans, suggesting GzmB has a preference for such substrates. Indeed, GzmB has affinity for the glycosaminoglycan side chains of PGs, as it is stored on serglycin in cytotoxic granules and has affinity for cell surface PG upon cellular internalization. Cleavage of biglycan and betaglycan occurs at a P1 residue of aspartic acid, consistent with the literature. I show that cleavage of decorin, biglycan and betaglycan releases active TGF- $\beta$  which remains fully active and induces SMAD-3 activation in human coronary artery smooth muscle cells.

A GzmB-dependent decrease in medial fibrillin-1 was characterized in murine models of AAA and atherosclerosis. ApoE-KO mice displayed a decrease in adventitial decorin levels in AAA that is restored in GzmB/apoE-DKO mice that may contribute to weakening the vessel wall and promoting aneurysm rupture. In skin aging, a decrease in decorin in the dermal-epidermal junction is apparent in apoE-KO mice, an area critical in skin wrinkling. GzmB/apoE-DKO mice were protected from this loss of decorin. Finally, both Perf/apoE-DKO and

GzmB/apoE-DKO mice display reduced atherosclerotic plaque compared to apoE-KO mice in a model of atherosclerosis, suggesting that the intracellular Perforin-dependent roles of the granzymes are also critical in atherosclerosis pathogenesis. This reduction in atherosclerosis was not due to a reduction in cholesterol or triglyceride levels and occurs through a separate mechanism.

The field of extracellular GzmB activity remains in its infancy, however this work has significantly increased our knowledge of extracellular GzmB activity in disease. Implications of extracellular GzmB activity is illustrated in Figure 37. Cleavage of ECM results in the release of growth factors from ECM and cell death due to a detachment from matrix, known as anoikis. GzmB can also activate cytokines extracellularly such as IL-1 $\alpha$  and IL-18. An increase in soluble active growth factors and cytokines can promote inflammation, which in turn facilitates tissue damage. We have shown that cleavage of fibrillin-1 co-responds to medial disruption in AAA and that cleavage of decorin results in collagen disorganization and a loss in tensile strength in AAA and skin aging [193-195]. Cleavage of decorin, biglycan and betaglycan also results in the release of TGF- $\beta$  from matrix and a reduction in decorin levels may increase collagen synthesis [417], all leading to fibrosis and consequently further tissue disruption.

## Bibliography

- 1      Trapani, J. A. (2001) Granzymes: a family of lymphocyte granule serine proteases. *Genome Biol* **2**, REVIEWS3014
- 2      Smyth, M. J., O'Connor, M. D. and Trapani, J. A. (1996) Granzymes: a variety of serine protease specificities encoded by genetically distinct subfamilies. *J Leukoc Biol* **60**, 555-562
- 3      Bleackley, R. C., Duggan, B., Ehrman, N. and Lobe, C. G. (1988) Isolation of two cDNA sequences which encode cytotoxic cell proteases. *FEBS Lett* **234**, 153-159
- 4      Brunet, J. F., Dosseto, M., Denizot, F., Mattei, M. G., Clark, W. R., Haqqi, T. M., Ferrier, P., Nabholz, M., Schmitt-Verhulst, A. M., Luciani, M. F. and et al. (1986) The inducible cytotoxic T-lymphocyte-associated gene transcript CTLA-1 sequence and gene localization to mouse chromosome 14. *Nature* **322**, 268-271
- 5      Masson, D., Nabholz, M., Estrade, C. and Tschopp, J. (1986) Granules of cytolytic T-lymphocytes contain two serine esterases. *EMBO J* **5**, 1595-1600
- 6      Pasternack, M. S. and Eisen, H. N. (1985) A novel serine esterase expressed by cytotoxic T lymphocytes. *Nature* **314**, 743-745
- 7      Strik, M. C., de Koning, P. J., Kleijmeer, M. J., Bladergroen, B. A., Wolbink, A. M., Griffith, J. M., Wouters, D., Fukuoka, Y., Schwartz, L. B., Hack, C. E., van Ham, S. M. and Kummer, J. A. (2007) Human mast cells produce and release the cytotoxic lymphocyte associated protease granzyme B upon activation. *Mol Immunol* **44**, 3462-3472
- 8      Kim, W. J., Kim, H., Suk, K. and Lee, W. H. (2007) Macrophages express granzyme B in the lesion areas of atherosclerosis and rheumatoid arthritis. *Immunol Lett* **111**, 57-65
- 9      Wagner, C., Iking-Konert, C., Deneffle, B., Stegmaier, S., Hug, F. and Hansch, G. M. (2004) Granzyme B and perforin: constitutive expression in human polymorphonuclear neutrophils. *Blood* **103**, 1099-1104
- 10     Tschopp, C. M., Spiegl, N., Didichenko, S., Lutmann, W., Julius, P., Virchow, J. C., Hack, C. E. and Dahinden, C. A. (2006) Granzyme B, a novel mediator of allergic inflammation: its induction and release in blood basophils and human asthma. *Blood* **108**, 2290-2299
- 11     Rissoan, M. C., Duhon, T., Bridon, J. M., Bendriss-Vermare, N., Peronne, C., de Saint Vis, B., Briere, F. and Bates, E. E. (2002) Subtractive hybridization reveals the expression of immunoglobulin-like transcript 7, Eph-B1, granzyme B, and 3 novel transcripts in human plasmacytoid dendritic cells. *Blood* **100**, 3295-3303
- 12     Namekawa, T., Wagner, U. G., Goronzy, J. J. and Weyand, C. M. (1998) Functional subsets of CD4 T cells in rheumatoid synovitis. *Arthritis Rheum* **41**, 2108-2116
- 13     Grossman, W. J., Verbsky, J. W., Tollefsen, B. L., Kemper, C., Atkinson, J. P. and Ley, T. J. (2004) Differential expression of granzymes A and B in human cytotoxic lymphocyte subsets and T regulatory cells. *Blood* **104**, 2840-2848
- 14     Horiuchi, K., Saito, S., Sasaki, R., Tomatsu, T. and Toyama, Y. (2003) Expression of granzyme B in human articular chondrocytes. *J Rheumatol* **30**, 1799-1810
- 15     Hernandez-Pigeon, H., Jean, C., Charruyer, A., Haure, M. J., Titeux, M., Tonasso, L., Quillet-Mary, A., Baudouin, C., Charveron, M. and Laurent, G. (2006) Human keratinocytes acquire cellular cytotoxicity under UV-B irradiation. Implication of granzyme B and perforin. *J Biol Chem* **281**, 13525-13532
- 16     Choy, J. C., McDonald, P. C., Suarez, A. C., Hung, V. H., Wilson, J. E., McManus, B. M. and Granville, D. J. (2003) Granzyme B in atherosclerosis and transplant vascular

- disease: association with cell death and atherosclerotic disease severity. *Mod Pathol* **16**, 460-470
- 17 Vernooy, J. H., Moller, G. M., van Suylen, R. J., van Spijk, M. P., Cloots, R. H., Hoet, P. H., Pennings, H. J. and Wouters, E. F. (2007) Increased granzyme A expression in type II pneumocytes of patients with severe chronic obstructive pulmonary disease. *Am J Respir Crit Care Med* **175**, 464-472
  - 18 Hirst, C. E., Buzza, M. S., Sutton, V. R., Trapani, J. A., Loveland, K. L. and Bird, P. I. (2001) Perforin-independent expression of granzyme B and proteinase inhibitor 9 in human testis and placenta suggests a role for granzyme B-mediated proteolysis in reproduction. *Mol Hum Reprod* **7**, 1133-1142
  - 19 Sasson, R., Dantes, A., Tajima, K. and Amsterdam, A. (2003) Novel genes modulated by FSH in normal and immortalized FSH-responsive cells: new insights into the mechanism of FSH action. *FASEB J* **17**, 1256-1266
  - 20 Waugh, S. M., Harris, J. L., Fletterick, R. and Craik, C. S. (2000) The structure of the pro-apoptotic protease granzyme B reveals the molecular determinants of its specificity. *Nat Struct Biol* **7**, 762-765
  - 21 Klein, J. L., Shows, T. B., Dupont, B. and Trapani, J. A. (1989) Genomic organization and chromosomal assignment for a serine protease gene (CSPB) expressed by human cytotoxic lymphocytes. *Genomics* **5**, 110-117
  - 22 Babichuk, C. K., Duggan, B. L. and Bleackley, R. C. (1996) In vivo regulation of murine granzyme B gene transcription in activated primary T cells. *J Biol Chem* **271**, 16485-16493
  - 23 Fregeau, C. J. and Bleackley, R. C. (1991) Transcription of two cytotoxic cell protease genes is under the control of different regulatory elements. *Nucleic Acids Res* **19**, 5583-5590
  - 24 Wargnier, A., Lafaurie, C., Legros-Maida, S., Bourge, J. F., Sigaux, F., Sasportes, M. and Paul, P. (1998) Down-regulation of human granzyme B expression by glucocorticoids. Dexamethasone inhibits binding to the Ikaros and AP-1 regulatory elements of the granzyme B promoter. *J Biol Chem* **273**, 35326-35331
  - 25 Haddad, P., Wargnier, A., Bourge, J. F., Sasportes, M. and Paul, P. (1993) A promoter element of the human serine esterase granzyme B gene controls specific transcription in activated T cells. *Eur J Immunol* **23**, 625-629
  - 26 Babichuk, C. K. and Bleackley, R. C. (1997) Mutational analysis of the murine granzyme B gene promoter in primary T cells and a T cell clone. *J Biol Chem* **272**, 18564-18571
  - 27 Griffiths, G. M. and Isaaz, S. (1993) Granzymes A and B are targeted to the lytic granules of lymphocytes by the mannose-6-phosphate receptor. *J Cell Biol* **120**, 885-896
  - 28 Brown, G. R., McGuire, M. J. and Thiele, D. L. (1993) Dipeptidyl peptidase I is enriched in granules of in vitro- and in vivo-activated cytotoxic T lymphocytes. *J Immunol* **150**, 4733-4742
  - 29 Smyth, M. J., McGuire, M. J. and Thia, K. Y. (1995) Expression of recombinant human granzyme B. A processing and activation role for dipeptidyl peptidase I. *J Immunol* **154**, 6299-6305
  - 30 Balaji, K. N., Schaschke, N., Machleidt, W., Catalfamo, M. and Henkart, P. A. (2002) Surface cathepsin B protects cytotoxic lymphocytes from self-destruction after degranulation. *J Exp Med* **196**, 493-503



- 31 Grujic, M., Braga, T., Lukinius, A., Eloranta, M. L., Knight, S. D., Pejler, G. and Abrink, M. (2005) Serglycin-deficient cytotoxic T lymphocytes display defective secretory granule maturation and granzyme B storage. *J Biol Chem* **280**, 33411-33418
- 32 Galvin, J. P., Spaeny-Dekking, L. H., Wang, B., Seth, P., Hack, C. E. and Froelich, C. J. (1999) Apoptosis induced by granzyme B-glycosaminoglycan complexes: implications for granule-mediated apoptosis in vivo. *J Immunol* **162**, 5345-5350
- 33 Metkar, S. S., Wang, B., Aguilar-Santelises, M., Raja, S. M., Uhlin-Hansen, L., Podack, E., Trapani, J. A. and Froelich, C. J. (2002) Cytotoxic cell granule-mediated apoptosis: perforin delivers granzyme B-serglycin complexes into target cells without plasma membrane pore formation. *Immunity* **16**, 417-428
- 34 Podack, E. R., Young, J. D. and Cohn, Z. A. (1985) Isolation and biochemical and functional characterization of perforin 1 from cytolytic T-cell granules. *Proc Natl Acad Sci U S A* **82**, 8629-8633
- 35 Masson, D. and Tschopp, J. (1985) Isolation of a lytic, pore-forming protein (perforin) from cytolytic T-lymphocytes. *J Biol Chem* **260**, 9069-9072
- 36 Horvath, A. J., Forsyth, S. L. and Coughlin, P. B. (2004) Expression patterns of murine antichymotrypsin-like genes reflect evolutionary divergence at the *Serpina3* locus. *J Mol Evol* **59**, 488-497
- 37 Keefe, D., Shi, L., Feske, S., Massol, R., Navarro, F., Kirchhausen, T. and Lieberman, J. (2005) Perforin triggers a plasma membrane-repair response that facilitates CTL induction of apoptosis. *Immunity* **23**, 249-262
- 38 Voskoboinik, I., Smyth, M. J. and Trapani, J. A. (2006) Perforin-mediated target-cell death and immune homeostasis. *Nat Rev Immunol* **6**, 940-952
- 39 Froelich, C. J., Orth, K., Turbov, J., Seth, P., Gottlieb, R., Babior, B., Shah, G. M., Bleackley, R. C., Dixit, V. M. and Hanna, W. (1996) New paradigm for lymphocyte granule-mediated cytotoxicity. Target cells bind and internalize granzyme B, but an endosomolytic agent is necessary for cytosolic delivery and subsequent apoptosis. *J Biol Chem* **271**, 29073-29079
- 40 Motyka, B., Korbitt, G., Pinkoski, M. J., Heibei, J. A., Caputo, A., Hobman, M., Barry, M., Shostak, I., Sawchuk, T., Holmes, C. F., Gaudie, J. and Bleackley, R. C. (2000) Mannose 6-phosphate/insulin-like growth factor II receptor is a death receptor for granzyme B during cytotoxic T cell-induced apoptosis. *Cell* **103**, 491-500
- 41 Pinkoski, M. J., Hobman, M., Heibei, J. A., Tomaselli, K., Li, F., Seth, P., Froelich, C. J. and Bleackley, R. C. (1998) Entry and trafficking of granzyme B in target cells during granzyme B-perforin-mediated apoptosis. *Blood* **92**, 1044-1054
- 42 Shi, L., Mai, S., Israels, S., Browne, K., Trapani, J. A. and Greenberg, A. H. (1997) Granzyme B (GraB) autonomously crosses the cell membrane and perforin initiates apoptosis and GraB nuclear localization. *J Exp Med* **185**, 855-866
- 43 Veugelers, K., Motyka, B., Goping, I. S., Shostak, I., Sawchuk, T. and Bleackley, R. C. (2006) Granule-mediated killing by granzyme B and perforin requires a mannose 6-phosphate receptor and is augmented by cell surface heparan sulfate. *Mol Biol Cell* **17**, 623-633
- 44 Raja, S. M., Metkar, S. S., Honing, S., Wang, B., Russin, W. A., Pipalia, N. H., Menaa, C., Belting, M., Cao, X., Dressel, R. and Froelich, C. J. (2005) A novel mechanism for protein delivery: granzyme B undergoes electrostatic exchange from serglycin to target cells. *J Biol Chem* **280**, 20752-20761

- 45 Bird, C. H., Sun, J., Ung, K., Karambalis, D., Whisstock, J. C., Trapani, J. A. and Bird, P. I. (2005) Cationic sites on granzyme B contribute to cytotoxicity by promoting its uptake into target cells. *Mol Cell Biol* **25**, 7854-7867
- 46 Gross, C., Schmidt-Wolf, I. G., Nagaraj, S., Gastpar, R., Ellwart, J., Kunz-Schughart, L. A. and Multhoff, G. (2003) Heat shock protein 70-reactivity is associated with increased cell surface density of CD94/CD56 on primary natural killer cells. *Cell Stress Chaperones* **8**, 348-360
- 47 Afonina, I. S., Cullen, S. P. and Martin, S. J. Cytotoxic and non-cytotoxic roles of the CTL/NK protease granzyme B. *Immunol Rev* **235**, 105-116
- 48 Talanian, R. V., Yang, X., Turbov, J., Seth, P., Ghayur, T., Casiano, C. A., Orth, K. and Froelich, C. J. (1997) Granule-mediated killing: pathways for granzyme B-initiated apoptosis. *J Exp Med* **186**, 1323-1331
- 49 Darmon, A. J., Nicholson, D. W. and Bleackley, R. C. (1995) Activation of the apoptotic protease CPP32 by cytotoxic T-cell-derived granzyme B. *Nature* **377**, 446-448
- 50 Adrain, C., Murphy, B. M. and Martin, S. J. (2005) Molecular ordering of the caspase activation cascade initiated by the cytotoxic T lymphocyte/natural killer (CTL/NK) protease granzyme B. *J Biol Chem* **280**, 4663-4673
- 51 Hengartner, M. O. (2000) The biochemistry of apoptosis. *Nature* **407**, 770-776
- 52 Jiang, X. and Wang, X. (2000) Cytochrome c promotes caspase-9 activation by inducing nucleotide binding to Apaf-1. *J Biol Chem* **275**, 31199-31203
- 53 Li, P., Nijhawan, D., Budihardjo, I., Srinivasula, S. M., Ahmad, M., Alnemri, E. S. and Wang, X. (1997) Cytochrome c and dATP-dependent formation of Apaf-1/caspase-9 complex initiates an apoptotic protease cascade. *Cell* **91**, 479-489
- 54 Goping, I. S., Sawchuk, T., Underhill, D. A. and Bleackley, R. C. (2006) Identification of {alpha}-tubulin as a granzyme B substrate during CTL-mediated apoptosis. *J Cell Sci* **119**, 858-865
- 55 Hostetter, D. R., Loeb, C. R., Chu, F. and Craik, C. S. (2007) Hip is a pro-survival substrate of granzyme B. *J Biol Chem* **282**, 27865-27874
- 56 Caruso, J. A. and Reiners, J. J., Jr. (2006) Proteolysis of HIP during apoptosis occurs within a region similar to the BID loop. *Apoptosis* **11**, 1877-1885
- 57 Bredemeyer, A. J., Carrigan, P. E., Fehniger, T. A., Smith, D. F. and Ley, T. J. (2006) Hop cleavage and function in granzyme B-induced apoptosis. *J Biol Chem* **281**, 37130-37141
- 58 Boivin, W. A., Cooper, D. M., Hiebert, P. R. and Granville, D. J. (2009) Intracellular versus extracellular granzyme B in immunity and disease: challenging the dogma. *Lab Invest* **89**, 1195-1220
- 59 Bird, C. H., Sutton, V. R., Sun, J., Hirst, C. E., Novak, A., Kumar, S., Trapani, J. A. and Bird, P. I. (1998) Selective regulation of apoptosis: the cytotoxic lymphocyte serpin proteinase inhibitor 9 protects against granzyme B-mediated apoptosis without perturbing the Fas cell death pathway. *Mol Cell Biol* **18**, 6387-6398
- 60 Sun, J., Bird, C. H., Sutton, V., McDonald, L., Coughlin, P. B., De Jong, T. A., Trapani, J. A. and Bird, P. I. (1996) A cytosolic granzyme B inhibitor related to the viral apoptotic regulator cytokine response modifier A is present in cytotoxic lymphocytes. *J Biol Chem* **271**, 27802-27809
- 61 Buzza, M. S., Hirst, C. E., Bird, C. H., Hosking, P., McKendrick, J. and Bird, P. I. (2001) The granzyme B inhibitor, PI-9, is present in endothelial and mesothelial cells, suggesting that it protects bystander cells during immune responses. *Cell Immunol* **210**, 21-29

- 62 Young, J. L., Sukhova, G. K., Foster, D., Kisiel, W., Libby, P. and Schonbeck, U. (2000) The serpin proteinase inhibitor 9 is an endogenous inhibitor of interleukin 1beta-converting enzyme (caspase-1) activity in human vascular smooth muscle cells. *J Exp Med* **191**, 1535-1544
- 63 Bots, M., L, V. A. N. B., Rademaker, M. T., Offringa, R. and Medema, J. P. (2006) Serpins prevent granzyme-induced death in a species-specific manner. *Immunol Cell Biol* **84**, 79-86
- 64 Sipione, S., Simmen, K. C., Lord, S. J., Motyka, B., Ewen, C., Shostak, I., Rayat, G. R., Dufour, J. M., Korbitt, G. S., Rajotte, R. V. and Bleackley, R. C. (2006) Identification of a novel human granzyme B inhibitor secreted by cultured sertoli cells. *J Immunol* **177**, 5051-5058
- 65 Macri, L., Silverstein, D. and Clark, R. A. (2007) Growth factor binding to the pericellular matrix and its importance in tissue engineering. *Adv Drug Deliv Rev* **59**, 1366-1381
- 66 Imai, K., Hiramatsu, A., Fukushima, D., Pierschbacher, M. D. and Okada, Y. (1997) Degradation of decorin by matrix metalloproteinases: identification of the cleavage sites, kinetic analyses and transforming growth factor-beta1 release. *Biochem J* **322** ( Pt 3), 809-814
- 67 Taylor, A. W. (2009) Review of the activation of TGF-beta in immunity. *J Leukoc Biol* **85**, 29-33
- 68 Schiller, M., Javelaud, D. and Mauviel, A. (2004) TGF-beta-induced SMAD signaling and gene regulation: consequences for extracellular matrix remodeling and wound healing. *J Dermatol Sci* **35**, 83-92
- 69 Dallas, S. L., Miyazono, K., Skerry, T. M., Mundy, G. R. and Bonewald, L. F. (1995) Dual role for the latent transforming growth factor-beta binding protein in storage of latent TGF-beta in the extracellular matrix and as a structural matrix protein. *J Cell Biol* **131**, 539-549
- 70 Lopez-Casillas, F., Payne, H. M., Andres, J. L. and Massague, J. (1994) Betaglycan can act as a dual modulator of TGF-beta access to signaling receptors: mapping of ligand binding and GAG attachment sites. *J Cell Biol* **124**, 557-568
- 71 Hildebrand, A., Romaris, M., Rasmussen, L. M., Heinegard, D., Twardzik, D. R., Border, W. A. and Ruoslahti, E. (1994) Interaction of the small interstitial proteoglycans biglycan, decorin and fibromodulin with transforming growth factor beta. *Biochem J* **302** ( Pt 2), 527-534
- 72 Hirani, R., Hanssen, E. and Gibson, M. A. (2007) LTBP-2 specifically interacts with the amino-terminal region of fibrillin-1 and competes with LTBP-1 for binding to this microfibrillar protein. *Matrix Biol* **26**, 213-223
- 73 Isogai, Z., Ono, R. N., Ushiro, S., Keene, D. R., Chen, Y., Mazzieri, R., Charbonneau, N. L., Reinhardt, D. P., Rifkin, D. B. and Sakai, L. Y. (2003) Latent transforming growth factor beta-binding protein 1 interacts with fibrillin and is a microfibril-associated protein. *J Biol Chem* **278**, 2750-2757
- 74 Jensen, S. A., Reinhardt, D. P., Gibson, M. A. and Weiss, A. S. (2001) Protein interaction studies of MAGP-1 with tropoelastin and fibrillin-1. *J Biol Chem* **276**, 39661-39666
- 75 Hanssen, E., Hew, F. H., Moore, E. and Gibson, M. A. (2004) MAGP-2 has multiple binding regions on fibrillins and has covalent periodic association with fibrillin-containing microfibrils. *J Biol Chem* **279**, 29185-29194

- 76 Freeman, L. J., Lomas, A., Hodson, N., Sherratt, M. J., Mellody, K. T., Weiss, A. S., Shuttleworth, A. and Kielty, C. M. (2005) Fibulin-5 interacts with fibrillin-1 molecules and microfibrils. *Biochem J* **388**, 1-5
- 77 Sengle, G., Charbonneau, N. L., Ono, R. N., Sasaki, T., Alvarez, J., Keene, D. R., Bachinger, H. P. and Sakai, L. Y. (2008) Targeting of bone morphogenetic protein growth factor complexes to fibrillin. *J Biol Chem* **283**, 13874-13888
- 78 Brown, D. C. and Vogel, K. G. (1989) Characteristics of the in vitro interaction of a small proteoglycan (PG II) of bovine tendon with type I collagen. *Matrix* **9**, 468-478
- 79 Santra, M., Eichstetter, I. and Iozzo, R. V. (2000) An anti-oncogenic role for decorin. Down-regulation of ErbB2 leads to growth suppression and cytodifferentiation of mammary carcinoma cells. *J Biol Chem* **275**, 35153-35161
- 80 Lewandowska, K., Choi, H. U., Rosenberg, L. C., Zardi, L. and Culp, L. A. (1987) Fibronectin-mediated adhesion of fibroblasts: inhibition by dermatan sulfate proteoglycan and evidence for a cryptic glycosaminoglycan-binding domain. *J Cell Biol* **105**, 1443-1454
- 81 Winnemoller, M., Schmidt, G. and Kresse, H. (1991) Influence of decorin on fibroblast adhesion to fibronectin. *Eur J Cell Biol* **54**, 10-17
- 82 Winnemoller, M., Schon, P., Vischer, P. and Kresse, H. (1992) Interactions between thrombospondin and the small proteoglycan decorin: interference with cell attachment. *Eur J Cell Biol* **59**, 47-55
- 83 Reinboth, B., Hanssen, E., Cleary, E. G. and Gibson, M. A. (2002) Molecular interactions of biglycan and decorin with elastic fiber components: biglycan forms a ternary complex with tropoelastin and microfibril-associated glycoprotein 1. *J Biol Chem* **277**, 3950-3957
- 84 Yamaguchi, Y., Mann, D. M. and Ruoslahti, E. (1990) Negative regulation of transforming growth factor-beta by the proteoglycan decorin. *Nature* **346**, 281-284
- 85 Penc, S. F., Pomahac, B., Winkler, T., Dorschner, R. A., Eriksson, E., Herndon, M. and Gallo, R. L. (1998) Dermatan sulfate released after injury is a potent promoter of fibroblast growth factor-2 function. *J Biol Chem* **273**, 28116-28121
- 86 Tufvesson, E. and Westergren-Thorsson, G. (2002) Tumour necrosis factor-alpha interacts with biglycan and decorin. *FEBS Lett* **530**, 124-128
- 87 Nili, N., Cheema, A. N., Giordano, F. J., Barolet, A. W., Babaei, S., Hickey, R., Eskandarian, M. R., Smeets, M., Butany, J., Pasterkamp, G. and Strauss, B. H. (2003) Decorin inhibition of PDGF-stimulated vascular smooth muscle cell function: potential mechanism for inhibition of intimal hyperplasia after balloon angioplasty. *Am J Pathol* **163**, 869-878
- 88 Schonherr, E., Sunderkotter, C., Iozzo, R. V. and Schaefer, L. (2005) Decorin, a novel player in the insulin-like growth factor system. *J Biol Chem* **280**, 15767-15772
- 89 Reed, C. C. and Iozzo, R. V. (2002) The role of decorin in collagen fibrillogenesis and skin homeostasis. *Glycoconj J* **19**, 249-255
- 90 Merle, B., Durussel, L., Delmas, P. D. and Clezardin, P. (1999) Decorin inhibits cell migration through a process requiring its glycosaminoglycan side chain. *J Cell Biochem* **75**, 538-546
- 91 Xaus, J., Comalada, M., Cardo, M., Valledor, A. F. and Celada, A. (2001) Decorin inhibits macrophage colony-stimulating factor proliferation of macrophages and enhances cell survival through induction of p27(Kip1) and p21(Waf1). *Blood* **98**, 2124-2133

- 92 Yamaguchi, Y. and Ruoslahti, E. (1988) Expression of human proteoglycan in Chinese hamster ovary cells inhibits cell proliferation. *Nature* **336**, 244-246
- 93 Schonherr, E., O'Connell, B. C., Schittny, J., Robenek, H., Fastermann, D., Fisher, L. W., Plenz, G., Vischer, P., Young, M. F. and Kresse, H. (1999) Paracrine or virus-mediated induction of decorin expression by endothelial cells contributes to tube formation and prevention of apoptosis in collagen lattices. *Eur J Cell Biol* **78**, 44-55
- 94 Danielson, K. G., Baribault, H., Holmes, D. F., Graham, H., Kadler, K. E. and Iozzo, R. V. (1997) Targeted disruption of decorin leads to abnormal collagen fibril morphology and skin fragility. *J Cell Biol* **136**, 729-743
- 95 Oksala, O., Salo, T., Tammi, R., Hakkinen, L., Jalkanen, M., Inki, P. and Larjava, H. (1995) Expression of proteoglycans and hyaluronan during wound healing. *J Histochem Cytochem* **43**, 125-135
- 96 Sayani, K., Dodd, C. M., Nedelec, B., Shen, Y. J., Ghahary, A., Tredget, E. E. and Scott, P. G. (2000) Delayed appearance of decorin in healing burn scars. *Histopathology* **36**, 262-272
- 97 Carrino, D. A., Onnerfjord, P., Sandy, J. D., Cs-Szabo, G., Scott, P. G., Sorrell, J. M., Heinegard, D. and Caplan, A. I. (2003) Age-related changes in the proteoglycans of human skin. Specific cleavage of decorin to yield a major catabolic fragment in adult skin. *J Biol Chem* **278**, 17566-17572
- 98 Sayers, T. J., Wiltrout, T. A., Sowder, R., Munger, W. L., Smyth, M. J. and Henderson, L. E. (1992) Purification of a factor from the granules of a rat natural killer cell line (RNK) that reduces tumor cell growth and changes tumor morphology. Molecular identity with a granule serine protease (RNKP-1). *J Immunol* **148**, 292-300
- 99 Sower, L. E., Klimpel, G. R., Hanna, W. and Froelich, C. J. (1996) Extracellular Activities of Human Granzymes. *Cell Immunol* **171**, 159-163
- 100 Buzza, M. S. and Bird, P. I. (2006) Extracellular granzymes: current perspectives. *Biol Chem* **387**, 827-837
- 101 Romero, V. and Andrade, F. (2008) Non-apoptotic functions of granzymes. *Tissue Antigens* **71**, 409-416
- 102 Kramer, M. D. and Simon, M. M. (1987) Are Proteinases Functional Molecules of Lymphocytes-T. *Immunology Today* **8**, 140-142
- 103 Tak, P. P., Spaeny-Dekking, L., Kraan, M. C., Breedveld, F. C., Froelich, C. J. and Hack, C. E. (1999) The levels of soluble granzyme A and B are elevated in plasma and synovial fluid of patients with rheumatoid arthritis (RA). *Clin Exp Immunol* **116**, 366-370
- 104 Spaeny-Dekking, E. H., Hanna, W. L., Wolbink, A. M., Wever, P. C., Kummer, A. J., Swaak, A. J., Middeldorp, J. M., Huisman, H. G., Froelich, C. J. and Hack, C. E. (1998) Extracellular granzymes A and B in humans: detection of native species during CTL responses in vitro and in vivo. *J Immunol* **160**, 3610-3616
- 105 Saito, S., Murakoshi, K., Kotake, S., Kamatani, N. and Tomatsu, T. (2008) Granzyme B induces apoptosis of chondrocytes with natural killer cell-like cytotoxicity in rheumatoid arthritis. *J Rheumatol* **35**, 1932-1943
- 106 Froelich, C. J., Pardo, J. and Simon, M. M. (2009) Granule-associated serine proteases: granzymes might not just be killer proteases. *Trends Immunol* **30**, 117-123
- 107 Pardo, J., Wallich, R., Ebnet, K., Iden, S., Zentgraf, H., Martin, P., Ekiciler, A., Prins, A., Mullbacher, A., Huber, M. and Simon, M. M. (2007) Granzyme B is expressed in mouse mast cells in vivo and in vitro and causes delayed cell death independent of perforin. *Cell Death Differ* **14**, 1768-1779

- 108 Caughey, G. H., Schaumberg, T. H., Zerweck, E. H., Butterfield, J. H., Hanson, R. D., Silverman, G. A. and Ley, T. J. (1993) The human mast cell chymase gene (CMA1): mapping to the cathepsin G/granzyme gene cluster and lineage-restricted expression. *Genomics* **15**, 614-620
- 109 Isaaz, S., Baetz, K., Olsen, K., Podack, E. and Griffiths, G. M. (1995) Serial killing by cytotoxic T lymphocytes: T cell receptor triggers degranulation, re-filling of the lytic granules and secretion of lytic proteins via a non-granule pathway. *Eur J Immunol* **25**, 1071-1079
- 110 Skold, S., Zeberg, L., Gullberg, U. and Olofsson, T. (2002) Functional dissociation between proforms and mature forms of proteinase 3, azurocidin, and granzyme B in regulation of granulopoiesis. *Exp Hematol* **30**, 689-696
- 111 Prakash, M. D., Bird, C. H. and Bird, P. I. (2008) Active and zymogen forms of granzyme B are constitutively released from cytotoxic lymphocytes in the absence of target cell engagement. *Immunol Cell Biol*
- 112 Malmstrom, C., Lycke, J., Haghighi, S., Andersen, O., Carlsson, L., Wadenvik, H. and Olsson, B. (2008) Relapses in multiple sclerosis are associated with increased CD8+ T-cell mediated cytotoxicity in CSF. *J Neuroimmunol* **196**, 159-165
- 113 Takahashi, Y., Mine, J., Kubota, Y., Yamazaki, E. and Fujiwara, T. (2009) A substantial number of Rasmussen syndrome patients have increased IgG, CD4(+) T cells, TNFalpha, and Granzyme B in CSF. *Epilepsia*
- 114 Tremblay, G. M., Wolbink, A. M., Cormier, Y. and Hack, C. E. (2000) Granzyme activity in the inflamed lung is not controlled by endogenous serine proteinase inhibitors. *J Immunol* **165**, 3966-3969
- 115 Bratke, K., Bottcher, B., Leeder, K., Schmidt, S., Kupper, M., Virchow, J. C., Jr. and Luttmann, W. (2004) Increase in granzyme B+ lymphocytes and soluble granzyme B in bronchoalveolar lavage of allergen challenged patients with atopic asthma. *Clin Exp Immunol* **136**, 542-548
- 116 Kurschus, F. C., Kleinschmidt, M., Fellows, E., Dornmair, K., Rudolph, R., Lilie, H. and Jenne, D. E. (2004) Killing of target cells by redirected granzyme B in the absence of perforin. *FEBS Lett* **562**, 87-92
- 117 Rowshani, A. T., Strik, M. C., Molenaar, R., Yong, S. L., Wolbink, A. M., Bemelman, F. J., Hack, C. E. and Ten Berge, I. J. (2005) The granzyme B inhibitor SERPINB9 (protease inhibitor 9) circulates in blood and increases on primary cytomegalovirus infection after renal transplantation. *J Infect Dis* **192**, 1908-1911
- 118 Froelich, C. J., Zhang, X., Turbov, J., Hudig, D., Winkler, U. and Hanna, W. L. (1993) Human granzyme B degrades aggrecan proteoglycan in matrix synthesized by chondrocytes. *J Immunol* **151**, 7161-7171
- 119 Buzza, M. S., Dyson, J. M., Choi, H., Gardiner, E. E., Andrews, R. K., Kaiserman, D., Mitchell, C. A., Berndt, M. C., Dong, J. F. and Bird, P. I. (2008) Antihemostatic activity of human granzyme B mediated by cleavage of von Willebrand factor. *J Biol Chem* **283**, 22498-22504
- 120 Mulligan-Kehoe, M. J., Drinane, M. C., Mollmark, J., Casciola-Rosen, L., Hummers, L. K., Hall, A., Rosen, A., Wigley, F. M. and Simons, M. (2007) Antiangiogenic plasma activity in patients with systemic sclerosis. *Arthritis Rheum* **56**, 3448-3458
- 121 Gahring, L., Carlson, N. G., Meyer, E. L. and Rogers, S. W. (2001) Granzyme B proteolysis of a neuronal glutamate receptor generates an autoantigen and is modulated by glycosylation. *J Immunol* **166**, 1433-1438

- 122 Casciola-Rosen, L., Miagkov, A., Nagaraju, K., Askin, F., Jacobson, L., Rosen, A. and Drachman, D. B. (2008) Granzyme B: evidence for a role in the origin of myasthenia gravis. *J Neuroimmunol* **201-202**, 33-40
- 123 Buzza, M. S., Zamurs, L., Sun, J., Bird, C. H., Smith, A. I., Trapani, J. A., Froelich, C. J., Nice, E. C. and Bird, P. I. (2005) Extracellular matrix remodeling by human granzyme B via cleavage of vitronectin, fibronectin, and laminin. *J Biol Chem* **280**, 23549-23558
- 124 Choy, J. C., Hung, V. H., Hunter, A. L., Cheung, P. K., Motyka, B., Goping, I. S., Sawchuk, T., Bleackley, R. C., Podor, T. J., McManus, B. M. and Granville, D. J. (2004) Granzyme B induces smooth muscle cell apoptosis in the absence of perforin: involvement of extracellular matrix degradation. *Arterioscler Thromb Vasc Biol* **24**, 2245-2250
- 125 Afonina, I. S., Tynan, G. A., Logue, S. E., Cullen, S. P., Bots, M., Luthi, A. U., Reeves, E. P., McElvaney, N. G., Medema, J. P., Lavelle, E. C. and Martin, S. J. (2011) Granzyme B-dependent proteolysis acts as a switch to enhance the proinflammatory activity of IL-1alpha. *Mol Cell* **44**, 265-278
- 126 Lauw, F. N., Simpson, A. J., Hack, C. E., Prins, J. M., Wolbink, A. M., van Deventer, S. J., Chaowagul, W., White, N. J. and van Der Poll, T. (2000) Soluble granzymes are released during human endotoxemia and in patients with severe infection due to gram-negative bacteria. *J Infect Dis* **182**, 206-213
- 127 van Woensel, J. B., Biezeveld, M. H., Hack, C. E., Bos, A. P. and Kuijpers, T. W. (2005) Elastase and granzymes during meningococcal disease in children: correlation to disease severity. *Intensive Care Med* **31**, 1239-1247
- 128 Hermesen, C. C., Konijnenberg, Y., Mulder, L., Loe, C., van Deuren, M., van der Meer, J. W., van Mierlo, G. J., Eling, W. M., Hack, C. E. and Sauerwein, R. W. (2003) Circulating concentrations of soluble granzyme A and B increase during natural and experimental *Plasmodium falciparum* infections. *Clin Exp Immunol* **132**, 467-472
- 129 ten Berge, I. J., Wever, P. C., Wolbink, A. M., Surachno, J., Wertheim, P. M., Spaeny, L. H. and Hack, C. E. (1998) Increased systemic levels of soluble granzymes A and B during primary cytomegalovirus infection after renal transplantation. *Transplant Proc* **30**, 3972-3974
- 130 Bade, B., Lohrmann, J., ten Brinke, A., Wolbink, A. M., Wolbink, G. J., ten Berge, I. J., Virchow, J. C., Jr., Luttmann, W. and Hack, C. E. (2005) Detection of soluble human granzyme K in vitro and in vivo. *Eur J Immunol* **35**, 2940-2948
- 131 Hodge, S., Hodge, G., Nairn, J., Holmes, M. and Reynolds, P. N. (2006) Increased airway granzyme b and perforin in current and ex-smoking COPD subjects. *COPD* **3**, 179-187
- 132 Kondo, H., Hojo, Y., Tsuru, R., Nishimura, Y., Shimizu, H., Takahashi, N., Hirose, M., Ikemoto, T., Ohya, K., Katsuki, T., Yashiro, T. and Shimada, K. (2009) Elevation of plasma granzyme B levels after acute myocardial infarction. *Circ J* **73**, 503-507
- 133 Skjelland, M., Michelsen, A. E., Krohg-Sorensen, K., Tennoe, B., Dahl, A., Bakke, S., Brosstad, F., Damas, J. K., Russell, D., Halvorsen, B. and Aukrust, P. (2007) Plasma levels of granzyme B are increased in patients with lipid-rich carotid plaques as determined by echogenicity. *Atherosclerosis* **195**, e142-146
- 134 Lyons, R. M., Keski-Oja, J. and Moses, H. L. (1988) Proteolytic activation of latent transforming growth factor-beta from fibroblast-conditioned medium. *J Cell Biol* **106**, 1659-1665
- 135 Kraan, M. C., Haringman, J. J., Weedon, H., Barg, E. C., Smith, M. D., Ahern, M. J., Smeets, T. J., Breedveld, F. C. and Tak, P. P. (2004) T cells, fibroblast-like synoviocytes,

- and granzyme B+ cytotoxic cells are associated with joint damage in patients with recent onset rheumatoid arthritis. *Ann Rheum Dis* **63**, 483-488
- 136 Kummer, J. A., Tak, P. P., Brinkman, B. M., van Tilborg, A. A., Kamp, A. M., Verweij, C. L., Daha, M. R., Meinders, A. E., Hack, C. E. and Breedveld, F. C. (1994) Expression of granzymes A and B in synovial tissue from patients with rheumatoid arthritis and osteoarthritis. *Clin Immunol Immunopathol* **73**, 88-95
  - 137 Roday, H. K., van der Laan, W. H., Tak, P. P., de Roos, J. A., Bank, R. A., TeKoppele, J. M., Froelich, C. J., Hack, C. E., Hogendoorn, P. C., Breedveld, F. C. and Verheijen, J. H. (2001) Human granzyme B mediates cartilage proteoglycan degradation and is expressed at the invasive front of the synovium in rheumatoid arthritis. *Rheumatology (Oxford)* **40**, 55-61
  - 138 Tak, P. P., Kummer, J. A., Hack, C. E., Daha, M. R., Smeets, T. J., Erkelens, G. W., Meinders, A. E., Kluin, P. M. and Breedveld, F. C. (1994) Granzyme-positive cytotoxic cells are specifically increased in early rheumatoid synovial tissue. *Arthritis Rheum* **37**, 1735-1743
  - 139 Loeb, C. R., Harris, J. L. and Craik, C. S. (2006) Granzyme B proteolyzes receptors important to proliferation and survival, tipping the balance toward apoptosis. *J Biol Chem* **281**, 28326-28335
  - 140 Hernandez-Pigeon, H., Jean, C., Charruyer, A., Haure, M. J., Baudouin, C., Charveron, M., Quillet-Mary, A. and Laurent, G. (2007) UVA induces granzyme B in human keratinocytes through MIF: implication in extracellular matrix remodeling. *J Biol Chem* **282**, 8157-8164
  - 141 Barilla, M. L. and Carsons, S. E. (2000) Fibronectin fragments and their role in inflammatory arthritis. *Semin Arthritis Rheum* **29**, 252-265
  - 142 Norris, D. A., Clark, R. A., Swigart, L. M., Huff, J. C., Weston, W. L. and Howell, S. E. (1982) Fibronectin fragment(s) are chemotactic for human peripheral blood monocytes. *J Immunol* **129**, 1612-1618
  - 143 Odekon, L. E., Frewin, M. B., Del Vecchio, P., Saba, T. M. and Gudewicz, P. W. (1991) Fibronectin fragments released from phorbol ester-stimulated pulmonary artery endothelial cell monolayers promote neutrophil chemotaxis. *Immunology* **74**, 114-120
  - 144 Stanton, H., Ung, L. and Fosang, A. J. (2002) The 45 kDa collagen-binding fragment of fibronectin induces matrix metalloproteinase-13 synthesis by chondrocytes and aggrecan degradation by aggrecanases. *Biochem J* **364**, 181-190
  - 145 Omoto, Y., Yamanaka, K., Tokime, K., Kitano, S., Kakeda, M., Akeda, T., Kurokawa, I., Gabazza, E. C., Tsutsui, H., Katayama, N., Yamanishi, K., Nakanishi, K. and Mizutani, H. Granzyme B is a novel interleukin-18 converting enzyme. *J Dermatol Sci* **59**, 129-135
  - 146 Boivin, W. A., Shackleford, M., Vanden Hoek, A., Zhao, H., Hackett, T. L., Knight, D. A. and Granville, D. J. Granzyme B Cleaves Decorin, Biglycan and Soluble Betaglycan, Releasing Active Transforming Growth Factor-beta1. *PLoS One* **7**, e33163
  - 147 Rucevic, M., Fast, L. D., Jay, G. D., Trespalacios, F. M., Sucov, A., Siryaporn, E. and Lim, Y. P. (2007) Altered levels and molecular forms of granzyme k in plasma from septic patients. *Shock* **27**, 488-493
  - 148 Hollestelle, M. J., Lai, K. W., van Deuren, M., Lenting, P. J., de Groot, P. G., Sprong, T. and Bovenschen, N. Cleavage of von Willebrand factor by granzyme M destroys its factor VIII binding capacity. *PLoS One* **6**, e24216
  - 149 Cooper, D. M., Pechkovsky, D. V., Hackett, T. L., Knight, D. A. and Granville, D. J. Granzyme K activates protease-activated receptor-1. *PLoS One* **6**, e21484



- 150 Tsuzuki, S., Kokado, Y., Satomi, S., Yamasaki, Y., Hirayasu, H., Iwanaga, T. and Fushiki, T. (2003) Purification and identification of a binding protein for pancreatic secretory trypsin inhibitor: a novel role of the inhibitor as an anti-granzyme A. *Biochem J* **372**, 227-233
- 151 Kam, C. M., Hudig, D. and Powers, J. C. (2000) Granzymes (lymphocyte serine proteases): characterization with natural and synthetic substrates and inhibitors. *Biochim Biophys Acta* **1477**, 307-323
- 152 Spaeny-Dekking, E. H., Kamp, A. M., Froelich, C. J. and Hack, C. E. (2000) Extracellular granzyme A, complexed to proteoglycans, is protected against inactivation by protease inhibitors. *Blood* **95**, 1465-1472
- 153 de Koning, P. J., Kummer, J. A., de Poot, S. A., Quadir, R., Broekhuizen, R., McGettrick, A. F., Higgins, W. J., Devreese, B., Worrall, D. M. and Bovenschen, N. Intracellular serine protease inhibitor SERPINB4 inhibits granzyme M-induced cell death. *PLoS One* **6**, e22645
- 154 Mahrus, S., Kisiel, W. and Craik, C. S. (2004) Granzyme M is a regulatory protease that inactivates proteinase inhibitor 9, an endogenous inhibitor of granzyme B. *J Biol Chem* **279**, 54275-54282
- 155 Wilharm, E., Parry, M. A., Friebel, R., Tschesche, H., Matschiner, G., Sommerhoff, C. P. and Jenne, D. E. (1999) Generation of catalytically active granzyme K from *Escherichia coli* inclusion bodies and identification of efficient granzyme K inhibitors in human plasma. *J Biol Chem* **274**, 27331-27337
- 156 Beresford, P. J., Zhang, D., Oh, D. Y., Fan, Z., Greer, E. L., Russo, M. L., Jaju, M. and Lieberman, J. (2001) Granzyme A activates an endoplasmic reticulum-associated caspase-independent nuclease to induce single-stranded DNA nicks. *J Biol Chem* **276**, 43285-43293
- 157 Chowdhury, D. and Lieberman, J. (2008) Death by a thousand cuts: granzyme pathways of programmed cell death. *Annu Rev Immunol* **26**, 389-420
- 158 Martinvalet, D., Zhu, P. and Lieberman, J. (2005) Granzyme A induces caspase-independent mitochondrial damage, a required first step for apoptosis. *Immunity* **22**, 355-370
- 159 Lieberman, J. and Fan, Z. (2003) Nuclear war: the granzyme A-bomb. *Curr Opin Immunol* **15**, 553-559
- 160 Fan, Z., Beresford, P. J., Oh, D. Y., Zhang, D. and Lieberman, J. (2003) Tumor suppressor NM23-H1 is a granzyme A-activated DNase during CTL-mediated apoptosis, and the nucleosome assembly protein SET is its inhibitor. *Cell* **112**, 659-672
- 161 Fan, Z., Beresford, P. J., Zhang, D. and Lieberman, J. (2002) HMG2 interacts with the nucleosome assembly protein SET and is a target of the cytotoxic T-lymphocyte protease granzyme A. *Mol Cell Biol* **22**, 2810-2820
- 162 Fan, Z., Beresford, P. J., Zhang, D., Xu, Z., Novina, C. D., Yoshida, A., Pommier, Y. and Lieberman, J. (2003) Cleaving the oxidative repair protein Ape1 enhances cell death mediated by granzyme A. *Nat Immunol* **4**, 145-153
- 163 Chowdhury, D., Beresford, P. J., Zhu, P., Zhang, D., Sung, J. S., Demple, B., Perrino, F. W. and Lieberman, J. (2006) The exonuclease TREX1 is in the SET complex and acts in concert with NM23-H1 to degrade DNA during granzyme A-mediated cell death. *Mol Cell* **23**, 133-142
- 164 Zhang, D., Beresford, P. J., Greenberg, A. H. and Lieberman, J. (2001) Granzymes A and B directly cleave lamins and disrupt the nuclear lamina during granule-mediated cytolysis. *Proc Natl Acad Sci U S A* **98**, 5746-5751

- 165 Zhang, D., Pasternack, M. S., Beresford, P. J., Wagner, L., Greenberg, A. H. and Lieberman, J. (2001) Induction of rapid histone degradation by the cytotoxic T lymphocyte protease Granzyme A. *J Biol Chem* **276**, 3683-3690
- 166 Zhao, T., Zhang, H., Guo, Y., Zhang, Q., Hua, G., Lu, H., Hou, Q., Liu, H. and Fan, Z. (2007) Granzyme K cleaves the nucleosome assembly protein SET to induce single-stranded DNA nicks of target cells. *Cell Death Differ* **14**, 489-499
- 167 MacDonald, G., Shi, L., Vande Velde, C., Lieberman, J. and Greenberg, A. H. (1999) Mitochondria-dependent and -independent regulation of Granzyme B-induced apoptosis. *J Exp Med* **189**, 131-144
- 168 Johnson, H., Scorrano, L., Korsmeyer, S. J. and Ley, T. J. (2003) Cell death induced by granzyme C. *Blood* **101**, 3093-3101
- 169 Kelly, J. M., Waterhouse, N. J., Cretney, E., Browne, K. A., Ellis, S., Trapani, J. A. and Smyth, M. J. (2004) Granzyme M mediates a novel form of perforin-dependent cell death. *J Biol Chem* **279**, 22236-22242
- 170 Bots, M. and Medema, J. P. (2006) Granzymes at a glance. *J Cell Sci* **119**, 5011-5014
- 171 Wang, S., Xia, P., Shi, L. and Fan, Z. FADD cleavage by NK cell granzyme M enhances its self-association to facilitate procaspase-8 recruitment for auto-processing leading to caspase cascade. *Cell Death Differ*
- 172 Fellows, E., Gil-Parrado, S., Jenne, D. E. and Kurschus, F. C. (2007) Natural killer cell-derived human granzyme H induces an alternative, caspase-independent cell-death program. *Blood* **110**, 544-552
- 173 Hou, Q., Zhao, T., Zhang, H., Lu, H., Zhang, Q., Sun, L. and Fan, Z. (2008) Granzyme H induces apoptosis of target tumor cells characterized by DNA fragmentation and Bid-dependent mitochondrial damage. *Mol Immunol* **45**, 1044-1055
- 174 Lu, H., Hou, Q., Zhao, T., Zhang, H., Zhang, Q., Wu, L. and Fan, Z. (2006) Granzyme M directly cleaves inhibitor of caspase-activated DNase (CAD) to unleash CAD leading to DNA fragmentation. *J Immunol* **177**, 1171-1178
- 175 Bratke, K., Klug, A., Julius, P., Kuepper, M., Lommatzsch, M., Sparmann, G., Luttmann, W. and Virchow, J. C. (2008) Granzyme K: a novel mediator in acute airway inflammation. *Thorax* **63**, 1006-1011
- 176 Hirayasu, H., Yoshikawa, Y., Tsuzuki, S. and Fushiki, T. (2008) A lymphocyte serine protease granzyme A causes detachment of a small-intestinal epithelial cell line (IEC-6). *Biosci Biotechnol Biochem* **72**, 2294-2302
- 177 Simon, M. M., Prester, M., Nerz, G., Kramer, M. D. and Fruth, U. (1988) Release of biologically active fragments from human plasma-fibronectin by murine T cell-specific proteinase 1 (TSP-1). *Biol Chem Hoppe Seyler* **369 Suppl**, 107-112
- 178 Simon, M. M., Kramer, M. D., Prester, M. and Gay, S. (1991) Mouse T-cell associated serine proteinase 1 degrades collagen type IV: a structural basis for the migration of lymphocytes through vascular basement membranes. *Immunology* **73**, 117-119
- 179 Vanguri, P., Lee, E., Henkart, P. and Shin, M. L. (1993) Hydrolysis of myelin basic protein in myelin membranes by granzymes of large granular lymphocytes. *J Immunol* **150**, 2431-2439
- 180 Brunner, G., Simon, M. M. and Kramer, M. D. (1990) Activation of pro-urokinase by the human T cell-associated serine proteinase HuTSP-1. *FEBS Lett* **260**, 141-144
- 181 Hansen, K. K., Sherman, P. M., Cellars, L., Andrade-Gordon, P., Pan, Z., Baruch, A., Wallace, J. L., Hollenberg, M. D. and Vergnolle, N. (2005) A major role for proteolytic activity and proteinase-activated receptor-2 in the pathogenesis of infectious colitis. *Proc Natl Acad Sci U S A* **102**, 8363-8368

- 182 Parry, M. A., Myles, T., Tschopp, J. and Stone, S. R. (1996) Cleavage of the thrombin receptor: identification of potential activators and inactivators. *Biochem J* **320** ( Pt 1), 335-341
- 183 Suidan, H. S., Clemetson, K. J., Brown-Luedi, M., Niclou, S. P., Clemetson, J. M., Tschopp, J. and Monard, D. (1996) The serine protease granzyme A does not induce platelet aggregation but inhibits responses triggered by thrombin. *Biochem J* **315** ( Pt 3), 939-945
- 184 Suidan, H. S., Bouvier, J., Schaerer, E., Stone, S. R., Monard, D. and Tschopp, J. (1994) Granzyme A released upon stimulation of cytotoxic T lymphocytes activates the thrombin receptor on neuronal cells and astrocytes. *Proc Natl Acad Sci U S A* **91**, 8112-8116
- 185 Irmeler, M., Hertig, S., MacDonald, H. R., Sadoul, R., Becherer, J. D., Proudfoot, A., Solari, R. and Tschopp, J. (1995) Granzyme A is an interleukin 1 beta-converting enzyme. *J Exp Med* **181**, 1917-1922
- 186 Sower, L. E., Klimpel, G. R., Hanna, W. and Froelich, C. J. (1996) Extracellular activities of human granzymes. I. Granzyme A induces IL6 and IL8 production in fibroblast and epithelial cell lines. *Cell Immunol* **171**, 159-163
- 187 Sower, L. E., Froelich, C. J., Allegretto, N., Rose, P. M., Hanna, W. D. and Klimpel, G. R. (1996) Extracellular activities of human granzyme A. Monocyte activation by granzyme A versus alpha-thrombin. *J Immunol* **156**, 2585-2590
- 188 Metkar, S. S., Menaa, C., Pardo, J., Wang, B., Wallich, R., Freudenberg, M., Kim, S., Raja, S. M., Shi, L., Simon, M. M. and Froelich, C. J. (2008) Human and mouse granzyme A induce a proinflammatory cytokine response. *Immunity* **29**, 720-733
- 189 Sower, L. E., Froelich, C. J., Carney, D. H., Fenton, J. W., 2nd and Klimpel, G. R. (1995) Thrombin induces IL-6 production in fibroblasts and epithelial cells. Evidence for the involvement of the seven-transmembrane domain (STD) receptor for alpha-thrombin. *J Immunol* **155**, 895-901
- 190 Joeckel, L. T., Wallich, R., Martin, P., Sanchez-Martinez, D., Weber, F. C., Martin, S. F., Borner, C., Pardo, J., Froelich, C. and Simon, M. M. Mouse granzyme K has pro-inflammatory potential. *Cell Death Differ* **18**, 1112-1119
- 191 Anthony, D. A., Andrews, D. M., Chow, M., Watt, S. V., House, C., Akira, S., Bird, P. I., Trapani, J. A. and Smyth, M. J. A role for granzyme M in TLR4-driven inflammation and endotoxemia. *J Immunol* **185**, 1794-1803
- 192 Young, L. H., Joag, S. V., Lin, P. Y., Luo, S. F., Zheng, L. M., Liu, C. C. and Young, J. D. (1992) Expression of cytolytic mediators by synovial fluid lymphocytes in rheumatoid arthritis. *Am J Pathol* **140**, 1261-1268
- 193 Chamberlain, C. M., Ang, L. S., Boivin, W. A., Cooper, D. M., Williams, S. J., Zhao, H., Hendel, A., Folkesson, M., Swedenborg, J., Allard, M. F., McManus, B. M. and Granville, D. J. (2010) Perforin-independent extracellular granzyme B activity contributes to abdominal aortic aneurysm. *Am J Pathol* **176**, 1038-1049
- 194 Ang, L. S., Boivin, W. A., Williams, S. J., Zhao, H., Abraham, T., Carmine-Simmen, K., McManus, B. M., Bleackley, R. C. and Granville, D. J. (2011) Serpina3n attenuates granzyme B-mediated decorin cleavage and rupture in a murine model of aortic aneurysm. *Cell Death Dis* **2**, e215
- 195 Hiebert, P. R., Boivin, W. A., Abraham, T., Pazooki, S., Zhao, H. and Granville, D. J. (2011) Granzyme B contributes to extracellular matrix remodeling and skin aging in apolipoprotein E knockout mice. *Exp Gerontol* **46**, 489-499

- 196 Chrysofakis, G., Tzanakis, N., Kyriakoy, D., Tsoumakidou, M., Tsiligianni, I., Klimathianaki, M. and Siafakas, N. M. (2004) Perforin expression and cytotoxic activity of sputum CD8+ lymphocytes in patients with COPD. *Chest* **125**, 71-76
- 197 Hodge, G., Mukaro, V., Reynolds, P. N. and Hodge, S. Role of increased CD8/CD28(null) T cells and alternative co-stimulatory molecules in chronic obstructive pulmonary disease. *Clin Exp Immunol* **166**, 94-102
- 198 Hashimoto, S., Kobayashi, A., Kooguchi, K., Kitamura, Y., Onodera, H. and Nakajima, H. (2000) Upregulation of two death pathways of perforin/granzyme and FasL/Fas in septic acute respiratory distress syndrome. *Am J Respir Crit Care Med* **161**, 237-243
- 199 Dourado, M., Bento, J., Mesquita, L., Marques, A., Vale-Pereira, S., Ribeiro, A. B. and Pinto, A. M. (2005) [Granzymes A and B in pulmonary sarcoidosis (experimental study)]. *Rev Port Pneumol* **11**, 111-133
- 200 Kurumagawa, T., Seki, S., Kobayashi, H., Koike, Y., Kanoh, S., Hiraide, H. and Motoyoshi, K. (2003) Characterization of bronchoalveolar lavage T cell subsets in sarcoidosis on the basis of CD57, CD4 and CD8. *Clin Exp Immunol* **133**, 438-447
- 201 Teymoortash, A., Tiemann, M., Schrader, C. and Werner, J. A. (2004) Characterization of lymphoid infiltrates in chronic obstructive sialadenitis associated with sialolithiasis. *J Oral Pathol Med* **33**, 300-304
- 202 Meade, J. L., de Wynter, E. A., Brett, P., Sharif, S. M., Woods, C. G., Markham, A. F. and Cook, G. P. (2006) A family with Papillon-Lefevre syndrome reveals a requirement for cathepsin C in granzyme B activation and NK cell cytolytic activity. *Blood* **107**, 3665-3668
- 203 Pham, C. T., Ivanovich, J. L., Raptis, S. Z., Zehnbauser, B. and Ley, T. J. (2004) Papillon-Lefevre syndrome: correlating the molecular, cellular, and clinical consequences of cathepsin C/dipeptidyl peptidase I deficiency in humans. *J Immunol* **173**, 7277-7281
- 204 Lage, D., Pimentel, V. N., Soares, T. C., Souza, E. M., Metze, K. and Cintra, M. L. Perforin and granzyme B expression in oral and cutaneous lichen planus - a comparative study. *J Cutan Pathol* **38**, 973-978
- 205 Kook, H., Zeng, W., Guibin, C., Kirby, M., Young, N. S. and Maciejewski, J. P. (2001) Increased cytotoxic T cells with effector phenotype in aplastic anemia and myelodysplasia. *Exp Hematol* **29**, 1270-1277
- 206 Xu, J. L., Nagasaka, T. and Nakashima, N. (2003) Involvement of cytotoxic granules in the apoptosis of aplastic anaemia. *Br J Haematol* **120**, 850-852
- 207 Papadaki, H. A., Coulocheri, S., Xylouri, I., Chatzivassili, A., Konsolas, J., Katrinakis, G., Karkavitsas, N. and Eliopoulos, G. D. (1998) Defective natural killer cell activity of peripheral blood lymphocytes correlates with the degree of neutropenia in patients with chronic idiopathic neutropenia of adults. *Ann Hematol* **76**, 127-134
- 208 Olsson, B., Andersson, P. O., Jernas, M., Jacobsson, S., Carlsson, B., Carlsson, L. M. and Wadenvik, H. (2003) T-cell-mediated cytotoxicity toward platelets in chronic idiopathic thrombocytopenic purpura. *Nat Med* **9**, 1123-1124
- 209 Wang, L., Zhang, F., Zhu, Y. Y., Li, L. Z., Ma, D. X. and Hou, M. (2005) [Mechanism of cell-mediated lysis of autologous platelets in chronic idiopathic thrombocytopenic purpura]. *Zhonghua Yi Xue Za Zhi* **85**, 3048-3051
- 210 Zhang, F., Chu, X., Wang, L., Zhu, Y., Li, L., Ma, D., Peng, J. and Hou, M. (2006) Cell-mediated lysis of autologous platelets in chronic idiopathic thrombocytopenic purpura. *Eur J Haematol* **76**, 427-431

- 211 Bodemer, C., Peuchmaur, M., Fraitag, S., Chatenoud, L., Brousse, N. and De Prost, Y. (2000) Role of cytotoxic T cells in chronic alopecia areata. *J Invest Dermatol* **114**, 112-116
- 212 Siebenhaar, F., Sharov, A. A., Peters, E. M., Sharova, T. Y., Syska, W., Mardaryev, A. N., Freyschmidt-Paul, P., Sundberg, J. P., Maurer, M. and Botchkarev, V. A. (2007) Substance P as an immunomodulatory neuropeptide in a mouse model for autoimmune hair loss (alopecia areata). *J Invest Dermatol* **127**, 1489-1497
- 213 Sato-Kawamura, M., Aiba, S. and Tagami, H. (2003) Strong expression of CD40, CD54 and HLA-DR antigen and lack of evidence for direct cellular cytotoxicity are unique immunohistopathological features in alopecia areata. *Arch Dermatol Res* **294**, 536-543
- 214 Berthou, C., Michel, L., Soulie, A., Jean-Louis, F., Flageul, B., Dubertret, L., Sigaux, F., Zhang, Y. and Sasportes, M. (1997) Acquisition of granzyme B and Fas ligand proteins by human keratinocytes contributes to epidermal cell defense. *J Immunol* **159**, 5293-5300
- 215 Trivedi, N. R., Gilliland, K. L., Zhao, W., Liu, W. and Thiboutot, D. M. (2006) Gene array expression profiling in acne lesions reveals marked upregulation of genes involved in inflammation and matrix remodeling. *J Invest Dermatol* **126**, 1071-1079
- 216 Hussein, M. R., Abdel-Magid, W. M., Saleh, R. and Nada, E. (2008) Phenotypical Characteristics of the Immune Cells in Allergic Contact Dermatitis, Atopic Dermatitis and Pityriasis Rosea. *Pathol Oncol Res*
- 217 Hussein, M. R., Aboulhagag, N. M., Atta, H. S. and Atta, S. M. (2008) Evaluation of the profile of the immune cell infiltrate in lichen planus, discoid lupus erythematosus, and chronic dermatitis. *Pathology* **40**, 682-693
- 218 Yawalkar, N., Hunger, R. E., Buri, C., Schmid, S., Egli, F., Brand, C. U., Mueller, C., Pichler, W. J. and Braathen, L. R. (2001) A comparative study of the expression of cytotoxic proteins in allergic contact dermatitis and psoriasis: spongiotic skin lesions in allergic contact dermatitis are highly infiltrated by T cells expressing perforin and granzyme B. *Am J Pathol* **158**, 803-808
- 219 Yawalkar, N., Schmid, S., Braathen, L. R. and Pichler, W. J. (2001) Perforin and granzyme B may contribute to skin inflammation in atopic dermatitis and psoriasis. *Br J Dermatol* **144**, 1133-1139
- 220 Oyarbide-Valencia, K., van den Boorn, J. G., Denman, C. J., Li, M., Carlson, J. M., Hernandez, C., Nishimura, M. I., Das, P. K., Luiten, R. M. and Le Poole, I. C. (2006) Therapeutic implications of autoimmune vitiligo T cells. *Autoimmun Rev* **5**, 486-492
- 221 van den Wijngaard, R., Wankowicz-Kalinska, A., Le Poole, C., Tigges, B., Westerhof, W. and Das, P. (2000) Local immune response in skin of generalized vitiligo patients. Destruction of melanocytes is associated with the prominent presence of CLA+ T cells at the perilesional site. *Lab Invest* **80**, 1299-1309
- 222 Ammar, M., Mokni, M., Boubaker, S., El Gaied, A., Ben Osman, A. and Louzir, H. (2008) Involvement of granzyme B and granulysin in the cytotoxic response in lichen planus. *J Cutan Pathol* **35**, 630-634
- 223 Santoro, A., Majorana, A., Bardellini, E., Gentili, F., Festa, S., Sapelli, P. and Facchetti, F. (2004) Cytotoxic molecule expression and epithelial cell apoptosis in oral and cutaneous lichen planus. *Am J Clin Pathol* **121**, 758-764
- 224 Shimizu, M., Higaki, Y., Higaki, M. and Kawashima, M. (1997) The role of granzyme B-expressing CD8-positive T cells in apoptosis of keratinocytes in lichen planus. *Arch Dermatol Res* **289**, 527-532

- 225 Santoro, A., Majorana, A., Roversi, L., Gentili, F., Marrelli, S., Vermi, W., Bardellini, E., Sapelli, P. and Facchetti, F. (2005) Recruitment of dendritic cells in oral lichen planus. *J Pathol* **205**, 426-434
- 226 Wenzel, J., Scheler, M., Proelss, J., Bieber, T. and Tuting, T. (2006) Type I interferon-associated cytotoxic inflammation in lichen planus. *J Cutan Pathol* **33**, 672-678
- 227 Hunger, R. E., Bronnimann, M., Kappeler, A., Mueller, C., Braathen, L. R. and Yawalkar, N. (2007) Detection of perforin and granzyme B mRNA expressing cells in lichen sclerosus. *Exp Dermatol* **16**, 416-420
- 228 Wenzel, J., Wiechert, A., Merkel, C., Bieber, T. and Tuting, T. (2007) IP10/CXCL10 - CXCR3 interaction: a potential self-recruiting mechanism for cytotoxic lymphocytes in lichen sclerosus et atrophicus. *Acta Derm Venereol* **87**, 112-117
- 229 Regauer, S., Liegl, B., Reich, O. and Beham-Schmid, C. (2004) Vasculitis in lichen sclerosus: an under recognized feature? *Histopathology* **45**, 237-244
- 230 Borchers, A. T., Lee, J. L., Naguwa, S. M., Cheema, G. S. and Gershwin, M. E. (2008) Stevens-Johnson syndrome and toxic epidermal necrolysis. *Autoimmun Rev* **7**, 598-605
- 231 Chave, T. A., Mortimer, N. J., Sladden, M. J., Hall, A. P. and Hutchinson, P. E. (2005) Toxic epidermal necrolysis: current evidence, practical management and future directions. *Br J Dermatol* **153**, 241-253
- 232 Nassif, A., Bensussan, A., Boumsell, L., Deniaud, A., Moslehi, H., Wolkenstein, P., Bagot, M. and Roujeau, J. C. (2004) Toxic epidermal necrolysis: effector cells are drug-specific cytotoxic T cells. *J Allergy Clin Immunol* **114**, 1209-1215
- 233 Posadas, S. J., Padial, A., Torres, M. J., Mayorga, C., Leyva, L., Sanchez, E., Alvarez, J., Romano, A., Juarez, C. and Blanca, M. (2002) Delayed reactions to drugs show levels of perforin, granzyme B, and Fas-L to be related to disease severity. *J Allergy Clin Immunol* **109**, 155-161
- 234 Nassif, A., Moslehi, H., Le Gouvello, S., Bagot, M., Lyonnet, L., Michel, L., Boumsell, L., Bensussan, A. and Roujeau, J. C. (2004) Evaluation of the potential role of cytokines in toxic epidermal necrolysis. *J Invest Dermatol* **123**, 850-855
- 235 Verneuil, L., Leboeuf, C., Vidal, J. S., Ratajczak, P., Comoz, F., Ameisen, J. C. and Janin, A. Endothelial damage in all types of T-lymphocyte-mediated drug-induced eruptions. *Arch Dermatol* **147**, 579-584
- 236 Hussein, M. R., Ali, F. M. and Omar, A. E. (2007) Immunohistological analysis of immune cells in blistering skin lesions. *J Clin Pathol* **60**, 62-71
- 237 Wenzel, J., Uerlich, M., Worrenkamper, E., Freutel, S., Bieber, T. and Tuting, T. (2005) Scarring skin lesions of discoid lupus erythematosus are characterized by high numbers of skin-homing cytotoxic lymphocytes associated with strong expression of the type I interferon-induced protein MxA. *Br J Dermatol* **153**, 1011-1015
- 238 Takahashi, H., Amagai, M., Tanikawa, A., Suzuki, S., Ikeda, Y., Nishikawa, T., Kawakami, Y. and Kuwana, M. (2007) T helper type 2-biased natural killer cell phenotype in patients with pemphigus vulgaris. *J Invest Dermatol* **127**, 324-330
- 239 Smeets, T. J., Kraan, M. C., Galjaard, S., Youssef, P. P., Smith, M. D. and Tak, P. P. (2001) Analysis of the cell infiltrate and expression of matrix metalloproteinases and granzyme B in paired synovial biopsy specimens from the cartilage-pannus junction in patients with RA. *Ann Rheum Dis* **60**, 561-565
- 240 Goldbach-Mansky, R., Suson, S., Wesley, R., Hack, C. E., El-Gabalawy, H. S. and Tak, P. P. (2005) Raised granzyme B levels are associated with erosions in patients with early rheumatoid factor positive rheumatoid arthritis. *Ann Rheum Dis* **64**, 715-721

- 241 Ren, J., Feng, Z., Lv, Z., Chen, X. and Li, J. Natural killer-22 cells in the synovial fluid of patients with rheumatoid arthritis are an innate source of interleukin 22 and tumor necrosis factor-alpha. *J Rheumatol* **38**, 2112-2118
- 242 Arvonnen, M., Ikni, L., Augustin, M., Karttunen, T. J. and Vahasalo, P. Increase of duodenal and ileal mucosal cytotoxic lymphocytes in juvenile idiopathic arthritis. *Clin Exp Rheumatol* **28**, 128-134
- 243 Smeets, T. J., Dolhain, R. J., Breedveld, F. C. and Tak, P. P. (1998) Analysis of the cellular infiltrates and expression of cytokines in synovial tissue from patients with rheumatoid arthritis and reactive arthritis. *J Pathol* **186**, 75-81
- 244 Bauer, J., Bien, C. G. and Lassmann, H. (2002) Rasmussen's encephalitis: a role for autoimmune cytotoxic T lymphocytes. *Curr Opin Neurol* **15**, 197-200
- 245 Bauer, J., Elger, C. E., Hans, V. H., Schramm, J., Urbach, H., Lassmann, H. and Bien, C. G. (2007) Astrocytes are a specific immunological target in Rasmussen's encephalitis. *Ann Neurol* **62**, 67-80
- 246 Bien, C. G., Bauer, J., Deckwerth, T. L., Wiendl, H., Deckert, M., Wiestler, O. D., Schramm, J., Elger, C. E. and Lassmann, H. (2002) Destruction of neurons by cytotoxic T cells: a new pathogenic mechanism in Rasmussen's encephalitis. *Ann Neurol* **51**, 311-318
- 247 Schwab, N., Bien, C. G., Waschbisch, A., Becker, A., Vince, G. H., Dornmair, K. and Wiendl, H. (2009) CD8+ T-cell clones dominate brain infiltrates in Rasmussen encephalitis and persist in the periphery. *Brain*
- 248 Kebir, H., Kreymborg, K., Ifergan, I., Dodelet-Devillers, A., Cayrol, R., Bernard, M., Giuliani, F., Arbour, N., Becher, B. and Prat, A. (2007) Human TH17 lymphocytes promote blood-brain barrier disruption and central nervous system inflammation. *Nat Med* **13**, 1173-1175
- 249 Pouly, S. and Antel, J. P. (1999) Multiple sclerosis and central nervous system demyelination. *J Autoimmun* **13**, 297-306
- 250 Rensing-Ehl, A., Malipiero, U., Irmeler, M., Tschopp, J., Constam, D. and Fontana, A. (1996) Neurons induced to express major histocompatibility complex class I antigen are killed via the perforin and not the Fas (APO-1/CD95) pathway. *Eur J Immunol* **26**, 2271-2274
- 251 Haile, Y., Simmen, K. C., Pasichnyk, D., Touret, N., Simmen, T., Lu, J. Q., Bleackley, R. C. and Giuliani, F. Granule-derived granzyme B mediates the vulnerability of human neurons to T cell-induced neurotoxicity. *J Immunol* **187**, 4861-4872
- 252 Niland, B., Miklossy, G., Banki, K., Biddison, W. E., Casciola-Rosen, L., Rosen, A., Martinvalet, D., Lieberman, J. and Perl, A. Cleavage of transaldolase by granzyme B causes the loss of enzymatic activity with retention of antigenicity for multiple sclerosis patients. *J Immunol* **184**, 4025-4032
- 253 Ilzecka, J. Granzymes A and B levels in serum of patients with amyotrophic lateral sclerosis. *Clin Biochem* **44**, 650-653
- 254 Wanschitz, J., Maier, H., Lassmann, H., Budka, H. and Berger, T. (2003) Distinct time pattern of complement activation and cytotoxic T cell response in Guillain-Barre syndrome. *Brain* **126**, 2034-2042
- 255 Heuss, D., Probst-Cousin, S., Kayser, C. and Neundorfer, B. (2000) Cell death in vasculitic neuropathy. *Muscle Nerve* **23**, 999-1004
- 256 Oka, N., Takahashi, M., Kawasaki, T. and Akiguchi, I. (2000) Apoptosis of perineurial cells in sensory perineuritis. *Acta Neuropathol* **99**, 317-320

- 257 Chaitanya, G. V. and Babu, P. P. (2008) Multiple apoptogenic proteins are involved in the nuclear translocation of Apoptosis Inducing Factor during transient focal cerebral ischemia in rat. *Brain Res* **1246**, 178-190
- 258 Chaitanya, G. V., Kolli, M. and Babu, P. P. (2008) Granzyme-b mediated cell death in the spinal cord-injured rat model. *Neuropathology*
- 259 Huarte, E., Rynda-Apple, A., Riccardi, C., Skyberg, J. A., Golden, S., Rollins, M. F., Ramstead, A. G., Jackiw, L. O., Maddaloni, M. and Pascual, D. W. Tolerogen-induced interferon-producing killer dendritic cells (IKDCs) protect against EAE. *J Autoimmun* **37**, 328-341
- 260 Chaitanya, G. V., Eeka, P., Munker, R., Alexander, J. S. and Babu, P. P. Role of cytotoxic protease granzyme-b in neuronal degeneration during human stroke. *Brain Pathol* **21**, 16-30
- 261 Casciola-Rosen, L., Andrade, F., Ulanet, D., Wong, W. B. and Rosen, A. (1999) Cleavage by granzyme B is strongly predictive of autoantigen status: implications for initiation of autoimmunity. *J Exp Med* **190**, 815-826
- 262 Blanco, P., Pitard, V., Viallard, J. F., Taupin, J. L., Pellegrin, J. L. and Moreau, J. F. (2005) Increase in activated CD8+ T lymphocytes expressing perforin and granzyme B correlates with disease activity in patients with systemic lupus erythematosus. *Arthritis Rheum* **52**, 201-211
- 263 Skoldberg, F., Ronnblom, L., Thornemo, M., Lindahl, A., Bird, P. I., Rorsman, F., Kampe, O. and Landgren, E. (2002) Identification of AHNAK as a novel autoantigen in systemic lupus erythematosus. *Biochem Biophys Res Commun* **291**, 951-958
- 264 Lee, K. J., Dong, X., Wang, J., Takeda, Y. and Dynan, W. S. (2002) Identification of human autoantibodies to the DNA ligase IV/XRCC4 complex and mapping of an autoimmune epitope to a potential regulatory region. *J Immunol* **169**, 3413-3421
- 265 Graham, K. L., Thibault, D. L., Steinman, J. B., Okeke, L., Kao, P. N. and Utz, P. J. (2005) Granzyme B is dispensable for immunologic tolerance to self in a murine model of systemic lupus erythematosus. *Arthritis Rheum* **52**, 1684-1693
- 266 Daca, A., Czuszyńska, Z., Smolenska, Z., Zdrojewski, Z., Witkowski, J. M. and Bryl, E. Two systemic lupus erythematosus (SLE) global disease activity indexes--the SLE Disease Activity Index and the Systemic Lupus Activity Measure--demonstrate different correlations with activation of peripheral blood CD4+ T cells. *Hum Immunol* **72**, 1160-1167
- 267 Shah, D., Kiran, R., Wanchu, A. and Bhatnagar, A. Soluble granzyme B and cytotoxic T lymphocyte activity in the pathogenesis of systemic lupus erythematosus. *Cell Immunol* **269**, 16-21
- 268 Nield, L. E., Silverman, E. D., Smallhorn, J. F., Taylor, G. P., Mullen, J. B., Benson, L. N. and Hornberger, L. K. (2002) Endocardial fibroelastosis associated with maternal anti-Ro and anti-La antibodies in the absence of atrioventricular block. *J Am Coll Cardiol* **40**, 796-802
- 269 Schachna, L., Wigley, F. M., Morris, S., Gelber, A. C., Rosen, A. and Casciola-Rosen, L. (2002) Recognition of Granzyme B-generated autoantigen fragments in scleroderma patients with ischemic digital loss. *Arthritis Rheum* **46**, 1873-1884
- 270 Ulanet, D. B., Flavahan, N. A., Casciola-Rosen, L. and Rosen, A. (2004) Selective cleavage of nucleolar autoantigen B23 by granzyme B in differentiated vascular smooth muscle cells: insights into the association of specific autoantibodies with distinct disease phenotypes. *Arthritis Rheum* **50**, 233-241



- 271 Polihronis, M., Tapinos, N. I., Theocharis, S. E., Economou, A., Kittas, C. and Moutsopoulos, H. M. (1998) Modes of epithelial cell death and repair in Sjogren's syndrome (SS). *Clin Exp Immunol* **114**, 485-490
- 272 Tapinos, N. I., Polihronis, M., Tzioufas, A. G. and Moutsopoulos, H. M. (1999) Sjogren's syndrome. Autoimmune epithelitis. *Adv Exp Med Biol* **455**, 127-134
- 273 Huang, M., Ida, H., Arima, K., Nakamura, H., Aramaki, T., Fujikawa, K., Tamai, M., Kamachi, M., Kawakami, A., Yamasaki, H., Origuchi, T. and Eguchi, K. (2007) La autoantigen translocates to cytoplasm after cleavage during granzyme B-mediated cytotoxicity. *Life Sci* **81**, 1461-1466
- 274 Kuwana, M., Okano, T., Ogawa, Y., Kaburaki, J. and Kawakami, Y. (2001) Autoantibodies to the amino-terminal fragment of beta-fodrin expressed in glandular epithelial cells in patients with Sjogren's syndrome. *J Immunol* **167**, 5449-5456
- 275 Fujihara, T., Fujita, H., Tsubota, K., Saito, K., Tsuzaka, K., Abe, T. and Takeuchi, T. (1999) Preferential localization of CD8+ alpha E beta 7+ T cells around acinar epithelial cells with apoptosis in patients with Sjogren's syndrome. *J Immunol* **163**, 2226-2235
- 276 Nagaraju, K., Cox, A., Casciola-Rosen, L. and Rosen, A. (2001) Novel fragments of the Sjogren's syndrome autoantigens alpha-fodrin and type 3 muscarinic acetylcholine receptor generated during cytotoxic lymphocyte granule-induced cell death. *Arthritis Rheum* **44**, 2376-2386
- 277 Huang, M., Ida, H., Kamachi, M., Iwanaga, N., Izumi, Y., Tanaka, F., Aratake, K., Arima, K., Tamai, M., Hida, A., Nakamura, H., Origuchi, T., Kawakami, A., Ogawa, N., Sugai, S., Utz, P. J. and Eguchi, K. (2005) Detection of apoptosis-specific autoantibodies directed against granzyme B-induced cleavage fragments of the SS-B (La) autoantigen in sera from patients with primary Sjogren's syndrome. *Clin Exp Immunol* **142**, 148-154
- 278 Rosen, A. and Casciola-Rosen, L. (2004) Altered autoantigen structure in Sjogren's syndrome: implications for the pathogenesis of autoimmune tissue damage. *Crit Rev Oral Biol Med* **15**, 156-164
- 279 Cherin, P., Herson, S., Crevon, M. C., Hauw, J. J., Cervera, P., Galanaud, P. and Emilie, D. (1996) Mechanisms of lysis by activated cytotoxic cells expressing perforin and granzyme-B genes and the protein TIA-1 in muscle biopsies of myositis. *J Rheumatol* **23**, 1135-1142
- 280 Levine, S. M., Raben, N., Xie, D., Askin, F. B., Tuder, R., Mullins, M., Rosen, A. and Casciola-Rosen, L. A. (2007) Novel conformation of histidyl-transfer RNA synthetase in the lung: the target tissue in Jo-1 autoantibody-associated myositis. *Arthritis Rheum* **56**, 2729-2739
- 281 Li, M. and Dalakas, M. C. (2000) Expression of human IAP-like protein in skeletal muscle: a possible explanation for the rare incidence of muscle fiber apoptosis in T-cell mediated inflammatory myopathies. *J Neuroimmunol* **106**, 1-5
- 282 Targoff, I. N. (2000) Update on myositis-specific and myositis-associated autoantibodies. *Curr Opin Rheumatol* **12**, 475-481
- 283 Estella, E., McKenzie, M. D., Catterall, T., Sutton, V. R., Bird, P. I., Trapani, J. A., Kay, T. W. and Thomas, H. E. (2006) Granzyme B-mediated death of pancreatic beta-cells requires the proapoptotic BH3-only molecule bid. *Diabetes* **55**, 2212-2219
- 284 Thomas, H. E. and Kay, T. W. Intracellular pathways of pancreatic beta-cell apoptosis in type 1 diabetes. *Diabetes Metab Res Rev* **27**, 790-796
- 285 Graham, K. L., Krishnamurthy, B., Fynch, S., Mollah, Z. U., Slattery, R., Santamaria, P., Kay, T. W. and Thomas, H. E. Autoreactive cytotoxic T lymphocytes acquire higher

- expression of cytotoxic effector markers in the islets of NOD mice after priming in pancreatic lymph nodes. *Am J Pathol* **178**, 2716-2725
- 286 Adriani, M., Jones, K. A., Uchiyama, T., Kirby, M. R., Silvin, C., Anderson, S. M. and Candotti, F. Defective inhibition of B-cell proliferation by Wiskott-Aldrich syndrome protein-deficient regulatory T cells. *Blood* **117**, 6608-6611
- 287 Drut, R. and Drut, R. M. (2004) Lymphocytic gastritis in pediatric celiac disease -- immunohistochemical study of the intraepithelial lymphocytic component. *Med Sci Monit* **10**, CR38-42
- 288 Suzuki, T., Ito, M., Hayasaki, N., Ishihara, A., Ando, T., Ina, K. and Kusugami, K. (2003) Cytotoxic molecules expressed by intraepithelial lymphocytes may be involved in the pathogenesis of acute gastric mucosal lesions. *J Gastroenterol* **38**, 216-221
- 289 Oberhuber, G., Bodingbauer, M., Mosberger, I., Stolte, M. and Vogelsang, H. (1998) High proportion of granzyme B-positive (activated) intraepithelial and lamina propria lymphocytes in lymphocytic gastritis. *Am J Surg Pathol* **22**, 450-458
- 290 Kaserer, K., Exner, M., Mosberger, I., Penner, E. and Wrba, F. (1998) Characterization of the inflammatory infiltrate in autoimmune cholangitis. A morphological and immunohistochemical study. *Virchows Arch* **432**, 217-222
- 291 Tsuda, M., Ambrosini, Y. M., Zhang, W., Yang, G. X., Ando, Y., Rong, G., Tsuneyama, K., Sumida, K., Shimoda, S., Bowlus, C. L., Leung, P. S., He, X. S., Coppel, R. L., Ansari, A. A., Lian, Z. X. and Gershwin, M. E. Fine phenotypic and functional characterization of effector cluster of differentiation 8 positive T cells in human patients with primary biliary cirrhosis. *Hepatology* **54**, 1293-1302
- 292 Ziol, M., Poirel, H., Kountchou, G. N., Boyer, O., Mohand, D., Mouthon, L., Tepper, M., Guillet, J. G., Guettier, C., Raphael, M. and Beaugrand, M. (2004) Intrasinusoidal cytotoxic CD8+ T cells in nodular regenerative hyperplasia of the liver. *Hum Pathol* **35**, 1241-1251
- 293 Mitomi, H., Ohkura, Y., Yokoyama, K., Sada, M., Kobayashi, K., Tanabe, S., Fukui, N., Kanazawa, H., Kishimoto, I. and Saigenji, K. (2007) Contribution of TIA-1+ and granzyme B+ cytotoxic T lymphocytes to cryptal apoptosis and ulceration in active inflammatory bowel disease. *Pathol Res Pract* **203**, 717-723
- 294 Schiller, N. K., Boisvert, W. A. and Curtiss, L. K. (2002) Inflammation in atherosclerosis: lesion formation in LDL receptor-deficient mice with perforin and Lyst(beige) mutations. *Arterioscler Thromb Vasc Biol* **22**, 1341-1346
- 295 Nakajima, T., Schulte, S., Warrington, K. J., Kopecky, S. L., Frye, R. L., Goronzy, J. J. and Weyand, C. M. (2002) T-cell-mediated lysis of endothelial cells in acute coronary syndromes. *Circulation* **105**, 570-575
- 296 Tsuru, R., Kondo, H., Hojo, Y., Gama, M., Mizuno, O., Katsuki, T., Shimada, K., Kikuchi, M. and Yashiro, T. (2008) Increased granzyme B production from peripheral blood mononuclear cells in patients with acute coronary syndrome. *Heart* **94**, 305-310
- 297 Hendel, A., Cooper, D., Abraham, T., Zhao, H., Allard, M. F. and Granville, D. J. (2012) Proteinase inhibitor 9 is reduced in human atherosclerotic lesion development. *Cardiovasc Pathol* **21**, 28-38
- 298 Altamari, A., Gruppioni, E., Capizzi, E., Bagni, A., Corti, B., Fiorentino, M., Lazzarotto, T., Lauro, A., Pinna, A. D., Ridolfi, L., Grigioni, W. F. and D'Errico-Grigioni, A. (2008) Blood monitoring of granzyme B and perforin expression after intestinal transplantation: considerations on clinical relevance. *Transplantation* **85**, 1778-1783

- 299 Cashion, A., Sabek, O., Driscoll, C., Gaber, L., Kotb, M. and Gaber, O. (2006) Correlation of genetic markers of rejection with biopsy findings following human pancreas transplant. *Clin Transplant* **20**, 106-112
- 300 Cashion, A. K., Sabek, O. M., Driscoll, C. J., Gaber, L. W. and Gaber, A. O. (2006) Serial peripheral blood cytotoxic lymphocyte gene expression measurements for prediction of pancreas transplant rejection. *Transplant Proc* **38**, 3676-3677
- 301 Corti, B., Altimari, A., Gabusi, E., Pinna, A. D., Lauro, A., Morselli-Labate, A. M., Gruppioni, E., Pirini, M. G., Fiorentino, M., Ridolfi, L., Grigioni, W. F. and D'Errico-Grigioni, A. (2005) Potential of real-time PCR assessment of granzyme B and perforin up-regulation for rejection monitoring in intestinal transplant recipients. *Transplant Proc* **37**, 4467-4471
- 302 D'Errico, A., Corti, B., Pinna, A. D., Altimari, A., Gruppioni, E., Gabusi, E., Fiorentino, M., Bagni, A. and Grigioni, W. F. (2003) Granzyme B and perforin as predictive markers for acute rejection in human intestinal transplantation. *Transplant Proc* **35**, 3061-3065
- 303 Kummer, J. A., Wever, P. C., Kamp, A. M., ten Berge, I. J., Hack, C. E. and Weening, J. J. (1995) Expression of granzyme A and B proteins by cytotoxic lymphocytes involved in acute renal allograft rejection. *Kidney Int* **47**, 70-77
- 304 Li, B., Hartono, C., Ding, R., Sharma, V. K., Ramaswamy, R., Qian, B., Serur, D., Mouradian, J., Schwartz, J. E. and Suthanthiran, M. (2001) Noninvasive diagnosis of renal-allograft rejection by measurement of messenger RNA for perforin and granzyme B in urine. *N Engl J Med* **344**, 947-954
- 305 Simon, T., Opelz, G., Wiesel, M., Ott, R. C. and Susal, C. (2003) Serial peripheral blood perforin and granzyme B gene expression measurements for prediction of acute rejection in kidney graft recipients. *Am J Transplant* **3**, 1121-1127
- 306 Yannarakis, M., Rebibou, J. M., Ducloux, D., Saas, P., Duperrier, A., Felix, S., Rifl e, G., Chalopin, J. M., Herve, P., Tiberghien, P. and Ferrand, C. (2006) Urinary cytotoxic molecular markers for a noninvasive diagnosis in acute renal transplant rejection. *Transpl Int* **19**, 759-768
- 307 Choy, J. C., Cruz, R. P., Kerjner, A., Geisbrecht, J., Sawchuk, T., Fraser, S. A., Hudig, D., Bleackley, R. C., Jirik, F. R., McManus, B. M. and Granville, D. J. (2005) Granzyme B induces endothelial cell apoptosis and contributes to the development of transplant vascular disease. *Am J Transplant* **5**, 494-499
- 308 Choy, J. C., Kerjner, A., Wong, B. W., McManus, B. M. and Granville, D. J. (2004) Perforin mediates endothelial cell death and resultant transplant vascular disease in cardiac allografts. *Am J Pathol* **165**, 127-133
- 309 Guzman-Cottrill, J. A., Garcia, F. L., Shulman, S. T. and Rowley, A. H. (2005) CD8 T lymphocytes do not express cytotoxic proteins in coronary artery aneurysms in acute Kawasaki disease. *Pediatr Infect Dis J* **24**, 382-384
- 310 Kuijpers, T. W., Biezeveld, M., Achterhuis, A., Kuipers, I., Lam, J., Hack, C. E., Becker, A. E. and van der Wal, A. C. (2003) Longstanding obliterative panarteritis in Kawasaki disease: lack of cyclosporin A effect. *Pediatrics* **112**, 986-992
- 311 Brown, T. J., Crawford, S. E., Cornwall, M. L., Garcia, F., Shulman, S. T. and Rowley, A. H. (2001) CD8 T lymphocytes and macrophages infiltrate coronary artery aneurysms in acute Kawasaki disease. *J Infect Dis* **184**, 940-943
- 312 Fujinaka, H., Yamamoto, T., Feng, L., Nameta, M., Garcia, G., Chen, S., El-shemi, A. A., Ohshiro, K., Katsuyama, K., Yoshida, Y., Yaoita, E. and Wilson, C. B. (2007) Anti-

- perforin antibody treatment ameliorates experimental crescentic glomerulonephritis in WKY rats. *Kidney Int* **72**, 823-830
- 313 Reynolds, J., Norgan, V. A., Bhambra, U., Smith, J., Cook, H. T. and Pusey, C. D. (2002) Anti-CD8 monoclonal antibody therapy is effective in the prevention and treatment of experimental autoimmune glomerulonephritis. *J Am Soc Nephrol* **13**, 359-369
- 314 Ikemoto, T., Hojo, Y., Kondo, H., Takahashi, N., Hirose, M., Nishimura, Y., Katsuki, T. and Shimada, K. (2009) Plasma granzyme B as a predicting factor of coronary artery disease--clinical significance in patients with chronic renal failure. *J Cardiol* **54**, 409-415
- 315 Clark, S. B., Rice, T. W., Tubbs, R. R., Richter, J. E. and Goldblum, J. R. (2000) The nature of the myenteric infiltrate in achalasia: an immunohistochemical analysis. *Am J Surg Pathol* **24**, 1153-1158
- 316 Resnick, M. B., Finkelstein, Y., Weissler, A., Levy, J. and Yakirevich, E. (1999) Assessment and diagnostic utility of the cytotoxic T-lymphocyte phenotype using the specific markers granzyme-B and TIA-1 in esophageal mucosal biopsies. *Hum Pathol* **30**, 397-402
- 317 Oberhuber, G., Puspok, A., Peck-Radosavlevic, M., Kutilek, M., Lamprecht, A., Chott, A., Vogelsang, H. and Stolte, M. (1999) Aberrant esophageal HLA-DR expression in a high percentage of patients with Crohn's disease. *Am J Surg Pathol* **23**, 970-976
- 318 Toquet, C., Hamidou, M. A., Renaudin, K., Jarry, A., Foulc, P., Barbarot, S., Labois, C. and Mussini, J. M. (2003) In situ immunophenotype of the inflammatory infiltrate in eosinophilic fasciitis. *J Rheumatol* **30**, 1811-1815
- 319 Yakirevich, E., Yanai, O., Sova, Y., Sabo, E., Stein, A., Hiss, J. and Resnick, M. B. (2002) Cytotoxic phenotype of intra-epithelial lymphocytes in normal and cryptorchid human testicular excurrent ducts. *Hum Reprod* **17**, 275-283
- 320 Ohshima, K., Shimazaki, K., Kume, T., Suzumiya, J., Kanda, M. and Kikuchi, M. (1998) Perforin and Fas pathways of cytotoxic T-cells in histiocytic necrotizing lymphadenitis. *Histopathology* **33**, 471-478
- 321 Mori, N., Yatabe, Y., Asai, J. and Nagasawa, T. (1997) Immunohistochemical study of necrotizing lymphadenitis: a possible mechanism for apoptosis involving perforin and granzyme-producing cytotoxic T cells. *Pathol Int* **47**, 31-37
- 322 Baetz, K., Isaaz, S. and Griffiths, G. M. (1995) Loss of cytotoxic T lymphocyte function in Chediak-Higashi syndrome arises from a secretory defect that prevents lytic granule exocytosis. *J Immunol* **154**, 6122-6131
- 323 Sandri, M., El Meslemani, A. H., Sandri, C., Schjerling, P., Vissing, K., Andersen, J. L., Rossini, K., Carraro, U. and Angelini, C. (2001) Caspase 3 expression correlates with skeletal muscle apoptosis in Duchenne and facioscapulo human muscular dystrophy. A potential target for pharmacological treatment? *J Neuropathol Exp Neurol* **60**, 302-312
- 324 Qiu, S., Du, Y., Duan, X., Geng, X., Xie, J., Gao, H. and Yang, P. C. Cytotoxic T lymphocytes mediate chronic inflammation of the nasal mucosa of patients with atypical allergic rhinitis. *N Am J Med Sci* **3**, 378-383
- 325 Kim, J. Y., Shin, E., Kim, H. J. and Park, K. Expression of Epstein-Barr virus and granzyme B in cytologic smears of histiocytic necrotizing lymphadenitis. *Diagn Cytopathol*
- 326 Hansson, G. K., Robertson, A. K. and Soderberg-Naucler, C. (2006) Inflammation and atherosclerosis. *Annu Rev Pathol* **1**, 297-329
- 327 Hansson, G. K. and Libby, P. (2006) The immune response in atherosclerosis: a double-edged sword. *Nat Rev Immunol* **6**, 508-519

- 328 Lloyd-Jones, D., Adams, R., Carnethon, M., De Simone, G., Ferguson, T. B., Flegal, K., Ford, E., Furie, K., Go, A., Greenlund, K., Haase, N., Hailpern, S., Ho, M., Howard, V., Kissela, B., Kittner, S., Lackland, D., Lisabeth, L., Marelli, A., McDermott, M., Meigs, J., Mozaffarian, D., Nichol, G., O'Donnell, C., Roger, V., Rosamond, W., Sacco, R., Sorlie, P., Stafford, R., Steinberger, J., Thom, T., Wasserthiel-Smoller, S., Wong, N., Wylie-Rosett, J. and Hong, Y. (2009) Heart disease and stroke statistics -- 2009 update: a report from the American Heart Association Statistics Committee and Stroke Statistics Subcommittee. *Circulation* **119**, e21-181
- 329 Daugherty, A. and Rateri, D. L. (2008) Atherosclerosis: cell biology and lipoproteins. *Curr Opin Lipidol* **19**, 328-329
- 330 Daugherty, A., Rateri, D. L. and Lu, H. (2008) As macrophages indulge, atherosclerotic lesions bulge. *Circ Res* **102**, 1445-1447
- 331 Bobryshev, Y. V. and Lord, R. S. (1995) S-100 positive cells in human arterial intima and in atherosclerotic lesions. *Cardiovasc Res* **29**, 689-696
- 332 Jonasson, L., Holm, J., Skalli, O., Bondjers, G. and Hansson, G. K. (1986) Regional accumulations of T cells, macrophages, and smooth muscle cells in the human atherosclerotic plaque. *Arteriosclerosis* **6**, 131-138
- 333 Kaartinen, M., Penttila, A. and Kovanen, P. T. (1994) Accumulation of activated mast cells in the shoulder region of human coronary atheroma, the predilection site of atheromatous rupture. *Circulation* **90**, 1669-1678
- 334 Rizas, K. D., Ippagunta, N. and Tilson, M. D., 3rd (2009) Immune cells and molecular mediators in the pathogenesis of the abdominal aortic aneurysm. *Cardiol Rev* **17**, 201-210
- 335 Verneuil, L., Ratajczak, P., Allabert, C., Leboeuf, C., Comoz, F., Janin, A. and Ameisen, J. C. (2009) Endothelial cell apoptosis in severe drug-induced bullous eruptions. *Br J Dermatol* **161**, 1371-1375
- 336 Hull, S. M., Nutbrown, M., Pepall, L., Thornton, M. J., Randall, V. A. and Cunliffe, W. J. (1991) Immunohistologic and ultrastructural comparison of the dermal papilla and hair follicle bulb from "active" and "normal" areas of alopecia areata. *J Invest Dermatol* **96**, 673-681
- 337 Ranki, A., Kianto, U., Kanerva, L., Tolvanen, E. and Johansson, E. (1984) Immunohistochemical and electron microscopic characterization of the cellular infiltrate in alopecia (areata, totalis, and universalis). *J Invest Dermatol* **83**, 7-11
- 338 Banda, M. J. and Werb, Z. (1981) Mouse macrophage elastase. Purification and characterization as a metalloproteinase. *Biochem J* **193**, 589-605
- 339 Gordon, S., Werb, Z. and Cohn, Z. A. (1976) Methods for Detection of Macrophage Secretory Enzymes. In *In vitro methods in cell mediated and tumor immunity* (Bloom, B. R. and David, J. R., eds.), pp. 349-350, Academic Press, New York
- 340 Backes, C., Kuentzer, J., Lenhof, H. P., Comtesse, N. and Meese, E. (2005) GraBCas: a bioinformatics tool for score-based prediction of Caspase- and Granzyme B-cleavage sites in protein sequences. *Nucleic Acids Res* **33**, W208-213
- 341 Gayzik, F. S., Yu, M. M., Danelson, K. A., Slice, D. E. and Stitzel, J. D. (2008) Quantification of age-related shape change of the human rib cage through geometric morphometrics. *J Biomech* **41**, 1545-1554
- 342 Muller-Rover, S., Handjiski, B., van der Veen, C., Eichmuller, S., Foitzik, K., McKay, I. A., Stenn, K. S. and Paus, R. (2001) A comprehensive guide for the accurate classification of murine hair follicles in distinct hair cycle stages. *J Invest Dermatol* **117**, 3-15

- 343 Paus, R., Stenn, K. S. and Link, R. E. (1990) Telogen skin contains an inhibitor of hair growth. *Br J Dermatol* **122**, 777-784
- 344 Mecklenburg, L., Tobin, D. J., Muller-Rover, S., Handjiski, B., Wendt, G., Peters, E. M., Pohl, S., Moll, I. and Paus, R. (2000) Active hair growth (anagen) is associated with angiogenesis. *J Invest Dermatol* **114**, 909-916
- 345 Willoughby, C. A., Bull, H. G., Garcia-Calvo, M., Jiang, J., Chapman, K. T. and Thornberry, N. A. (2002) Discovery of potent, selective human granzyme B inhibitors that inhibit CTL mediated apoptosis. *Bioorg Med Chem Lett* **12**, 2197-2200
- 346 Medema, J. P., Toes, R. E., Scaffidi, C., Zheng, T. S., Flavell, R. A., Melief, C. J., Peter, M. E., Offringa, R. and Krammer, P. H. (1997) Cleavage of FLICE (caspase-8) by granzyme B during cytotoxic T lymphocyte-induced apoptosis. *Eur J Immunol* **27**, 3492-3498
- 347 Hendel, A., Hiebert, P. R., Boivin, W. A., Williams, S. J. and Granville, D. J. (2010) Granzymes in age-related cardiovascular and pulmonary diseases. *Cell Death Differ* **17**, 596-606
- 348 Raja, S. M., Wang, B., Dantuluri, M., Desai, U. R., Demeler, B., Spiegel, K., Metkar, S. S. and Froelich, C. J. (2002) Cytotoxic cell granule-mediated apoptosis. Characterization of the macromolecular complex of granzyme B with serglycin. *J Biol Chem* **277**, 49523-49530
- 349 Fleischmajer, R., Fisher, L. W., MacDonald, E. D., Jacobs, L., Jr., Perlish, J. S. and Termine, J. D. (1991) Decorin interacts with fibrillar collagen of embryonic and adult human skin. *J Struct Biol* **106**, 82-90
- 350 Schonherr, E., Witsch-Prehm, P., Harrach, B., Robenek, H., Rauterberg, J. and Kresse, H. (1995) Interaction of biglycan with type I collagen. *J Biol Chem* **270**, 2776-2783
- 351 Gambichler, T., Tomi, N. S., Skrygan, M., Altmeyer, P. and Kreuter, A. (2007) Significant decrease of decorin expression in human skin following short-term ultraviolet exposures. *J Dermatol Sci* **45**, 203-205
- 352 Mukhopadhyay, A., Wong, M. Y., Chan, S. Y., Do, D. V., Khoo, A., Ong, C. T., Cheong, H. H., Lim, I. J. and Phan, T. T. (2010) Syndecan-2 and decorin: proteoglycans with a difference--implications in keloid pathogenesis. *J Trauma* **68**, 999-1008
- 353 Carrino, D. A., Mesiano, S., Barker, N. M., Hurd, W. W. and Caplan, A. I. (2012) Proteoglycans of uterine fibroids and keloid scars: similarity in their proteoglycan composition. *Biochem J*
- 354 Wu, J., Utani, A., Endo, H. and Shinkai, H. (2001) Deficiency of the decorin core protein in the variant form of Ehlers-Danlos syndrome with chronic skin ulcer. *J Dermatol Sci* **27**, 95-103
- 355 Corsi, A., Xu, T., Chen, X. D., Boyde, A., Liang, J., Mankani, M., Sommer, B., Iozzo, R. V., Eichstetter, I., Robey, P. G., Bianco, P. and Young, M. F. (2002) Phenotypic effects of biglycan deficiency are linked to collagen fibril abnormalities, are synergized by decorin deficiency, and mimic Ehlers-Danlos-like changes in bone and other connective tissues. *J Bone Miner Res* **17**, 1180-1189
- 356 Sweetwyne, M. T. and Murphy-Ullrich, J. E. Thrombospondin1 in tissue repair and fibrosis: TGF-beta-dependent and independent mechanisms. *Matrix Biol*
- 357 Young, G. D. and Murphy-Ullrich, J. E. (2004) Molecular interactions that confer latency to transforming growth factor-beta. *J Biol Chem* **279**, 38032-38039
- 358 Hogg, P. J., Owensby, D. A. and Chesterman, C. N. (1993) Thrombospondin 1 is a tight-binding competitive inhibitor of neutrophil cathepsin G. Determination of the kinetic

- mechanism of inhibition and localization of cathepsin G binding to the thrombospondin 1 type 3 repeats. *J Biol Chem* **268**, 21811-21818
- 359 Lee, N. V., Sato, M., Annis, D. S., Loo, J. A., Wu, L., Mosher, D. F. and Iruela-Arispe, M. L. (2006) ADAMTS1 mediates the release of antiangiogenic polypeptides from TSP1 and 2. *Embo J* **25**, 5270-5283
- 360 Trask, T. M., Trask, B. C., Ritty, T. M., Abrams, W. R., Rosenbloom, J. and Mecham, R. P. (2000) Interaction of tropoelastin with the amino-terminal domains of fibrillin-1 and fibrillin-2 suggests a role for the fibrillins in elastic fiber assembly. *J Biol Chem* **275**, 24400-24406
- 361 Miosge, N., Gotz, W., Sasaki, T., Chu, M. L., Timpl, R. and Herken, R. (1996) The extracellular matrix proteins fibulin-1 and fibulin-2 in the early human embryo. *Histochem J* **28**, 109-116
- 362 Zhang, H. Y., Timpl, R., Sasaki, T., Chu, M. L. and Ekblom, P. (1996) Fibulin-1 and fibulin-2 expression during organogenesis in the developing mouse embryo. *Dev Dyn* **205**, 348-364
- 363 Kainulainen, V., Wang, H., Schick, C. and Bernfield, M. (1998) Syndecans, heparan sulfate proteoglycans, maintain the proteolytic balance of acute wound fluids. *J Biol Chem* **273**, 11563-11569
- 364 Subramanian, S. V., Fitzgerald, M. L. and Bernfield, M. (1997) Regulated shedding of syndecan-1 and -4 ectodomains by thrombin and growth factor receptor activation. *J Biol Chem* **272**, 14713-14720
- 365 Yamaguchi, Y. (2000) Leticans: organizers of the brain extracellular matrix. *Cell Mol Life Sci* **57**, 276-289
- 366 Hockfield, S., Kalb, R. G., Zaremba, S. and Fryer, H. (1990) Expression of neural proteoglycans correlates with the acquisition of mature neuronal properties in the mammalian brain. *Cold Spring Harb Symp Quant Biol* **55**, 505-514
- 367 Bandtlow, C. E. and Zimmermann, D. R. (2000) Proteoglycans in the developing brain: new conceptual insights for old proteins. *Physiol Rev* **80**, 1267-1290
- 368 Hedlund, H., Mengarelli-Widholm, S., Heinegard, D., Reinholt, F. P. and Svensson, O. (1994) Fibromodulin distribution and association with collagen. *Matrix Biol* **14**, 227-232
- 369 Leung, L. L. (1984) Role of thrombospondin in platelet aggregation. *J Clin Invest* **74**, 1764-1772
- 370 Munjal, I. D., Crawford, D. R., Blake, D. A., Sabet, M. D. and Gordon, S. R. (1990) Thrombospondin: biosynthesis, distribution, and changes associated with wound repair in corneal endothelium. *Eur J Cell Biol* **52**, 252-263
- 371 Taraboletti, G., Roberts, D., Liotta, L. A. and Giavazzi, R. (1990) Platelet thrombospondin modulates endothelial cell adhesion, motility, and growth: a potential angiogenesis regulatory factor. *J Cell Biol* **111**, 765-772
- 372 Volpert, O. V., Tolsma, S. S., Pellerin, S., Feige, J. J., Chen, H., Mosher, D. F. and Bouck, N. (1995) Inhibition of angiogenesis by thrombospondin-2. *Biochem Biophys Res Commun* **217**, 326-332
- 373 Noh, Y. H., Matsuda, K., Hong, Y. K., Kunstfeld, R., Riccardi, L., Koch, M., Oura, H., Dadras, S. S., Streit, M. and Detmar, M. (2003) An N-terminal 80 kDa recombinant fragment of human thrombospondin-2 inhibits vascular endothelial growth factor induced endothelial cell migration in vitro and tumor growth and angiogenesis in vivo. *J Invest Dermatol* **121**, 1536-1543
- 374 Kyriakides, T. R., Tam, J. W. and Bornstein, P. (1999) Accelerated wound healing in mice with a disruption of the thrombospondin 2 gene. *J Invest Dermatol* **113**, 782-787

- 375 Amalinei, C., Caruntu, I. D. and Balan, R. A. (2007) Biology of metalloproteinases. *Rom J Morphol Embryol* **48**, 323-334
- 376 Chang, C. and Werb, Z. (2001) The many faces of metalloproteases: cell growth, invasion, angiogenesis and metastasis. *Trends Cell Biol* **11**, S37-43
- 377 Wakefield, L. M., Smith, D. M., Flanders, K. C. and Sporn, M. B. (1988) Latent transforming growth factor-beta from human platelets. A high molecular weight complex containing precursor sequences. *J Biol Chem* **263**, 7646-7654
- 378 Mythreya, K. and Blobel, G. C. (2009) Proteoglycan signaling co-receptors: roles in cell adhesion, migration and invasion. *Cell Signal* **21**, 1548-1558
- 379 Velasco-Loyden, G., Arribas, J. and Lopez-Casillas, F. (2004) The shedding of betaglycan is regulated by pervanadate and mediated by membrane type matrix metalloprotease-1. *J Biol Chem* **279**, 7721-7733
- 380 Arribas, J. and Borroto, A. (2002) Protein ectodomain shedding. *Chem Rev* **102**, 4627-4638
- 381 Zhang, Y. E. (2009) Non-Smad pathways in TGF-beta signaling. *Cell Res* **19**, 128-139
- 382 Ito, S., Taguchi, H., Hamada, S., Kawauchi, S., Ito, H., Senoura, T., Watanabe, J., Nishimukai, M., Ito, S. and Matsui, H. (2008) Enzymatic properties of cellobiose 2-epimerase from *Ruminococcus albus* and the synthesis of rare oligosaccharides by the enzyme. *Appl Microbiol Biotechnol* **79**, 433-441
- 383 Kratzer, R., Pukl, M., Egger, S., Vogl, M., Brecker, L. and Nidetzky, B. (2011) Enzyme identification and development of a whole-cell biotransformation for asymmetric reduction of o-chloroacetophenone. *Biotechnol Bioeng* **108**, 797-803
- 384 Bae, Y. A., Kim, S. H., Lee, E. G., Sohn, W. M. and Kong, Y. (2011) Identification and biochemical characterization of two novel peroxiredoxins in a liver fluke, *Clonorchis sinensis*. *Parasitology* **138**, 1143-1153
- 385 Chau, Y., Tan, F. E. and Langer, R. (2004) Synthesis and characterization of dextran-peptide-methotrexate conjugates for tumor targeting via mediation by matrix metalloproteinase II and matrix metalloproteinase IX. *Bioconjug Chem* **15**, 931-941
- 386 Ling, H. B., Wang, G. J., Li, J. E. and Tan, H. R. (2008) sanN encoding a dehydrogenase is essential for Nikkomycin biosynthesis in *Streptomyces ansochromogenes*. *J Microbiol Biotechnol* **18**, 397-403
- 387 Casciola-Rosen, L., Garcia-Calvo, M., Bull, H. G., Becker, J. W., Hines, T., Thornberry, N. A. and Rosen, A. (2007) Mouse and human granzyme B have distinct tetrapeptide specificities and abilities to recruit the bid pathway. *J Biol Chem* **282**, 4545-4552
- 388 Kaiserman, D., Bird, C. H., Sun, J., Matthews, A., Ung, K., Whisstock, J. C., Thompson, P. E., Trapani, J. A. and Bird, P. I. (2006) The major human and mouse granzymes are structurally and functionally divergent. *J Cell Biol* **175**, 619-630
- 389 Harris, J. L., Peterson, E. P., Hudig, D., Thornberry, N. A. and Craik, C. S. (1998) Definition and redesign of the extended substrate specificity of granzyme B. *J Biol Chem* **273**, 27364-27373
- 390 Van Damme, P., Maurer-Stroh, S., Plasman, K., Van Durme, J., Colaert, N., Timmerman, E., De Bock, P. J., Goethals, M., Rousseau, F., Schymkowitz, J., Vandekerckhove, J. and Gevaert, K. (2009) Analysis of protein processing by N-terminal proteomics reveals novel species-specific substrate determinants of granzyme B orthologs. *Mol Cell Proteomics* **8**, 258-272
- 391 Thomas, D. A. and Massague, J. (2005) TGF-beta directly targets cytotoxic T cell functions during tumor evasion of immune surveillance. *Cancer Cell* **8**, 369-380
- 392 Granville, D. J. Granzymes in disease: bench to bedside. *Cell Death Differ* **17**, 565-566



- 393 Ramirez, F., Sakai, L. Y., Dietz, H. C. and Rifkin, D. B. (2004) Fibrillin microfibrils: multipurpose extracellular networks in organismal physiology. *Physiol Genomics* **19**, 151-154
- 394 Reinhardt, D. P., Keene, D. R., Corson, G. M., Poschl, E., Bachinger, H. P., Gammee, J. E. and Sakai, L. Y. (1996) Fibrillin-1: organization in microfibrils and structural properties. *J Mol Biol* **258**, 104-116
- 395 Carta, L., Pereira, L., Arteaga-Solis, E., Lee-Arteaga, S. Y., Lenart, B., Starcher, B., Merkel, C. A., Sukoyan, M., Kerkis, A., Hazeki, N., Keene, D. R., Sakai, L. Y. and Ramirez, F. (2006) Fibrillins 1 and 2 perform partially overlapping functions during aortic development. *J Biol Chem* **281**, 8016-8023
- 396 Pereira, L., Lee, S. Y., Gayraud, B., Andrikopoulos, K., Shapiro, S. D., Bunton, T., Biery, N. J., Dietz, H. C., Sakai, L. Y. and Ramirez, F. (1999) Pathogenetic sequence for aneurysm revealed in mice underexpressing fibrillin-1. *Proc Natl Acad Sci U S A* **96**, 3819-3823
- 397 Tamarina, N. A., Grassi, M. A., Johnson, D. A. and Pearce, W. H. (1998) Proteoglycan gene expression is decreased in abdominal aortic aneurysms. *J Surg Res* **74**, 76-80
- 398 Mohamed, S. A., Sievers, H. H., Hanke, T., Richardt, D., Schmidtke, C., Charitos, E. I., Belge, G. and Bullerdiek, J. (2009) Pathway analysis of differentially expressed genes in patients with acute aortic dissection. *Biomark Insights* **4**, 81-90
- 399 Beresford, P. J., Xia, Z., Greenberg, A. H. and Lieberman, J. (1999) Granzyme A loading induces rapid cytolysis and a novel form of DNA damage independently of caspase activation. *Immunity* **10**, 585-594
- 400 Paus, R. and Foitzik, K. (2004) In search of the "hair cycle clock": a guided tour. *Differentiation* **72**, 489-511
- 401 Alonso, L. and Fuchs, E. (2006) The hair cycle. *J Cell Sci* **119**, 391-393
- 402 Foitzik, K., Lindner, G., Mueller-Roeve, S., Maurer, M., Botchkareva, N., Botchkarev, V., Handjiski, B., Metz, M., Hibino, T., Soma, T., Dotto, G. P. and Paus, R. (2000) Control of murine hair follicle regression (catagen) by TGF-beta1 in vivo. *Faseb J* **14**, 752-760
- 403 Hansen, L. A., Alexander, N., Hogan, M. E., Sundberg, J. P., Dlugosz, A., Threadgill, D. W., Magnuson, T. and Yuspa, S. H. (1997) Genetically null mice reveal a central role for epidermal growth factor receptor in the differentiation of the hair follicle and normal hair development. *Am J Pathol* **150**, 1959-1975
- 404 McElwee, K. J. and Sinclair, R. (2008) Hair physiology and its disorders. *Drug Discovery Today: Disease Mechanisms* **5**, e163-e171
- 405 Ang, L. S., Cruz, R. P., Hendel, A. and Granville, D. J. (2008) Apolipoprotein E, an important player in longevity and age-related diseases. *Exp Gerontol* **43**, 615-622
- 406 Hafezi-Moghadam, A., Thomas, K. L. and Wagner, D. D. (2007) ApoE deficiency leads to a progressive age-dependent blood-brain barrier leakage. *Am J Physiol Cell Physiol* **292**, C1256-1262
- 407 Guo, Y., Zhang, C., Du, X., Nair, U. and Yoo, T. J. (2005) Morphological and functional alterations of the cochlea in apolipoprotein E gene deficient mice. *Hear Res* **208**, 54-67
- 408 Bolitho, P., Voskoboinik, I., Trapani, J. A. and Smyth, M. J. (2007) Apoptosis induced by the lymphocyte effector molecule perforin. *Curr Opin Immunol* **19**, 339-347
- 409 Mikhail, G. R. and Miller-Milinska, A. (1964) Mast Cell Population in Human Skin. *J Invest Dermatol* **43**, 249-254
- 410 Zackheim, H. S. and Langs, L. (1962) The bald area of the guinea-pig. *J Invest Dermatol* **38**, 347-349

- 411 Paus, R., Maurer, M., Slominski, A. and Czarnecki, B. M. (1994) Mast cell involvement  
in murine hair growth. *Dev Biol* **163**, 230-240
- 412 Botchkarev, V. A., Paus, R., Czarnecki, B. M., Kupriyanov, V. S., Gordon, D. S. and  
Johansson, O. (1995) Hair cycle-dependent changes in mast cell histochemistry in  
murine skin. *Arch Dermatol Res* **287**, 683-686
- 413 Maurer, M., Paus, R. and Czarnecki, B. M. (1995) Mast cells as modulators of hair  
follicle cycling. *Exp Dermatol* **4**, 266-271
- 414 Maurer, M., Fischer, E., Handjiski, B., von Stebut, E., Algermissen, B., Bavandi, A. and  
Paus, R. (1997) Activated skin mast cells are involved in murine hair follicle regression  
(catagen). *Lab Invest* **77**, 319-332
- 415 Lattanand, A. and Johnson, W. C. (1975) Male pattern alopecia a histopathologic and  
histochemical study. *J Cutan Pathol* **2**, 58-70
- 416 Arck, P. C., Handjiski, B., Hagen, E., Joachim, R., Klapp, B. F. and Paus, R. (2001)  
Indications for a 'brain-hair follicle axis (BHA)': inhibition of keratinocyte proliferation  
and up-regulation of keratinocyte apoptosis in telogen hair follicles by stress and  
substance P. *Faseb J* **15**, 2536-2538
- 417 Mietz, H., Chevez-Barrios, P., Lieberman, M. W., Wendt, M., Gross, R. and Basinger, S.  
F. (1997) Decorin and suramin inhibit ocular fibroblast collagen production. *Graefes  
Arch Clin Exp Ophthalmol* **235**, 399-403